



Davidson, Matthew Alexander (2018) Analysis of potential driver genes in oral squamous cell carcinoma. PhD thesis.

<http://theses.gla.ac.uk/9018/>

Copyright and moral rights for this work are retained by the author

A copy can be downloaded for personal non-commercial research or study, without prior permission or charge

This work cannot be reproduced or quoted extensively from without first obtaining permission in writing from the author

The content must not be changed in any way or sold commercially in any format or medium without the formal permission of the author

When referring to this work, full bibliographic details including the author, title, awarding institution and date of the thesis must be given

Enlighten:Theses
<http://theses.gla.ac.uk/>
theses@gla.ac.uk

Analysis of Potential Driver Genes in Oral Squamous Cell Carcinoma

Matthew Alexander Davidson
BSc (Hons)



University
of Glasgow



CANCER
RESEARCH
UK

BEATSON
INSTITUTE

Submitted in fulfilment of the requirements of
the Degree of Doctor of Philosophy

Institute of Cancer Sciences
College of Medical, Veterinary and Life Sciences
University of Glasgow

November 2017

Abstract

The 5-year survival rate of head and neck squamous cell carcinoma (HNSCC) has remained at ~50% for over 50 years. HNSCC is categorised by multiple anatomical sites, but oral (oral SCC) and oropharyngeal squamous cell carcinoma (OPSCC) account for approximately 90% of all cases. At the time of writing, only one targeted agent, cetuximab (a monoclonal antibody targeting the epithelial growth factor receptor), has been approved for the treatment of recurrent/metastatic HNSCC. However, despite the high expression of EGFR in oral SCC tumour samples, the clinical benefit of cetuximab has been modest thus far. Using a phenotypic screening approach, I sought to identify putative therapeutic targets.

A whole genome siRNA screen carried out using an aggressive patient-derived cell line ('Liv7k') in normoxic and hypoxic conditions provided the foundation for this project. In addition, a drug-repurposing screen tested the efficacy of 1,351 compounds, approved for cancer and non-cancer indications. A number of approaches were used to identify potential targets, including a whole genome siRNA screen in normoxic and hypoxic conditions, a drug-repurposing screen, and a data multiplexing approach combining the two screens with pathway analysis and datasets from The Cancer Genome Atlas and the International Cancer Genome Consortium.

Genomic characterisation of oral cancer cell lines confirmed the importance of a previously identified frequently amplified region of chromosome three, which contains a number of driver genes in HNSCC. In addition, a differential susceptibility of oral SCC cells in hypoxia formed the basis of a line of inquiry centred on triglyceride and ether lipid metabolism. Finally, compound screening identified a dependence of oral SCCs on cysteinyl leukotriene signalling, which is involved in inflammatory conditions such as asthma.

Table of Contents

Contents

| | |
|--|----|
| Abstract | 2 |
| Table of Contents | 3 |
| List of Tables..... | 9 |
| List of Figures..... | 10 |
| List of Accompanying Material..... | 14 |
| Acknowledgments | 15 |
| Author's Declaration | 16 |
| Definitions/Abbreviations | 17 |
| Chapter 1 Introduction | 18 |
| 1.1 Disease Characterisation | 19 |
| 1.1.1 Anatomic Definition | 19 |
| 1.1.2 Epidemiology | 19 |
| 1.1.3 TNM Staging | 20 |
| 1.2 Hallmarks of Head and Cancer | 23 |
| 1.3 Molecular Landscape | 25 |
| 1.3.1 Somatic Mutation | 25 |
| 1.3.2 Structural Variations | 26 |
| 1.3.2.1 Epithelial Growth Factor Receptor (EGFR) | 27 |
| 1.3.3 Summary | 27 |
| 1.4 Genetic Progression | 28 |
| 1.4.1 Precursor Lesions | 28 |
| 1.4.2 Field cancerisation..... | 28 |
| 1.4.2 Major Copy Number Events in HNSCC | 30 |
| 1.5 IGF Signalling in HNSCC | 32 |
| 1.5.1 Overview | 32 |
| 1.5.2 Clinical Trials..... | 34 |
| 1.5.3 IGF binding proteins..... | 35 |
| 1.5.4 Regulation of IGF2BP2 | 35 |
| 1.5.5 Target Transcripts of IGF2BP2 | 37 |
| 1.5.6 IGF2BP2 in cancer | 38 |
| 1.5.7 Summary | 39 |
| 1.6 The Significance of Hypoxia..... | 40 |
| 1.6.1 Clinical Definition | 40 |
| 1.6.2 Transcriptional Regulation by HIF-1A..... | 42 |
| 1.6.3 Hypoxia and Clinical Failure | 44 |

| | | |
|-----------|---|----|
| 1.6.4 | Summary | 46 |
| 1.7 | Lipid Metabolism..... | 47 |
| 1.7.1 | Fatty Acid Metabolism | 47 |
| 1.7.2 | Fatty Acid Synthesis..... | 49 |
| 1.7.3 | Dynamic Lipid Storage | 50 |
| 1.7.4 | The Role of Hypoxia in Lipid Metabolism | 51 |
| 1.7.5 | Lipid Rafts and Metastasis..... | 53 |
| 1.7.6 | Summary | 54 |
| 1.8 | Cysteinyl Leukotrienes and Inflammation..... | 55 |
| 1.8.1 | Eicosanoids | 55 |
| 1.8.2 | Lipoxygenases (LOX pathway) | 56 |
| 1.8.3 | Leukotrienes and Cancer | 58 |
| 1.8.4 | Summary | 60 |
| 1.9 | Thesis Aims and Objectives | 61 |
| Chapter 2 | Materials and Methods | 62 |
| 2.1 | Cell lines..... | 62 |
| 2.2 | Reagents and Vendors | 62 |
| 2.3 | Cell Culture Methods..... | 64 |
| 2.3.1 | General Maintenance | 64 |
| 2.3.2 | Thawing stocks..... | 64 |
| 2.3.3 | Passage of cell cultures..... | 65 |
| 2.3.4 | Cell Counting..... | 65 |
| 2.3.5 | Creation of frozen cell stocks..... | 65 |
| 2.4 | Plasmid Manipulation | 65 |
| 2.4.1 | pTRIPZ_IGF2BP2 (tet-inducible)..... | 66 |
| 2.5 | Bacterial Transformation..... | 67 |
| 2.6 | Plasmid cloning, purification and sequencing..... | 67 |
| 2.7 | Lentiviral transfection of mammalian cells..... | 67 |
| 2.7.1 | Packaging and envelope system | 67 |
| 2.7.2 | Puromycin kill curves and selection | 68 |
| 2.7.3 | Lentiviral transfection into 293T cells..... | 68 |
| 2.7.4 | Concentration of lentivirus..... | 68 |
| 2.7.5 | Lentiviral transduction of Liv7k cells | 69 |
| 2.7.6 | Determination of viral titer | 69 |
| 2.7.7 | Puromycin selection of stably expressing cells..... | 70 |
| 2.8 | Molecular Biology Techniques: RNA..... | 70 |
| 2.8.1 | Isolation of RNA from mammalian cell lines..... | 70 |
| 2.8.2 | Normalisation and reverse transcription of RNA..... | 70 |

| | | |
|-----------|---|----|
| 2.8.3 | Generation of cDNA standard curves | 71 |
| 2.8.4 | Real time quantitative PCR (RTq-PCR) | 71 |
| 2.8.5 | Primer Design | 72 |
| 2.9 | Molecular Biology Techniques: Protein..... | 73 |
| 2.9.1 | Cell Lysis (6 well plate) | 73 |
| 2.9.2 | Protein Quantification (BCA Assay) | 73 |
| 2.9.3 | Sodium Dodecyl Sulfate Polyacrylamide Gel Electrophoresis (SDS-PAGE) 73 | |
| 2.9.4 | Western Blotting | 74 |
| 2.10 | Statistical Analysis | 75 |
| 2.11 | RNA Sequencing | 75 |
| 2.12 | High Throughput Screening: siRNA | 77 |
| 2.12.1 | Liquid Handling Quality Control..... | 78 |
| 2.12.2 | Preparation of source plates | 78 |
| 2.12.3 | Experimental Design | 80 |
| 2.12.4 | Fixation and Staining | 81 |
| 2.12.5 | Hit Selection | 81 |
| 2.13 | High Throughput Screening: Drug-Repurposing..... | 84 |
| 2.14 | RNAi transfection (96 well plate)..... | 85 |
| 2.15 | Functional Assays: Incucyte Zoom3®..... | 87 |
| 2.15.1 | Propagation | 87 |
| 2.15.2 | Migration (Wound Assay) | 87 |
| 2.15.3 | Invasion (Wound Assay) | 87 |
| 2.15.4 | Inverse Invasion Assay (Transwell®) | 88 |
| 2.15.5 | 3D Spheroid Formation | 88 |
| 2.15.6 | Neutral Lipid Staining | 89 |
| 2.15.7 | MitoStress Assay (Seahorse, Agilent) | 89 |
| 2.15.8 | Proteasome Activity Kit | 89 |
| 2.16 | Liquid Chromatography Mass Spectrometry (LCMS) | 89 |
| 2.16.1 | Lipid Extraction | 89 |
| 2.16.2 | LCMS | 90 |
| 2.17 | <i>In vivo</i> xenografts | 90 |
| 2.18 | Immunohistochemistry | 91 |
| 2.19 | Patient sample acquisition and processing..... | 92 |
| Chapter 3 | Results - High Throughput Screening | 92 |
| 3.1 | siRNA Screen | 93 |
| 3.2 | Drug-Repurposing Screen..... | 97 |
| 3.3 | Screening Analysis..... | 98 |

| | |
|--|-----|
| Chapter 4 Results - Identification of HNSCC survival significant genes in the 3q26-29 amplicon..... | 99 |
| 4.1 Amplification of chromosome 3q26-29 in oral SCC cell lines..... | 100 |
| 4.2 Identification of pro-oncogenic factors in 3q26-29..... | 102 |
| 4.3 10 genes are implicated in HNSCC patient survival (TCGA)..... | 103 |
| 4.4 <i>IGF2BP2</i> and <i>PSMD2</i> are required for Liv7k viability in vitro and are highly significant for patient survival..... | 106 |
| 4.5 Discussion..... | 107 |
| Chapter 5 Results - Validation of <i>IGF2BP2</i> as a driver gene in oral squamous cell carcinoma | 111 |
| 5.1 Introduction..... | 111 |
| 5.2 <i>IGF2BP2</i> expression in a series of oral SCC cell lines and validation of growth inhibition..... | 112 |
| 5.3 Predicted Binding Sites of <i>IGF2BP2</i> | 114 |
| 5.4 <i>IGF2</i> is highly expressed in tumour cell lines compared to immortalised oral keratinocytes..... | 115 |
| 5.5 Knockdown of insulin signalling genes results in suppression of fitness in Liv7k cell line..... | 117 |
| 5.6 Quantification of <i>IGF2BP2</i> levels in patient tumour vs matched normal tissue..... | 119 |
| 5.7 Generation of an sh <i>IGF2BP2</i> knockdown model..... | 120 |
| 5.8 <i>IGF2BP2</i> knockdown does not significantly affect oral cell line propagation..... | 121 |
| 5.9 <i>IGF2BP2</i> knockdown does not significantly affect oral cell line migration..... | 123 |
| 5.10 <i>IGF2BP2</i> knockdown does not impair oral cell line invasion..... | 124 |
| 5.11 The role of <i>IGF2BP2</i> in epithelial to mesenchymal transition (EMT)..... | 127 |
| 5.12 <i>IGF2BP2</i> depletion did not significantly impair chemotactic invasion in Liv37k cells..... | 128 |
| 5.13 <i>IGF2BP2</i> knockdown did not affect spheroid growth..... | 129 |
| 5.14 The role of <i>IGF2BP2</i> in mitochondrial metabolism..... | 131 |
| 5.15 The role of <i>IGF2BP2</i> in the regulation of oncogenic signalling..... | 132 |
| 5.16 Discussion..... | 134 |
| Chapter 6 Results - Validation of <i>PSMD2</i> as a driver gene in oral squamous cell carcinoma | 136 |
| 6.1 Introduction..... | 136 |
| 6.2 <i>PSMD2</i> is frequently overexpressed in HNSCC patient samples..... | 139 |
| 6.3 Concurrent downregulation of <i>PSMD6</i> is a common event in HNSCC patient samples..... | 140 |
| 6.4 <i>PSMD6</i> gene copy number loss renders tumour cells more vulnerable to suppression of remaining copies..... | 143 |

| | | |
|-----------|---|-----|
| 6.5 | Copy number amplification of proteasomal subunit genes does not predict sensitivity to bortezomib..... | 148 |
| 6.6 | Silencing of <i>PSMD2</i> does not alter the response of oral cancer cells to proteasomal inhibition by bortezomib..... | 150 |
| 6.7 | Proteasomal activity is not altered by gene expression of <i>PSMD2</i> (preliminary data) | 151 |
| 6.8 | Discussion | 153 |
| Chapter 7 | Results - The Role of Lipid Metabolism Genes in Hypoxia | 156 |
| 7.1 | Triglyceride Metabolism | 156 |
| 7.1.1 | Lipid metabolism genes are upregulated in hypoxia | 156 |
| 7.1.2 | A subset of triglyceride metabolism genes are important for cell survival in hypoxia | 161 |
| 7.1.3 | Validation of differential growth inhibition did not confirm screen findings..... | 163 |
| 7.1.4 | Silencing of <i>MGLL</i> leads to a build-up of triglycerides in tumour cells | 166 |
| 7.2 | Ether Lipid Metabolism | 169 |
| 7.2.1 | A subset of genes involved in ether lipid synthesis are essential for cell viability in hypoxia | 171 |
| 7.2.2 | Validation of <i>AGPS</i> knockdown in oral SCC cell lines..... | 172 |
| 7.2.3 | Lipid profiling of <i>AGPS</i> knockdown cells in hypoxia | 174 |
| 7.2.4 | Hypoxia alters levels of ether lipid species..... | 176 |
| 7.2.5 | <i>AGPS</i> knockdown selectively decreases ether lipid species in hypoxia | 178 |
| 7.3 | Discussion | 180 |
| Chapter 8 | Results - <i>In vivo</i> significance of cysteinyl leukotrienes in oral SCC | 185 |
| 8.1 | Introduction | 185 |
| 8.2 | Cysteinyl leukotriene pathway inhibitors inhibit growth of oral SCC cells in a drug screen | 187 |
| 8.3 | Serum-containing media protects cells from leukotriene pathway inhibition..... | 189 |
| 8.4 | Montelukast is a selective antagonist of <i>CysLT₁R</i> | 190 |
| 8.5 | Knockdown of <i>CysLT₁R</i> causes growth inhibition in Liv7k cell line..... | 191 |
| 8.6 | Montelukast induces cell death in the Liv7k cell line | 192 |
| 8.7 | Preliminary data shows montelukast slows growth in a 3D culture model | 193 |
| 8.8 | Montelukast tends toward reduced tumour volume in Liv7k xenograft model..... | 194 |
| 8.9 | Montelukast does not significantly delay time to tumour endpoint..... | 196 |
| 8.10 | Montelukast does not affect the proliferation of Liv7k xenograft cells | 197 |

| | | |
|-----------|--|-----|
| 8.11 | Montelukast treatment did not significantly alter the innate immune response to tumour cells | 199 |
| 8.12 | Discussion | 201 |
| Chapter 9 | Concluding Remarks | 204 |
| | List of References | 210 |

List of Tables

Table 1.1 TNM Staging

Table 1.2 Hypoxia gene classifier set.

Table 2.1 Cell lines used in this thesis.

Table 2.2 List of reagents.

Table 2.3 Optimal primer attributes.

Table 2.4 Primers used in this thesis, custom made and off the shelf

Table 2.5 List of antibodies.

Table 2.6 List of automated equipment used in the screens.

Table 2.7 List of screening plastic ware used in the screens.

Table 2.8 Classes of siRNA used in the screen.

Table 2.9 Z-factor and its interpretation.

Table 2.10 SSMD values and effect size.

Table 2.11 Details of compound libraries used in the drug-repurposing screen.

Table 2.12 List of siRNA sequences.

Table 2.13 List of primary antibodies used for immunohistochemistry.

Table 3.1 Details of the Dharmacon siRNA library.

Table 5.1 Reactome analysis reveals predicted IGF2BP2 function.

Table 7.1 Mean percentage growth inhibition after knockdown of triglyceride metabolism genes (comparison of data from siRNA screen with validation experiments).

Table 7.2 siRNA screen results showing percentage growth inhibition for ether lipid biosynthesis genes in Liv7k cell line.

List of Figures

- Figure 1.1 Cervical lymph nodes classified according to anatomic group.
- Figure 1.2 Hallmarks of cancer, and the influence of hypoxia in HNSCC.
- Figure 1.3 Genetic progression model of HNSCC.
- Figure 1.4 Major arm-level and focal copy number alterations in HNSCC.
- Figure 1.5 Insulin Signalling in HNSCC.
- Figure 1.6 Oxygen diffusion gradient in a solid tumour.
- Figure 1.7 The fate of HIF-1 α in the cell.
- Figure 1.8 Overview of lipid metabolism.
- Figure 1.9 Structure of a lipid raft.
- Figure 1.10 Pathways of arachidonic acid metabolism.
- Figure 1.11 Overview of cysteinyl leukotriene metabolism.
- Figure 2.1 pTRIPZ lentiviral vector map, provided by Dharmacon.
- Figure 2.2 Generation of a standard curve for RTq-PCR experiments.
- Figure 2.3 Stamping of source plates into 384 well experimental plates.
- Figure 2.4 Experimental design of a screen batch.
- Figure 3.1 Screening workflow summary.
- Figure 3.2 Average nuclei count for control wells throughout the siRNA screen.
- Figure 3.3 siRNA screen z score values (per plate).
- Figure 3.4 Frequency distribution chart of percentage growth inhibition in normoxic and hypoxic conditions.
- Figure 3.5 SSMD values for all tested siRNAs, relative to NTC, in (A) normoxic and (B) hypoxic conditions.
- Figure 3.6 Scatter plot showing percentage growth inhibition of Liv7k cell line in response to treatment with FDA-approved compounds.
- Figure 4.1 Copy number analysis of chromosome 3 from whole exome sequencing.
- Figure 4.2 Expression profile of genes contained within 3q26-29 amplicon.
- Figure 4.3 Survival significant genes are scattered throughout 3q26-29.
- Figure 4.4 Pathway analysis of survival significant genes reveals links to known oncogenes.
- Figure 4.5 Highly expressed genes are also important for Liv7k cell viability.
- Figure 4.6 *IGF2BP2* and *PSMD2* overexpression is significantly correlated with reduced overall survival in HNSCC patients.
- Figure 5.1 : Bar chart showing mRNA expression of *IGF2BP2* in four oral SCC cell lines (Liv7k, Liv52k, KR19, Liv52k) and two oral keratinocyte cell lines (OKF4, OKG4).
- Figure 5.2 Silencing of *IGF2BP2* results in growth inhibition in oral SCC and oral keratinocyte cell lines.

Figure 5.3 RNA sequencing reveals fold change gene expression of insulin signalling genes between Liv7k and OKF/OKG4 cell lines.

Figure 5.4 RNA sequencing reveals gene expression of insulin signalling genes.

Figure 5.5 Scatter plot showing percentage growth inhibition in the Liv7k (median) cell line versus fold change of gene expression between Liv7k and OKF4 cell line.

Figure 5.6 The effect on Liv7k growth of knockdown of insulin pathway genes in siRNA screen.

Figure 5.7 *IGF2BP2* mRNA expression was measured in patient tumour and matched normal samples.

Figure 5.8 Generation of an inducible shRNA knockdown model.

Figure 5.9 Cell propagation quantification following silencing of *IGF2BP2* in (A) Liv7k and (B) Liv37k.

Figure 5.10 Measurement of cell migration following silencing of *IGF2BP2* in (A) Liv7k and (B) Liv37k cells.

Figure 5.11 Schematic representation of scratch assay used to assess oral SCC invasion.

Figure 5.12 Cell invasion analysis following *IGF2BP2* knockdown in (A) Liv7k and (B) Liv37k cells.

Figure 5.13 Confirmation of RFP induction in Liv37k cells stably expressing the plasmid.

Figure 5.14 *IGF2BP2* knockdown leads to decreased Snail expression in Liv37k cell line.

Figure 5.15 Inverse invasion assays were performed on sh*IGF2BP2*-induced Liv37k cell line.

Figure 5.16 Spheroid formation assay, showing the effect of *IGF2BP2* knockdown in the Liv7k cell line.

Figure 5.17 The effect of *IGF2BP2* depletion on OCR and ECAR in Liv7k cell line.

Figure 5.18 The effect of *IGF2BP2* knockdown on oncogenic signalling in the Liv7k cell line.

Figure 5.19 Western blot showing expression of phospho and total IGF1R, *IGF2BP2*, phospho and total AKT and phospho and total MAPK upon IGF1R knockdown in Liv7k cell line.

Figure 6.1 Structure of the 26S proteasome.

Figure 6.2 Genomic profiling of upregulated genes encoding proteasomal subunits.

Figure 6.3 Genomic profiling of downregulated genes encoding proteasomal subunits.

Figure 6.4 Genomic profile of *PSMD6* expression in TCGA patient samples.

Figure 6.5 RNA sequencing analysis reveals differential expression of proteasomal subunit genes in oral SCC cells versus immortalised keratinocytes.

Figure 6.6 Proteasomal subunit RNA expression profile.

Figure 6.7 Copy number analysis of *PSMD2*, *PSMC2*, *PSME4* and *PSMD6* using Taqman RTq-PCR assays in oral SCC/keratinocyte cell lines.

Figure 6.8 Western blot analysis of the expression of the proteins encoded by *PSMD2* and *PSMD6*, RPN1 and RPN7 respectively, in two oral SCC and two oral keratinocyte cell lines.

Figure 6.9 Mean growth inhibition after knockdown of proteasomal subunit genes.

Figure 6.10 Bortezomib IC50 values from the Genomics of Drug Sensitivity in Cancer Screen (Sanger Institute).

Figure 6.11 Bortezomib dose response curves in BT-474, oral SCC and immortalised keratinocyte cell lines.

Figure 6.12 Bortezomib dose response curve +/- *PSMD2* in Liv7k cell line.

Figure 6.13 Basal proteasomal activity measured in oral SCC and immortalised keratinocyte cell lines.

Figure 6.14 The effect of bortezomib treatment on proteasome activity.

Figure 7.1 Primary siRNA screen results showing median percentage growth inhibition relative to non-targeting control in normoxic and hypoxic conditions.

Figure 7.2 Metacore GeneGo™ analysis of the hypoxic gene set.

Figure 7.3 SREBP-mediated regulation of cholesterol/fatty acid biosynthesis.

Figure 7.4 Window of percentage growth inhibition versus fold change in gene expression between hypoxic and normoxic conditions.

Figure 7.5 Mean percentage growth inhibition after knockdown of triglyceride metabolism genes (data from siRNA screen).

Figure 7.6 Knockdown of triglyceride metabolism genes leads to growth inhibition in oral cancer cells and immortalised keratinocytes.

Figure 7.7 Quantification of neutral lipid droplets in oral cell lines.

Figure 7.8 Overview of Ether Lipid Synthesis.

Figure 7.9 Gene expression of major ether lipid pathway components from TCGA HNSCC dataset.

Figure 7.10 Validation of growth inhibition upon silencing of ether lipid genes in Liv7k cell line.

Figure 7.11 Validation of AGPS knockdown in Liv7k cell line.

Figure 7.12 Pre-processing of LC-MS Data.

Figure 7.13 Principal Component Analysis (PCA) plot of ether lipid species in hypoxia and normoxia.

Figure 7.14 Hypoxia significantly altered levels of certain ether lipids.

Figure 7.15 PCA plot showing distribution of correlations between groups.

Figure 7.16 Heat map and hierarchical clustering of ether lipid metabolites upon knockdown of AGPS in hypoxia and normoxia.

Figure 8.1 Overview of cysteinyl leukotriene metabolism.

Figure 8.2 Scatter plot showing percentage growth inhibition of the Liv7k cell line in a drug-repurposing screen.

Figure 8.3 Bar chart showing percentage growth inhibition in a panel of cancer cell lines treated with CysLT₁R antagonists.

Figure 8.4 Percentage growth inhibition (IC₅₀ values) of leukotriene pathway antagonists in a series of oral cell lines.

Figure 8.5 Molecular structure of montelukast and its known interactions.

Figure 8.6 Bar chart showing percentage growth inhibition upon knockdown of montelukast target genes in the Liv7k cell line.

Figure 8.7 Liv7k cells were treated for 16 h with montelukast (0.75-10µM).

Figure 8.8 Rate of spheroid growth in a 3D spheroid model (preliminary data).

Figure 8.9 Tumour size as a percentage of start volume for montelukast (n=10) and vehicle control groups (n=10).

Figure 8.10 Tumour size as a percentage of start volume for individual montelukast and vehicle control mice.

Figure 8.11 Survival curve of montelukast (n=10) versus vehicle control (n=10) mice, up to 100 days since the start of treatment.

Figure 8.12 Ki67 histological staining.

Figure 8.13 H&E, macrophage (F4/80) and neutrophil (NIMP) histological staining.

List of Accompanying Material

Publications arising from this work:

REVIEW: Davidson MA, Shanks EJ (2017) 3q26-29 amplification in head and neck squamous cell carcinoma: a review of established and prospective oncogenes. FEBS J. 2017 Sep; 284(17):2705-2731.

Acknowledgments

I would like to thank Dr Emma Shanks for giving me the opportunity to do a PhD in her lab and utilise the full range of screening facilities. Thank you for all of your support throughout my time here. I have found your guidance essential for the completion of this project and for my own development as a scientist. I would also like to thank Lynn McGarry for showing me the ropes of the screening facility and ensuring that all of my work was of a high standard. In addition, I would like to thank other members of the screening facility for their support throughout my project, both personally and academically. These people are Daniel James, who made the analysis of massive data bundles quick and simple; Kay Hewit, who offered so much support throughout; and Grant McGregor, who was very helpful in the final year of my project. I am very grateful to Marc Jones for his advice and help during my PhD.

I would also like to thank the fantastic staff at the Beatson Institute and all of the service groups who made my work possible. These include Susan Mason and Karen Blyth, who put so much work into the *in vivo* aspect of the project. Thanks to Colin Nixon and his histology team, William Clark, Andrew Keith, Gabriela Kalna, Ann Hedley, Matt Neilson, Gillian Mackay, Sergey Tumanov, members of R2 and R6 and the central services team, who made working here so much easier. I am very grateful to have received direction from Eyal Gottlieb, Peter Adams, Karen Blyth and Mike Olsen.

I reserve a special mention for Kim-Moran Jones, who tirelessly provided guidance and assistance throughout my project and has been a wonderful friend and mentor. I am thankful for the support of my family and friends that I have met here in Glasgow. Lastly, I would like to thank Christin Bauer for her personal support throughout my project and for putting up with me for four years. My time here would not have been the same without her.

The results here are in part based upon data generated by the TCGA Research Network: <http://cancergenome.nih.gov/>

Author's Declaration

I declare that, except where explicit reference is made to the contribution of others, this thesis is the result of my own work and that it has not been submitted for any other degree at the University of Glasgow or any other institution.

Signature

Printed name: Matthew Alexander Davidson

Definitions/Abbreviations

| | |
|--------|---|
| AJCC | American Joint Committee on Cancer |
| ARCON | Accelerated Radiotherapy with Carbogen and Nicotinamide |
| CGH | Comparative Genomic Hybridization |
| CNA | Copy number alteration (somatic) |
| CNV | Copy number variation (germline) |
| DISC | Death-inducing signalling complex |
| ECS | Extracapsular Spread |
| EGFR | Epithelial Growth Factor Receptor |
| EMT | Epithelial to mesenchymal transition |
| FDA | Food and Drug Administration |
| FISH | Fluorescent In Situ Hybridization |
| GBM | Glioblastoma Multiforme |
| GISTIC | Genomic Identification of Significant Targets In Cancer |
| HPV | Human Papilloma Virus |
| ICD | International Classification of Disease |
| ICGC | International Cancer Genome Consortium |
| IGF | Insulin-like growth factor |
| LOH | Loss of heterozygosity |
| MMP | Matrix metalloprotease |
| OS | Overall Survival |
| PFS | Progression Free Survival |
| TCGA | The Cancer Genome Atlas |

Chapter 1 Introduction

Head and neck cancer is the sixth most common cancer in the world with more than 11,000 new cases in the UK in 2014[1, 2]. More than 90% of head and neck cancers are squamous cell carcinomas (head and neck squamous cell carcinoma; HNSCC)[3], and these are further categorised by biological subsite, HPV status and TNM stage. Current five-year survival rates have lingered at approximately 50% for decades in patients where spread to regional lymph nodes has occurred[4]. Metastasis, abetted by late presentation and detection, is the major factor leading to the failure of treatment in head and neck patients[5, 6], and in contrast to other solid tumours, head and neck tumours spread almost exclusively lymphatically[7].

The mainstay treatment for HNSCC remains (often disfiguring) surgery with adjuvant chemo/radiotherapy. At the time of writing, only one targeted therapy has been approved for the treatment of local recurrent/metastatic HNSCC. In 2006, cetuximab (Erbix; Bristol-Myers Squibb, NY, USA) a humanised monoclonal antibody targeting epithelial growth factor receptor (EGFR) was approved. However, given the strong evidence for the importance of EGFR in HNSCC progression, the overall improvement in patient survival upon cetuximab treatment has been modest. Overexpression of the protein occurs in more than 90% of cases and is predictive of a poor prognosis[8], however combined cetuximab and radiotherapy led to only a 10% overall survival benefit versus radiotherapy alone[9-11].

Pembrolizumab (Keytruda; Merck & Co. Inc, Kenilworth, NJ, USA), is an immune modifying therapy which has been approved for use in unresectable, metastatic melanoma (2014)[12], non-small cell lung cancer (2014)[13] and in HNSCC (2016)[14]. The humanised monoclonal antibody binds programmed cell death protein 1 (PD-1) receptor on the surface of T cells and prevents their binding to PD-L1 and PD-L2 on tumour cells, thus stimulating T-cell mediated tumour cell destruction[12]. Its approval in recurrent and/or metastatic HNSCC was accelerated based on early results of the phase 1b KEYNOTE-012 trial, which showed an overall response rate (ORR) of 18%[14]. A later phase II clinical trial (KEYNOTE-055) which sought to assess the efficacy of pembrolizumab in patients

who were refractory to cetuximab treatment showed an ORR of 16%[15]. More recently, its use has extended to cover any solid tumour with mismatch repair deficiency or high microsatellite instability. This is because tumours with high mutation rates have increased levels of abnormal antigens and are therefore more responsive to immune modulation[16]. Another immune checkpoint inhibitor, nivolumab (Opvigo), was approved later in 2016 following on from the successful phase III CheckMate-141 trial[17]. Ongoing phase III trials are encouraging but further studies are required to understand the full potential of immunotherapy in HNSCC.

1.1 Disease Characterisation

1.1.1 Anatomic Definition

The primary focus of this body of work is oral squamous cell carcinoma (oral SCC), which represents 38% of head and neck cancers in males and 50% in females[2]. The disease encompasses multiple anatomic sites, including the lip, buccal mucosa, anterior two thirds of the tongue, upper and lower gingiva, the floor of the mouth and the hard palate (ICD-10: C00-06)[18]. The base of the tongue, the squamous-lined tonsils (palatine and lingual), the side and back walls of throat and the soft palate are classified as oropharyngeal cancer (ICD-10: C09-10) and were not investigated in this study. Individual subsites have varying degrees of access to local venous and lymphatic systems, and are therefore accompanied by different risk factors and treatment options. While these classifications serve as a useful guide, there is no internationally agreed anatomical definition of oral SCC in the wider literature and data from multiple sites are often combined. Where possible, it has been specified whether a referenced study focused specifically on squamous cell carcinomas of the oral cavity or HNSCCs in general.

1.1.2 Epidemiology

Although the highest prevalence of oral SCC is seen in the over 65 age bracket, there has been a dramatic rise in younger populations (<45 years) in recent years[19]. Socio-economic factors weigh heavily on these statistics, with alcohol and smoking cooperatively exacerbating risk[20]. However, the increased

incidence largely reflects an atypical younger population who have minimal exposure to the classic risk factors[21-24]. HPV has an established role in oropharyngeal cancer, with up to 70% of these patients testing positive for the virus[25, 26]. However, HPV is predominantly absent in oral SCC. Moreover, those patients presenting with HPV-positive tumours generally have a more favourable prognosis, even in recurrence[27-29], suggesting a distinct disease aetiology. Despite this, current evidence suggests that cetuximab and pembrolizumab benefit patients with either HPV status[30].

The complexity of HNSCC is further compounded by the intrinsic heterogeneity of the disease, as revealed by molecular analyses[31-34]. The last decade has seen the release of an unprecedented amount of genomic characterisation, thanks to projects such as The Cancer Genome Atlas (TCGA) and the International Cancer Genome Consortium (ICGC). This freely available data has vastly improved the understanding of disease processes and opened the door to a number of innovative personalised therapeutic strategies. To date, HNSCC has not truly benefitted from this wealth of information, when compared to the leaps made in the molecular subtyping of other cancer types[35, 36]. This project capitalises on large sequencing datasets in order to help identify novel molecular subtypes.

1.1.3 TNM Staging

Oral SCCs are defined clinically by the TNM (Tumour, Node and Metastasis) system, which allows for the successful management of disease prognosis. The three factors relate to: (1) the primary tumour, including size and location; (2) the extent of nodal involvement; and (3) the presence of distant metastasis. Tumour and nodal status are staged from 1-4, with sub-classifications a, b or c (Table 1.1). For example, T4aN2aM0 indicates a moderately advanced tumour with local invasion into tongue muscle or mandible and involving more than one lymph node. The oral cavity is one of the most common sites of SCC incidence, owing to its exposure to external carcinogens. Primary treatment for most tumours is surgery, often in combination with radiotherapy with postoperative chemotherapy to improve local disease control. Platinum-based therapies such

as 5-fluorouracil and cisplatin have a modest impact on patient survival and decrease time to recurrence[37].

| Primary Tumour (T) | |
|--------------------------|---|
| Tx | Primary tumour cannot be assessed |
| T0 | No evidence of primary tumour |
| T1 | Tumour <2cm in greatest dimension |
| T2 | Tumour 2-4cm in greatest dimension |
| T3 | Tumour >4cm in greatest dimension |
| T4a | Moderately advanced local disease, with invasion into cortical bone, deep extrinsic muscle of the tongue, maxillary sinus, or skin of face |
| T4b | Very advanced local disease, with invasion into masticator space, pterygoid plates, or skull base and/or encases internal carotid artery |
| Regional Lymph Nodes (N) | |
| Nx | Nodal involvement cannot be assessed |
| N1 | No regional lymph node involvement |
| N2 | Metastasis in a single ipsilateral lymph node, <3cm in greatest dimension |
| N2a | Metastasis in a single ipsilateral lymph node 3-6cm in greatest dimension; or in multiple ipsilateral nodes, none >6cm; or in bilateral or contralateral nodes, none >6cm |
| N2b | Metastasis in a single ipsilateral lymph node 3-6cm in greatest dimension |
| N2c | Metastasis in a multiple ipsilateral lymph nodes, none >6cm in greatest dimension |
| N3 | Metastasis in a bilateral/contralateral lymph nodes, none >6cm in greatest dimension |
| Distant Metastasis (M) | |
| Mx | Distant metastasis cannot be assessed |
| M0 | No evidence of distant metastasis |
| M1 | Distant metastasis |

Table 1.1 TNM Staging (American Joint Committee on Cancer, AJCC).

Lymph node metastasis is estimated to occur in approximately 40% of oral cancer patients[38]. The proximity of the oral SCCs to regional lymph nodes has a major impact on rate of recurrence and distant metastasis of tumour cells, with one study finding cervical lymph node metastasis in ~62% of T3/T4 tumours[39]. Extracapsular spread (ECS) is another major prognostic factor in oral SCC. Its significance is widely recognised in the prognosis of oral cancer, with average 5-year survival dropping to 24% in patients with ECS in cervical lymph nodes[40]. So far, ECS has not been shown to predict worse disease-free survival in HPV-positive or negative oral SCCs[41]. There are approximately 300 lymph nodes in

the neck, which are classified by their location. These are the submental and submandibular group, the upper jugular group, the middle jugular group, the lower jugular group, the posterior triangle group and the anterior compartment [42](Figure 1.1).

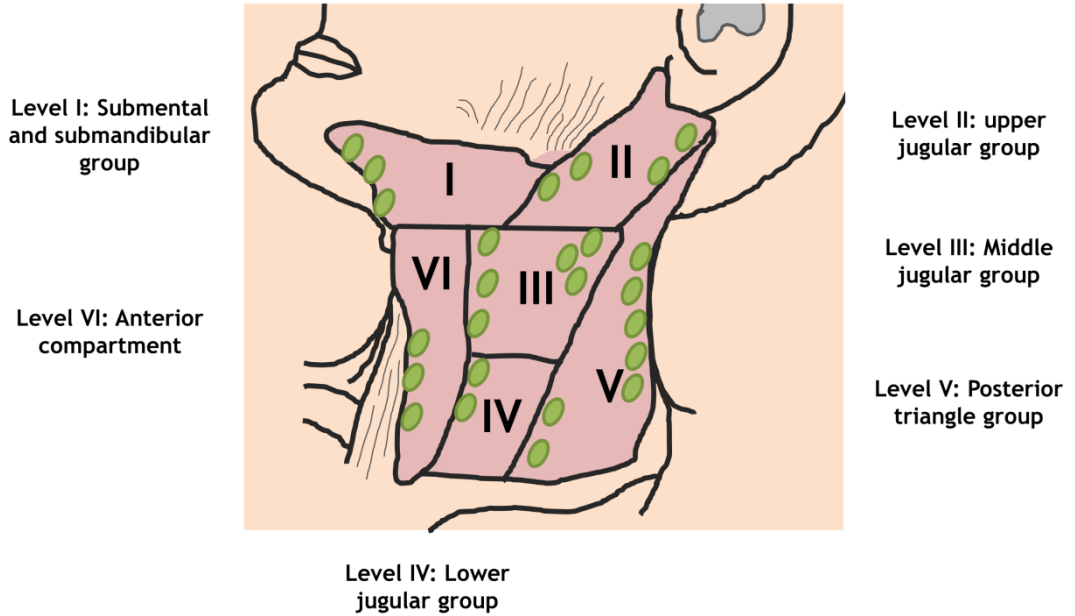


Figure 1.1 Cervical lymph nodes classified according to anatomic group.

1.2 Hallmarks of Head and Cancer

Hanahan and Weinberg's "Hallmarks of Cancer" (Figure 1.2) describe the eight defining features of all cancers, which are enabled by genome instability and inflammation[43]. These hallmarks underpin the development and progression of HNSCC, which remains a major therapeutic challenge. This introduction touches on many of these defining characteristics but focuses primarily on three key hallmarks: genomic instability, deregulated metabolism and inflammation. HNSCC is a highly heterogeneous cancer, characterised by mutations and somatic copy number alterations[44]. This is an underlying reason for treatment failure, and explains why so many targeted therapies fail to bring wide-reaching benefit, despite success in pre-clinical studies[45].

Genomic instability is exaggerated by another defining feature of solid tumours such as HNSCC. Hypoxia, which occurs when tumour growth outpaces that of oxygen and nutrient supplying blood vessels, brings about a strong selective pressure on cells[46]. Hypoxia promotes a more aggressive phenotype that is associated with resistance to chemo/radiotherapy[47]. Lack of oxygen also perturbs cellular metabolism, which forms the second major theme of this thesis. These changes in energy utilisation are a direct result of successive genetic alterations and limited availability of nutrients and include a shift to a glycolytic phenotype and increased production of lipids[48]. Herein, a subset of genes involved in triglyceride metabolism was identified as part of an unbiased genomic screen. Maintaining a steady supply of lipids is essential to the survival of rapidly proliferating cells. Lipids exist in a wide variety of forms owing to different lengths of fatty acid chains and the position and number of double bonds. This multiplicity allows lipids to play a range of roles within the cell, including as cell membrane constituents, second messengers in signalling and storage of energy[49].

Finally, an FDA-approved compound screen led to the identification of a class of non-steroidal anti-inflammatory drugs (NSAIDs), which caused >90% growth inhibition in oral SCC cell lines. Tumour growth is dependent on the surrounding extracellular matrix and the ancillary processes that occur within it[50]. Infiltrating immune cells can facilitate tumour development through the release

of cytokines and growth factors that promote tumour growth and promote invasion[51]. Moreover, it has been shown that NSAIDs can impair the growth and development of HNSCCs[52]. This introduction reviews the known roles of inflammation in HNSCC and presents novel findings from *in vivo* work targeting a major inflammatory pathway.

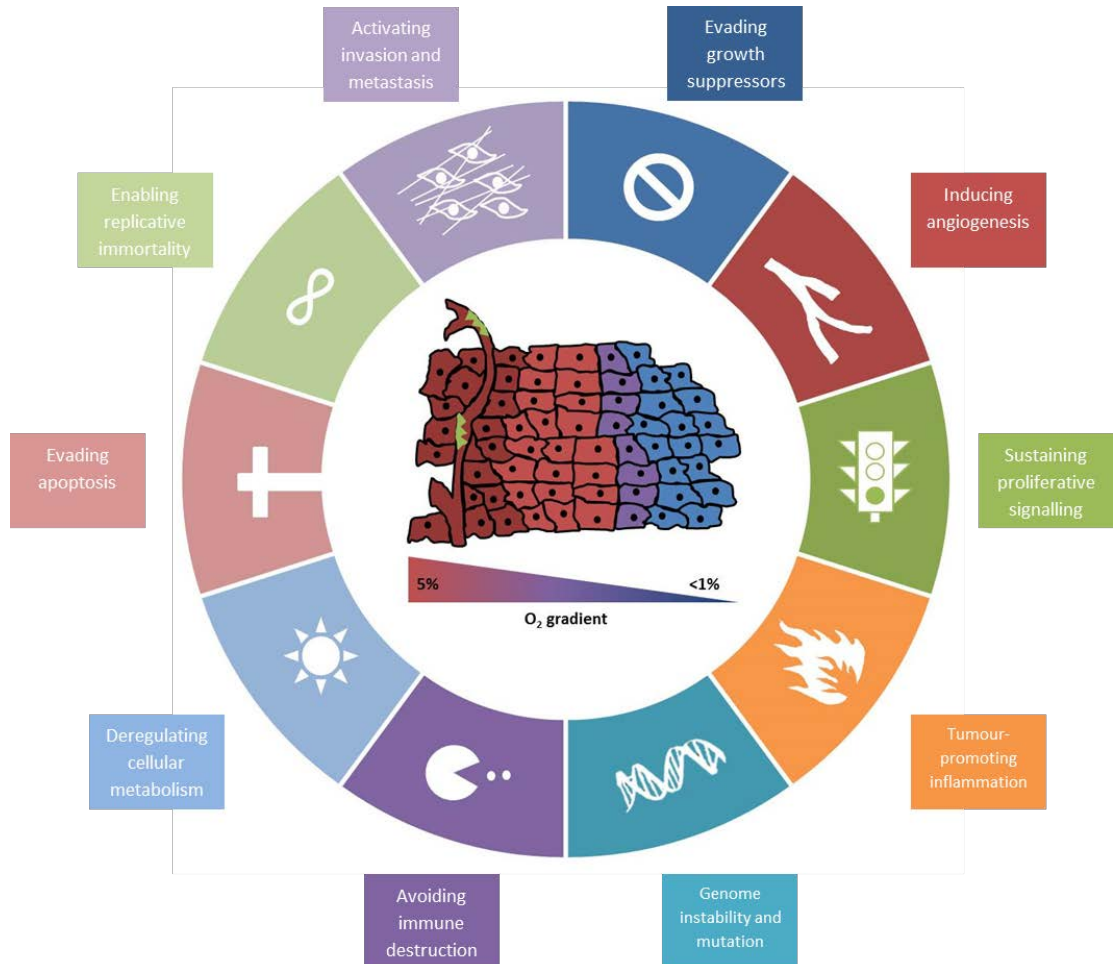


Figure 1.2 Hallmarks of cancer, and the influence of hypoxia in HNSCC. Adapted from [43].

1.3 Molecular Landscape

Head and neck cancer is a highly heterogeneous disease, with genetic variation between patient tumour samples and within the tumour itself, and accounts for approximately 550,000 cases and 380,000 deaths every year[53]. However, at present, complete and standardised genomic profiles exist for just 522 patients in TCGA dataset - a snapshot of the overall situation. Like most solid tumours, HNSCC occurs through a series of genetic alterations, which occur over an individual's lifetime. Epigenetic mechanisms also play a key role (although have not been investigated further here). There are two functional classes of genetic alteration: somatic mutation and structural variation.

1.3.1 Somatic Mutation

Several key alterations in HNSCC had been discovered before the widespread implementation of high throughput platforms for gene expression analysis, with the most frequent being those found in *TP53* (17p13), a tumour suppressor gene in which activating mutations are known to play an important role in the pathogenesis of HPV-negative HNSCC[44]. Loss-of-function mutations in *TP53* are almost universal and are recognised as one of the earliest genetic alterations in HNSCC[54].

Also common are inactivating deletions or mutations in *CDKN2A* (9p21), which occur in >50% of HNSCC tumours, and amplification of *CCND1* (11q13), found in approximately one third of HPV-negative HNSCCs[55, 56]. In addition, up to one third of HNSCCs harbour activating mutations in the oncogenic PI3K pathway, with the largest percentage occurring in the *PIK3CA* gene (3q26)[57]. *PTEN*, a negative regulator of the PI3K pathway and tumour suppressor gene is also frequently lost or downregulated in aggressive HNSCC[54, 58, 59].

As a result of sequencing data, inactivating mutations in *NOTCH1* have been confirmed in 10-15% of HNSCCs[44, 60, 61], suggesting a tumour suppressor role, a function validated in several studies[62-64]. However, NOTCH1 dysregulation is more complicated than mere loss-of-function. Increased NOTCH pathway signalling occurs in approximately one third of HNSCCs, and is accompanied by an oncogenic phenotype[65-67].

The *NOTCH1* gene encodes a transmembrane receptor which belongs to a family of interrelated signalling molecules which can regulate many aspects of cell biology, including stem cell renewal[68], proliferation and cell survival[69]. In oral SCC tumours, NOTCH1 is localised at the invasive edge where its expression is positively correlated with lymph node metastasis and depth of local invasion[69-71]. Furthermore, inhibition or knockdown of NOTCH1 reduces cell proliferation and invasion[69, 72]. The conflicting roles of NOTCH1 are likely influenced by the presence of other genetic alterations and the surrounding microenvironment[73, 74].

1.3.2 Structural Variations

HNSCCs exhibit a high degree of chromosomal instability, which contributes to the vast heterogeneity of the disease and represents a major clinical challenge. Structural variations occur frequently through mutational mechanisms, including errors in DNA recombination, replication and repair processes[75]. These include insertions, deletions, duplications, translocations and inversions, all of which can lead to changes in gene copy number. Originally, structural variation was defined as a genomic alteration involving a segment of DNA larger than 1 Kb; however improvements in detection have led to a revision of this definition to include changes involving more than 50 base pairs[76]. In contrast, insertions and deletions (INDELs) normally involve only a few base pairs.

Copy number alteration (CNA) refers to copy number changes occurring in somatic cells and should not to be confused with copy number variation (CNV) which is germline in origin. A recent analysis of 3,299 tumour samples spanning 12 cancer types revealed two major classes of genetic alteration in cancer that are characterised by recurrent somatic mutation (M class) or copy number alteration (C class), with HNSCC primarily falling under the latter category[77].

Using various techniques, a high incidence of LOH/deletion on chromosomes 3p, 5q, 8p, 9p and 18q[78-80] and high levels of gain/amplification on 3q, 5p, 7p, 8q and 11q have been identified in HNSCC, many of which have been confirmed in recent years utilising high-throughput sequencing methods.

1.3.2.1 Epithelial Growth Factor Receptor (EGFR)

Focal amplification of 7p11.2 occurs in approximately 31% of HNSCCs[81]. The region is home to the gene encoding EGFR, a receptor tyrosine kinase which is expressed in over 90% of HNSCCs[82]. Increased protein expression of EGFR is observed early in carcinogenesis, and increases with the degree of dysplasia[83]. Protein overexpression has been shown to occur in a similar percentage of oral SCC samples[84-86]. Moreover, EGFR has been repeatedly verified as a negative prognostic indicator in HNSCC with its overexpression correlating with significantly decreased overall and disease-free survival in addition to high rates of loco-regional relapse[87]. Similar findings are found in patients with tumours with increased EGFR copy number[88, 89]. Activation of EGFR signalling brings about a malignant phenotype which is characterised by enhanced angiogenesis, decreased apoptosis and a propensity to metastasize to local and distant sites[90]. This is achieved through activation of downstream signalling pathways such as AKT, STAT3 and MAPK[91-94]. Despite a solid biological rationale to target EGFR, inhibitors of the receptor have met with limited success as a monotherapy, indicating a requirement for additional therapeutics in this disease.

1.3.3 Summary

A number of studies have sought to capitalise on recent technological advances in order to associate key molecular alterations to specific pathological traits. Overall, a complex pattern of chromosomal alteration has emerged in which the gains and losses commonly observed in HNSCC translates into clinically relevant prognoses, and correlates with poorer survival in patients[95]. While some of these regions contain key oncogenes and tumour suppressor genes, the importance of other regions to disease progression is currently unknown[96].

Distinguishing driver mutations from randomly occurring passenger mutations (which result from a higher basal rate of alteration in tumour cells), remains a challenge[97]. A driver mutation has a causal role in oncogenesis and confers a growth advantage to the tumour cell that is passed on to daughter cells, allowing it to alter core processes, overcome cell cycle restriction and activate survival and invasion pathways[43]. In contrast, passenger mutations are not

selected for and generally do not confer a growth advantage. These somatic mutations are passed on with no functional consequence[98]. In addition, facilitator mutation events, which are not oncogenic by themselves, often promote the genetic diversity that enables tumour cells to overcome restrictions on their growth. The difficulty is in distinguishing the types of mutation, which relies largely on measuring how randomly they are distributed. Inevitably, a number of mutations will be falsely classified and should be interpreted with caution. Consolidation of driver mutations is achieved by investigating their phenotypic consequence.

1.4 Genetic Progression

1.4.1 Precursor Lesions

Genetic alterations occur in a stepwise progression, accompanied by macroscopic changes in the oral mucosa known as precursor lesions. The most common of these is the appearance of a white patch on the mucosal lining termed oral leukoplakia. These lesions occur in approximately 1.5% of the population and are associated with an increased risk of malignant transformation[99]. The rate of development into invasive carcinoma differs depending on population cohort and variation in assessment, but it is currently thought that ~1% of leukoplakia make the transition into oral SCC[99].

By the time leukoplakias are visible to the naked eye, the cells will have undergone a number of histological and genetic alterations. The first genetic multi-step progression model of HNSCC was proposed in 1996 (updated in **Figure 1.3**). The model provides a link between instances of chromosomal loss and histopathological observations in early and late stage tumours.

1.4.2 Field cancerisation

Early genetic changes can also be present in the macroscopically normal epithelium surrounding lesions[100]. 'Field Cancerisation' describes the existence of a pre-neoplastic field of epithelium outside the surgical margins defined by macroscopically visible lesions[101]. The field arises from a single cell which develops a genetic alteration and clonally expands, later giving rise to

a secondary invasive carcinoma[102, 103]. Slaughter *et al.* was the first to link the existence of such fields to the high propensity of HNSCCs to recur in patients[104]. An analysis of macroscopically normal mucosa surrounding HNSCC revealed genetic alteration in 36% of patients[105]. HNSCCs have the second highest percentage of multiple primary tumours (15%) of all cancer types[106].

However, fixed linear models of progression, such as that in **Figure 1.3**, do not fully capture the heterogeneous nature of HNSCC, which has been shown to involve multiple molecular routes to a metastatic endpoint.

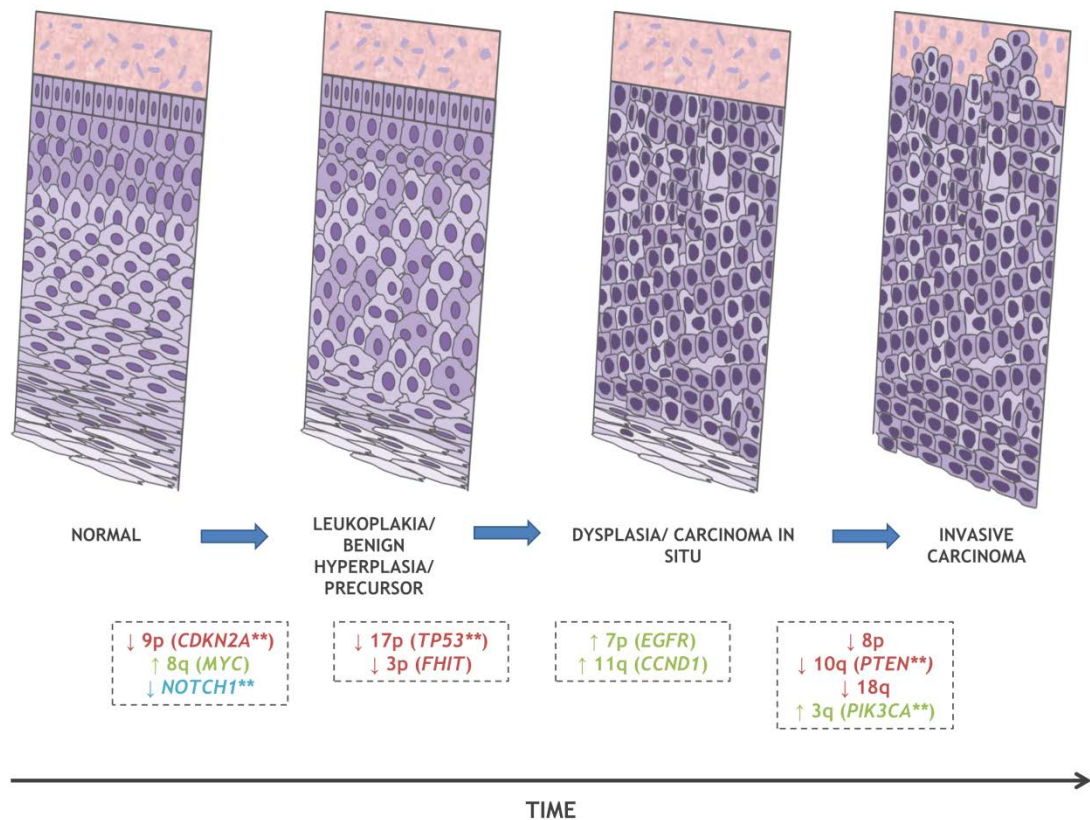


Figure 1.3 Genetic progression model of HNSCC. Chromosomal regions with frequent copy number alterations are presented, along with associated oncogenes or tumour suppressors. *NOTCH1* has been reported as both an oncogene and tumour suppressor gene in HNSCC, indicating its function may vary depending on genetic context. Adapted from [107].

1.4.2 Major Copy Number Events in HNSCC

Somatic copy number alterations affect a larger proportion of the cancer genome than any other type of genetic alteration[108]. Much like somatic mutations, it is important to distinguish driver events that contribute to cancer progression from passenger events that are acquired throughout the lifetime of a tumour, but do not impart a phenologic change[109]. Driver CNAs that provide a growth advantage occur more often and similar patterns of alteration are seen in cancers of similar tissue types[110]. Copy number alterations can be divided into “arm-level” events encompassing entire arms or smaller “focal” events, which occur within a specific region[111]. Additional copies of certain genes can lead to over activity of the protein product. Oncogenes are often activated in this way and lead to cellular transformation. **Figure 1.4** shows the most significant chromosomal alteration events in HNSCC, according to GISTIC 2.0 analysis[112].

Amplification of chromosome 3q26-29 is a defining feature of squamous type cancers and is estimated to occur in up to 75% of HNSCCs[113]. The region contains a number of established and prospective oncogenes, including *PIK3CA*, *TP63* and *SOX2*[114-116]. Furthermore, it has a demonstrated ability to enhance migration and invasion and is consistently associated with a poor prognosis in HNSCC patients[117-119]. The 3q26-29 amplicon forms a major part of this project and will be discussed further in chapters four, five and six. In particular, the role of a binding protein involved in insulin signalling will be assessed.

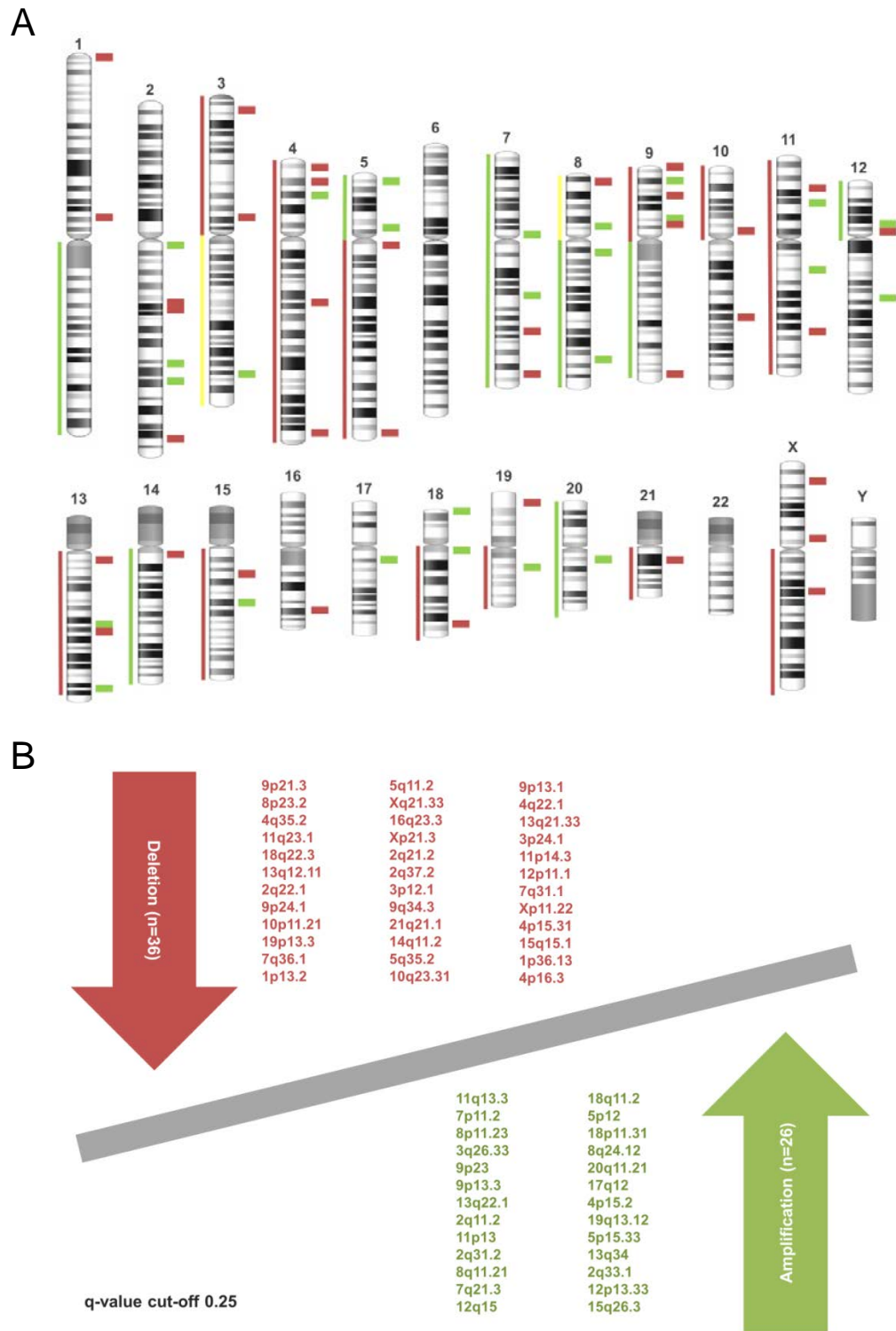


Figure 1.4 Major arm-level and focal copy number alterations in HNSCC. (A) Graphical representation of significant chromosomal alterations in HNSCC in TCGA dataset, as determined by GISTIC 2.0, $n = 279$ samples (green = amplification; red = deletion, yellow, both). Vertical lines represent arm level events and rectangles depict focal alterations with significance set at a q -value = 0.25. (B) Major focal copy number alterations in HNSCC. GISTIC 2.0 analysis reveals 36 significantly recurring deletion events and 26 amplification events, ranked by descending residual q -value. Data adapted from [51].

1.5 IGF Signalling in HNSCC

3q26-29 copy number amplification is the most frequent genomic alteration in HNSCC and is universally associated with a poor prognosis[113]. Whole exome sequencing revealed the presence of this amplicon in a number of oral SCC cell lines used in this project. Subsequent analysis of the region identified a number of genes, which are highly significant for survival in patients (TCGA HNSCC dataset). The most significant gene in terms of overall survival was *insulin-like growth factor 2 binding protein 2 (IGF2BP2)*. In the cell, IGF2BP2 binds to and stabilises specific gene transcripts, thus regulating their translation. One of the confirmed targets of the gene is insulin-like growth factor 2 (IGF2), which acts through the IGF1 receptor (IGF1R) to activate downstream growth and survival pathways. A central aim of this project was to determine if *IGF2BP2* acts as a key driver gene in HNSCC progression.

1.5.1 Overview

The IGF signalling pathway represents a very attractive target in cancer therapy, however effective inhibition of the network has proven challenging. To date, most inhibitors have IGF1R, a heterodimeric transmembrane receptor that is associated with poorer survival in advanced stage oral SCC [120] and is preferentially overexpressed in HPV-negative HNSCC[121]. IGF1R was found to be significantly expressed in a series of oral cancer biopsies taken from patients prior to treatment[122]. Moreover, it has been shown that elevated expression of IGF1R, in combination with its binding protein, IGFBP3, correlates with a significantly shorter time to progression in HNSCC[123]. *In vivo* studies also support a role for IGF1R in tumour progression. Constitutive activity of IGF1R led to the rapid induction of tumours in a transgenic mice model, while a small-molecule inhibitor of the receptor reduced the tumour burden[124]. Conversely, deletion of IGF1R or genetic reduction of circulating IGF1 has been shown to negate tumour progression[125, 126].

The IGF1R receptor is composed of two extracellular α subunits which mediate ligand binding and two transmembrane β subunits with tyrosine kinase activity (Figure 1.5)[127]. There is a 60% amino acid sequence homology between the IGF1R receptor and the insulin receptor (IR)[128], which allows the formation of

hybrid receptors which can bind both IGF ligands[129]. Ligand binding of IGF1 or IGF2 to IGF1R (or hybrid/insulin receptors) leads to autophosphorylation of the receptor and activation of insulin receptor substrate (IRS)[130]. There are six distinct IRS proteins but IRS-1/2 mediate most of the downstream signalling[131]. Phosphorylation of IRS-1 at Tyr⁶¹² activates the p85 regulatory subunit of PI3K and subsequently AKT[132, 133], while phosphorylation at Tyr⁸⁹⁶ promotes binding of Grb2 and activation of the MAPK pathway[134]. AKT activation frees mTOR from tuberous sclerosis complex 2 (TSC2)-driven inhibition, thus promoting cell growth and survival[135]. PI3K activity is negatively regulated through PTEN-mediated dephosphorisation of PIP₃[136], however the *PTEN* tumour suppressor gene is commonly mutated/deleted in HNSCC (8-23% of cases)[44, 137].

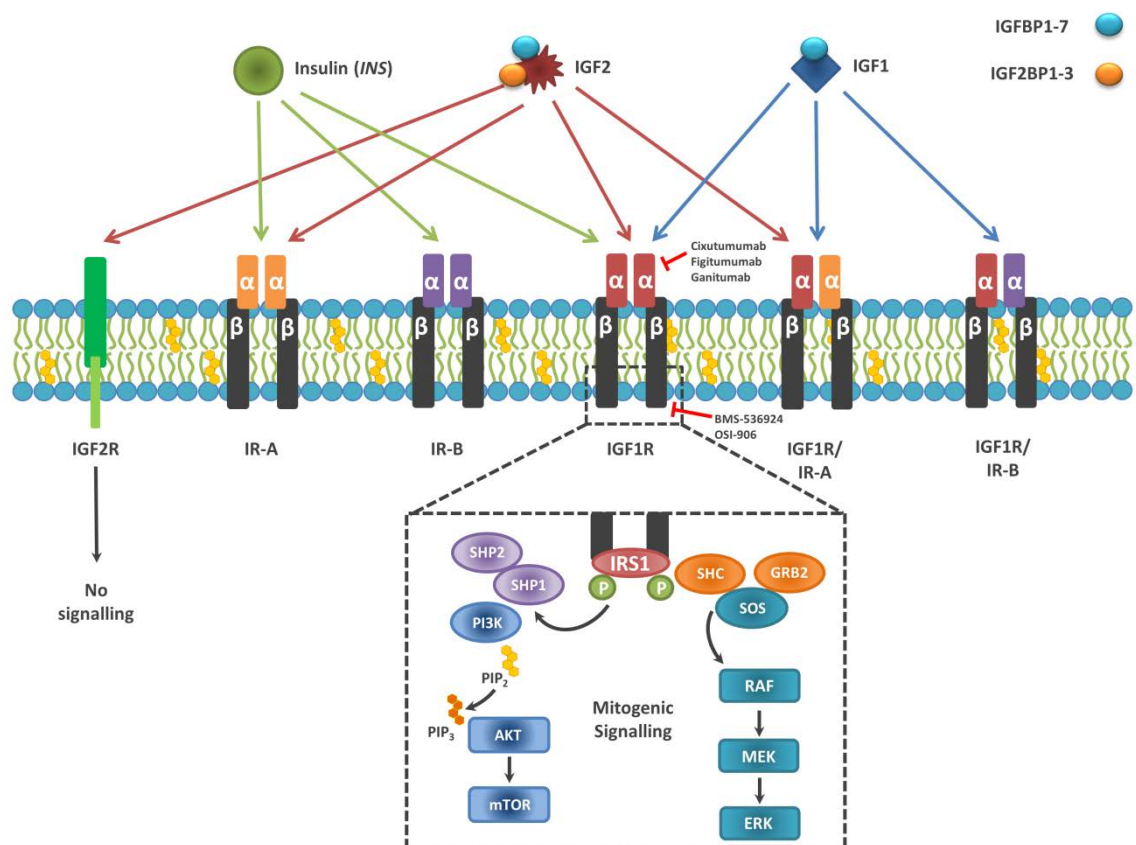


Figure 1.5 Insulin Signalling in HNSCC. An overview of the insulin signalling pathway, depicting the interaction of IGF-binding proteins with IGF ligands, IGF ligand-receptor binding and targeted therapeutics of IGF1R which have been trialed in HNSCC.

1.5.2 Clinical Trials

Despite promising pre-clinical results, IGF1R inhibitors and monoclonal antibodies have lacked efficacy in human trials. One such monoclonal therapy, figitumumab, provided no benefit to patients with palliative HNSCC in a phase II clinical study[138]. Another phase II trial assessing cixutumumab (IMC-A12) in combination with cetuximab is ongoing in HNSCC patients (ClinicalTrials.gov identifier: NCT00957853), however the same regimen held no benefit for colorectal cancer patients[139]. In fact, lack of efficiency has led to early termination in some trials and one phase II study comparing cetuximab with/without the dual IGF1R/IR inhibitor OSI-906 (ClinicalTrials.gov identifier:NCT01427205) was withdrawn prior to enrolment.

A possible reason for the failure of IGF1R inhibition is the compensatory action of homologous receptors, such as IR or hybrid receptors. High IR to IGF1R ratios have been associated with IGF1R inhibitor resistance[140, 141]. Indeed, the stimulation of IR can maintain cellular proliferation in the absence of IGF1R[142]. Furthermore, downregulation of IR in LCC6 cells was shown to reduce the growth rate of xenografts in athymic mice independently of IGF1R[143]. Dual blockade of IGF1R and IR tyrosine kinase activity is a feasible therapeutic option[144] and has been shown to synergise with approved cytotoxic agents as well as targeted Src-kinase inhibition and hormonal modulation[145-147].

Crosstalk with other growth factor receptors can also contribute to treatment failure. Upregulation of EGFR is associated with resistance to IGF1R inhibition *in vitro* and vice versa[148, 149]. Barnes *et al.* showed that stimulation with either IGF or EGF resulted in heterodimerisation of both IGF1R and EGFR and that simultaneous blockade of the receptors lead to a greater reduction in cellular proliferation and migration than single receptor inhibition[150]. In support of this resistance mechanism, EGF-EGFR binding was shown to directly phosphorylate IRS and activate AKT and MAPK pathways, independently of IGF1R[151]. However, other studies have found that dual inhibition of IGF1R and EGFR provided no added benefit[152].

Combination with other forms of therapy has also yielded positive results. Concurrent administration of ganitumab (AMG-479) and panitumumab with radiation resulted in significantly higher rates of success than the use of either given alone with radiotherapy[153].

1.5.3 IGF binding proteins

IGF2BP2 belongs to a conserved family of three mRNA-binding proteins, IGF2BP1, IGF2BP2 and IGF2BP3 (also known as IMP1, IMP2 and IMP3), which bind multiple gene transcripts with unique and overlapping functions[154]. Expression of the gene family is predominantly embryonic, but is often upregulated in aggressive cancer[155]. IGF2BP2 is the most divergent family member with moderate to high expression in a wide range of adult tissues, including the testis, colon and kidneys[156].

Alternative translational initiation gives rise to two isoforms of IGF2BP2 with molecular weights of 62 and 66kDa[157]. IGF2BPs contain four C-terminal K-homology (KH) domains which bind RNA transcripts[158] and two N-terminal RNA recognition motifs (RRMs) which stabilise the interaction[159]. The process involves the formation of large, granular complexes called ribonucleoprotein (RNPs) which facilitate the transport of transcripts to their target destination, while maintaining the integrity of mRNA molecules[160].

1.5.4 Regulation of IGF2BP2

While a comprehensive network of IGF2BP2 interactions has yet to be completed, recent studies suggest an important role for high-mobility-group A2 (HMGA2). HMGA2 is a transcription factor which exhibits a very similar expression pattern to IGF2BP2 and is correlated with decreased overall survival in HNSCC[161]. Embryonic HMGA2 has been shown to regulate the level of *IGF2BP2* mRNA in the cell, and promote its transcription in cooperation with NFKB1[162, 163]. Furthermore, *IGF2BP2* is significantly downregulated in HMGA2 knockout mice, which exhibit impaired skeletal muscle development and reduced myoblast proliferation. Rescuing of this phenotype was partially achieved by overexpressing IGF2BP2 in knockout myocytes[164]. The study also found that knockdown of IGF2BP2 led to reduced protein expression of c-MYC

and IGF1R but did not alter mRNA expression of these genes. This suggests that IGF2BP2 alters the rate at which mRNAs are translated without affecting overall mRNA levels.

In the last decade, microRNAs (miRNAs) have garnered increasing interest in cancer research stemming from their role as regulators of gene expression[165]. Luciferase gene reporting revealed that miR-1193 directly targets the 3'UTR of IGF2BP2 and reduces its expression in breast cancer. miR-1193 mediated suppression of IGF2BP2 led to deactivation of the PI3K and ERK signalling pathways and a significant diminution of proliferative and invasive capacity[166].

A recent global miRNA profiling analysis of 51 locally advanced HNSCC tumour samples reported consistent downregulation of Let-7 miRNA family members, Let-7a and Let-7c[167]. In line with this, Let-7 miRNAs have been shown to negatively regulate the expression of *IGF2BP2*, *HMGA2*, *CCND1* and *IGF1R*[168]. The study also showed that the RNA binding protein, Lin28bc can inhibit Let-7, thus upregulating the expression of its target genes, including *IGF2BP2*. Importantly, the expression of Lin28b, IGF2BP2 and IGF2 are significantly correlated with high rates of disease relapse[168].

The same Lin28b/Let-7 axis was later shown to drive oncogenic *SOX2* expression in HNSCC, where it reprograms cells to a stem-like state[169, 170]. Stem cells are capable of initiating and sustaining tumour growth, thus they represent a valuable therapeutic target in HNSCC[171]. This supports previous findings that Let-7 negatively regulates expression of stemness genes[172]. Interestingly, stemness is maintained in Let-7 expressing primary GBM cultures in the absence of Lin28b, suggesting other mechanisms must exist to preserve tumour cell stemness[173]. IGF2BP2 has been shown to protect Let-7 target transcripts (including *HMGA2*) from gene silencing. Loss of tumour-initiating capacity incurred by IGF2BP2 depletion was restored by overexpressing *Lin28b*[173, 174]. Disruption of this reciprocal relationship between Let-7 miRNA and IGF2BP2 could be important in the promotion of HNSCC tumour progression.

1.5.5 Target Transcripts of IGF2BP2

At present, little has been confirmed about the role of IGF2BP2 in cancer, but there is mounting evidence that it facilitates oncogene expression[175-177]. As one of 422 predicted RNA-binding proteins in mammalian cells, IGF2BP2 could potentially regulate the translation of numerous gene transcripts with wide ranging cellular functions[178]. The range of roles carried out by an RNA-binding protein is include pre-mRNA splicing, post-transcriptional modification, and regulation of translation. The key question is what its target transcripts within a cell are, and following on from this, does IGF2BP2 bind different targets in different cancer types?

Janiszewska *et al.* employed a RIP-CHIP microarray in glioblastoma spheroid cultures and found approximately 400 transcripts that were bound to the IGF2BP2-RNP complex with a significant overrepresentation of genes involved in mitochondrial metabolism[179]. A number of IGF2BP2 binding partners have also been identified in mouse myoblasts, including *MYC*, *SP1*, *IGF1R*, *CCNG1*, *NOTCH2*, *CDK6*, *AKT3*, *MDM2*, *KI67*, *ARF1*, and *MAPK1*[164]. Surprisingly, no strong IGF2BP2-*IGF2* binding was observed in these cells. A similar study in colorectal cancer revealed IGF2BP2 binding of *MAPK1*, *EFF2F*, *RAF1*, *SP1*, *CCNB1*, *CCNA2*, *NUCKS1* and importantly, *IGF2*. However, *IGF2* was the least enriched of the aforementioned gene transcripts[175].

IGF2BP2 binds to and stabilises *IGF2* mRNA within the cell, positively regulating its translation[180]. Like IGF1, IGF2 is a major growth factor involved in development as evidenced by growth retardation in mice lacking it[181]. Mature IGF2 is a 7.5 kDa peptide growth factor produced mainly in the liver, but it can be secreted by most tissues where it acts in an autocrine or paracrine manner[182]. Like IGF2BP2, it is highly expressed in the embryonic tissue where it promotes foetal growth, and its expression declines rapidly after birth[183]. While IGF2 is a major growth factor in the prenatal state, IGF1 takes over during post-natal development and remains until puberty[184].

The growth factor is able to exert its effects through binding and activating either the IGF1 receptor (IGF1R), insulin receptor A (IR-A) or heterodimeric

IGF1R/IR-A[185-187]. IGF2R specifically binds IGF2, but lacks an intracellular tyrosine kinase domain required for signalling. IGF2R is responsible for regulating IGF2 levels in the extracellular matrix, thus acting as a negative regulator of its mitogenic activity[188, 189]. Circulating levels of IGF2 are regulated by interactions with secreted IGFbps, which stabilise the growth factor and limit its bioavailability for other receptors as unbound IGF2 has a half-life of only a few minutes[190, 191]. The majority of circulating IGF2 is bound to IGFBP3 and a glycoprotein called acid-labile subunit (ALS), and to a smaller extent, IGFBP5[192, 193]. IGFbps and IGF2bps interact widely with IGF-independent ligands and thus are capable of both promoting and suppressing tumour progression[194].

1.5.6 IGF2BP2 in cancer

While re-expression of IGF2BP1 and IGF2BP3 has been observed in a number of aggressive malignancies[195-197], studies on IGF2BP2 have mainly focused on its putative role in type II diabetes[198, 199] and an unrelated role in the regulation of smooth muscle cell adhesion and motility[200]. Since the original discovery that the p62 splice variant of IGF2BP2 elicits an auto-antibody response in hepatocellular carcinoma (HCC)[201], other immune responses have been documented in oesophageal adenocarcinoma (ESCC) and breast cancer[202, 203]. Elevated expression of IGF2BP2 has also been correlated with higher rates of metastasis and shorter survival in oesophageal adenocarcinoma[176]. In addition, IGF2BP2 was recently shown to promote colorectal cancer cell proliferation by protecting *RAF1* mRNA from miR-195 mediated degradation[175]. *RAF1* is an essential component of the mitogen-activated protein kinase (MAPK) pathway, where it phosphorylates and activates the mitogen-activated protein kinase (MEK)-1/2, which in turn phosphorylate and activate extracellular-related kinase (ERK)-1/2[204, 205].

The gene is frequently overexpressed in glioblastoma multiforme (GBM)[206, 207] where it has been shown to control oxidative phosphorylation in stem cells through stabilisation of gene transcripts involved in the mitochondrial respiratory chain[179]. Further evidence suggests that IGF2BP2 modulates GBM progression through an IGF2-IGF1R-PI3K axis[177]. Interestingly, IGF2BP2 also

inhibits translation of the mitochondrial transport protein, uncoupling protein-1 (UCP1), in breast cancer[208]. This preferential interaction of IGF2BP2 with mRNA components of mitochondrial complex could provide the metabolic link between its involvements in cancer, obesity and type-II diabetes[209].

Enhanced invasion is a key hallmark of cancer, and is often a precursor to full-blown metastasis. Epithelial to mesenchymal transition (EMT) describes a process in which an adherent epithelial cell acquires a more motile phenotype and is underwritten by a series of molecular alterations[210]. The loss of E-cadherin (encoded by *CDH1*) is one such alteration and is driven by transcriptional repressors such as Snail (*SNAI1*) and Slug (*SNAI2*)[211, 212].

IGF2BP2 is implicated in the EMT process in breast cancer[213] and its overexpression has been shown to enhance the invasive phenotype of GBM through modulation of EMT components[177]. Moreover, knockdown of IGF2BP2 led to a reduced ability of cells to migrate and invade. A key upstream regulator of IGF2BP2, HMGA2, was recently shown to be essential for TGF β -mediated EMT in breast cancer where it localises at the invasive front of tumour cells and regulates Snail expression[214, 215]. In addition, overexpression of HMGA2 has been strongly correlated with HNSCC progression and survival where it upregulates Snail and promotes EMT[216].

1.5.7 Summary

It is clear that IGF2BP2 is not merely a passive reservoir of IGFs, but exerts control over a multitude of genes with wide-reaching consequences throughout the cell. Expression analyses have revealed elevated expression of *IGF2BP2* in tumour compared to normal tissue and a carcinogenic role has already been established in certain cancer types. Through its regulation of IGF2 and subsequent activation of downstream oncogenic signalling nodes, IGF2BP2 has been shown to promote cell growth and survival in addition to maintaining metabolic integrity. However, a role in head and neck cancer has yet to be assessed. Herein, the process of IGF2BP2 identification from a comprehensive analysis of patient data combined with genomic screening, and validation of its phenologic influence in a series of patient-derived HNSCC cell lines is described.

1.6 The Significance of Hypoxia

One of the primary aims of this thesis was to identify genes that were selectively essential in hypoxia. To this end, a whole genome siRNA screen was carried out to determine genes, which are selectively essential in hypoxia. These genes represented ~10% of the total 18,075 genes knocked down. However, a more manageable number of hits were needed to follow up so the results of the siRNA screen were combined with pathway analysis to determine if these genes had common functions in the cell. The top hit returned a subset of genes involved in the metabolism of fatty acids and cholesterol biosynthesis. The importance of hypoxia and lipid metabolism in HNSCC is discussed in the remainder of the introduction.

1.6.1 Clinical Definition

Hypoxia results from the tumour mass growing faster than the vascular supply, leading to regions with a decreased supply of nutrients and oxygen[217, 218]. Hypoxia is a defining feature of solid tumours, including head and neck cancers[219, 220]. There is a strong correlation between tumour volume and the degree of hypoxia in HNSCC tumours and hypoxic tumour volume is an independent prognostic factor for survival in patients [221]. Approximately two thirds of TCGA primary HNSCC tumours are stage 3 or 4, which suggests that at least this many tumour samples are hypoxic to some degree[54].

Well-oxygenated peripheral tissue generally has an oxygen tension of approximately 40 mmHg (5% O₂)[222]. Tumours are considered to be hypoxic when the oxygen tension within the tumour falls below that of the surrounding tissue and is generally accepted to be ≤ 8 mmHg (1% O₂), however a cellular response to hypoxia can be activated anywhere below 5% O₂, and the exact value will vary between different tumours[223]. The diffusion limit of oxygen falls between 70-200 μ m from the nearest blood vessel[223]. This diffusion limit also applies to anti-cancer drugs, which often fail to penetrate the tumour mass and reach internal cells at a lethal concentration (**Figure 1.6**). In addition, hypoxia brings about a slowing of cell growth, which renders a number of conventional chemotherapies ineffective[224].

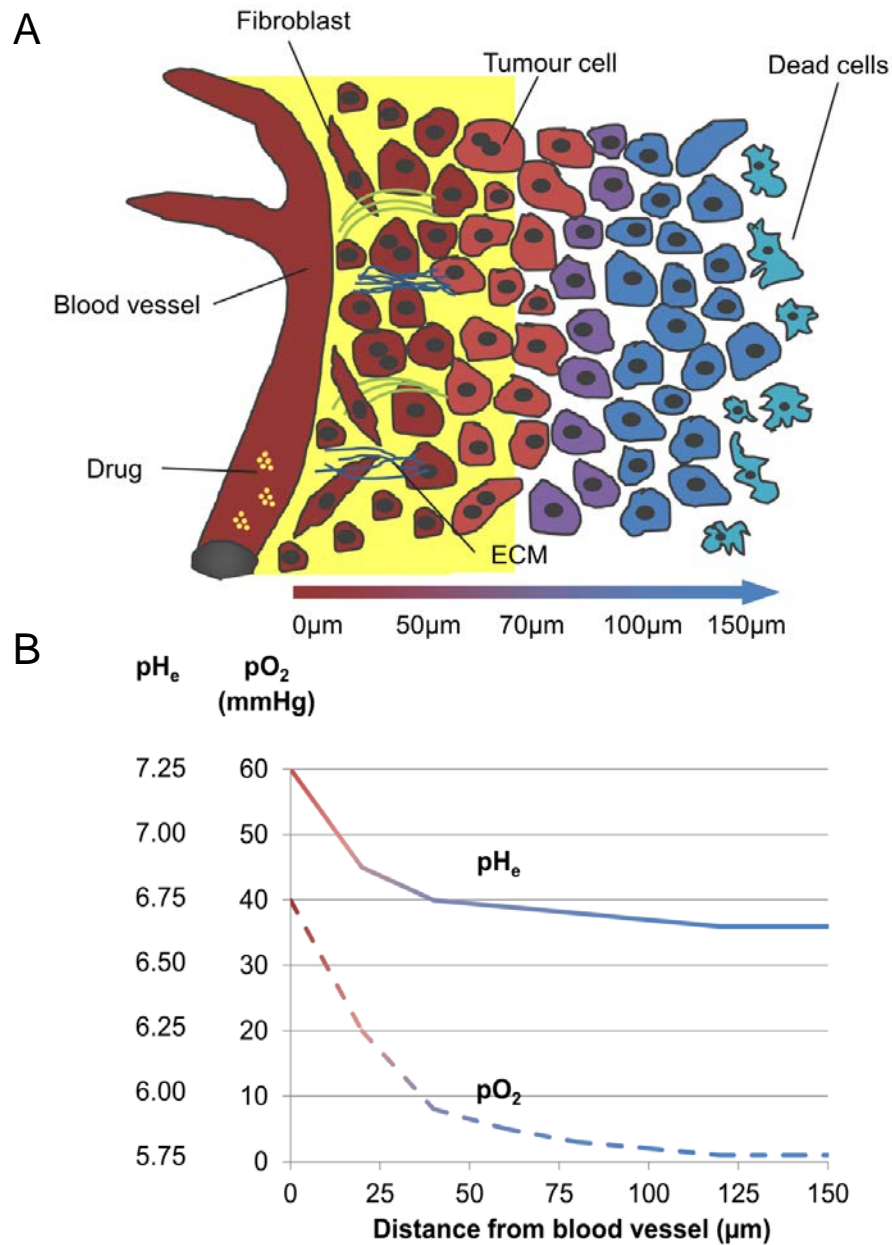


Figure 1.6 Oxygen diffusion gradient in a solid tumour. (A) Diagram shows tumour cells in relation to the nearest blood vessel and the extracellular matrix (ECM). Anti-cancer drugs fail to reach isolated tumour cells furthest from blood supply. (B) The partial oxygen pressure (pO_2) drops from 40 mmHg in peripheral tissue to less than 5 mmHg in tumours and is accompanied by a drop in physiological pH, creating a more acidic environment.

1.6.2 Transcriptional Regulation by HIF-1A

Hypoxia exerts a strong selective pressure on tumour cells, promoting genomic instability and increasing rates of mutation[225]. This in turn drives a more aggressive phenotype with enhanced proliferative, invasive and metastatic potential[226]. Hypoxia-responsive genes are estimated to make up about 1.5% of the human genome and effect wide-ranging adaptive changes to aid cells in their survival of a low oxygen environment[227]. Genetic changes occur predominantly, but not exclusively through hypoxia inducible factor-1 α (HIF-1 α)[228].

HIF-1 α is the master regulator of hypoxia. It exists as a dimer with HIF-1 β (not induced by hypoxia) and acts as a transcription factor, which binds to hypoxia response elements (HREs) in the promoter region of target genes. At normal oxygen tension, HIF-1 α is kept under a constant state of hydroxylation and is marked for destruction by the von Hippel-Lindau protein (VHL)[229, 230]. This hydroxylation cannot occur in low oxygen, leading to stabilisation of HIF-1 α and increased transcription of genes containing a HRE (Figure 1.7)[46].

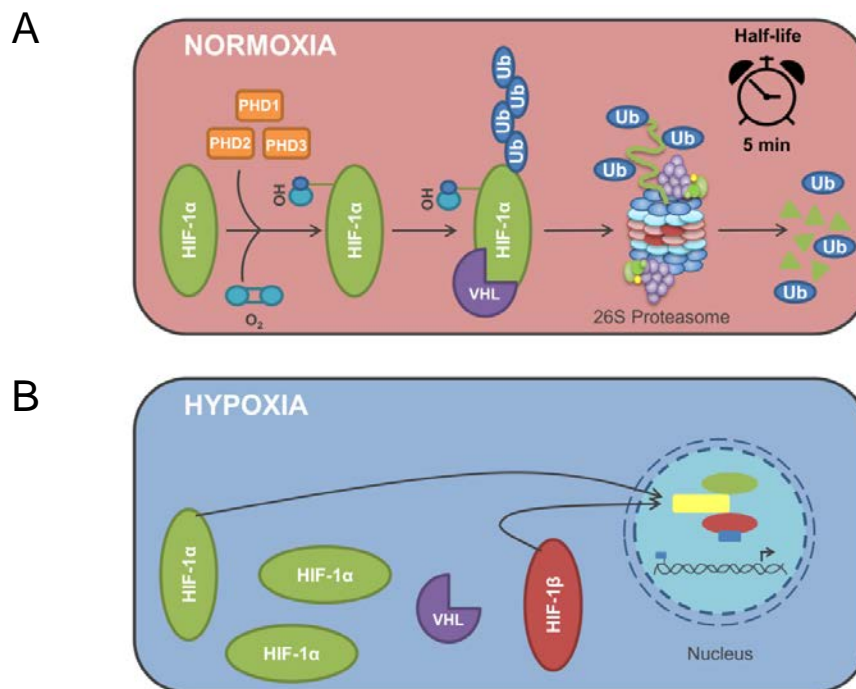


Figure 1.7 The fate of HIF-1 α in the cell. (A) HIF-1 α is rapidly degraded in normoxic conditions via hydroxylation by prolyl hydroxylase-domain enzymes (PHDs), recruitment of VHL and subsequent ubiquitination/proteasomal degradation. (B) In hypoxia, HIF-1A binds hypoxia-response elements within target genes, and activates their transcription.

In addition, the activation of HNSCC oncogenes such as *PIK3CA*, and loss of tumour suppressors such as *PTEN*, can compensate for the degradation of HIF-1 α in oxygenated environments by increasing its translation[231]. This highlights the tumour cell's dependence on HIF-1 α to maintain an aggressive phenotype under conditions of stress. To date, no HIF-1 α inhibitors have been approved for use in cancer due to their lack of efficacy or low tolerability. The tumour microenvironment produces discrepancies between *in vitro* and *in vivo* efficacy studies, often resulting in clinical failure. In addition to the challenge of delivery, no robust hypoxic marker exists for the preselection of patients with high HIF-1 α activity[232].

The significance of low oxygen has been well documented within a metabolic context where it exerts great physiological stress on tumour cells, requiring adaptation in order to best utilise the limited oxygen available[233, 234]. One of the outcomes of this is an increased reliance on glycolysis as the primary means of ATP production rather than (the more efficient) oxidative phosphorylation. Interestingly, this preference is also observed in areas of tumours which are not oxygen limited, in a process termed "aerobic glycolysis"[235]. This has led to the conclusion that the glycolytic phenotype confers a survival advantage to tumour cells, despite the lower output of ATP and the acidification of the surrounding extracellular matrix (ECM)[236].

The evolutionary drive to survive in these low oxygen/ATP/pH conditions occurs in the early stages of tumour formation, when the tumour epithelial boundary expands beyond the oxygen diffusion limit (>70-200 μ m) [236, 237]. The scarce resources drives the selection of cells favouring those less sensitive to growth restraints and therefore more capable of survival in low oxygen, acidic environments[238]. This is supported by the upregulation of H⁺ transporters in cancer cells[239], in addition to increased expression of high performance glucose transporters (e.g. GLUT1)[240]. Lactate production and the resulting acidification of the surrounding ECM have also been shown to enhance invasion and stimulate the activation of tumour-associated macrophages[241, 242].

To date, two major hypoxic gene signatures have been developed. Winters *et al.* developed a 99-gene set that was shown to be a significant prognostic factor for

recurrence-free survival in HNSCC patients[243]. Toustrup *et al.* developed a 15-gene hypoxic classifier set in HNSCC (Table 1.2), based on the gene expression profiles of cell lines exposed *in vitro* to different oxygen and pH levels, and followed up with *in vivo* xenograft studies[244, 245]. The list predominantly comprises genes involved in cell metabolism, stress response and apoptosis. *ALDOA*, which codes for a glycolytic enzyme and catalyses the conversion of fructose-1,6-bisphosphate to glyceraldehyde 3-phosphate and dihydroxyacetone phosphate, is frequently upregulated in oral SCC [246] but has not as yet been linked to patient outcome. Higher expression of *SLC2A1* (GLUT1) is consistently associated with a poor prognosis in patients with oral SCC [240, 247] while HNSCC cells treated with a GLUT1 inhibitor demonstrate enhanced chemosensitivity to cisplatin[248].

| Hypoxia Responsive Genes | | |
|--------------------------|---------|--------|
| ADM | C3orf28 | P4HA1 |
| ALDOA | EGLN3 | P4HA2 |
| ANKRD37 | KCTD11 | PDK1 |
| BNIP3 | LOX | PFKFB3 |
| BNIP3L | NDRG1 | SLC2A1 |

Table 1.2 Hypoxia gene classifier set. Gene set developed by Toustrup *et al.* [244].

1.6.3 Hypoxia and Clinical Failure

Tumour hypoxia is consistently correlated with poorer prognosis in HNSCC, and is a major determinant of resistance to chemo/radiotherapy[249]. A large multi-centre study of 397 patients with HNSCC found that overall survival was significantly impaired in tumours with pre-treatment oxygen tensions of less than 2.5 mmHg[250]. Concomitant chemo/radiotherapy is the cornerstone postoperative treatment for HNSCC patients, and despite improving the prognosis of patients with locally advanced disease[251], recurrence occurs in >50% of patients with stage 3/4 tumours, in which the median survival is <12 months[252]. In normoxic tissue, the high oxygen tension acts as a radiosensitising agent by prolonging the lifespan of the highly reactive hydroxyl radicals produced when tightly bound electrons are removed from water in the sheath surrounding DNA (radiolysis)[253]. These free radicals cause damage to DNA in the form of double strand breaks (DSBs), single strand breaks (SSBs), DNA

base damage and DNA-DNA/DNA-protein crosslinking[254]. In hypoxic tissue, fewer hydroxyl radicals are produced, thus decreasing the frequency of DNA damaging events.

Rapidly dividing tumour cells are more vulnerable to DNA damage than normal cells with their lower turnover. Radioresistance arises when oxygen tension drops to ≤ 5 mmHg in HNSCC tumours[253], although less severe oxygen levels are sufficient to cause a multitude of gene expression changes[255, 256]. It has been demonstrated in head and neck cancer that hypoxic radioresistance can be counteracted by hypoxia modifying approaches, such as treating with nitroimidazoles (which mimic oxygen during irradiation) [257] or by increasing oxygen delivery to the affected area, potentially via the ARCON (accelerated fractionated radiotherapy with carbogen and nicotinamide) strategy[258]. The high cytotoxicity of the drugs has hampered their implementation at a clinically relevant dose[259], but there has been a small, but significant improvement in locoregional control over radiotherapy alone[260].

Cells in hypoxic conditions can exhibit resistance to drugs, primarily owing to their distance from blood vessels, which can decrease the effective concentration to which they are exposed [261], depending on the structure and metabolic stability of the drug. In addition, some drugs require oxygen in order to be maximally cytotoxic (e.g. bleomycin)[262]. A study by Yoshihara *et al.* showed that hypoxia was able to induce resistance to 5-fluorouracil in oral cancer cells by inducing cell cycle arrest at the G1/S transition phase[263]. Similarly, knockdown of GLUT1 in a panel of oral cancer cell lines sensitised hypoxic cells to cisplatin-mediated apoptosis[264]. Cells in a hypoxic environment exhibit a slower cell cycle progression, which enhances their resistance to anticancer drugs[265]. Furthermore, the selection pressure exerted by hypoxia favours cells expressing mutant p53, as p53-dependent apoptosis will eliminate susceptible cells with wild-type p53[225], thus decreasing sensitivity to treatment. In this way, hypoxia can also compromise surgical outcome and increasing rates of relapse[266].

1.6.4 Summary

Hypoxia is one of the defining characteristics of head and neck squamous cell carcinoma, and one of the major causes of the chemo/radioresistance and the resulting poor prognosis. Identifying pathways involved in the hypoxic response (HIF-1 α dependent or not) and how they influence the behaviour of tumour cells and the surrounding extracellular matrix, is essential if the efficacy of therapies are to be improved. To some extent, hypoxia underpins every hallmark of cancer by promoting genomic instability. This, in turn, drives the selection of cells with an aggressive phenotype that are highly adapted to their harsh environment. The role of hypoxia in HNSCC has been extensively studied and this has shown that it carries a consistently negative prognosis. This is compounded by the lack of a robust biomarker in the clinic, which will impede the implementation of targeted therapies. To this end, hypoxic gene signatures have been developed that can successfully predict treatment outcome. However, this approach is limited by highly heterogeneous tumours such as HNSCCs. This study seeks to identify genes that are not only highly expressed in hypoxia, but are also essential for cell survival under these conditions.

1.7 Lipid Metabolism

Hypoxia creates an environment in which a tumour cell must adapt in order to survive. Immediate changes occur in cellular metabolism in order to compensate for the loss of ATP resulting from decreased oxidative phosphorylation[267]. To date, most metabolism studies in cancer have focused on changes in glucose and glutamine; however, the roles of lipids in tumour progression are increasingly recognised. Implementation of an unbiased genomic screen has identified a subset of genes involved in triglyceride metabolism, with potential importance in HNSCC progression. In addition, the role of a class of lipids known as ether lipids (plasmalogens), which are present at higher levels in tumours than normal tissue[268], is investigated in a panel of oral SCC cell lines.

1.7.1 Fatty Acid Metabolism

A number of metabolic changes occur in cells undergoing malignant transformation, including a switch to a glycolytic energy profile, heightened glutaminolysis and an increase in *de novo* fatty synthesis[269-271]. Reprogramming of lipid metabolism is increasingly recognised as a hallmark of cancer and involves the fine-tuning of synthesis, storage and degradation of triglycerides (TGs), phospholipids (PLs), cholesterol (CLs) and cholesterol esters (CEs)[272]. **Figure 1.8** provides a graphical overview of the key events in lipid metabolism. Free fatty acids (FAs) are the essential building blocks for the synthesis of membrane lipids and lipid second messengers such as phosphatidylinositol-3,4,5-trisphosphate (PIP₃), as well as acting as substrates for energy production[273]. FAs can come from exogenous sources in the diet or can be synthesised *de novo* in the cytoplasm.

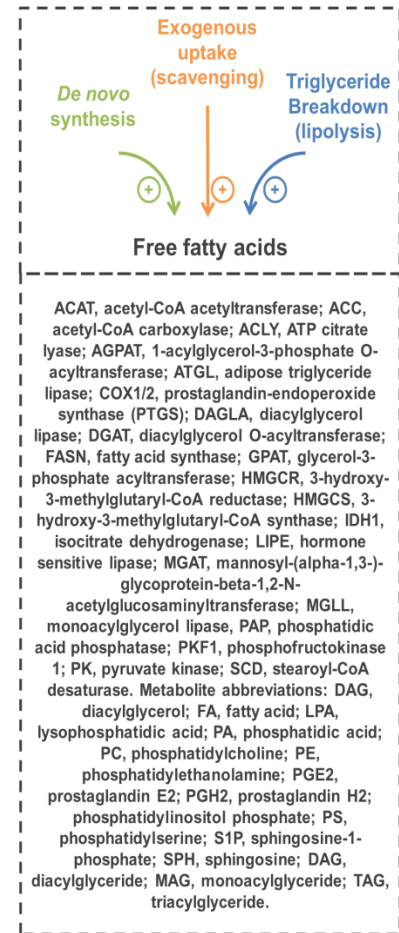
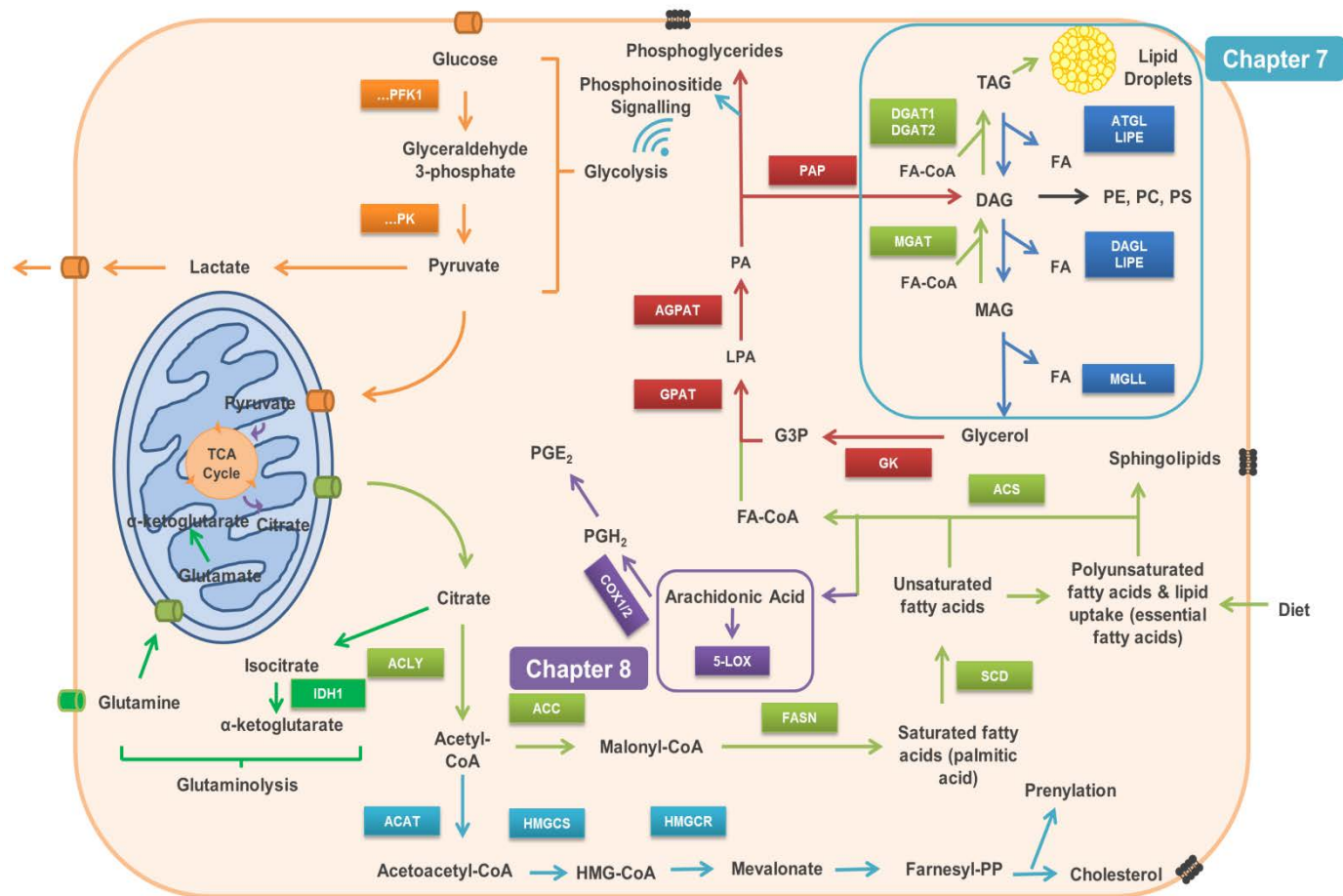


Figure 1.8 Overview of lipid metabolism.

1.7.2 Fatty Acid Synthesis

Sterol regulatory element-binding proteins (SREBPs) are transcription factors which act as master regulators of lipid metabolism by controlling the synthesis of FAs, TGs and CLs[274]. Three isoforms exist in mammalian cells (SREBP-1a, -1c and -2), with distinct but overlapping roles, and encoded by *SREBP-1a/1c* and *SREBP2*, respectively[275]. Fatty acids are primarily synthesized from tricarboxylic acid (TCA) cycle-derived citrate, which is converted to oxaloacetate and acetyl-CoA by ATP citrate lyase (ACLY). Acetyl-CoA is then carboxylated to malonyl-CoA by acetyl-CoA carboxylase (ACC) and condensed to palmitate by fatty acid synthase (FASN). This basic, 16-carbon FA can be elongated and desaturated to various degrees, generating a wide range of FAs with different functionalities[276]. In order to become biologically active, a FA must gain one molecule of coenzyme A in a two-step reaction catalysed by acyl-CoA synthetase (ACS). In this form, FAs can be further modified to triglycerides through esterification with glycerol and stored in lipid droplets for future use. There are currently 26 genes encoding ACS enzymes, which are categorised according to the length of the acyl chain they generate[277].

At this stage, fatty acid chains are completely saturated and must gain at least one double bond in order to perform their complete range of functions. The insertion of a cis double bond at the delta-9 position of short chain fatty acids (C-16, C-18) is catalysed by stearoyl-CoA desaturase (SCD) and significantly alters the physical properties of FAs[278]. There are two SCD isoforms in mammalian cells - SCD1 and SCD5. The former is the most extensively studied and its overexpression has been implicated in a number of human cancers[279]. Limiting the supply of fatty acids by blocking their synthesis or decreasing their release from storage could prove to be an effective strategy for slowing tumour cell proliferation. Inhibition of enzymes required for the synthesis of fatty acids should theoretically limit tumour cell growth while having a negligible effect on normal cells.

Indeed, knockdown or inhibition of ACLY in cancer cell lines has been shown to limit *in vitro* proliferation and survival as well as *in vivo* xenograft growth[280, 281]. Similarly, ACC1 knockdown induced apoptosis in prostate and breast cancer, but not in non-malignant control cells[282, 283]. However, knockdown

of either of the two ACC isoforms, ACC1 and ACC2, was shown to accelerate proliferation in lung cancer cells by maintaining NADPH generation in the absence of AMP-activated protein kinase (AMPK)[284]. Increased FASN expression has been reported in HNSCC[285, 286] and its expression is linked with tumour metastasis and recurrence[287]. Likewise, high levels of phosphorylated ACC is correlated with decreased overall survival in HNSCC patients[288]. FASN has been the focus of a number of drug discovery efforts leading to the generation of specific inhibitors (e.g. C75) which has been shown to have an effect on cancer cell proliferation and viability[289-291]. In HNSCC, inhibition of FASN sensitises cells to radiotherapy[292]. However, their development has been plagued by poor pharmacokinetics and off-target toxicities[293, 294].

SCD1 inhibition or knockdown has been shown to induce apoptosis in malignant cell lines of the lung and hypopharynx when cultured in reduced serum in a response attributed to the ER stress pathway[295]. A similar study found that SCD1 inhibition caused apoptosis in colorectal cancer cells via stimulation of the ceramide synthesis pathway[296]. Endogenous levels of ceramide (a sphingosine attached to a fatty acid chain) are increased under stresses such as hypoxia or radio/chemotherapy[297, 298]. Ceramide expression is consistently lower in HNSCCs compared to normal or pre-malignant keratinocytes and is inversely correlated with rates of nodal metastasis[299, 300]. Moreover, treatment with ceramide enhanced the cell killing effect of paclitaxel and knockdown of ceramide synthase led to apoptotic resistance in HNSCC cells[301, 302].

1.7.3 Dynamic Lipid Storage

De novo lipogenesis is essential for the dynamic remodelling of lipid membranes required for rapidly proliferating cells. Cancer cells, with their rapid proliferation rates are heavily dependent on *de novo* synthesis, favouring this method over extracellular scavenging of fatty acids[303]. However, cancer cells retain their dynamism through a complementary lipolytic pathway that can liberate free fatty acids from neutral and phospholipid stores (lipid droplets) when needed for lipid-mediated intracellular signalling[49]. Elevated numbers of lipid droplets are commonly observed in tumour cells and have been correlated to the malignant potential of cancers[304-307]. The stepwise synthesis of triglycerides is catalysed by monoacylglycerol and diacylglycerol acyltransferases

(MGATs and DGATs) of which a number of isoforms exist depending on cellular context[308, 309]. An alternative pathway, the glycerol-3-phosphate pathway (G-3-P), exists, but both pathways converge on the final step to generate TGs[310].

The breakdown of TGs is mediated by an antagonistically acting set of enzymes, including hormone-sensitive lipase (LIPE), adipose triglyceride lipase (ATGL)[311] and monoacylglycerol lipase (MGLL), which governs the final step in the lipolytic cascade resulting in the generation of FAs and glycerol. The enzyme has been shown to be tumourigenic in ovarian, breast and melanoma by liberating FAs to serve as building blocks for lipid signalling molecules such as lysophosphatidic acid (LPA) and prostaglandins (e.g. PGE₂), which effect a diverse lipid signalling network thus stimulating survival, migration and invasion[312]. The authors of this study also showed that inhibition of MGLL simultaneously stimulates anti-tumourigenic cannabinoid pathways and depresses pro-tumourigenic lipid signalling in aggressive prostate cancer[313].

Other studies have shown the blockade of MGLL inhibits the proliferation of colorectal cancer cells *in vitro*[314, 315] and attenuate the growth of colorectal and hepatocellular carcinoma xenografts *in vivo*[316, 317]. Furthermore, MGLL is able to promote a more invasive phenotype in nasopharyngeal carcinoma through positive regulation of EMT proteins[318]. Conversely, a tumour suppressive role for MGLL was reported in colorectal cancer, where it negatively regulates PI3K/AKT signalling[319], which serves to highlight the complexity of the signalling networks involved. While current evidence strongly favours an oncogenic role, it is possible that MGLL has dual roles in cell growth regulation depending on cellular context. Clearly, more work is needed to affirm its role in cancer progression.

1.7.4 The Role of Hypoxia in Lipid Metabolism

Fluctuations in oxygen levels may drive the selection of cells that are able to switch between anabolic and catabolic processes[320, 321]. Hypoxia increases fatty acid synthesis and FASN expression through the activation of AKT and SREBP1. FASN protein was recently shown to localise to hypoxic regions in breast cancer xenografts[322]. Increasingly, evidence suggests that aggressive tumours

are highly reliant on acetate as a carbon source in the generation of lipids. A recent study showed that a short chain variant of ACS, cytoplasmic acetyl-CoA synthetase (ACSS2), becomes essential under metabolically limiting conditions such as hypoxia.

In the absence of oxygen, entry of pyruvate into the TCA cycle is inhibited and acetyl-CoA must be generated from other sources. An alternative source is the condensation of acetate by ACSS2, which is stimulated in hypoxia-induced metabolic stress[323, 324]. Furthermore, its expression is positively correlated with tumour stage and patient survival and it was recently identified as a critical enzyme for the growth and survival of breast cancer cells screened in low oxygen and low serum[325]. A follow up study found that knockout of ACSS2 inhibited growth of breast cancer xenografts in mice[325]. Loss of ACSS2 was also shown to reduce tumour burden in a genetic mouse model of hepatocellular carcinoma[326]. Additional compensation of lipogenesis comes from increased uptake of exogenous lipids in hypoxia and the promotion of lipid droplet formation[327]. Lipids stored in droplets can also be deployed as an antioxidant buffer if there is a sudden increase in available oxygen[328].

Cancer cells thrive on an abundance of fatty acids, which they use for membrane building, energy storage and production of signalling molecules[329]. Various competing mechanisms exist to regulate the synthesis, storage and release of fatty acids from lipid storage droplets[330]. The correct functioning of this system revolves around the action of enzymes, which are vulnerable to hijacking by aberrant signalling processes in cancer. However, this dependence on enzymes to catalyse rate-limiting steps in lipid metabolism also leaves cancer cells vulnerable to targeted therapeutics, which selectively target highly proliferative cells. As ever, the vast heterogeneity of cancers may undermine this approach through differential expression of various isoforms, crosstalk with other signalling networks and other compensatory measures including the development of resistance. Successful application will require studying the specific metabolic dysregulations of any given tumour.

1.7.5 Lipid Rafts and Metastasis

Cell membranes consist of a variety of lipid structures, the proportions of which influence the fluidity of the membrane[331]. Lipid rafts are low-density membrane domains, which consist of tightly packed saturated fatty acids in the form of sphingolipids and cholesterol (Figure 1.9). Lipid rafts also act as platforms for signalling molecules and facilitate the transduction of cell death and/or survival signals throughout the cell[332]. These include the insulin and EGF receptors, which play a major role in HNSCC progression[333].

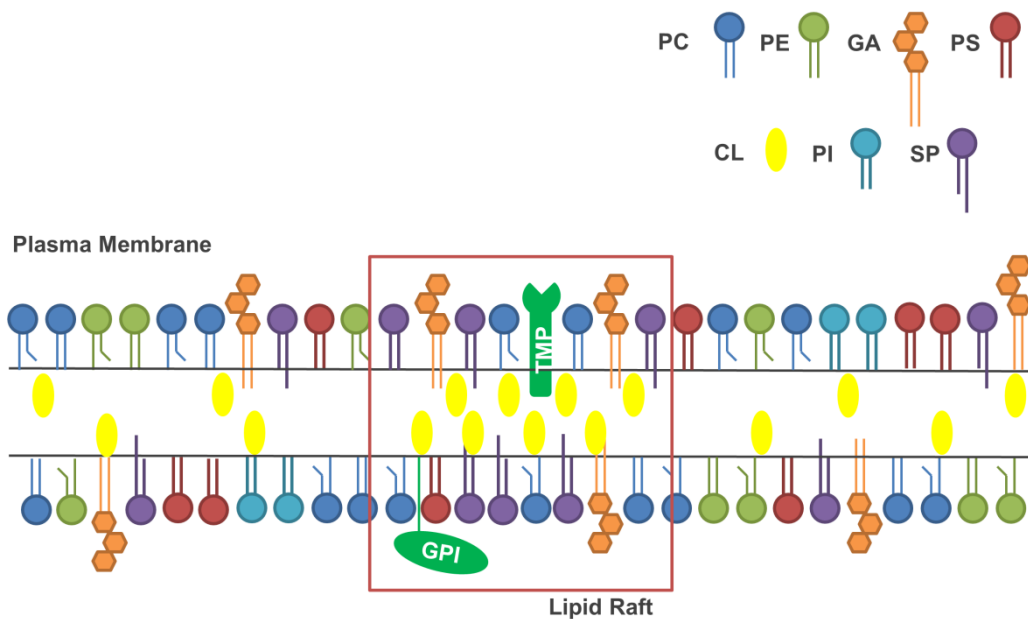


Figure 1.9 Structure of a lipid raft. Lipid rafts are membrane domains that are rich in certain lipid species such as sphingosine, cholesterol and gangliosides. Lipids within the structure are very tightly packed, leading to the formation of distinct “floating” rafts that can diffuse freely throughout the plasma membrane. Lipid rafts are dynamic structures, capable of rapid assembly and disassembly, and contain a number of transmembrane proteins (TMP) and glycosylphosphatidylinositols (GPI). PC, phosphatidylcholine; PE, phosphatidylethanolamine; GA, gangliosides; PS, phosphatidylserine; CL, cholesterol; PI, phosphatidylinositol; SP, sphingomyelin.

Dynamic reorganisation of lipid raft domains in cell membranes has been shown to influence the response of HNSCC cells to radiation treatment[334]. Radiation and other cellular insults such as cisplatin stimulate the reorganisation of these domains, and the recruitment of receptors such as FasR/CD95 or EGFR[335]. Moreover, elevated levels of cholesterol have been observed in oral SCC tumour compared to normal tissue[336], while elevated levels of sphingosine kinase 1 (*SPHK1*), which catalyses the phosphorylation of sphingosine, have been implicated in HNSCC invasion through positive regulation of EGFR and

STAT3[337]. The metabolism of the major sphingolipid component, ceramide, has been shown to play an important part in HNSCC pathogenesis[338]. The levels of C₁₈-ceramide were significantly decreased in advanced HNSCCs compared to normal tissue and correlated with increased nodal invasion and metastasis[300]. Ceramide is a potent inducer of apoptosis and has been shown to enhance the growth inhibition effect of paclitaxel in *in vitro* HNSCC assays[301, 339].

1.7.6 Summary

Lipids represent an important source of energy for the cell, and are an essential biosynthetic resource. The structural variation of fatty acids gives rise to a number of lipid species with different characteristics. The relative ratios of these lipids dictate membrane fluidity and function and can influence tumour cell migration and invasion[340]. *De novo* lipid synthesis is an essential process in tumour development and generates up to 95% of the lipids required by the rapidly dividing cells[341]. Neutral lipids such as triglycerides are stored in lipid droplets, which are vital for survival under energy stress and are frequently found in higher numbers in tumour cells[305]. Recently, it was shown that cancer stem cells have a higher ratio of unsaturated versus saturated fatty acids and that this ratio is essential for the maintenance of stemness[342]. Interfering with the lipogenic process was shown to impair stemness and tumour initiation capacity in ovarian cancer stem cells[343]. A complete picture of how metabolic alterations sustain an aggressive phenotype in HNSCC has yet to emerge, as research in this field is limited. However, an increased requirement for lipids is common to all cancer cells, including those of the head and neck. A better understanding of deregulated metabolic pathways could lead to novel therapeutics, which are so greatly needed in HNSCC.

1.8 Cysteinyl Leukotrienes and Inflammation

Inflammation is an important micro-environmental factor in the progression of cancer[344]. The innate immune response is responsible for the clearing of infection from affected areas, but it is also advantageous for the tumour to recruit inflammatory mediators. Tumour cells release chemical signals to lure macrophages and granulocytes to the site of tumour growth and stimulate them to release cytokines, which drive angiogenesis and aid in the restructuring of surrounding stroma[344]. A drug-repurposing screen (conducted as part of this project) identified a family of compounds involved in the regulation of inflammation, which significantly inhibited the growth of an aggressive, patient-derived oral cancer cell line.

The oral cavity is the first point of contact with exogenous carcinogens, such as alcohol, tobacco and betel quid. Prolonged exposure to these agents damages the mucosal lining and leads to the accumulation of mutations over a lifetime[345]. Cigarette smoke in particular has a significant effect on the innate immune system through the generation of reactive oxygen species, which activate pro-inflammatory signalling cascades in oral epithelial cells[346].

The NF- κ B transcription factor is the primary regulator of genes involved in the inflammatory response and is the central hub through which inflammatory agents act[347]. Inactive NF- κ B exists in a sequestered state in all mammalian cells; it is only upon translocation to the nucleus that it becomes an active inflammatory mediator. Constitutive activation of NF- κ B is detected in head and neck cancer cells and its expression is positively correlated with tumour stage[348, 349]. NF- κ B upregulates the expression of pro-inflammatory cytokines interleukin-8 (IL-8) and tumour necrosis factor- α (TNF α)[350]. The latter has been shown to regulate the activity of a group of lipid inflammation mediators called eicosanoids[351].

1.8.1 Eicosanoids

The eicosanoid (greek: eicosa, 20) family of lipophilic signalling molecules are important regulators of inflammation[352]. In response to stimulation, cysteinyl leukotrienes are rapidly generated from arachidonic acid (AA), a 20-carbon,

polyunsaturated fatty acid which is esterified to glycerol in cell membrane phospholipids[353]. AA is released directly into the cytosol through activation of calcium-dependent cytosolic phospholipase A2 (cPLA₂) which catalyses the hydrolysis of phospholipid molecules. Phospholipase C and D can also liberate AA indirectly by generating diacylglycerol and phosphatidic acid, (intermediate lipid products from which fatty acids can be released by the action of diacylglycerol and monoacylglycerol lipases)[354]. Free AA that does not diffuse into the extracellular matrix is metabolised within the cell via three major pathways[355], giving rise to lipid molecules with overlapping and distinct roles in inflammation (Figure 1.10). This project focuses specifically on the role of the lipoxygenase pathway in oral cancer.

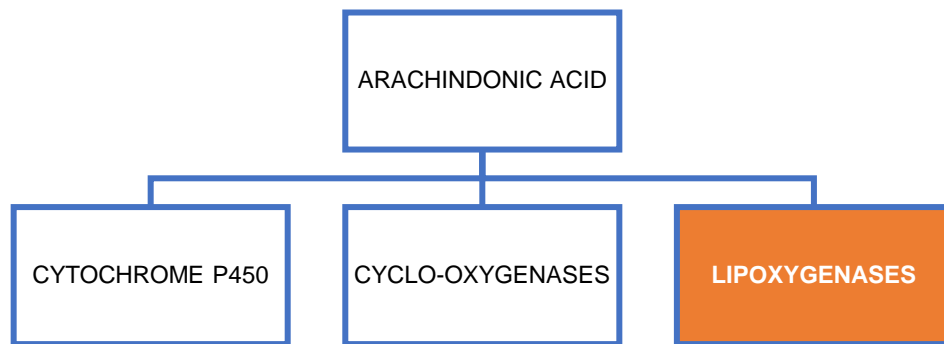


Figure 1.10 Pathways of arachidonic acid metabolism.

1.8.2 Lipoxygenases (LOX pathway)

Liberated AA can be converted to a group of lipid molecules known as leukotrienes, which play a pivotal role in the inflammatory response and feature predominantly in asthma[356]. The first step in the synthesis of leukotrienes is the translocation of cytosolic AA to the phospholipid membranes of the nucleus, endoplasmic reticulum and Golgi apparatus[357]. Here, 5-LOX activating protein (FLAP) presents AA to 5-lipoxygenase (5-LOX) which catalyses the sequential oxidation at the C-5 position to generate 5-hydroperoxyeicosatetraenoic acid (5-HPETE), and dehydration to form the unstable intermediate, leukotriene A₄ (LTRA₄)[358].

The pathway branches off at this point to produce either LTB₄, which acts as a chemotactic for neutrophils or the cysteinyl leukotrienes (CysLTs) - LTC₄, LTD₄

and LTE_4 [359, 360]. CysLTs get their name from the presence of a conserved cysteine residue and are the primary lipid mediators of inflammatory disease and are mainly produced by eosinophils, mast cells and macrophages[361]. Despite structural similarities, the CysLTs are functionally diverse. LTRA_4 is processed into the intermediate metabolite, 5-HETE, which is hydrolysed by LTRA_4 synthase to form LTB_4 . LTC_4 is generated through the enzymatic activity of LTC_4 synthase exported from cells where it is sequentially metabolised to LTD_4 and LTE_4 (Figure 1.11). Small molecule inhibitors, which target the 5-LOX pathway, have been approved for the treatment of asthma.

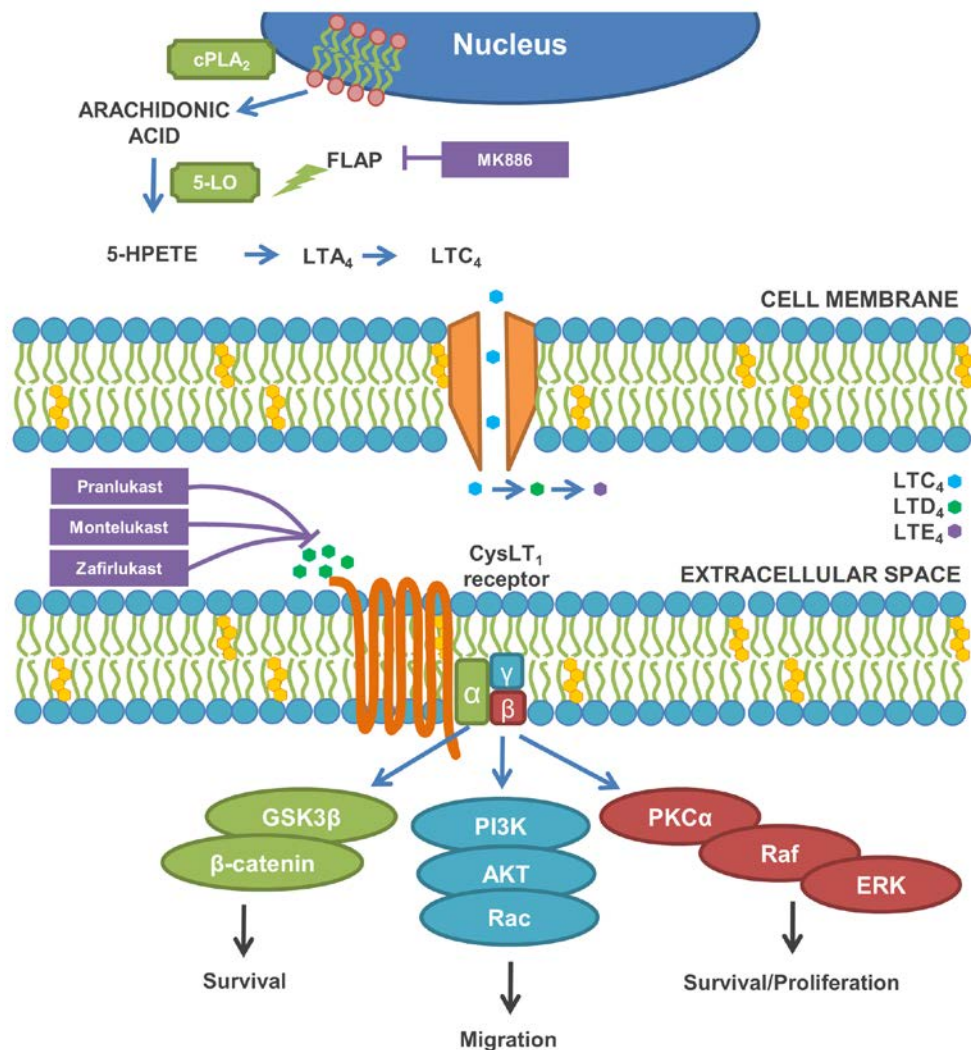


Figure 1.11 Overview of cysteinyl leukotriene metabolism. CysLT₁R has been shown to activate downstream pathways including PI3K[362], ERK[363] and GSK3β[364]. Inhibitors act on various points in this pathway (purple boxes). LTRA_4 , C_4 , D_4 , leukotriene A_4 , C_4 , D_4 ; FLAP, 5-lipoxygenase-activating protein; 5-LO, 5-lipoxygenase; 5-HPETE, 5-hydroperoxyeicosatetraenoic acid; GSK3β, glycogen synthase kinase 3 beta; PI3K, phosphoinositide 3-kinase; PKCα, protein kinase C α; ERK, extracellular signal-related kinase; MEK, mitogen-activated protein kinase kinase; cPLA₂, cytosolic phospholipase A₂.

LTB₄ binds its cognate GPCRs, BLT₁ and BLT₂, with a high and low affinity, respectively[365, 366]. BLT₁ expression is confined mainly to peripheral leukocytes, whereas BLT₂ is fairly ubiquitous with peak expression in the spleen, liver and lymphocytes[367]. LTD₄ has the highest *in vivo* activity of the terminal CysLTs and can act through two GPCRs termed CysLT₁R and CysLT₂R. The receptors exhibit different affinities for their respective ligands, with CysLT₁R selectively binding LTD₄ and CysLT₂R having a lower but equal affinity for LTC₄ and LTD₄[368, 369].

At the site of inflammation, CysLTs can be produced by leukocytes alone, which produce all of the enzymes required for their synthesis. However, the situation *in vivo* is often more complex and involves a degree of cellular cooperation. On one hand, epithelial and endothelial cells expressing LTRA₄ hydrolase can generate leukotrienes from LTRA₄, which is released from neutrophils; conversely, leukocytes can utilise AA released from these cells as fuel to generate leukotrienes[370, 371]. This transcellular metabolism highlights the shortcomings of simple 2D *in vitro* assays in determining the role of leukotrienes in inflammation and cancer.

1.8.3 Leukotrienes and Cancer

To date, the majority of work exploring the role of leukotrienes in a disease setting has centred on pre-existing inflammatory conditions. Inflammatory bowel disease (IBD) such as ulcerative colitis and Crohn's disease are known risk factors of colorectal (bowel) cancer (CRC)[372], the fourth most common cancer and the second most common cause of cancer death in the UK[373]. A recent meta-analysis showed that the risk of bowel cancer was 70% higher in people with IBD compared to the general population[374]. IBD is characterised by high levels of AA-derived pro-inflammatory metabolites such as CysLTs and prostaglandins in the intestinal wall, which are produced by infiltrating leukocytes. Correspondingly, high levels of LTE₄ have been detected in the urine of IBD sufferers[375].

Overexpression of CysLT₁R has been found in a number of cancer types, including those of the bladder, prostate, breast and bowel, and are associated with decreased patient survival[376-379]. On the other hand, high CysLT₂R

expression is predictive of a favourable prognosis in CRC[380]. This expression pattern may be explained by the counteracting role of the CysLT₂R which keeps CysLT₁R locked in a heterodimer under basal conditions in intestinal epithelial cells[381, 382]. Upon LTC₄ stimulation, CysLT₂R induces internalisation of the heterodimeric complex, negatively regulating the plasma membrane expression of CysLT₁R[382].

LTD₄ stimulation of CysLT₁R leads to enhanced cell survival signalling in intestinal epithelial cells with a concomitant increase in proteins such as COX-2, β -catenin and Bcl-2[383], as well as increased proliferation and migration via the ERK1/2-p90^{RSK} and PI3K-Rac pathway, respectively[362, 384]. The anti-tumourigenic signalling protein IFN- α has been shown to induce CysLT₂R promoter activity, whereas mitogenic EGF suppresses it. Furthermore, EGF-induced cell migration in the colon cancer cell line, Caco-2, was mitigated by LTC₄ stimulation of CysLT₂R[385]. At the time of writing, no studies have established a role for CysLTs in oral cancer, although one study found significantly elevated levels of LTB₄ in oral SCC compared to normal control tissue[386].

A number of CysLT₁R antagonists (montelukast, pranlukast, zafirlukast) have been approved for the treatment of asthma[387] and drug-repurposing studies have shown that the compounds can induce apoptosis in cancer cell lines *in vitro*[376, 378, 388, 389]. Antagonism of CysLT₁R in colon cancer cell lines has been shown to reduce proliferation and combination treatments of the COX-2 inhibitor (celecoxib) with either a 5-LOX inhibitor (MK-886) or CysLT₁R antagonist (LY171883) produced an additive effect[390, 391]. Subsequent *in vivo* work has shown that CysLT₁R antagonists negatively regulate VEGF expression in mice and reduce vascular permeability[392]. Furthermore, in a murine Lewis lung carcinoma model, pranlukast and montelukast prevented tumour metastasis by inhibiting capillary permeability[393]. In line with these findings, Savari *et al.* showed that Montelukast treatment successfully inhibited the growth of human colon cancer xenografts in nude mice[394].

1.8.4 Summary

The crosstalk of the host's immune system with tumour cells is highlighted by the recent approval of pembrolizumab for the treatment of recurrent/metastatic HNSCC[14]. It is increasingly evident that chronic inflammation contributes to the development and progression of cancer. Repeated inflammatory insults, such as those experienced by smokers or IBD sufferers, predispose to the development of dysplasia. The recruitment of pro-inflammatory cytokines and growth factors promote the growth and survival of tumour cells and facilitate their invasion through the extracellular matrix. Further evidence for the tumour-promoting role of inflammation stems from the success of non-steroidal anti-inflammatory drugs (NSAIDs) in preventing carcinogenesis[395].

Cysteinyl leukotrienes have been less well studied than their COX pathway counterparts, but early evidence suggests an equally important role in tumour progression. By promoting the transcription of oncogenic genes[396], leukotrienes have been shown to sustain proliferation and enhance migration and invasion in colon cancer cells[397]. Through its interaction with VEGF, they can also induce angiogenesis[398], while inhibition of the CysLT₁R inhibited the growth of tumours in a xenograft model[394]. CysLT₁R signalling is linked with a number of cancer hallmarks and targeting the receptor shows promise as a therapeutic strategy.

Herein, a drug-repurposing screen reveals a group of CysLT₁R inhibitors that are highly effective at inhibiting the growth of oral SCC cell lines. This study sought to validate the significance of the pathway for *in vivo* tumour growth.

1.9 Thesis Aims and Objectives

HNSCC survival rates have remained stagnant for decades in the absence of effective targeted therapies. This project sought to identify novel driver genes in the disease through the application of large-scale genomic and compound screening. Hypoxia was chosen as the differential in these screens, owing to its prognostic significance in solid tumours. Following on from this, potential targets were followed up using a combination of bioinformatic and functionality-based approaches. Three major themes emerged from this work: (1) the amplification of chromosome 3q36-29, (2) the role of hypoxia in lipid metabolism and (3) tumour-related inflammation. Chapter 3 will give a brief overview of the screen results, while chapters 4, 5 and 6 will focus on the identification and validation of 3q26-29 genes that are frequently overexpressed in HNSCC and significant for patient survival. Chapter 7 will investigate the destabilising effect of hypoxia on the HNSCC genome and the importance of lipid metabolism genes. Chapter 8 assesses the effect of anti-inflammatory compounds on HNSCC progression.

Chapter 2 Materials and Methods

2.1 Cell lines

The patient-derived epithelial cell lines used in this thesis are listed in Table 2.1. All cell lines were adherent and HPV-negative. Cell lines were grown in keratinocyte serum free medium supplemented with 25µg/mL bovine pituitary extract (BPE) and 2.5ng/mL epithelial growth factor (EGF), unless otherwise stated.

| # | Cell Line | Tissue | Gender/Age | TNM Stage | Disease | Ref |
|---|------------------------------|---------|------------|-----------|---------|----------|
| 1 | Liv7k | Tongue | ? / ? | T3N2b | SCC | R. Shaw |
| 2 | Liv37k | FoM | M / 57 | T3N2b | SCC | R. Shaw |
| 3 | Liv52k | Tongue | M / 30 | T2N0 | SCC | R. Shaw |
| 4 | Liv72k | Tongue | F / 79 | T3N2c | SCC | R. Shaw |
| 5 | KR19 | Tongue | F / 19 | T4aN2b | SCC | In-house |
| 6 | OKF4/tert1 (puro) | FoM | M / 28 | - | - | [399] |
| 7 | OKG4/bmi1 (puro)/tert1 (bsd) | Gingiva | ? / 27 | - | - | [400] |

Table 2.1 Cell lines used in this thesis. Details include the tissue of origin, patient details and TNM stage. FoM, floor of mouth; TrigRE, retromolar trigone.

The “Liv” series of cell lines were generously gifted by Professor Richard Shaw (University of Liverpool, UK) and the OKF4 and OKG4 lines were purchased from the Rheinwald Lab (Boston, USA). The KR19 cell line was extracted from primary patient tissue by Dr Lynn McGarry (CRUK Beatson Institute, UK).

2.2 Reagents and Vendors

Reagents were purchased from various companies for use in this work. Reagents and company details are listed in Table 2.2.

| Product | Catalog Number |
|--|----------------|
| Thermo Fisher Scientific | |
| NuPAGE™ Transfer Buffer | NP0006 |
| NuPAGE™ Tris-Acetate SDS Running Buffer | LA0041 |
| NuPAGE™ MOPS SDS Running Buffer | NP000102 |
| NuPAGE™ MES SDS Running Buffer | NP000202 |
| Restore™ Fluorescent Western Blot Stripping Buffer | 62300 |

| | |
|--|-----------------|
| Halt™ Phosphatase Inhibitor Cocktail | 78420 |
| Keratinocyte-SFM Medium (Kit) with L-glutamine, EGF, and BPE | 17005075 |
| DMEM, high glucose, pyruvate, no glutamine | 21969035 |
| DMEM/F-12, no glutamine | 21331020 |
| MEM α , nucleosides | 22571020 |
| RPMI 1640 Medium, no glutamine | 31870074 |
| Foetal Bovine Serum, qualified, E.U.-approved, South America origin | 10270106 |
| Lipofectamine™ RNAiMAX Transfection Reagent | 13778500 |
| Lipofectamine™ 2000 Transfection Reagent | 11668019 |
| NuPAGE™ LDS Sample Buffer | NP0007 |
| NuPAGE™ Sample Reducing Agent | NP0004 |
| NuPAGE™ Antioxidant | NP0005 |
| Trypan Blue Stain (0.4%) for use with the Countess™ Automated Cell Counter | T10282 |
| RNaseZap™ RNase Decontamination Solution | AM9780 |
| High-Capacity cDNA Reverse Transcription Kit | 4368814 |
| RNaseOUT™ Recombinant Ribonuclease Inhibitor | 10777019 |
| Pierce™ BCA Protein Assay Kit | 23225 |
| NuPAGE™ 4-12% Bis-Tris Protein Gels, 1.0 mm, 12-well | NP0322PK2 |
| PageRuler™ Prestained Protein Ladder, 10 to 180 kDa | 26617 |
| PVDF Transfer Membrane, 0.45 μ m | 88518 |
| FastDigest NheI | FD0973 |
| FastDigest BamHI | FD0054 |
| FastDigest Sall | FD0644 |
| FastDigest Esp3I (BamHI) | FD0454 |
| FastDigest Buffer | B64 |
| Orange DNA Loading Dye | R0631 |
| MAX Efficiency™ DH5 α ™ Competent Cells | 18258012 |
| GeneRuler 1 kb DNA Ladder | SM0312 |
| T4 Polynucleotide Kinase (10 U/ μ L) | EK0031 |
| T4 DNA Ligase Buffer | 46300018 |
| TaqMan™ Gene Expression Master Mix | 4369016 |
| TaqMan™ RNase P Detection Reagents Kit | 4316831 |
| GE Healthcare (Dharmacon) | |
| 5X siRNA Buffer | B-002000-UB-100 |
| Sigma-Aldrich Company | |
| DAPI, dilactate | D9564 |
| Triton™ X-100 | X100 |
| Zafirlukast | Z4152 |
| Staurosporine from Streptomyces sp. | S4400 |
| Doxycycline Hydrochloride | D3072 |
| RNase-Free Water | W3513 |
| Rapid DNA Ligation Kit | 11635379001 |
| cComplete™, Mini Protease Inhibitor Cocktail | 04693124001 |
| Bovine Serum Albumin Fraction V | 10735086001 |
| TWEEN® 20 | P9416 |

| Qiagen | |
|--|-----------|
| QIAshredder | 79654 |
| RNeasy Mini Kit | 74104 |
| QIAprep Spin Miniprep Kit | 27104 |
| AllPrep DNA/RNA Mini Kit | 80204 |
| RNase-Free DNase Set | 79254 |
| Santa Cruz | |
| Bortezomib | sc-217785 |
| Tocris Bioscience | |
| MK 886 | 1311 |
| Invivogen | |
| Puromycin | ant-pr-1 |
| Clontech | |
| Lenti-X™ Concentrator | 631231 |
| In-Fusion® HD EcoDry™ Cloning Plus | 638912 |
| Stellar™ Competent Cells | 636763 |
| Macherey-Nagel™ NucleoSpin™ Gel and PCR Clean-up Kit | 12303368 |
| Dimethyl Sulfoxide | 10213810 |
| SelleckChem | |
| Carfilzomib | S2853 |
| Cayman Chemical | |
| Montelukast (sodium salt) | 10008318 |

Table 2.2 List of reagents.

2.3 Cell Culture Methods

2.3.1 General Maintenance

The media for cell lines used in this thesis are detailed in section 2.1. Stocks were maintained to keep a good stock of low passage cells. All procedures were carried out using aseptic techniques in a class II laminar flow hood with HEPA filtration. Cells were centrifuged at 300 x g for 5 minutes using a Beckman Coulter Allegra X-22R benchtop centrifuge. Cells were incubated at 37°C / 5% CO₂, unless otherwise stated.

2.3.2 Thawing stocks

Cells were thawed from liquid nitrogen stocks in 37°C water bath and resuspended in pre-warmed culture medium. The cell suspension was pelleted by centrifugation, medium removed and the cells resuspended in fresh medium for seeding in an appropriate flask.

2.3.3 Passage of cell cultures

Cell lines were split upon reaching confluence to continue growing stocks or seed for experiments. Spent medium was removed by aspiration and cells were washed once in sterile 1 x PBS. This was removed and a small volume of trypsin was added to the cell layer (3mL for T175, 2mL for T75 and 1mL for T25). Gentle rocking of flasks ensured even coverage of the cell layer. Flasks were incubated at 37°C for 5-10 minutes to maximise enzyme activity. Once cell detachment was confirmed under a light microscope, 10mL of serum-containing media was added to inactivate the trypsin. This suspension was centrifuged to pellet, the supernatant was removed and the pellet was resuspended in fresh medium and the cells seeded into a new flask.

2.3.4 Cell Counting

An aliquot of live cell suspension was mixed 1:1 with trypan blue stock solution (0.4%) and pipetted into a Countess chamber slide. Cells were counted using a Countess™ automated cell counter (Thermo Scientific). Dead cells were subtracted from total cell count and live cell counts were used.

2.3.5 Creation of frozen cell stocks

Stocks of early passage cells were generated for all cell lines used in this thesis. Cells were pelleted as in section 2.5.3 and resuspended in freezing solution. This solution consisted of 70% culture medium, 20% FBS and 10% DMSO. Cells in this solution were aliquoted into labelled and barcoded 2mL cryo-vials, scanned into the cell stock spreadsheet and placed into a freezing container (Mr Frosty, Nalgene) to allow gradual cooling. This was stored at -80°C overnight and frozen cells were transferred to liquid nitrogen stores the next day.

2.4 Plasmid Manipulation

A number of cell lines were modified by plasmid integration in order to achieve gene knockdown. SnapGene software (GSL Biotech LLC) and free-to-use ApE software (M. Wayne Davis, University of Utah, USA) were used to design plasmids in this project.

2.4.1 pTRIPZ_IGF2BP2 (tet-inducible)

Glycerol stocks of five custom-made pTRIPZ plasmids, three containing a unique shRNA sequence targeting IGF2BP2, one positive GAPDH shRNA control and one non-targeting shRNA control, were ordered from Dharmacon. The plasmid contains a tetracycline-inducible promoter, so gene expression can be switched on and off. Glycerol stock were thawed on wet ice and grown in AMP-containing LB-broth. Plasmid DNA was extracted and purified by maxiprep.

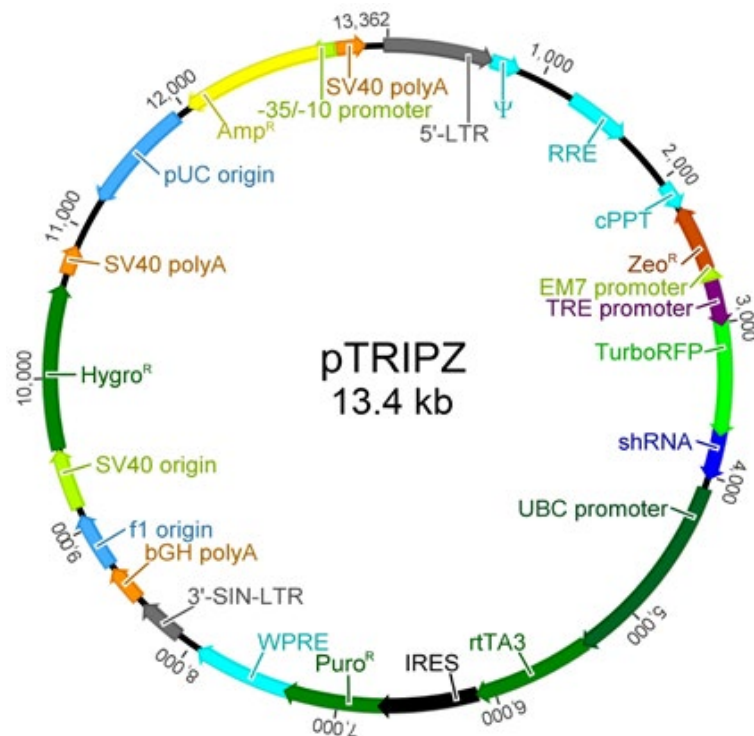


Figure 2.1 pTRIPZ lentiviral vector map, provided by Dharmacon. The empty vector is 13,362bp in size.

The plasmid DNA was subsequently digested using Fast Digest Sall (Thermo Fisher Scientific) as a quality control check. This was incubated for 5 minutes at 37° and run on a 1% agarose gel to generate bands of approximately 7104bp, 4028bp, 2188bp. The sequencing primer used for the plasmid was GGAAAGAATCAAGGAGG.

2.5 Bacterial Transformation

Either DH5 α [™] (Thermo Fisher Life Technologies) or Stellar[™] competent cells (Clontech) were used for transformation reactions, depending on RecA status required. Competent cells were thawed on wet ice prior to use and mixed gently to ensure even distribution. 50 μ L of competent cells were transferred to a 14mL round-bottomed falcon tube and 1 μ L of ligated DNA was added. The cells were kept on ice for 25 minutes and then heat shocked for 45 seconds at 42°C. Tubes were then placed on ice for 2 minutes and 500 μ L of pre-warmed (37°C) SOC medium was added. Cells were incubated with shaking at for 45 minutes at 37°C and 100 μ L of neat and diluted transformation reaction was plated onto agar plates containing appropriate antibiotic. Plates were incubated overnight at 37°C.

2.6 Plasmid cloning, purification and sequencing

Colonies were picked from agar plates using sterile pipette tips and placed into 14mL round-bottomed falcon tubes containing 5mL of LB broth, supplemented with antibiotic. Tubes were incubated overnight at 37°C with constant shaking. The following day, bacterial cells were pelleted by centrifugation, the supernatant was removed and a QIAprep Spin Miniprep Kit (Qiagen) was used to purify plasmid DNA according to manufacturer's instructions. The eluted DNA was sequenced with appropriate primer(s) and compared to the plasmid map. Following this, correct sequences were transformed into competent cells again and grown up for maxiprep by a Genomic-tip 500/G kit (Qiagen). Maxiprep was performed as directed by manufacturer. Minipreps and maxipreps were carried out by Andrew Keith (CRUK Beatson Institute). DNA was sequenced using the Applied Biosystems 3130xl Genetic Analyser, according to manufacturer instructions.

2.7 Lentiviral transfection of mammalian cells

2.7.1 Packaging and envelope system

Plasmids with the correct sequence were transfected into 293T cells using the psPAX2 lentiviral packaging and pCMV-VSV-G envelope plasmids in order to generate lentiviral particles. psPAX2 is a 2nd generation lentiviral packaging

plasmid and contains Gag, Pol, Rev and Tat HIV-1 genes. psPAX2 and pCMV-VSV-G are available from Addgene (plasmid #12260 and #8454) and were kindly gifted by Loic Fort (Laura Machesky Lab). They were originally deposited by Didier Trono and Bob Weinberg, respectively.

2.7.2 Puromycin kill curves and selection

To generate stable cell lines expressing the plasmid, a dose response curve of puromycin was applied to determine the minimum amount of antibiotic required to kill 100% of non-transfected cells. Cells of interest were seeded in a 24 well plate and incubated overnight. The next day, the media was replaced with media containing puromycin at concentrations ranging from 0-2µg/mL. Cells were examined daily to identify the minimal concentration of antibiotic that efficiently kills all non-transfected cells between 4-7 days after addition. Media was changed as necessary.

2.7.3 Lentiviral transfection into 293T cells

Briefly, 2.5×10^6 293T cells were seeded in a 10cm dish in 10mL of full growth medium (DMEM, 10% FBS, 2mM L-glut) and incubated overnight at 37°C / 5%CO₂. The next day, 15µg psPAX2, 5µg pCMV-VSV-G and 10µg target plasmid were added to 1mL of serum-free medium in a 1.5mL eppendorf and mixed well. In a separate tube, 30µL Lipofectamine 2000 (Thermo Fisher Scientific) was added to 1mL of serum-free medium and mixed. The packaging mix was combined with the transfection mix by gentle inversion. The mixture was incubated at room temperature for 15 minutes and added dropwise to 293T cells. Gentle rocking of the dish ensured even coverage of the plasmid mix and cells were then incubated overnight at 37°C / 5%CO₂. *Containment Level II procedure from this point*. The next day, the virus containing media was removed from 293T cells and discarded in a 1% virkon solution. New growth media was added gently to 293T cells to avoid detachment of cells.

2.7.4 Concentration of lentivirus

Virus-containing media was harvested from 293T cells into a sterile 50mL falcon tube. Virus containing media was centrifuged briefly at 500 x g for 10 minutes at 4°C and filtered through a 0.45 polyethersulfone (PES) filter into a new sterile

50mL falcon (do not use nitrocellulose - it binds surface proteins on the lentiviral envelope). One volume of Lenti-X concentrator (Clontech) was added to 3 volumes of clarified supernatant, and mixed by gentle inversion. This solution was incubated overnight at 4°C. The next day, the solution was centrifuged at 1,500 x g for 45 minutes at 4°C to pellet the virus and the supernatant was discarded in a 1% virkon solution. Next, the pellet was gently resuspended in 1/10 the original volume of keratinocyte serum-free media. The concentrated virus was used immediately for titration or stored at -80°C. Repeat the next day.

2.7.5 Lentiviral transduction of Liv7k cells

Liv7k cells were seeded at 1.5×10^6 per 10cm dish and incubated overnight at 37°C / 5%CO₂. The next day, concentrated virus was added dropwise to cells and the plate was gently rocked to ensure even distribution. Cells were incubated overnight and fresh media containing virus was added to target cells. After another overnight incubation, virus-containing media was removed and cells were allowed recover for 24-48 hours in full growth media.

2.7.6 Determination of viral titer

This was carried out on the cell line of interest, in order to determine the optimal multiplicity of infection (MOI), which is defined as the number of transducing units per cell. Cells of interest were seeded at 25,000 cells/well in a 24-well plate. Cells should be 40-50% confluence the next day. A five-fold dilution series of concentrated viral stock was created in a sterile V-bottomed 96 well plate using serum free medium, and mixed well by pipetting up and down at each dilution stage. Media was removed from target cells and 225µL of serum-free medium was added to each well. Then, 25uL was transferred from the viral source plate to the cell plate and incubated for 4 hours at 37°C / 5%CO₂. Virus containing medium was removed from cells followed by a gently rinse with 1x PBS. Full medium containing 1 µg/mL of doxycycline was added and incubated for a further 72 hours. Then, the number of turbo-RFP expressing cells was counted and the number of transducing units per mL was calculated:

$$\#TU/mL = \# \text{ of } tRFP \text{ expressing cells} * \text{viral } DF * 40$$

2.7.7 Puromycin selection of stably expressing cells

Target cells were allowed to recover for 24-48 hours after lentiviral infection and passaged if necessary. Following this, a pre-determined concentration of puromycin was added to cells in full growth medium and incubated for up to 7 days, until only stably transduced cells remained. These cells were expanded and frozen down as stocks.

2.8 Molecular Biology Techniques: RNA

2.8.1 Isolation of RNA from mammalian cell lines

Extraction of total RNA was performed using RNase-free reagents and plastic ware. Surfaces and pipettes were cleaned with RNaseZap™ RNase Decontamination Solution (Thermo Fisher Scientific) prior to work. RNA was isolated from cells using an RNeasy® Mini Kit (Qiagen), according to manufacturer's instructions. A QIAshredder spin column (Qiagen) was used to homogenise the cell pellet. DNase digestion was performed using an RNase-Free DNase Kit (Qiagen) for every RNA sample used within this body of work. RNA concentration was measured and assessed for purity using a NanoDrop spectrophotometer. RNA was stored at -80°C until use.

2.8.2 Normalisation and reverse transcription of RNA

Each RNA sample was normalised to 100ng/μL and reverse transcribed using a High-Capacity cDNA Reverse Transcription Kit (Applied Biosystems™), according to manufacturer's instructions. RNase Out (Thermo Fisher Scientific) solution was used for every sample. RNA samples were stored at -20°C until needed.

2.8.3 Generation of cDNA standard curves

A four-point standard curve was created for each experiment. First, the neat cDNA samples were diluted 1:1 in RNase-free water. Next, a pool of all cDNA samples was created and diluted 1:4 in RNase-free water, with careful mixing at each step. Individual samples were diluted 1:24 in RNase-free water and mixed well (Figure 2.2).

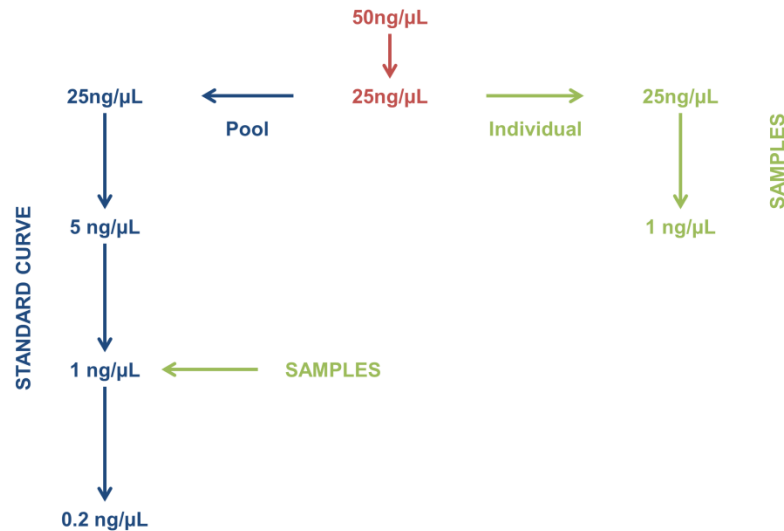


Figure 2.2 Generation of a standard curve for RTq-PCR experiments.

2.8.4 Real time quantitative PCR (RTq-PCR)

RT-qPCR was primarily used to measure knockdown efficiency of RNAi transfections but was also used to quantify gene expression in panels of cell lines grown in different oxygen conditions. 2 x qPCR Mastermix was ordered from Primer Design and all primers were either designed using NCBI primer blast (<https://www.ncbi.nlm.nih.gov/tools/primer-blast/>) or ordered from Qiagen. Melt curves were generated to assess primer specificity. The optimal reference gene was determined on an experiment-to-experiment basis. RTq-PCR was performed using an Applied Biosystems 7500 Fast system.

2.8.5 Primer Design

Standard parameters were used to design forward and reverse primers which covered a region of 100-300bp in length, and spanned an exon-exon junction (Table 2.3). Both primers were assessed for off-target binding using BLAST. Primers are listed in Table 2.4.

| Primer Attribute | Optimal Range |
|-----------------------------|------------------------|
| Sequence Length | 18-23 bp |
| PCR Product Size | 100-300 bp |
| GC Content | 40-60% |
| Melting Temp | 57-63°C (max 3°C diff) |
| Max Self-Complementarity | 2 |
| Max 3' Self-Complementarity | 1 |

Table 2.3 Optimal primer attributes.

| Target Gene | Primer Sequence | | Amplicon Length (bp) | |
|-------------|------------------------------------|-----------------------------------|----------------------|----------------------|
| IGF2BP2 | For 5'-GGCTTGACCATAAAGAACATCAC-3' | Rev 5'-GGAATCTCTTCGGCTAGTTTGG-3' | 190 | |
| CDH1 | For 5'-GTCAGTTCAGACTCCAGCCC-3' | Rev 5'-AAATTCACTCTGCCCAGGACG-3' | 295 | |
| SNAI1 | For 5'-ACTCTAATCCAGAGTTTACCTTCC-3' | Rev 5'-CAGGACAGAGTCCCAGATGAG-3' | 124 | |
| SNAI2 | For 5'-TCAAGGACACATTAGAACTCACAC-3' | Rev 5'-CTACACAGCAGCCAGATTCC-3' | 199 | |
| CDH1 | For 5'-CGAACTATATTCTTCTGTGAGAGG-3' | Rev 5'-ATGATAGATTCTTGGGTTGGGTC-3' | 160 | |
| VIM | For 5'-CTTAAAGGAACCAATGAGTCCCT-3' | Rev 5'-GCAGGTCTTGGTATTCACGA-3' | 162 | |
| HIF1A | For 5'-TTTTTCAAGCAGTAGGAATTGGA-3' | Rev 5'-GTGATGTAGTAGCTGCATGATCG-3' | 66 | |
| ARNT | For 5'-CTACCCGCTCAGGCTTTTC-3' | Rev 5'-CACCAAAGTGGGAAGTACGAG-3' | 75 | |
| 18S | For 5'-GTAACCCGTTGAACCCATT-3' | Rev 5'-CCATCCAATCGGTAGTAGCG-3' | 151 | |
| GAPDH | For 5'-GAAGGTGAAGGTCGGAGTC-3' | Rev 5'-GAAGATGGTGATGGGATTTTC-3' | 226 | |
| ACTB | For 5'-CCAACCGCGAGAAGATGA-3' | Rev 5'-CCAGAGGCGTACAGGGATAG-3' | 97 | |
| Target Gene | Oiagen cat # | Lot # | Exon(s) Detected | Amplicon Length (bp) |
| PSME4 | Hs_PSME4_1_SG | 203776661 | 12/13 | 107 |
| CYSLTR1 | Hs_CYSLTR1_1_SG | 197629900 | 1/2/3 | 126/209/186 |
| PSMC2 | Hs_PSMC2_2_SG | 197629899 | N/A | 106 |
| PSMD6 | Hs_PSMD6_1_SG | 197629898 | 5/6 | 91 |
| PSMD2 | Hs_PSMD2_1_SG | 187169669 | 3/4 | 120 |

| | | | | |
|--------|-----------------|-----------|----------|-----|
| IGF2BP | Hs_IGF2BP2_1_SG | 187163099 | 9/10 | 87 |
| MGLL | Hs_MGLL_1_SG | 172785459 | 5/6 | 64 |
| DGAT2 | Hs_DGAT2_1_SG | 172757566 | 2/3 | 95 |
| GNPAT | Hs_GNPAT_1_SG | 180726532 | 4/5 | 84 |
| FAR2 | Hs_FAR2_1_SG | 180726539 | 8/9 | 103 |
| FAR1 | Hs_FAR1_1_SG | 180726538 | 5/6/7 | 106 |
| SCD | Hs_SCD_1_SG | 174465809 | 2/3 | 66 |
| DGAT1 | Hs_DGAT1_1_SG | 174465808 | 2/3/4 | 67 |
| LIPE | Hs_LIPE_1_SG | 174464740 | 6/7 | 120 |
| DAGLA | Hs_DAGLA_1_SG | 174464739 | 15/16/17 | 130 |
| AGPS | Hs_AGPS_1_SG | 174465765 | 15/16/17 | 140 |
| PNPLA2 | Hs_PNPLA2_1_SG | 174465764 | 4/5 | 80 |

Table 2.4 Primers used in this thesis, custom made and off the shelf

2.9 Molecular Biology Techniques: Protein

2.9.1 Cell Lysis (6 well plate)

Cell plates were placed on wet ice and medium aspirated. Cells were then washed once with cold PBS and 80µL of cold RIPA buffer (50mM Tris HCl (pH 8, 150mM NaCl, 1% NP-40, 0.5% sodium deoxycholate, 0.1% SDS, 1x protease inhibitor, 2x phosphatase inhibitor) was added to each well, after which the cell layer was scraped and transferred to a 1.5mL eppendorf tube. Samples were mixed by vortexing and kept on wet ice for 30 minutes, with further vortexing every 10 minutes. Samples were passed through a 0.5mm diameter needle five times and centrifuged for 10 minutes at 10,000 x g at 4°C. The supernatant was transferred to a new eppendorf tube and stored at -20°C.

2.9.2 Protein Quantification (BCA Assay)

Protein samples were quantified using a Pierce™ BCA assay kit (Thermo Fisher Scientific), according to the manufacturer's instructions. Samples were normalised to equivalent concentrations.

2.9.3 Sodium Dodecyl Sulfate Polyacrylamide Gel Electrophoresis (SDS-PAGE)

Samples were mixed 1:3 with NuPAGE® 4x LDS Sample Buffer and 1:9 with NuPAGE® 10x Reducing Agent (Thermo Fisher Scientific) and heated at 70°C for 10 minutes. 10-30µg of protein was pipetted into each lane of a pre-cast

NuPAGE™ 4-12% Bis-Tris Protein Gel held in an XCell SureLock™ Mini-Cell gel electrophoresis tank (Thermo Fisher Scientific). 10µL of PageRuler™ Prestained Protein Ladder (10 to 180 kDa) was run alongside samples for size estimation. Electrophoresis was performed at 120V for 80 minutes or until the running front reached the bottom of the gel.

2.9.4 Western Blotting

Gels were transferred onto 0.45µm polyvinyl difluoride (PVDF) membrane using a Bio-Rad Mini-Protean Tetra Cell at 70V for 120 minutes. The membrane was then stained with 0.1% Ponceau S solution (diluted in 5% acetic acid) for 10 minutes to ensure complete transfer. The membrane was rinsed for 15 minutes in 1 x TBST to remove the stain and then blocked for 1 hour at room temperature in 5% BSA/TBST. After blocking, the membrane was placed in a 50mL falcon containing 5mL of primary antibody/5% BSA/TBST. The membrane was incubated overnight at 4°C with constant rolling. The following day, the membrane was washed 3 times for 10 minutes with 1 x TBST and incubated with secondary antibody in 5% BSA/TBST for 1 hour at room temperature. The membrane was washed three more times and imaged on a LI-COR CLx (LI-COR Biosciences).

A full list of antibodies used for western blotting in this body of work is detailed in Table 2.5. Secondary antibodies were used at a 1:2000 dilution in 5% BSA/TBST (either goat anti-rabbit IgG (H+L) Cross Adsorbed Secondary Antibody, DyLight 800 or goat anti-mouse IgG (H+L) Cross Adsorbed Secondary Antibody, Alexa Fluor 680).

| Target protein | Company | Catalog # | Species/ isotype | Dilution |
|---------------------------|-----------------|------------|------------------|----------|
| AGPS | Atlas | HPA030210 | Rb IgG | 1:500 |
| Akt (p) Ser473 | Cell Signalling | 4060 | Rb IgG | 1:1000 |
| Akt (pan) | Cell Signalling | 2920 | Ms IgG1 κ | 1:1000 |
| GAPDH | Cell Signalling | 2118 | Rb IgG | 1:1000 |
| IMP2 | Cell Signalling | 14672 | Rb IgG | 1:1000 |
| MAPK (p) Thr202/Tyr204 | Cell Signalling | 9101 | Rb IgG | 1:1000 |
| MGLL | ProteinTech | 14986-1-AP | Rb IgG | 1:1000 |
| p70 S6K | Cell Signalling | 2708 | Rb IgG | 1:1000 |
| p70 S6K | Cell Signalling | 9206 | Ms IgG | 1:1000 |
| p70 S6K (p) Thr389 | Cell Signalling | 9206 | Ms IgG2a | 1:1000 |
| PSMD2 | Cell Signalling | 14141 | Rb IgG | 1:1000 |
| PSMD6 | Bethyl Labs | A303-827A | Rb IgG | 1:1000 |
| PSME4 | Bethyl Labs | A303-880A | Rb IgG | 1:1000 |
| α -tubulin | Cell Signalling | 3873 | Ms IgG1 | 1:1000 |
| β -Actin | Cell Signalling | 3700 | Ms IgG2b | 1:1000 |

Table 2.5 List of antibodies. (p) phospho.

2.10 Statistical Analysis

Data was analysed for significance using GraphPad Prism (San Diego, CA, USA). Statistical significance was set at $p < 0.05$ unless otherwise stated.

2.11 RNA Sequencing

RNA was extracted as described in section 2.8. Library generation and sequencing was carried out by William Clark (CRUK Beatson Institute). The quality of RNA was assessed using a RNA ScreenTape assay with the 2200 TapeStation system (Agilent Technologies). RNA-seq libraries were generated using the TruSeq Stranded mRNA LT Kit (Illumina), according to an adapted version of manufacturer's instructions from Fisher *et al.*[401]. cDNA synthesis and adaptor ligation was performed as in Bailey *et al.*[402]. The quality and quantity of the DNA libraries was assessed using a DNA D1000 ScreenTape assay with the 2200 TapeStation system (Agilent Technologies) and Qubit Fluorometric Quantitation system (Thermo Fisher Life Technologies), respectively. All libraries were sequenced using the Illumina NextSeq 500 system with the High Output Kit v2 (75 cycles) to generate 2x36 paired-end reads.

RNA sequencing analysis was carried out by Ann Hedley and Gabriela Kalna (CRUK Beatson Institute). Quality checks on the raw RNASeq data files were done

using fastqc: (<https://www.bioinformatics.babraham.ac.uk/projects/fastqc/>) and fastq_screen: (http://www.bioinformatics.babraham.ac.uk/projects/fastq_screen/). RNASeq reads were aligned to the GRCh38[403] version of the human genome using TopHat2 version 2.0.10[404] with Bowtie version 2.1.0[405]. Expression levels were determined and statistically analysed by a combination of HTSeq version 0.5.4p3: (http://htseq.readthedocs.io/en/release_0.9.1/), the R 3.1.1 environment, utilizing packages from the Bioconductor data analysis suite and differential gene expression analysis based on the negative binomial distribution using the DESeq2[406]. Pathway analysis of genes with a fold change >2.0 and an adjusted P value <0.05 was performed using GeneGo Pathways Software (MetaCore; <https://portal.genego.com/> version 6.22.67265).

2.12 High Throughput Screening: siRNA

Two high throughput screens were performed in this project, including a whole genome siRNA screen and an FDA-approved compound screen. Both screens were carried out on the Liv7k cell line in normoxic and hypoxic conditions and included three replicates per condition. Automated liquid handling machinery was used in order to reduce variability between batches and minimise human error (Table 2.6). Sterile technique was maintained throughout the screen. All surfaces and plastic ware were sprayed with 70% ethanol before work and gloves and PPE were worn at all times. The automated machines were used inside laminar flow hoods to maintain sterility. All screening plastic ware used in the course of this project are listed in Table 2.7.

| Equipment |
|--|
| Janus Varispan and MDT automated workstation (Perkin Elmer) |
| Matrix WellMate [®] liquid dispenser (Thermo Fisher Scientific) |
| Envision 2102 plate reader (Perkin Elmer) |
| ALPS 3000 plate sealer (Thermo Fisher) |
| Operetta high content microscope (Perkin Elmer) |
| Opera high content confocal microscope (Perkin Elmer) |

Table 2.6 List of automated equipment used in the screens.

| Greiner Bio One | |
|--|-----------|
| Product | Catalog # |
| Cell culture microplate, 96 well, polystyrene, flat-bottom (chimney well), μ clear [®] , black, CellStar [®] , tissue culture, lid with condensation rings, sterile, 8 pcs/bag | 655090 |
| Cell culture microplate, 384 well, polystyrene, flat-bottom, μ clear [®] , black, CellStar [®] , tissue culture, lid, sterile, 8 pcs/bag | 781091 |
| Microplate, 96 well, polypropylene, V-bottom, chimney well, natural, 10pcs/bag | 651201 |
| Microplate, 384 well, polypropylene, flat-bottom, natural, 10pcs/bag | 781201 |
| Cell culture microplate, 96 well, polystyrene, flat-bottom, chimney well, μ clear [®] , white, CellStar [®] , tissue culture, lid with condensation rings, sterile, 8pcs/bag | 655098 |

Table 2.7 List of screening plastic ware used in the screens.

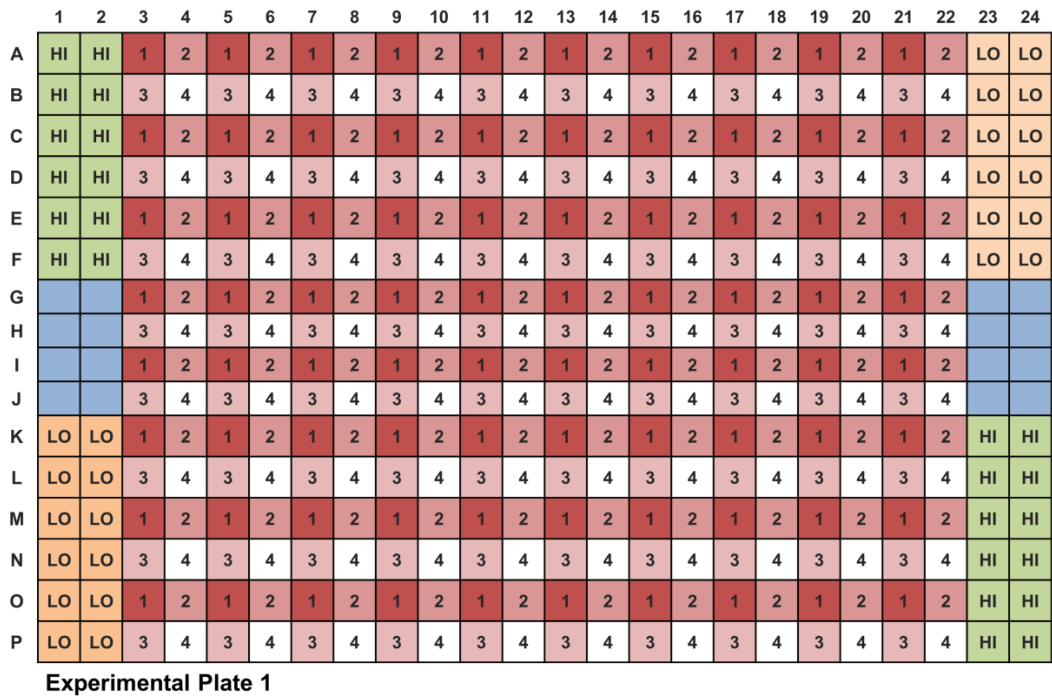
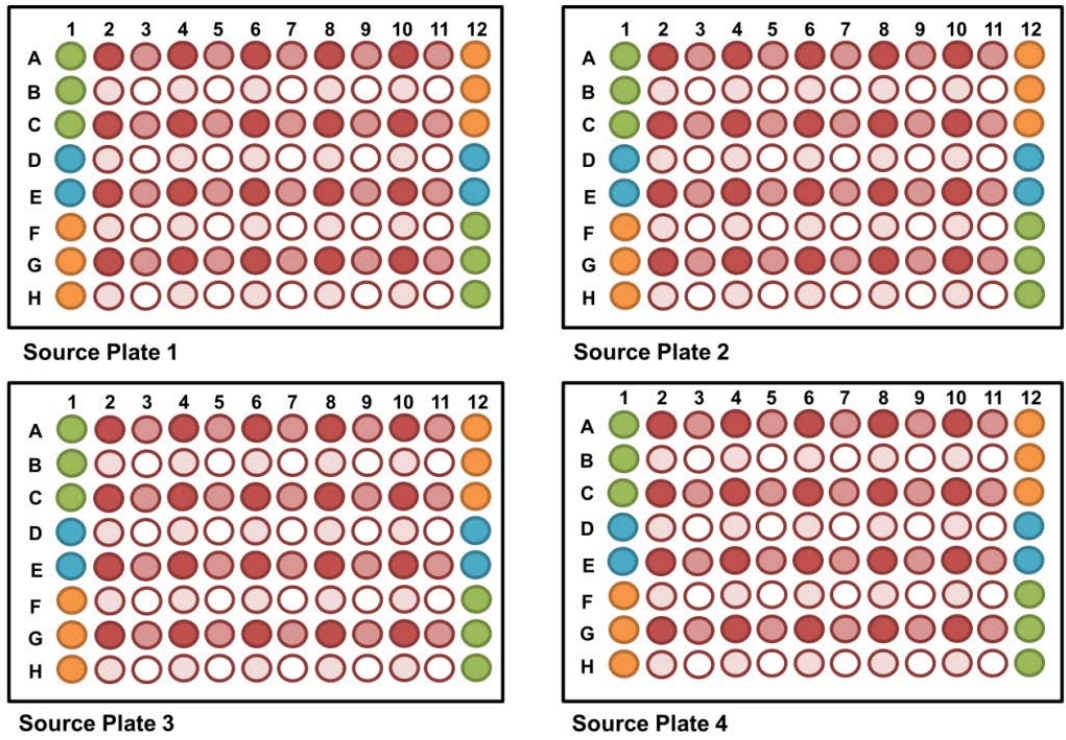
2.12.1 Liquid Handling Quality Control

To ensure even dispensing throughout plates, a quality control check of the automated workstation was performed prior to the screen. A 96 well V-bottomed plate containing 50µL 2.5mM Orange G dye was used in place of the siRNA source plate. 2.5µL of Orange G was transferred to every well of a black, clear-bottomed 384 well plate. Then, a WellMate was used to dispense 47.5µL of sterile ddH₂O to each well containing Orange G. The plate was shaken for 15 minutes at room temperature, and absorbance was measured at 460nm on an Envision plate reader. The mean, standard deviation and the coefficient of variation (CV) was calculated for each plate. A CV of <10% was deemed within acceptable limits.

$$\% CV = \frac{sd}{mean} * 100$$

2.12.2 Preparation of source plates

96-well source plates containing “siGENOME” pooled siRNA were purchased from Dharmacon (GE Healthcare) and diluted to a concentration of 500nM. On the day of screening, source plates were removed from -20°C storage and allowed to thaw at room temperature. While the source plates were thawing, control plates were prepared containing All Stars[®] cell death control (Qiagen) (LO control) and non-targeting negative control (Dharmacon “On-Target Plus”) (HI control) in the relevant wells. The percentage growth inhibition caused by target siRNAs will be normalised to that of the non-targeting control siRNA. All Stars siRNA will be used as a positive control to confirm successful transfection. See plate layout in **Figure 2.3**. The concentration of siRNA in the control plate was also 500nM. Once thawed, plates were spun down for one minute at 2000rpm in batches of six and placed inside the laminar airflow hood. Plate seals were peeled off and plates were placed in six stacks of four with a lid on the top plate.



LO control (siAllStars)
 HI control (siNTC)
 Cells only control

Figure 2.3 Stamping of source plates into 384 well experimental plates.

2.12.3 Experimental Design

Prior to beginning the screen, a number of transfection reagents were tested at a range of concentrations in the Liv7k cell line. RNAiMax was chosen because it had the highest on-target effect with minimal toxicity.

The classes of siRNA target are detailed in **Table 2.8**, and contained siRNAs to 18,075 genes in total. The screen was designed to include three replicates per oxygen condition and was carried out in 10 batches. Each batch consisted of 24 x 96-well siRNA source plates being stamped into 36 x 384-well experimental plates. Six “cells only” plates were also included to assess edge effects (**Figure 2.4**). In total, 231 source plates were stamped into 342 experimental plates, with an additional 60 cell only plates (total 402 x 384-well plates).

The Janus automated workstation was used to stamp each experimental plate with 2.5µL of control and target siRNA. 7.5µL of RNAiMAX transfection reagent (diluted in serum-free media) was then added to the siRNA using the WellMate and placed on a plate shaker at 600rpm for 15 minutes. Following this, 40µL of cell suspension was added using the WellMate and plates were incubated at 37°C / 5% CO₂ in either normoxic or hypoxic conditions for 72 hours.

| Class | Number of source plates |
|----------------------------|-------------------------|
| Kinase | 9 |
| G-Protein Coupled Receptor | 5 |
| Phosphatase | 4 |
| Ion Channel | 5 |
| Drug Target | 60 |
| Protease | 6 |
| Ubiquitin | 9 |
| Rest of Genome | 133 |
| Total | 231 |

Table 2.8 Classes of siRNA used in the screen.



Figure 2.4 Experimental design of a screen batch.

2.12.4 Fixation and Staining

At the 72-hour time point, cells were fixed with 4% formaldehyde for 15 minutes followed by a PBS wash. Then, cells were permeabilised with 0.1% TX-100 and stained with 1 μ g/mL DAPI for 2 hours. Cells were washed once more with PBS and plates were sealed for imaging on the Operetta high content microscope (Perkin Elmer). A nuclei count was carried out using Harmony software, and analysed with Dotmatics browser.

2.12.5 Hit Selection

The percentage growth inhibition of each siRNA was normalised to negative control values from the same plate. The mean, median and standard deviation were calculated from three technical replicates. To identify hypoxia-specific hits, the difference between the median of the normoxic condition was subtracted from the median of the hypoxic condition. A threshold of minimum growth inhibition of 10% in hypoxia and a window of 20% between the two conditions was applied. Genes that met these criteria were selected for rescreen. In addition, a number of plate-level calculations were performed.

2.12.5.1 Signal to Background Ratio (S2B)

The signal to background ratio is the difference between the mean of the positive and negative control samples. As it does not take standard deviation in to account, it does not provide any information about data variability. X_p and X_n represent the sample mean of the positive and negative controls, respectively.

$$S2B = \frac{X_p}{X_n}$$

2.12.5.2 Z-factor (Z')

The Z-factor (or Z prime, Z') accounts for variability in the positive and negative controls and involves four parameters:

$$Z' = \frac{(X_p - X_n) - 3(S_p - S_n)}{(X_p - X_n)}$$

where X_p and X_n represent the mean of the positive and negative control samples while S_p and S_n denote standard deviations of the same. The constant in the equation is based on three standard deviations from the mean, assuming a normal distribution. The Z' gives an indication of how difference the positive and negative controls are and thus the quality of the experiment (Table 2.9).

| Z' | Category | Interpretation |
|---------------------|-----------|--|
| $Z' = 1$ | Ideal | A perfect assay - Z factors cannot exceed 1 |
| $1 > Z' \geq 0.5$ | Excellent | There is a large difference between positive and negative controls |
| $0.5 > Z' \geq 0.3$ | Marginal | There is a moderate difference between positive and negative controls |
| $0.3 > Z' > 0$ | Poor | There is too much overlap between positive and negative controls |
| $Z' < 0$ | Failed | There is no difference between positive and negative controls - redesign assay |

Table 2.9 Z-factor and its interpretation.

2.12.5.3 Coefficient of Variation (CV)

A CV was calculated for both the positive and negative controls:

$$\% CV = \frac{sd}{mean} * 100$$

2.12.5.4 Strictly Standardised Mean Difference (SSMD)

The inclusion of three replicates allowed for an accurate estimation of siRNA variability. To this end, the uniformly minimal variance unbiased estimate of strictly standardised mean difference (umvue SSMD) was calculated to assess the size of siRNA effects:

$$SSMD = \frac{\Gamma\left(\frac{(n-1)}{2}\right)}{\Gamma\left(\frac{(n-2)}{2}\right)} \sqrt{\frac{2}{n-1} \frac{di}{si}}$$

where n is the number of replicates, di and si are the sample mean and standard deviation of the difference between the i^{th} siRNA and the negative control and $\Gamma()$ is a gamma function (i represents a specific siRNA). Table 2.10 provides a breakdown of SSMD rankings in terms of effect size.

| Effect Ranking | Negative SSMD thresholds (inhibition) | Positive SSMD thresholds (activation) |
|------------------|---------------------------------------|---------------------------------------|
| Extremely Strong | $SSMD \geq 5$ | $SSMD \leq -5$ |
| Very Strong | $5 > SSMD \geq 3$ | $-5 < SSMD \leq -3$ |
| Strong | $3 > SSMD \geq 2$ | $-3 < SSMD \leq -2$ |
| Fairly Strong | $2 > SSMD \geq 1.645$ | $-2 < SSMD \leq -1.645$ |
| Moderate | $1.645 > SSMD \geq 1.28$ | $-1.645 < SSMD \leq -1.28$ |
| Fairly Moderate | $1.28 > SSMD \geq 1$ | $-1.28 < SSMD \leq -1$ |
| Fairly Weak | $1 > SSMD \geq 0.75$ | $-1 < SSMD \leq -0.75$ |
| Weak | $0.75 > SSMD > 0.5$ | $-0.75 < SSMD < -0.5$ |
| Very weak | $0.5 \geq SSMD > 0.25$ | $-0.5 \leq SSMD < -0.25$ |
| Extremely Weak | $0.25 \geq SSMD > 0$ | $-0.25 \leq SSMD < 0$ |
| Zero | $SSMD = 0$ | $SSMD = 0$ |

Table 2.10 SSMD values and effect size.

2.13 High Throughput Screening: Drug-Repurposing

The Liv7k cell line was subjected to 1,351 FDA-approved compounds for oncology and non-oncology indications in normoxic and hypoxic conditions. The library was tested at a single concentration of 10 μ M. Candidates were prioritised based on three criteria: (1) drugs which were maximally effective (\geq 90% kill); (2) selectivity in the hypoxic condition; and (3) selectivity for Liv7k cells. The latter criterion was based on comparisons from previous drug screens carried out within the Screening Facility. Drug libraries are listed in Table 2.11.

| Library Name | Number of Compounds |
|--|---------------------|
| NIH Evotec Clinical Collection 1 | 281 |
| NIH Evotec Clinical Collection 2 | 446 |
| LOPAC Pfizer (Sigma Aldrich) | 90 |
| Selleck FDA-Approved Library | 420 |
| Developmental Therapeutics Program (DTP) FDA-Approved Oncology Set | 114 |

Table 2.11 Details of compound libraries used in the drug-repurposing screen.

The drug screen was performed in normoxic and hypoxic conditions with three replicate plates per condition. Similar to the siRNA screen, automated liquid handling machinery was used. On day 0, Liv7k cells were seeded in 190 μ L of K-SFM at 5000 cells per well in black, clear bottomed 96-well plates. The cells were incubated overnight at 37°C / 5% CO₂. The next day, drug source plates (stock concentration 10mM in DMSO) were removed from -20°C storage and allowed to thaw. Plates were centrifuged at 2000 rpm for 1 minute.

In a laminar airflow hood, plate seals were removed and replaced with a sterile plastic lid. For every compound source plate, an intermediate dilution plate was created. 98 μ L of serum-free media was dispensed into a PP V-bottomed plate using the WellMate and covered with a sterile lid. Relevant controls were then added to the intermediate plate. Staurosporine (stock 1mM, final concentration 1 μ M) was used as a positive control to confirm successful stamping of drugs and DMSO was used a negative control at a concentration of 0.1%.

Using the Janus, 2 μ L of drug stock was transferred from the source plate to the intermediate dilution plate to create a 1 in 50 dilution. The intermediate plates

were placed on a plate shaker for 30 minutes at 750 rpm to ensure complete mixing. After 30 minutes, 10 μ L of drug-containing media from the intermediate plates was stamped into six cell plates to create a further 1:20 dilution. The final concentration in the well was 10 μ M of compound.

Cell plates were incubated at the relevant oxygen condition for 72 hours, after which the cells were fixed and stained as for the siRNA screen. A nuclei count was performed using the Operetta high content microscope.

2.14 RNAi transfection (96 well plate)

Stock siRNA was diluted to a working concentration of 500nM. 10 μ L of diluted siRNA was dispensed into each well and 30 μ L of diluted RNAiMax transfection reagent was added on top. Incubation for 15 minutes at room temperature with shaking ensured complex formation. Cells are a concentration of 5000/well were seeded in a 160 μ L of full media. The final concentration of siRNA in each well was 25nM and the final volume of transfection reagent was 0.125 μ L/well. Cells were incubated at 37°C / 5% CO₂ for 72 hours unless otherwise stated. At experiment end-point, cells were fixed and stained as in the siRNA screen. A list of siRNAs used in transfections is provided in Table 2.12.

| siRNA ID | Sequence(s) | Catalog # |
|---------------|------------------------|------------|
| Qiagen | | |
| Hs_MGLL_1 | CTGGACCTACCTTAATGGTTA | SI00096250 |
| Hs_MGLL_2 | AAGACAGAGGTCGACATTTAT | SI00096257 |
| Hs_MGLL_3 | TCAGAGCTTGATGCTACTGTA | SI00096264 |
| Hs_MGLL_5 | CAGCGTGCTCTCTCGGAATAA | SI03067729 |
| Hs_AGPS_4 | CACCATGGAGTGGGCAAGTTA | SI00293440 |
| Hs_AGPS_5 | AAGCGCAAGAAGTTATGAAA | SI04211795 |
| Hs_AGPS_6 | CTGAGGAGTGATACACGTGTA | SI04221994 |
| Hs_AGPS_7 | ATGGTAACACCTAGAGGTATA | SI04263553 |
| Hs_GNPAT_1 | CACGTAATTACTCTCATCGAA | SI00103887 |
| Hs_GNPAT_3 | CTCGATCAAGGTACCTCTCAA | SI00103901 |
| Hs_GNPAT_5 | CAGCGCTGTCTGCTCCTCTA | SI03067232 |
| Hs_GNPAT_6 | GAGGCTCGGAGTAGTGGAGAA | SI03103870 |
| Hs_FAR2_5 | ATCCAGCACGCTCAAAGTTTA | SI03149293 |
| Hs_FAR2_6 | TTCGTCCCTATTCCTTAACTA | SI03242673 |
| Hs_FAR2_7 | ACAGTCGTC AATCTCATGCTA | SI04139821 |
| Hs_FAR2_8 | CCCAGGTTGGGTTGATAATAT | SI04199881 |
| Hs_FAR1_3 | CAGGATAGCCTACTAAATTTAA | SI00646513 |
| Hs_FAR1_5 | TGGATGGATGATGGCCTAGTA | SI04207546 |
| Hs_FAR1_6 | AGCGAACTCACCCAACCTAAA | SI04261481 |
| Hs_FAR1_7 | CAAGTTGCGGAATATACGTTA | SI04263119 |
| Hs_DGAT2_1 | CAGGAACTATATCTTTGGATA | SI00363097 |
| Hs_DGAT2_3 | CACGCTCGTCTAGTCCTGAAA | SI00363111 |

| | | |
|----------------------------------|------------------------|-------------|
| Hs_DGAT2_6 | CAGCCGGGACACCATAGACTA | SI04273626 |
| Hs_DGAT2_7 | CCTGTTCTAGGTGGTGGCTAA | SI04342667 |
| HS_PNPLA2_3 | CTGAAATATGTGTGTGAAGAA | SI00688289 |
| HS_PNPLA2_4 | CGCCAAAGCACATGTAATAAA | SI00688296 |
| HS_PNPLA2_5 | CAAGTTCATTGAGGTATCTAA | SI03019310 |
| HS_PNPLA2_6 | GACGGCGAGAATGTCATTATA | SI03019611 |
| Hs_SCD_4 | TAGGTCATCATGAAAGGTTAA | SI00711704 |
| Hs_SCD_5 | AAAGATGGTTGTAGCATTAA | SI03019177 |
| Hs_SCD_6 | AGGGCAGACAATAGTATAGAA | SI04184488 |
| Hs_SCD_7 | TGGGCAAGTCACTTAACTATA | SI04217843 |
| Hs_DAGLA_1 | CCCACAGTATCCGACCCTCAA | SI00084686 |
| Hs_DAGLA_2 | CACCAAGTACCTCGACCCTCAA | SI00084693 |
| Hs_DAGLA_3 | CTGCAGTGCTGTACATGTTTA | SI00084700 |
| Hs_DAGLA_5 | CTGACAAGATCCGGACTTCTA | SI03093034 |
| Hs_DGAT1_5 | CACTTTGTGCTACGAGCTCAA | SI04891999 |
| Hs_DGAT1_8 | CTGGTTGAGTCTATCACTCCA | SI03246754 |
| Hs_DGAT1_9 | CACCGTGAGCTACCCGGACAA | SI04145330 |
| Hs_DGAT1_12 | CGGGTCCGAGGGTGTCAATAA | SI05462086 |
| Hs_IGF2BP2_4 | CCCGGGTAGATATCCATAGAA | SI04367020 |
| Hs_IGF2BP2_3 | CAGCGAAAGGATGGTCATCAT | SI04138820 |
| Hs_IGF2BP2_2 | TCCGCTAGCCAAGAACCTATA | SI03232481 |
| Hs_IGF2BP2_1 | CAGGGCGTTAAATTCACAGAT | SI03176593 |
| Hs_CYSLTR1_4 | AAAGCAGACATTCGTAGAGAA | SI00090573 |
| Hs_CYSLTR1_3 | CTGTATATATTGGCTAGCAA | SI00090566 |
| Hs_CYSLTR1_2 | CACCTATGCTTTGTATGTCAA | SI00090559 |
| Hs_CYSLTR1_1 | CAAGTATACATGATTAATTTA | SI00090552 |
| Hs_PSME4_6 | CTCGATTGGCTACAGATAATA | SI04297251 |
| Hs_PSME4_5 | AAGCGGTCTGCTACAGTGTA | SI04220510 |
| Hs_PSME4_8 | TAGGTCTGTCTTCTACGTTTA | SI04360041 |
| Hs_PSME4_7 | AAGATTCTCAAAGAACCCTA | SI04336969 |
| Hs_PSM2_6 | CTCCGGAGGGCTGTACCTTTA | SI02779791 |
| Hs_PSM2_5 | TGGGTGTGTTCCGAAAGTTTA | SI02779763 |
| Hs_PSM2_8 | CTGCGTCCACACTATGGCAA | SI03095603 |
| Hs_PSM2_7 | CTGATCCAGAAGTTTCTCTATA | SI03093811 |
| Hs_IGF1R_8 | CTGGACTCAGTACGCCGTTTA | SI03096926 |
| Hs_IGF1R_7 | TCGAAGAATCGCATCATCATA | SI02624552 |
| Hs_IGF1R_6 | AGGATTGAGTTTCTCAACGAA | SI02624545 |
| Hs_IGF1R_1 | ATGGAGAATAATCCAGTCCTA | SI00017521 |
| GE Healthcare (Dharmacon) | | |
| PSMD6-1 | CCUJAGGAUJGGCUJAUUU | D-021249-01 |
| PSMD6-2 | GAUCUCAUCACACGAAACA | D-021249-02 |
| PSMD6-3 | UCGAUACUAUGUAAGAGAA | D-021249-03 |
| PSMD6-4 | CAUJAGCGGUUGUGGAACA | D-021249-04 |
| PSMC2-1 | GCACGACUGUGUCCAAUA | D-008180-01 |
| PSMC2-2 | UACAGACCUGAUACUUUG | D-008180-02 |
| PSMC2-3 | GUACAAAGAUAAUCAUUGC | D-008180-03 |
| PSMC2-4 | GAUJUCAGAUUUGAACUGU | D-008180-04 |

Table 2.12 List of siRNA sequences.

2.15 Functional Assays: Incucyte Zoom3®

2.15.1 Propagation

On day 0, cells were seeded at a range of concentrations in black, clear-bottomed 96-well plates in 200µL of K-SFM. Cells were incubated overnight at 37°C / 5% CO₂. The next day, plates were added to the Incucyte and imaged every 3 hours for 72-96 hours. Propagation was calculated from the confluence mask generated by the device's software.

2.15.2 Migration (Wound Assay)

Cells were seeded in 100µL K-SFM at 30,000 cells per well in Essen Imagelock™ 96-well plates and incubated overnight at 37°C / 5% CO₂. The next day, a scratch was made using a woundmaker tool™ (Essen Bioscience), according to manufacturer's instructions. The cell layer was checked to ensure a good scratch was made and washed once with 1 x PBS. 200µL of full media was added carefully to avoid disturbing the cells around the wound. Plates were added to the Incucyte and imaged every 3 hours for 72-96 hours until complete wound closure. Migration is quantified using device software using relative wound density (RWD). RWD is calculated as the cell density in the wound area relative to the cell density outside of the wound area over time.

2.15.3 Invasion (Wound Assay)

The day before making the wound, growth factor reduced matrigel (stock 9mg/mL) was placed in a fridge on wet ice and allowed to thaw. On the same day, cells were seeded in 100µL K-SFM at 30,000 cells per well in Essen Imagelock 96-well plates and incubated overnight at 37°C / 5% CO₂. The next day, matrigel was diluted 1:1 in full media to a concentration of 4.5mg/mL, and kept on wet ice. A scratch was made as for migration, and the cell layer was washed once with 1 x PBS. PBS was tipped into a container containing 1% virkon solution and the cell plate was placed in a coolbox to ensure the matrigel remains between 4-8°C. 100µL of diluted matrigel was added to each well using a multichannel pipette and the plates were incubated at 37°C / 5% CO₂ for one hour to allow matrigel to set. 100µL of full media (plus 2 x compound if

required) was added on top of the matrigel and added to the Incucyte. RWD was the primary readout for this assay.

2.15.4 Inverse Invasion Assay (Transwell®)

Matrigel (9mg/mL) was allowed to thaw slowly on ice and diluted 1:1 in full media. 100µL of diluted matrigel was carefully pipetted into the centre of each transwell insert (6.5mm Transwell® with 8.0µm Pore Polycarbonate Membrane Insert, Corning) and incubated for one hour at 37°C / 5% CO₂. During this time, a cell suspension was prepared containing 5x10⁶ cells per mL in full media. When the matrigel had set, the Transwell inserts were inverted and 100µL of the cell suspension was pipetted onto the underside of the filter (which is now uppermost). Transwell inserts were covered using the base of the 24-well culture plate, which was carefully lowered until it contacted the droplet of cell suspension. The inverted plate was incubated for 4 hours to allow the cells to attach. After 4 hours, the plate was turned upright again. Transwell inserts were dipped sequentially in 3 x 1 ml serum free medium to wash and left in wash 3 for incubation. 100µl of full media plus extra growth factor (insulin/IGF1) was gently pipetted into the insert on top of the matrigel/media. The plates were incubated at 37°C / 5% CO₂ for 5 days.

Cells were live stained with 4µM Calcein AM and 2µM Hoechst 33342 for one hour and the lower side of the insert was imaged on an Olympus FLUOVIEW FV1000 confocal laser-scanning microscope. The experiment is carried out in three sets of technical duplicates with five fields imaged in Z-stacks ranging from 0µm (base) up to 120µm into the membrane. Quantification was performed using ImageJ.

2.15.5 3D Spheroid Formation

Spheroids were created using Cultrex® 3D Spheroid Cell Invasion Assay (Trevigen catalog # 3500-096-K), according to manufacturer instructions. A seeding density of 5000 cells per well was used.

2.15.6 Neutral Lipid Staining

Cells were fixed in 4% formaldehyde for 15 minutes, followed by permeabilisation with 0.1% TX-100 in 1 x PBS for 1 hour. Cells were then washed once with 1 x PBS and sequentially stained with 1µg/mL DAPI (sigma # D9564, 0.5µg/mL Deep Red Cell Mask (Thermo Fisher #H32721) and 2µg/mL BODIPY 493/503 neutral lipid stain (Thermo Fisher # D3922). Cells were imaged using the Operetta high content microscope (Perkin Elmer).

2.15.7 MitoStress Assay (Seahorse, Agilent)

The day before the assay, cells were plated at 5000 cells/well in a Seahorse XF96 cell culture microplate (Agilent). The next day, Seahorse XF media was modified to have the same concentration of L-glutamine, D-glucose and pyruvate as keratinocyte serum free media, and 1M NaOH was added until a pH of 7.4 was achieved. Next, oligomycin, FCCP, rotenone and antimycin-A were diluted in seahorse media in order to give a final concentration of 1µM in the cell plate. One hour before the assay, the media in the cell plate was exchanged for seahorse media and incubated at 37°C. The assay was performed according to manufacturer's instructions and oxygen consumption rate/extracellular acidification rate was normalised to cellular nuclei count.

2.15.8 Proteasome Activity Kit

Proteasome activity was measured according to manufacturer's instructions (Promega #G8660).

2.16 Liquid Chromatography Mass Spectrometry (LCMS)

2.16.1 Lipid Extraction

Cells were seeded into a 6 well plate and siRNA/TR mix was added. After a 72-hour knockdown, the cell layer was washed once with ice-cold PBS. Lipids were extracted by adding 0.75mL of ice-cold methanol:PBS (1:1) to each well and scraping cells into a 1.5mL eppendorf. At this point, internal standard controls were spiked into each sample (pos-mode, PC 170/170; neg-mode, PE 170/170). 0.5mL of ice-cold chloroform was added and the tubes were vortexed for 1

minute, followed by centrifugation (14000rpm) at 4°C for 10 minutes. Carefully, the lower layer of chloroform containing dissolved lipids was moved into a glass autosampler vial. Butylated hydroxytoluene (BHT) was added to each sample and the lipid-containing chloroform was evaporated using nitrogen gas. Dried lipids were sealed in the glass autosampler vials and stored at -20°C until reconstitution in chloroform:methanol:water (1:1:0.3) (pos-mode) or isopropyl alcohol:chloroform:methanol (90:5:5) (neg-mode).

2.16.2 LCMS

Lipidomic analysis was performed by Gillian Mackay and Sergey Tumanov (CRUK Beatson Institute) using Q Exactive orbitrap mass spectrometer coupled to Dionex UltiMate 3000 LC system (Thermo Scientific). The LC parameters were as follows: 3 µL of sample was injected onto a 1.7 µm particle 100 x 2.1mm ID Waters Acquity CSH C18 column (Waters) which was kept at 50°C. A gradient of (A) water/acetonitrile (40:60, v/v) with 10 mM ammonium formate and (B) acetonitrile/2-propanol (10:90, v/v) with 10 mM ammonium formate at a flow rate of 0.3 mL/min was used. The gradient ran from 0% to 40% B over 6 min, then from 40% to 100% B in the next 24 min, followed by 100% B for 4 min, and then returned to 0% B in 2 min where it was kept for 4 min (40 min total). Lipids were analysed in both positive and negative mode. The electrospray and mass spec settings were as follows: spray voltage 3 kV (positive mode) and 3.5 kV (negative mode), capillary temperature 300°C, sheath gas flow 50 (arbitrary units), auxiliary gas flow 7 (arbitrary units) and sweep gas flow 5 (arbitrary units). The mass spec analysis was performed in a full MS and data dependent MS2 (Top 10) mode, with a full scan range of 300-1200 m/z, resolution 70,000, automatic gain control at 1 x10⁶ and a maximum injection time of 250 ms. MS2 parameters were: resolution 17,500, automatic gain control was set at 1 x10⁵ with a maximum injection time of 120 ms.

2.17 *In vivo* xenografts

Animal handling in this project was carried out by Susan Mason (Karen Blyth lab, CRUK Beatson Institute). Project license number: PPL70/8645. 5x10⁶ Liv7k cells were subcutaneously injected into NOD/SCID mice (n=20). Mice were split into treatment or control groups by cage assignment (n=10 per group). Montelukast (5

mg/kg) or vehicle control were administered daily by oral gavage once tumours were palpable and had reached a predetermined size (~5 mm). Tumour volume was calculated as $(\text{length} \times \text{width}^2) / 2$, and statistical significance between the two groups was determined by unpaired t-test. Thereafter, measurements were taken using calipers three times weekly until tumour size reached 15mm in any direction, as per licence conditions. Mice were taken at this point and survival curves were plotted. Statistical significance of survival was determined using Log-rank test.

2.18 Immunohistochemistry

Immunohistochemistry (IHC) was carried out by Colin Nixon and the Beatson histology department. Tumour xenografts were fixed in 4% formaldehyde for 24-36 hours and embedded in paraffin. Slices were adhered to glass slides for staining. Prior to staining, slides were washed twice in 1 x PBST and blocked for six minutes in peroxidase-blocking solution (Dako #S2023). Staining was performed using the Dako Autostainer. Sections were washed twice in 1 x PBST and blocked for 30 minutes in 2.5% normal horse serum (Vector #MP-6401-15) or Mouse on Mouse Blocking Reagent (Vector #MKB-2213). Primary antibodies and their dilutions used are listed in Table 2.13. Secondary antibodies, HRP conjugated goat anti-mouse (Dako #K4001), and horse anti-rabbit (Vector #MP-6401-15) were used as appropriate. After further washing 1 x PBST, 3,3'-diaminobenzidine tetrahydrochloride (Dako #K3468) was added and slides were counterstained with haematoxylin Z solution, and mounted with DPX (Sigma #44581). Tissue sections were scanned and images uploaded into Halo (Indica Labs) for staining analysis.

| Target | Species | Supplier | Catalog # | Dilution |
|------------------|---------|-----------------|-----------|----------|
| Ki67 | Rabbit | Thermo Fisher | RM-9106 | 1:500 |
| AKT (phospho) | Rabbit | Cell Signalling | 4060 | 1:250 |
| ERK1/2 (phospho) | Rabbit | Cell Signalling | 9101 | 1:250 |
| ERK1/2 | Rabbit | Cell Signalling | 9102 | 1:250 |
| MTOR (phospho) | Rabbit | Cell Signalling | 2976 | 1:100 |
| HLA | Mouse | Abcam | ab70328 | 1:100 |
| F4/80 | Rat | Abcam | ab6640 | 1:250 |
| NIMP | Rat | Abcam | ab2557 | 1:100 |

Table 2.13 List of primary antibodies used for immunohistochemistry.

2.19 Patient sample acquisition and processing

Patient samples were acquired from the NHS Queen Elizabeth University Hospital in Glasgow and were restricted to HPV- negative primary tumours with evidence of lymph node involvement. Processing of samples involved either snap freezing for RNA/DNA extraction, fixation in formaldehyde for immunohistochemical staining or culturing of fresh tissue for the generation of primary cell lines. Frozen samples were processed as in Biankin[407] *et al.*, 2012.

Chapter 3 Results – High Throughput Screening

The over-arching aim of this project was to identify novel driver genes in oral squamous cell carcinoma. We chose to approach this using an aggressive (T42Nb) patient derived cell line (Liv7k), utilising hypoxic conditions to mimic the common feature of HNSCC tumours. As such, siRNA and drug-repurposing screens were performed in both hypoxia (0.1% O₂) and normoxic (21% O₂) conditions. This allowed for the selection of genes or drugs based on their response in each condition. A complete protocol for both screens can be found in chapter 2, but a brief summary of the process is provided in Figure 3.1.

Percentage growth inhibition was the primary output in both the siRNA and drug screens, and was calculated relative to the non-targeting control siRNA and DMSO vehicle control, respectively. The negative controls were also used to

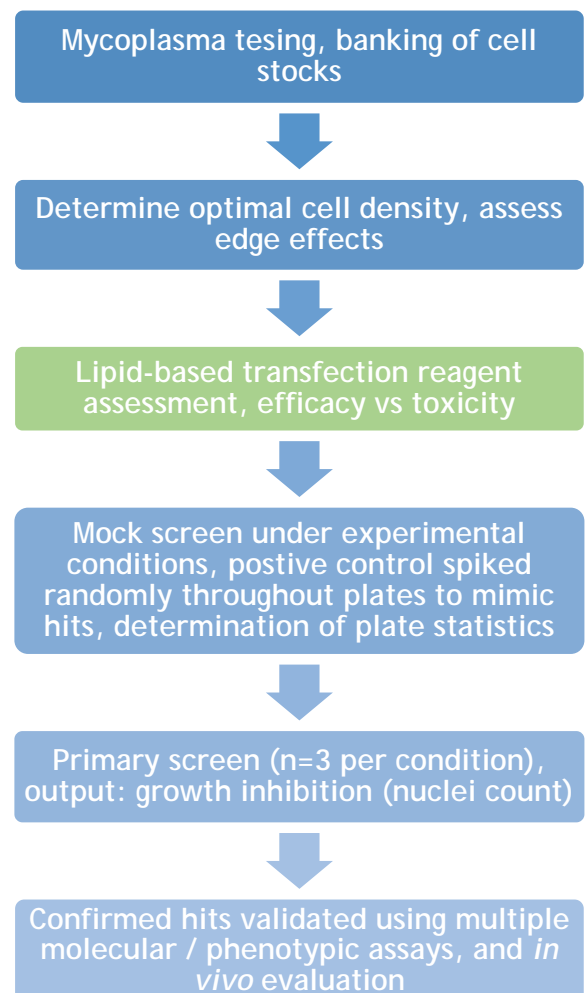


Figure 3.1 Screening workflow summary.

The process applies to both compound and siRNA screens, except for transfection reagent assessment (green).

monitor data variability across all plates throughout the screen. The positive control (siAllStars in the siRNA screen and staurosporine in the drug screen) was used to monitor the consistency of data produced and aid in the selection of hits. This chapter provides an overview of the quality assessment of the siRNA and drug screens.

3.1 siRNA Screen

The primary screen was performed in normoxic and hypoxic (0.1% O₂) conditions in an effort to recapitulate the low oxygen environment often found in solid HNSCCs [408]. In total, 18,175 genes were silenced using the Dharmacon siGENOME library (GE Healthcare) which is broken down into functional classes in Table 3.1.

| siRNA Library Class | Number of Genes |
|----------------------------|-----------------|
| Kinase | 720 |
| G-Protein Coupled Receptor | 390 |
| Phosphatase | 256 |
| Ion Channel | 352 |
| Drug Target | 4,795 |
| Protease | 480 |
| Ubiquitin | 600 |
| Rest of Genome | 10,582 |
| Total | 18,175 |

Table 3.1 Details of the Dharmacon siRNA library.

In the siRNA screen, the positive and negative controls used were All Stars siRNA (Qiagen) and non-targeting control siRNA (NTC; Dharmacon On-Target Plus), respectively. The cell nuclei counts for the control cells were highly consistent within each batch, although normoxic negative controls typically had a higher cell count than hypoxic cells, indicating a faster rate of proliferation (Figure 3.2). The primary method of assessing the quality of the siRNA screen was plate z score, which calculates the difference in growth inhibition between the positive and negative controls. A z score of > 0.3 is typically deemed acceptable, but the majority of plates fell above 0.4, indicating a highly robust assay (Figure 3.3).

Binning of the results revealed a normal distribution of percentage growth inhibition in both oxygen conditions (Figure 3.4), with most of the siRNAs yielding a percentage growth inhibition of between 0-20%. A greater percentage growth inhibition was observed in the normoxic condition, possibly owing to a higher rate of proliferation in these cells. Given this, the percentage growth inhibition in the hypoxic condition was mean-normalised to the normoxic condition in order to make the results more comparable. The strictly standardised mean difference (SSMD) was used as a measure of effect size, with more negative values representing a higher percentage growth inhibition (Figure 3.5). This also allowed the confirmation of the effect of silencing genes that are known to be essential for cell viability, such as WEE1 or PLK1. All calculations used in the analysis of the siRNA screen can be found in chapter 2. In order to identify a greater number of hits, the median growth inhibition was used in the initial screen. However, validation experiments utilised the mean growth inhibition in order to provide greater stringency.

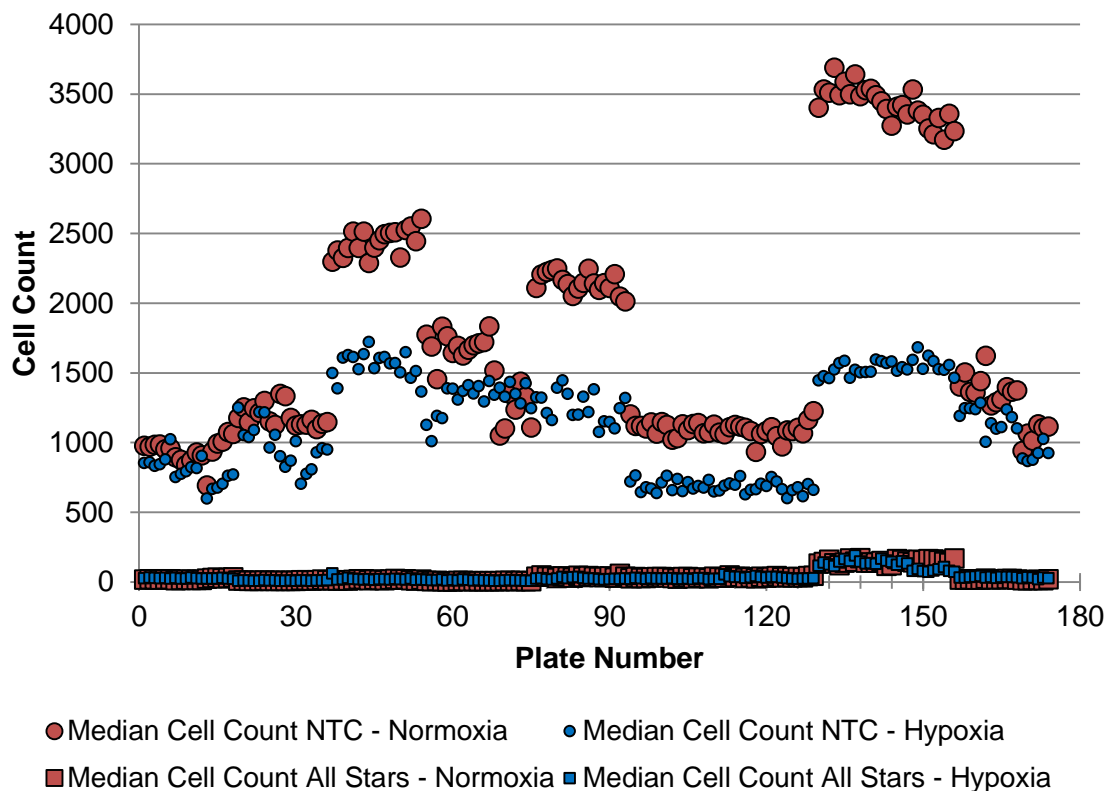


Figure 3.2 Average nuclei count for control wells throughout the siRNA screen. Values are plate averages of non-targeting (NTC) and All Stars control wells. Control outliers were excluded prior to analysis.

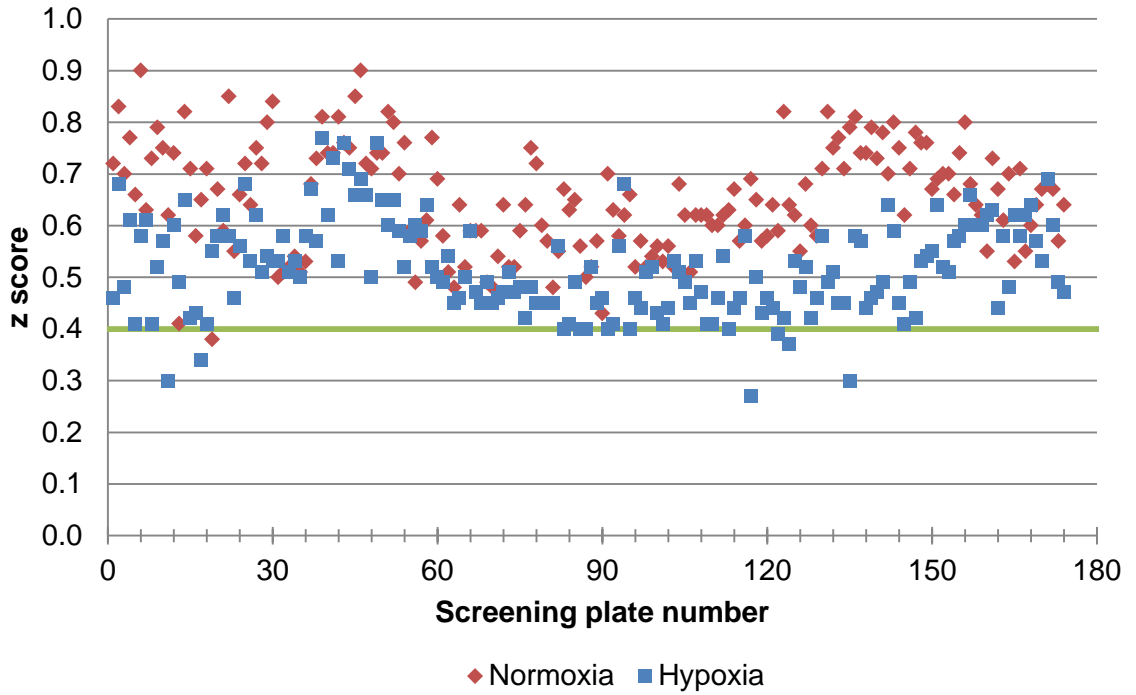


Figure 3.3 siRNA screen z score values (per plate). Values of ≥ 0.3 (indicated by green line) were considered within the acceptable limits. Greater variability was observed in the hypoxic condition. Plates that dropped below the 0.3 threshold were repeated.

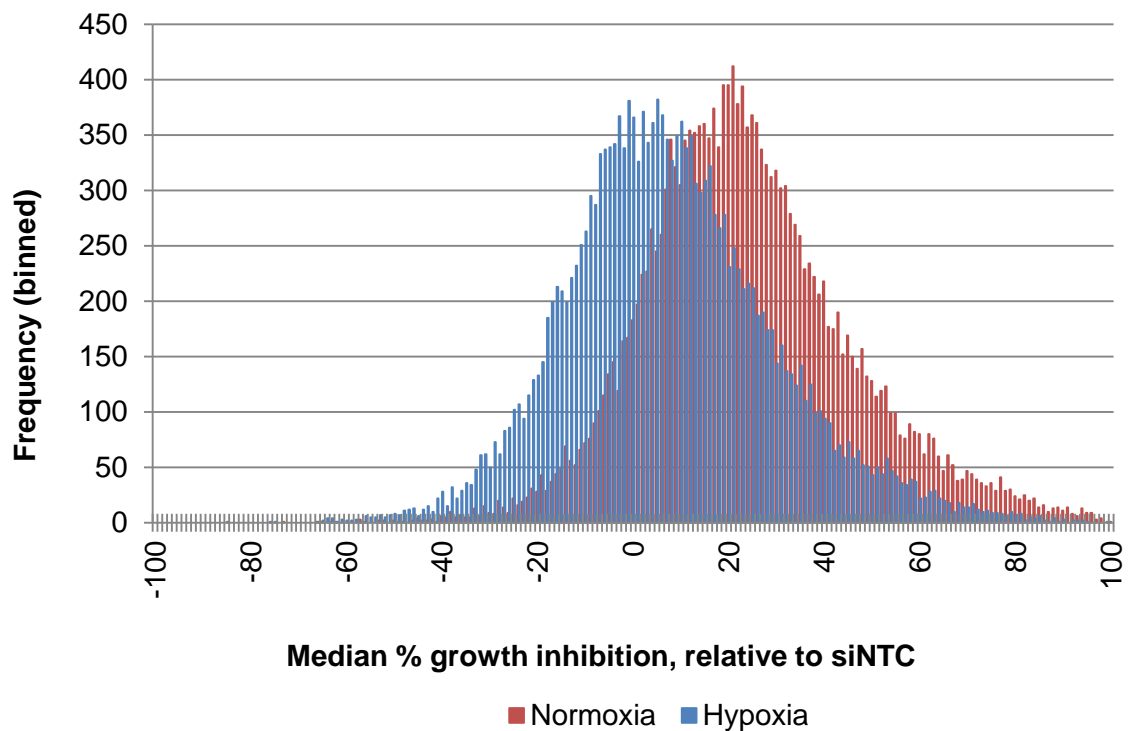
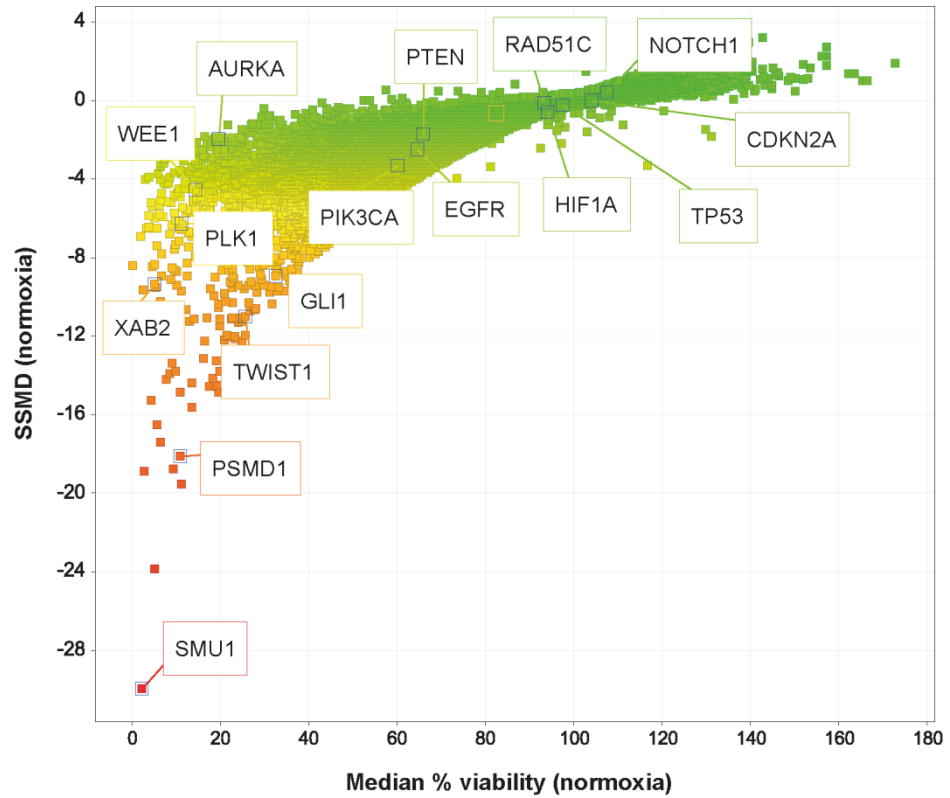


Figure 3.4 Frequency distribution chart of percentage growth inhibition in normoxic and hypoxic conditions. A clear shift was observed in the mean percentage growth inhibition of cells grown in the normoxic condition compared to the hypoxic condition.

A



B

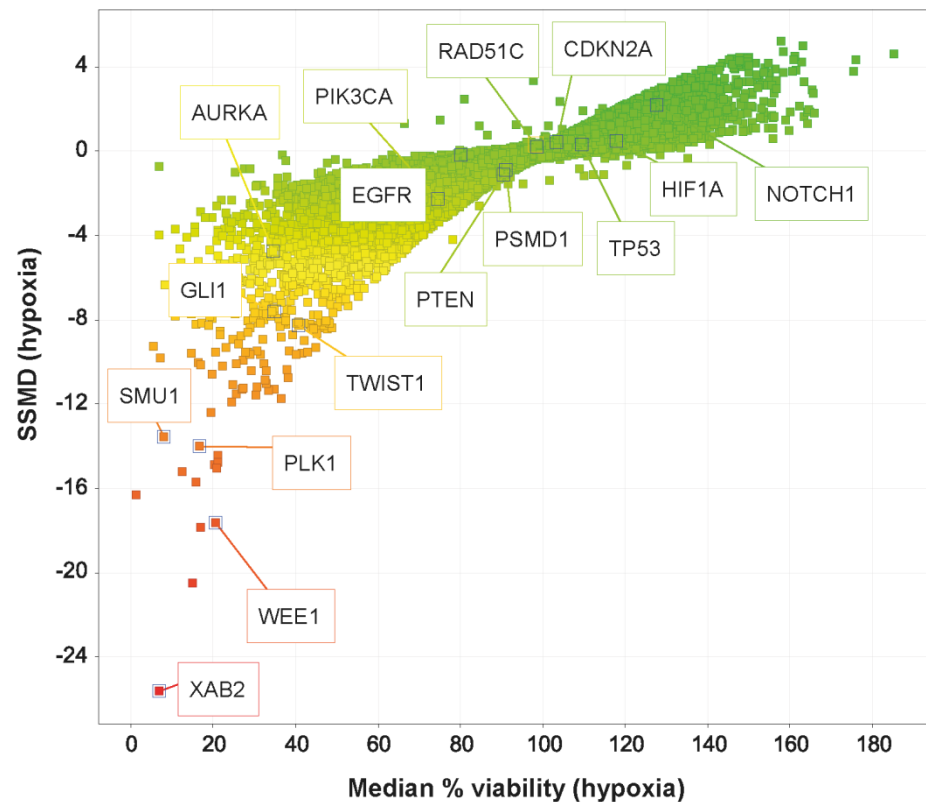


Figure 3.5 SSMD values for all tested siRNAs, relative to NTC, in (A) normoxic and (B) hypoxic conditions. SSMD is a measure of effect size - the more negative the value, the higher the percentage growth inhibition (or the lower the cell viability). Some known driver genes in HNSCC, as well as genes essential for cell viability are labelled.

3.2 Drug-Repurposing Screen

As an additional method of identifying targetable genes in HNSCC, a drug-repurposing screen was employed, where the efficacy of 1,351 FDA-approved drugs developed for cancer and non-cancer indications were assessed for their ability to inhibit the growth of Liv7k cells *in vitro*. The drug libraries used are listed in chapter 2. Drugs chosen for further investigation were required to meet three main criteria: (1) result in over 90% growth inhibition; (2) exhibit higher efficacy under hypoxia; and (3) exhibit selectivity for Liv7k cells over non-cancer cells/other cancer types. The last was included, based on comparisons from previous drug screens carried out within the Screening Facility. The results from the drug screen are shown in Figure 3.6 in which drugs are coloured based on their library of origin. Interestingly, the procollagen C-proteinase inhibitor (UK-383367) and estradiol valerate were found to have a greater effect on cell viability in hypoxia, but this angle was not followed up in this project.

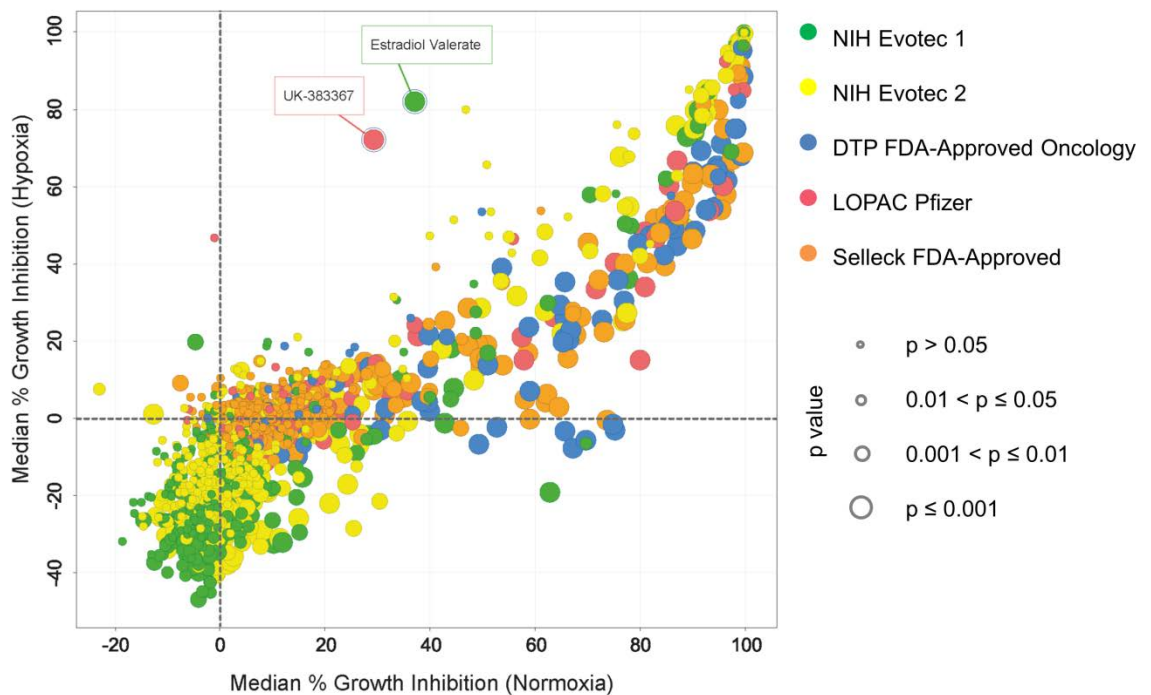


Figure 3.6 Scatter plot showing percentage growth inhibition of Liv7k cell line in response to treatment with FDA-approved compounds. A single concentration of 10 μ M was used for all compounds, and growth inhibition values were normalised to DMSO vehicle control. Results are the median of three screening replicates. Colours indicate the compound library used: Green, NIH Evotec Collection 1; Yellow, NIH Evotec Collection 2; Blue, Developmental Therapeutics Program (DTP) FDA-Approved Oncology Set; Red, LOPAC Pfizer (Sigma Aldrich); Orange, Selleck FDA-Approved Library. Circle size depicts significance according to unpaired t-test (p value). Dashed lines indicate 0% growth inhibition in both conditions.

3.3 Screening Analysis

The results from both screens were analysed and combined with data from a number of other sources, including RNA and whole exome sequencing, pathway analysis software, in-house screening data and publically available patient datasets such as The Cancer Genome Atlas (TCGA). This allowed for the selection of the genes most likely to be involved in HNSCC progression. The validation approach of genes of interest largely depended on their function within the cell (i.e. metabolism, cell movement, epigenetics). Whole exome sequencing revealed the presence of a commonly amplified region of chromosome three, while a differential susceptibility to gene silencing in hypoxia formed the basis of a project centred on triglyceride and ether lipid metabolism. Finally, the drug-repurposing screen identified a dependence of oral cancer cells on cysteinyl leukotriene signalling (involved in the inflammatory response).

Chapter 4 Results – Identification of HNSCC survival significant genes in the 3q26-29 amplicon

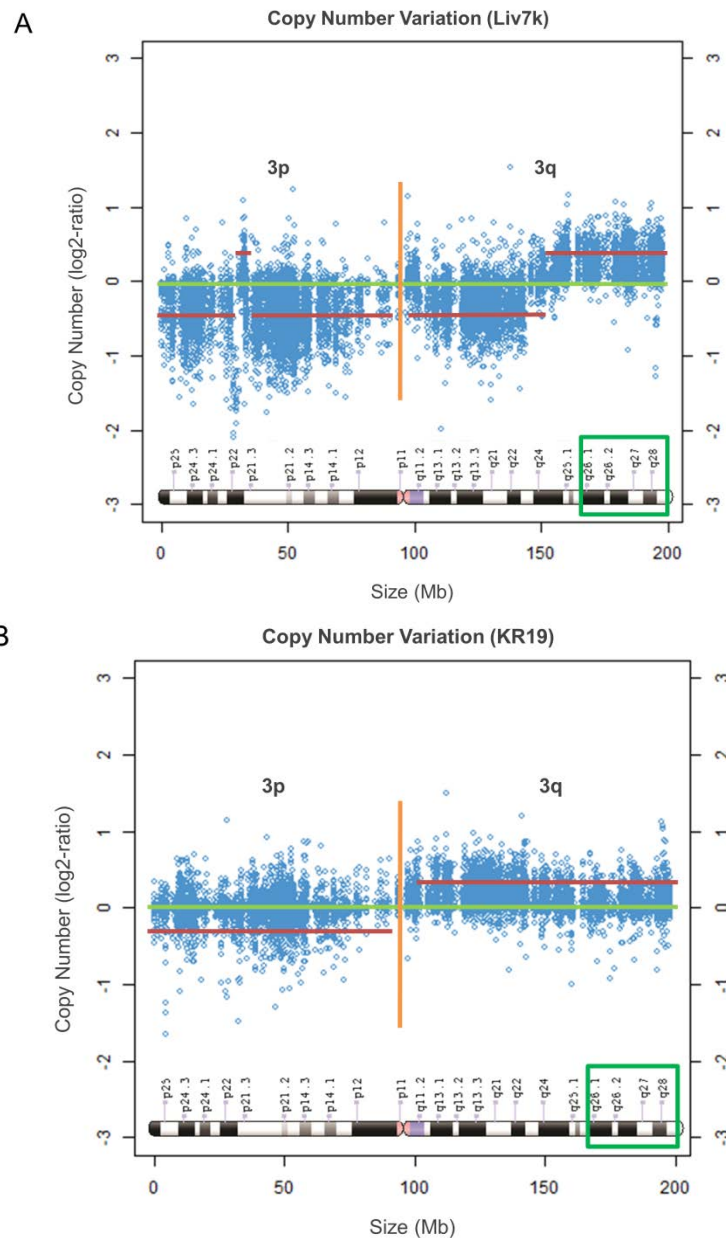
Whole exome sequencing of aggressive patient derived oral cancer cell lines revealed copy number amplification of a region at the terminal end of chromosome three (3q26-29). The region harbours 366 genes, 188 of which are protein coding. This chapter presents an analysis of genes within the amplicon, supported by transcriptomic data from The Cancer Genome Atlas (TCGA, n = 522 samples), experimental screening data and pathway analysis. This led to the generation of a 6-gene set, which was statistically significant for patient survival. Knockdown of these highly expressed genes led to high percentage growth inhibition in an oral SCC cell line. Two genes were selected for target validation studies.

Chromosome 3q26-29 is the most frequently amplified region in HNSCC and is a negative prognostic factor associated with increased invasive potential and decreased overall survival [409]. The region harbours multiple driver genes including *PIK3CA*, which encodes the p110 catalytic subunit of PI3K[410]; *SOX2*, a key regulator of stem cell differentiation[116]; *TP63*, a relative of *TP53* with pleiotropic functions[411]; *TERC*, which encodes the RNA component of telomerase[412] and *PRKCI*, a serine/threonine kinase in the NF-KB pathway[413].

The close proximity of these genes makes an independent assessment of their oncogenic potential difficult and this complexity is further compounded by the co-amplification of other genes in the region. It is likely that most of the genes residing in these regions are passengers experiencing copy number gain in parallel with driver genes[414]; however, the presence of yet unidentified driver genes remains a possibility.

4.1 Amplification of chromosome 3q26-29 in oral SCC cell lines

In order to determine if our patient derived cell lines contained the same pattern of copy number alteration as those in the TCGA dataset (see Figure 1.4), whole exome sequencing (outsourced to Oxford Gene Technology, UK) was performed. This revealed copy number gain of 3q26-29 in the Liv7k and KR19 cell lines but deletion in the Liv37k cell line, when compared to a reference human genome HG19 (Figure 4.1). The Liv7k cell line was used for the majority of subsequent phenotypic experiments, as they were a good representation of the 20% of patient tumour samples with the amplicon.



4.2 Identification of pro-oncogenic factors in 3q26-29

Chromosome 3 is the third largest chromosome and contains 1078 protein coding genes[415]. 3q26-29 amplification is not unique to HNSC - it is a feature of squamous cell carcinomas in general, including those of the lung[113], cervix[416], oesophagus[417] and skin[418], and is consistently correlated with poor prognosis in these cancers. The 3q26-29 amplicon consists of four cytogenetic bands and contains 366 genes (188 of which are protein coding). TCGA analysis reveals that 117 (62%) of the 366 genes are upregulated at mRNA level (z score > 2) in more than 10% of patients with HNSCC (Figure 4.2).

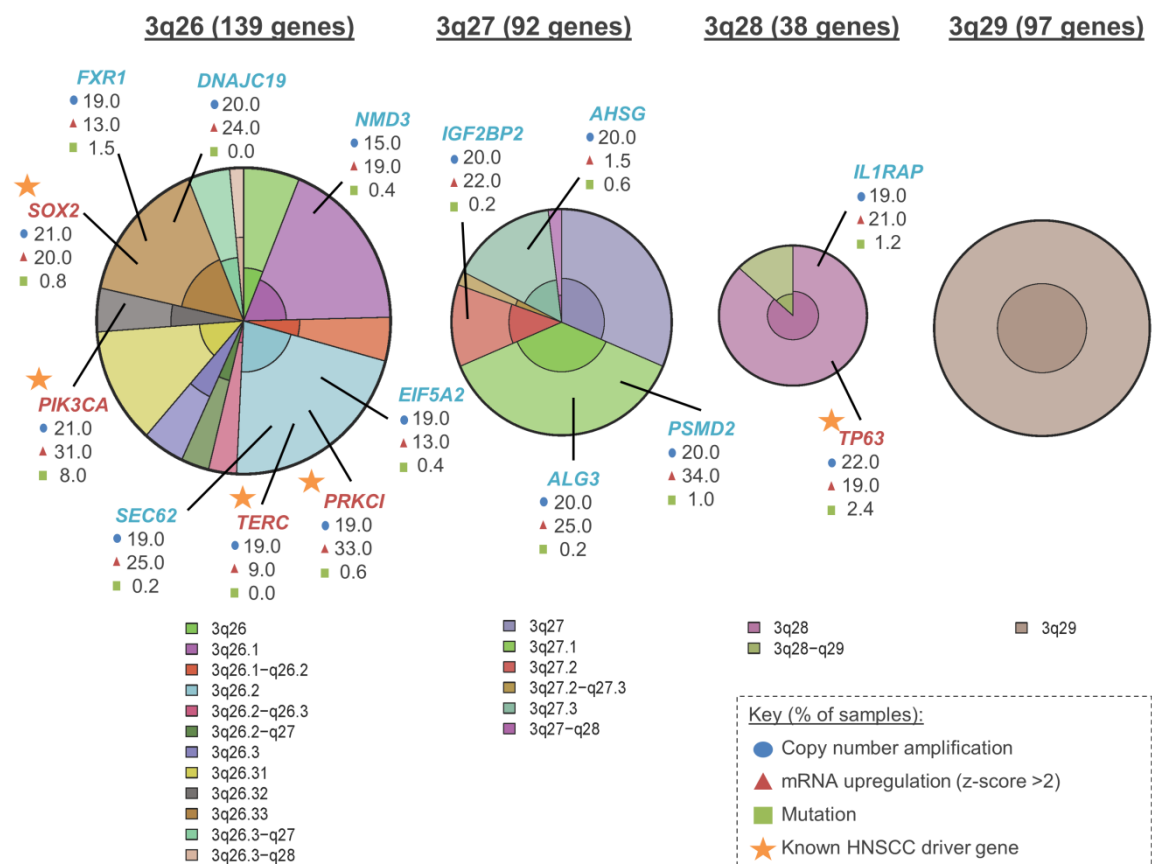


Figure 4.2 Expression profile of genes contained within 3q26-29 amplicon. 3q26-29 contains 366 gene identities, which are split between four sub-regions. Genes are arranged by chromosomal location; the size of the circle depicts the total number of genes within the denoted chromosomal locus and inner segments represent the number of genes within that locus with mRNA upregulation (defined by a statistical cut-off of z score > 2 in > 10% samples, TCGA HNSCC dataset, n = 522 samples). Copy number amplification, mRNA upregulation and mutation frequencies are listed for known HNSCC driver genes (red, starred) and genes that we have identified to be significant for survival in our analysis (blue). Published in [419].

4.3 10 genes are implicated in HNSCC patient survival (TCGA)

In order to determine which of the 188 protein-coding genes were most relevant to HNSCC progression, additional criteria were applied. Interrogation of gene mRNA expression data in combination with patient survival statistics allowed for the identification of oncogenic targets with potential therapeutic significance. Using this approach, a total of ten genes (*AHSG*, *EIF5A2*, *FXR1*, *IGF2BP2*, *PSMD2*, *SEC62*, *ALG3*, *DNAJC19*, *IL1RAP* and *NMD3*) were identified as having a negative effect on overall and disease free survival when overexpressed at mRNA level in HNSCCs ($p \leq 0.05$) (Figure 4.3).

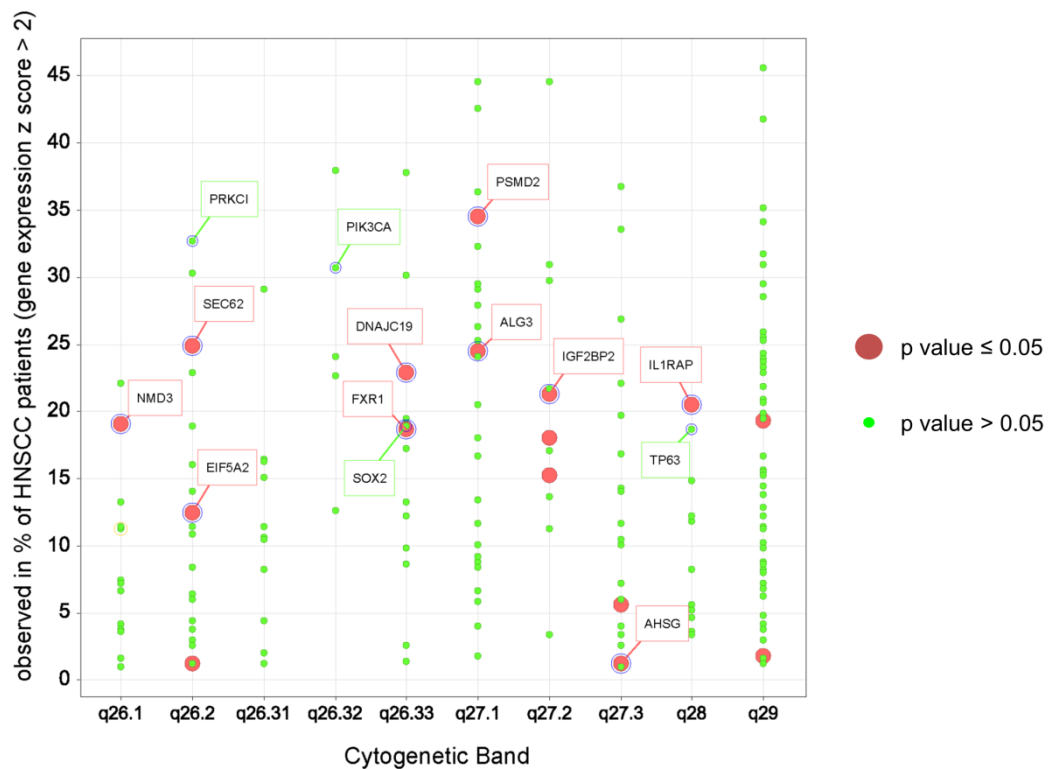


Figure 4.3 Survival significant genes are scattered throughout 3q26-29. Correlation plot of genes showing the percentage of patients with increased mRNA expression as defined by a z score of ≥ 2 versus chromosomal location (TCGA HNSCC dataset, $n = 522$ samples). Circle size and colour denote significance of reduced overall survival. Genes identified as being highly significant for patient survival in this analysis and known HNSCC driver genes are labelled. Published in [419].

These genes are spread over the 3q26-29 amplicon with no obvious clustering. In addition, six genes (*AHSG*, *EIF5A2*, *FXR1*, *IGF2BP2*, *PSMD2* and *SEC62*) have a greater cumulative effect on survival when overexpressed simultaneously (Figure 4.4a) (overall survival $p=2.78 \times 10^{-06}$, disease-free survival $P=1.63 \times 10^{-03}$). Although not the most frequently overexpressed gene in the analysis, overexpression of *IGF2BP2* correlated with most significant decrease in survival.

Four of the identified genes in the 6-gene set (*AHSG*, *EIF5A2*, *FXR1* and *IGF2BP2*) encode RNA-binding proteins (RBPs) which regulate the translation of numerous gene transcripts and hence influence a wide range of cellular functions. Pathway analysis of survival significant genes identified interactions with known oncogenes in HSNCC which are also frequently amplified or overexpressed, including *PRKCI*, *SOX2* and *ECT2* (Figure 4.4b).

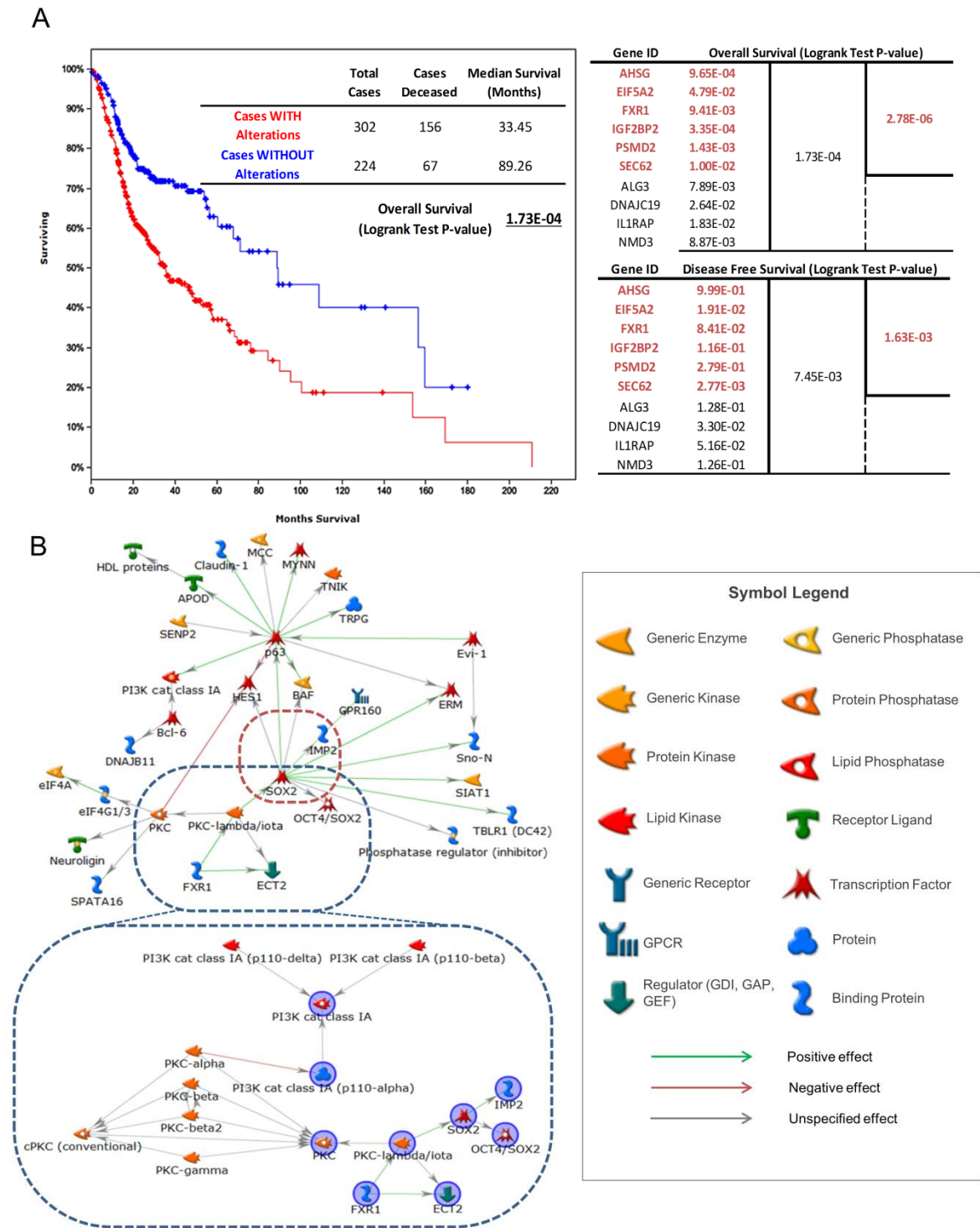


Figure 4.4 Pathway analysis of survival significant genes reveals links to known oncogenes.

(A) Survival analysis: left: Kaplan–Meier curves showing overall survival of patients with (red) or without (blue) overexpression of the 10-gene survival set identified in our analysis; right: table showing overall and disease-free survival p-values for overexpression of individual genes and concurrent overexpression of the gene set. Survival significance is categorised by log rank value: $*10^{-1}$ $**10^{-2}$ $***10^{-3}$ $****10^{-4}$. Survival is based on mRNA upregulation (z score ≥ 2) only. (B) Pathway analysis identifies interactions between survival significant genes and a module of core genes (PRKCI, SOX2, ECT2 and FXR1) which are known to be significant in HNSCC progression. GeneGo MetaCore™ was used to generate the signalling network of gene connections. Published in [419].

4.4 *IGF2BP2* and *PSMD2* are required for Liv7k viability in vitro and are highly significant for patient survival

A number of survival-associated genes were found to be significantly upregulated at mRNA level in both the Liv7k cell line and TCGA dataset (blue dots, Figure 1.9). Cross-referencing TCGA data with results from a whole genome siRNA screen identifies genes that are important for cell viability in the Liv7k cell line. Two genes (*IGF2BP2*, *PSMD2*) met all criteria, exhibiting amplified gene copy number, mRNA upregulation and significance for survival in patients, in addition to being required for Liv7k viability (Figure 4.5 and Figure 4.6).

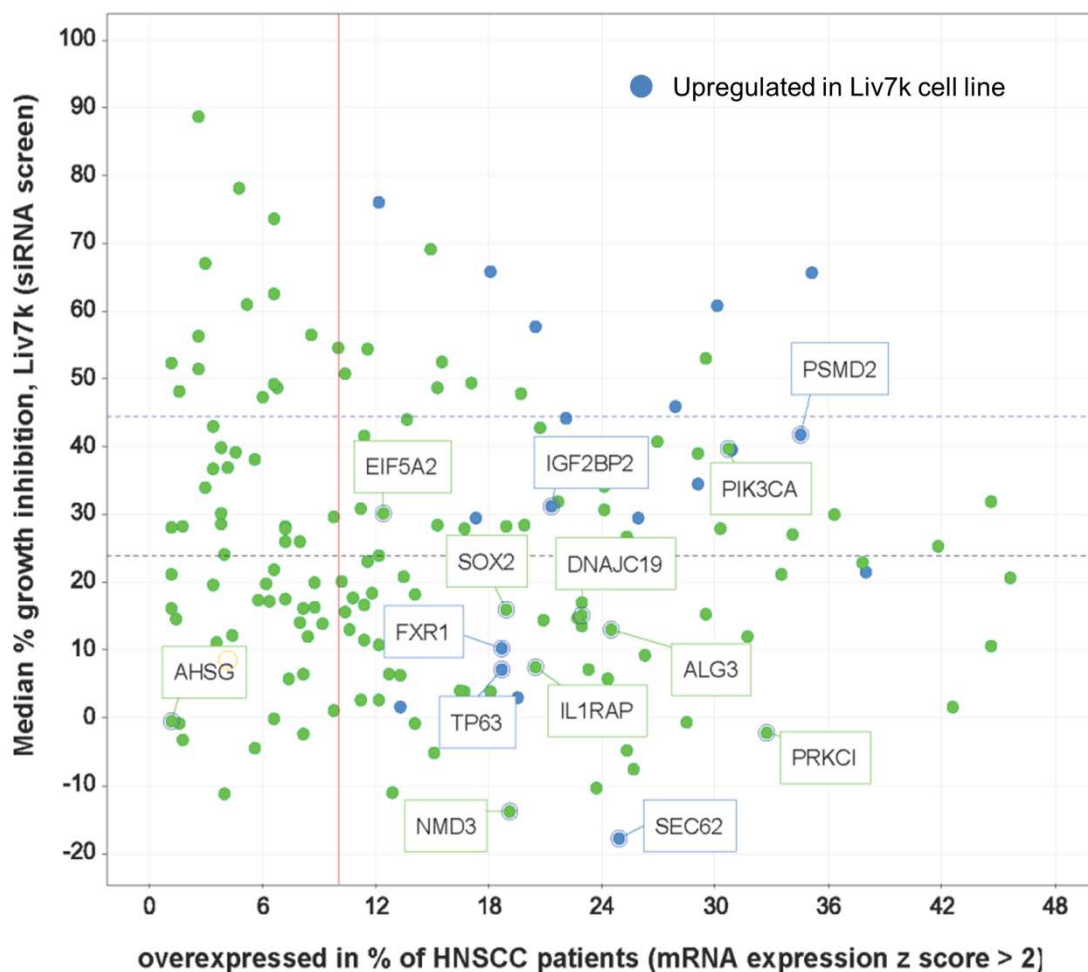


Figure 4.5 Highly expressed genes are also important for Liv7k cell viability. Scatter plot of mRNA expression in TCGA patient data (percentage of patients with a z score ≥ 2 , cut-off minimum 10% patients, red vertical line) and Liv7k siRNA screen (percentage growth inhibition $>$ mean + 1SD, blue upper horizontal line) identifies genes most substantially upregulated in patient samples and required for Liv7k viability. Blue dots represent 22 most highly expressed genes from RNA sequencing of Liv7k cell line, while 10 genes identified as significant for patient survival are labelled with gene symbol.

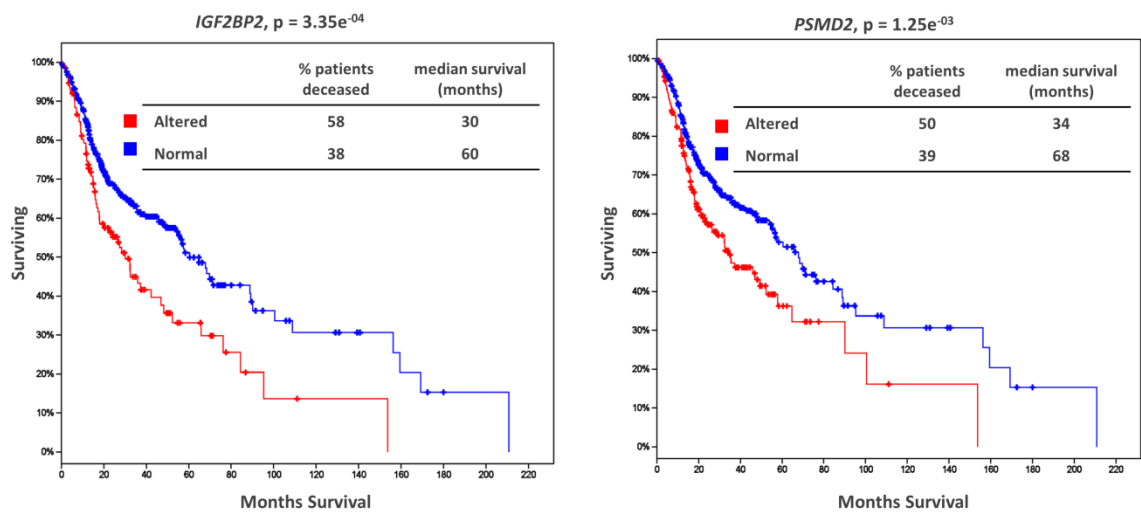


Figure 4.6 *IGF2BP2* and *PSMD2* overexpression is significantly correlated with reduced overall survival in HNSCC patients. mRNA overexpression (z score > 2) of either *IGF2BP2* or *PSMD2* is highly significant for overall survival in patients, as shown in Kaplan-Meier curves (log-rank test, $p < 0.01$). Data generated from TCGA HNSCC dataset ($n = 522$ patients). Percentage of deceased patients at time of publication and median survival statistics are presented in graph.

4.5 Discussion

In this chapter, the process of identifying potential oncogenic driver genes in HNSCC is described. First, amplification of a region located at the terminal end of chromosome 3q in patient derived cell lines was confirmed. This region is amplified in a number of squamous cell carcinomas and is consistently associated with a poor prognosis in patients[113]. The region itself contains 188 protein-coding genes, of which 117 (62%) are overexpressed (z score > 2) in more than 10% of patients with HNSCC (see Figure 4.5). Additionally, 10 genes in the amplicon were found to be statistically correlated with for patient survival ($p < 0.05$) in the TCGA HNSCC dataset (*AHSG*, *EIF5A2*, *FXR1*, *IGF2BP2*, *PSMD2*, *SEC62*, *ALG3*, *DNAJC19*, *IL1RAP* and *NMD3*). These genes are spread throughout the 3q26-29 region, with no obvious clustering. Moreover, six of these genes have a greater negative effect on overall survival when overexpressed simultaneously (*AHSG*, *EIF5A2*, *FXR1*, *IGF2BP2*, *PSMD2* and *SEC62*).

Pathway analysis of the 10-gene set uncovered a number of interactions with known HNSCC driver genes, such as the stem cell maintenance gene *SOX2* and

the protein kinase *PRKCI*. Of the 117 overexpressed genes, knockdown of 46 genes (39%) caused a loss of viability greater than mean ± 1 SD in a patient derived cell line. In the 10-gene set, overexpression of insulin-like growth factor 2 binding protein 2 (*IGF2BP2*, 3q27.2) correlated most significantly with decreased patient survival, and silencing of the gene in Liv7k cells led to significant growth inhibition in a whole genome siRNA screen. Taking all of the data into account, *IGF2BP2* was the first gene chosen for validation.

Similarly, overexpression of proteasome 26S subunit, non-ATPase (*PSMD2*, 3q27.1) correlates significantly with reduced patient survival. Moreover, silencing of the gene led to the highest percentage growth inhibition of survival significant genes in the Liv7k cell line. The gene encodes a subunit of the 19S regulatory cap, which flanks the 20S catalytic core of the 26S proteasome. Rapidly proliferating cells exhibit high rates of protein turnover and thus have an increased reliance on proteasomal machinery[420]. Chemical inhibition of the proteasome is an approved therapy for multiple myeloma[421], but has failed to provide a similar benefit in solid cancers such as HNSCC[422]. This is despite *in vitro* success, where treatment with the proteasomal inhibitor, bortezomib, was shown to induce apoptosis synergistically with cisplatin in HNSCC cells[423]. Moreover, bortezomib-induced proteasomal inhibition of HPV-positive HNSCC cells led to the restoration of functional p53 and the induction of cell cycle arrest[424]. In lung cancer, *PSMD2* was identified as part of a metastatic gene signature, while silencing of the gene resulted in growth inhibition in lung adenocarcinoma cells[425, 426]. Given the importance of proteasomal activity in cancer and the inhibitory effect of *PSMD2* silencing in a patient derived cell line, the gene was selected for follow up.

Although not chosen for validation, previous studies have shown that other genes in the set can drive SCC progression and display a striking degree of cooperation in doing so. Four genes (*AHSG*, *EIF5A2*, *FXR1* and *IGF2BP2*) encode RNA-binding proteins (RBPs), which can regulate the translation and stability of a number of gene targets and potentially affect a host of signalling pathways. Interestingly, HNSCCs have been shown to be enriched for genes encoding RBPs compared to matched normal tissue ($p < 0.05$)[427].

In a study of 81 HNSCC tumour samples, increased levels of fragile X-related gene 1 (*FXR1*, 3q26.33) mRNA was correlated with metastasis-free survival[428]. The same study also showed that FXR1 binds to and regulates the expression of two other 3q26-29 genes, epithelial cell transforming sequence 2 (*ECT2*) and protein kinase C iota (*PRKCI*), in non-small cell lung carcinoma (NSCLC). *ECT2* was overexpressed in 29% of patient tumour samples in this analysis, and has been shown to drive cell proliferation in oral SCC[429]. *PRKCI* is co-amplified with sex determining region Y (*SOX2*) and both genes cooperate to activate hedgehog signalling in lung squamous cell carcinoma (LSCC)[430]. FXR1 has also been shown to overcome cellular senescence in HNSCC through its joint modulation of p21 and stabilisation of TERC mRNA[431].

Similarly, increased protein expression of SEC62 (*SEC62*, 3q26.2) was correlated with reduced overall and disease-free survival in 35 pre-treatment biopsies taken from patients with locally advanced HNSCC[432]. SEC62, another RBP, was identified as a potential oncogenic driver in prostate cancer and silencing of the gene significantly reduced the invasive potential of a number of cancer cell lines[433, 434]. Additionally, expression of the protein is essential for the maintenance of ER stress tolerance in the disease[435].

Although not directly studied in HNSCC, eukaryotic translation initiation factor 5A2 (*EIF5A2*, 3q26.3) is overexpressed in a number of malignancies, where it is correlated with a poor prognosis and/or an aggressive phenotype[436-439]. Knockdown of the gene significantly impaired proliferation, migration and invasion processes in gastric cancer cell lines and was accompanied by downregulation of cyclin D1 (*CCND1*)[440]. Recent studies have shown that EIF5A2 promotes oncogenesis through its upregulation of the metastasis-associated protein 1 gene (*MTA1*) in a c-MYC dependent process, which positively regulates epithelial to mesenchymal transition (EMT)[438]. Recently, it was discovered that functional EIF5A is essential for HIF-1 α activation during hypoxia[441]. In this way, the 3q26-29 amplicon may promote the adaption of HNSCC cells low oxygen environments, thereby driving the selection of cells with a more aggressive phenotype.

The majority of alpha-2-HS-glycoprotein (*AHSG*, 3q27) is synthesized in the liver and secreted into serum where it is involved in bone remodelling[442]. However,

the oral cavity is unique in that it can produce endogenous AHSG, which has been shown to promote a more invasive phenotype in HNSCC cell lines[443]. In support of this role, it has been demonstrated that circulating AHSG can protect matrix metalloprotease 9 (MMP9) from autolytic degradation potentially enhancing invasion[444]. *In vivo* studies have shown that AHSG can also promote the progression of breast cancer through its modulation of TGF β signalling[445], while AHSG^{-/-} mice show a reduced tumour burden in a Lewis Lung carcinoma model[446].

Overall, it is clear that the 3q26-29 amplicon contributes to HNSCC progression through the overexpression of one or more of its constituent genes. However, extricating the network of genes and the role each plays is difficult. Moreover, the degree of cooperation between these genes in HNSCC is unknown and makes the identification of putative driver genes even more challenging. Some of the genes contained within the amplicon are known oncogenes in the disease and a small number are targeted by currently available drugs, for example *PIK3CA*[447] and *PRKCI*[448]. Given the degree of interaction between certain genes, combination therapy may be the optimal way forward. However, the fact that overexpression of known HNSCC oncogenes (such as the two aforementioned genes) did not significantly affect patient survival in the TCGA dataset could place a greater importance on as yet undiscovered upstream mediators.

The PI3K pathway is the most frequently mutated pathway in HNSCC, with a third of pathway genes containing driver mutations[57]. However, of the 162 HNSCC samples overexpressing *PIK3CA* in this analysis, only 21.5% contain activating mutations in the gene. This substantiates the importance of 3q26-29 amplification in HNSCC. Refinement of existing therapies to improve efficacy is a worthwhile venture, however intrinsic heterogeneity of tumours and the development of resistance will always be an obstacle to successful treatment. The development of novel targeted therapeutics is essential to maximise benefit to patients with HSNCC in the long run. There was a strong rationale to follow up of a number of 3q26-29 genes as potential therapeutic targets and/or predictive biomarkers, but based on patient survival data, two genes (*IGF2BP2* and *PSMD2*) were selected to be characterised more fully for their role in HNSCC progression.

Chapter 5 Results – Validation of *IGF2BP2* as a driver gene in oral squamous cell carcinoma

5.1 Introduction

Overexpression of *IGF2BP2* had the most significant correlation in terms of overall patient survival in an analysis of TCGA data. The gene was also shown to be important for viability in a patient derived oral cancer cell line. An RNA-binding protein (RBP), known to be upregulated in many cancers[177], *IGF2BP2* was selected as one of the targets for further investigation in this body of work. A comprehensive summary of what is known about the role of *IGF2BP2* is provided in chapter 1.5. First, validation of knockdown and the effect on growth was carried out using deconvolved siRNA (the same as those used in the screen). Next, pathway analysis was performed on computationally predicted mRNA targets of *IGF2BP2* from a collection of experimentally probed RBP binding sites in human transcriptomes[449]. The wider role of IGF signalling components was assessed using results from the siRNA screen and RNA sequencing data, which were carried out as part of this study.

Based on the purported role of *IGF2BP2* in IGF2-IGF1R-PI3K-AKT signalling[177], a major aim of this project was to determine the effect of *IGF2BP2* depletion on cellular function. To this end, a number of models were created for use in phenotypic assays. These included knockdown of *IGF2BP2* using siRNA, shRNA and CRISPR technologies. Upon validation of effective knockdown, these models were employed in proliferation, migration and invasion assays, as well as other 3D models and metabolic measurements. In addition, western blots were performed to determine if *IGF2BP2* is involved in oncogenic signalling.

5.2 *IGF2BP2* expression in a series of oral SCC cell lines and validation of growth inhibition

Gene expression levels of *IGF2BP2* were measured in a panel of oral cancer and immortalised “normal” control cell lines using qRT-PCR (Figure 5.1). This allowed for categorisation of cell lines, which have high and low gene expression of *IGF2BP2*. In the panel, Liv7k cells had the highest expression of the gene, while Liv37k cells had the lowest, which corresponded to measured copy number. Two immortalised keratinocyte cell lines, OKF4 and OKG4, exhibited moderate expression of *IGF2BP2*. The inhibitory effect on cell growth was validated using a deconvolved pool of the screen siRNA set (Figure 5.2A). The percentage growth inhibition caused by *IGF2BP2* knockdown varied with no obvious selectivity for carcinoma cell lines over the immortalised cell lines. Knockdown efficiency of each deconvolved siRNA is shown in Figure 5.2B, as determined by qRT-PCR and western blot.

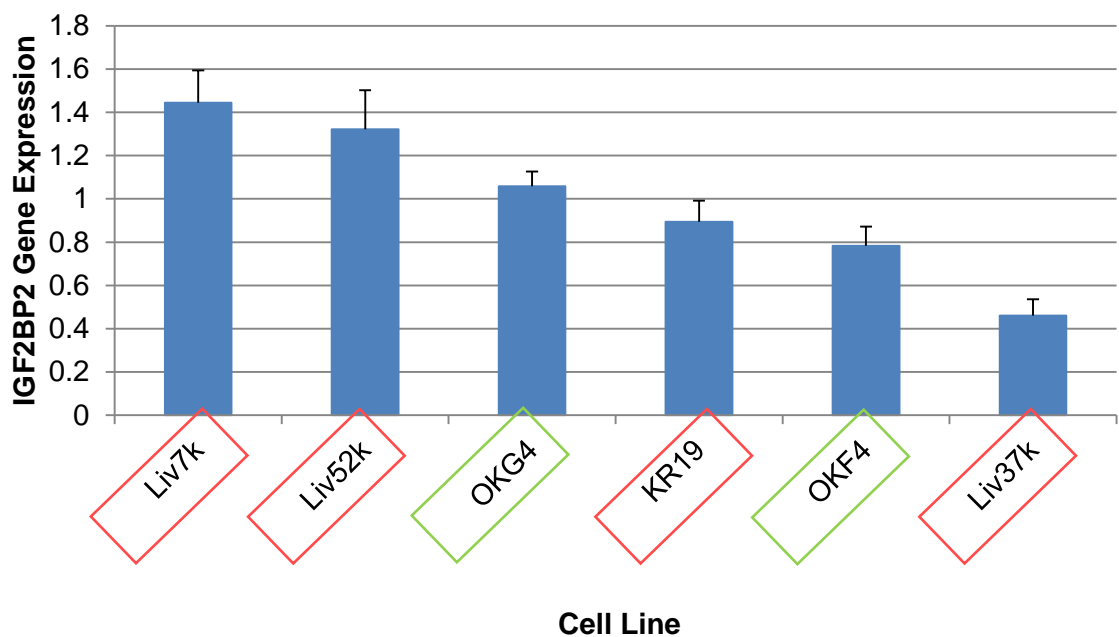


Figure 5.1 : Bar chart showing mRNA expression of *IGF2BP2* in four oral SCC cell lines (Liv7k, Liv52k, KR19, Liv52k) and two oral keratinocyte cell lines (OKF4, OKG4). Gene expression was measured by qRT-PCR and normalised to ACTB. Data is mean \pm SD of three independent experiments.

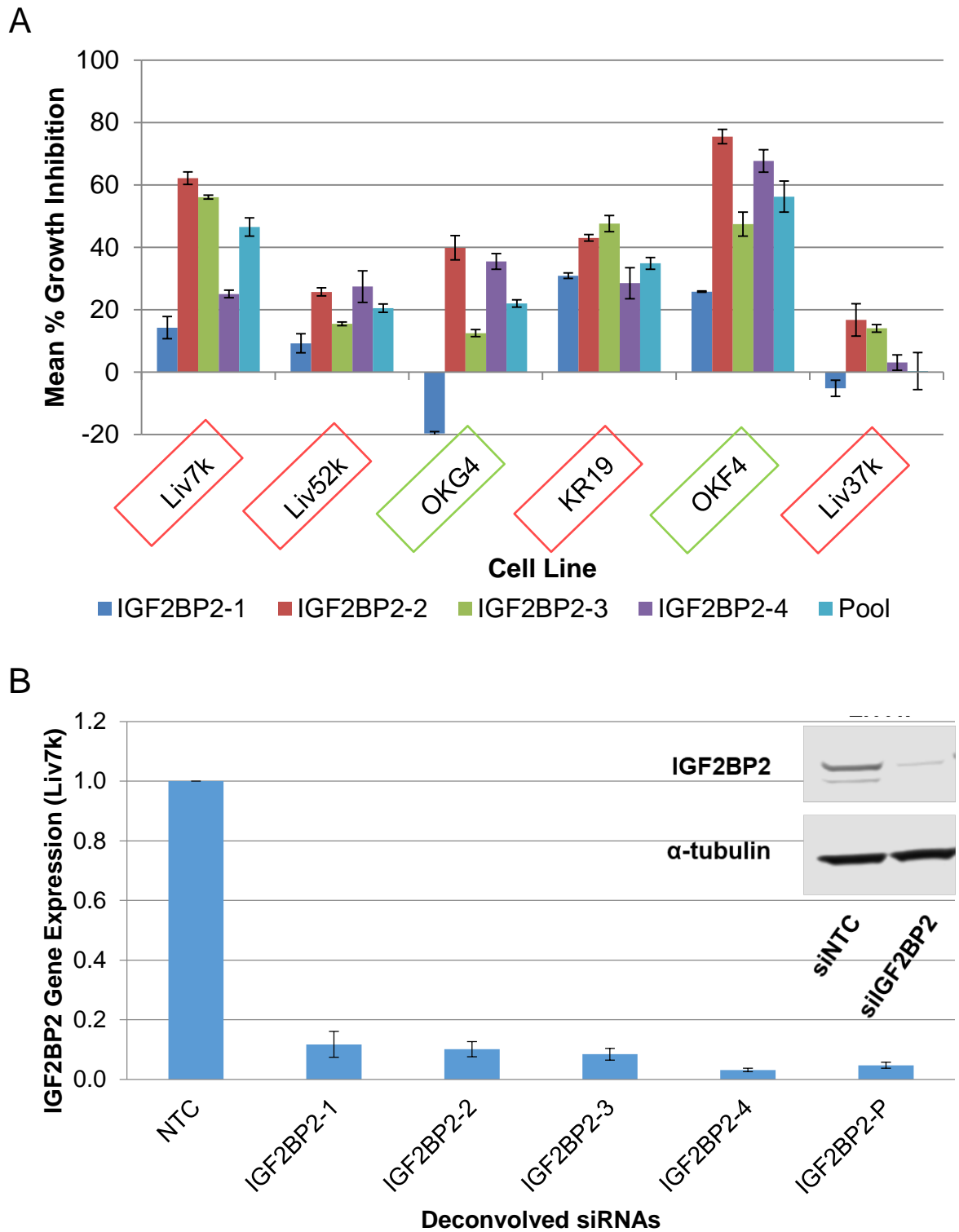


Figure 5.2 Silencing of IGF2BP2 results in growth inhibition in oral SCC and oral keratinocyte cell lines. (A) Bar chart showing the effect of *IGF2BP2* knockdown on cell growth. Results are plotted relative to non-targeting control siRNA (NTC). Data is mean \pm SD of three technical replicates. (B) qRT-PCR showing reduction in *IGF2BP2* gene expression after siRNA knockdown in Liv7k cells. *IGF2BP2* expression was normalised to *ACTB* and presented relative to NTC. Data is mean \pm SD of three biological replicates. Inset: western blot of IGF2BP2 expression after transfection with pooled siRNA used in screen. α -tubulin was used as a loading control.

5.3 Predicted Binding Sites of IGF2BP2

In order to determine a potential role for IGF2BP2 in human cancer, predicted binding targets of the protein were acquired from a publically available database, (POSTAR, platform for exploring POST-trAnscriptional Regulation coordinated by RNA-binding proteins)[449]. These were input into the Reactome (<http://www.reactome.org>)[450] database to determine if IGF2BP2 preferentially bound genes involved in a particular biological process. The POSTAR database contained mRNA targets of the protein in HEK293 cells only, in which there were over 100,000 sequence clusters recognised by IGF2BP2, with preferential binding to a CAUH (H = A/U/C) consensus sequence[451]. Overall, IGF2BP2 binding sequences were present in 3,442 protein coding mRNA transcripts (“Piranha” peak-calling, p-value < 0.01)[449]. Analysis of these transcripts using the Reactome database revealed significant overrepresentation of genes involved in cell cycle progression and metabolism of RNA (Table 5.1) [452, 453].

| Rank | Pathway Identifier | Pathway Name | Genes Found | Genes Total | Ratio | P value | FDR |
|------|--------------------|---|-------------|-------------|--------|----------|----------|
| 1 | R-HSA-69278 | Cell Cycle, Mitotic | 239 | 566 | 0.0418 | 8.33E-10 | 1.72E-06 |
| 2 | R-HSA-1640170 | Cell Cycle | 272 | 680 | 0.0503 | 8.08E-09 | 8.34E-06 |
| 3 | R-HSA-72163 | mRNA Splicing | 96 | 185 | 0.0136 | 2.27E-08 | 1.56E-05 |
| 4 | R-HSA-72203 | Processing of Capped Intron-Containing Pre-mRNA | 121 | 254 | 0.0187 | 3.91E-08 | 2.02E-05 |
| 5 | R-HSA-72172 | mRNA Splicing | 97 | 196 | 0.0145 | 1.62E-07 | 6.69E-05 |
| 6 | R-HSA-69620 | Cell Cycle Checkpoints | 121 | 279 | 0.0206 | 3.75E-06 | 1.29E-03 |
| 7 | R-HSA-8953854 | RNA Metabolism | 285 | 782 | 0.0578 | 7.35E-06 | 2.16E-03 |
| 8 | R-HSA-453279 | Mitotic G1-G1/S phases | 80 | 170 | 0.0125 | 1.10E-05 | 2.83E-03 |
| 9 | R-HSA-3247509 | Chromatin modification | 110 | 257 | 0.0190 | 1.73E-05 | 3.46E-03 |
| 10 | R-HSA-4839726 | Chromatin organization | 110 | 257 | 0.0190 | 1.73E-05 | 3.46E-03 |

Table 5.1 Reactome analysis reveals predicted IGF2BP2 function. The top 10 biological processes of 3,442 protein-coding genes containing IGF2BP2 binding sites in HEK293 cells, as predicted by POSTAR[449]. Pathway hits are ranked by p value. FDR, false discovery rate.

All three IGF2BP family members appear to recognise a similar set of target transcripts, suggesting a degree overlapping functionality [451]. However, this study used exogenously expressed IGF2BP2 and it has been shown that this can lead to aberrant sedimentation of RNA, as evidenced by sucrose gradient sedimentation [155]. Therefore, further validation is needed to confirm binding of IGF2BP2 to its proposed mRNA target.

5.4 IGF2 is highly expressed in tumour cell lines compared to immortalised oral keratinocytes

In chapter 4, *IGF2BP2* was identified as part of an amplified region of chromosome 3 in two oral SCC cell lines (Liv7k, KR19). However, several layers of regulation exist between genomic DNA and the finished gene transcript. Most studies have reported a reasonable correlation between gene copy number (CN) and mRNA expression (GE) [454, 455]. As a rule, CN amplification is a stronger predictor of increased GE than vice versa. Pollock *et al.* reported that 40-60% of high level CN amplifications in human breast cancer tumours also showed elevated GE, while only ~10% of highly expressed genes were amplified [456]. In line with this, approximately 36% of patients with amplified *IGF2BP2* copy number in the TCGA HNSCC database also exhibit overexpression of *IGF2BP2* mRNA.

Previous studies have shown that IGF2BP2 binds to and stabilises *IGF2* mRNA, thus regulating its translation [180, 457, 458], making the insulin signalling pathway a primary target for functional validation. IGF2 is a growth factor, which is most highly expressed in the early developmental stages. To this end, RNA sequencing of two patient-derived oral SCC (Liv7k, KR19) and two purchased oral keratinocyte cell lines (OKF4, OKG4) revealed mRNA expression levels of insulin pathway components (Liv7k comparisons are shown in **Figure 5.3** and **5.4**, but KR19 was similar). The mRNA expression level of *IGF2* was significantly higher in the SCC cell lines compared to oral keratinocyte cell lines, whereas *IGF2BP2* was similarly expressed in all tested cell lines. Negligible levels of *IGF1*, *IGFBP1* and *INS* and *INSR* were observed in tested cell lines. Copy number analysis of *IGF2BP2* in the oral keratinocyte cell lines was not performed, so the correlation between copy number and mRNA could not be directly assessed for these lines.

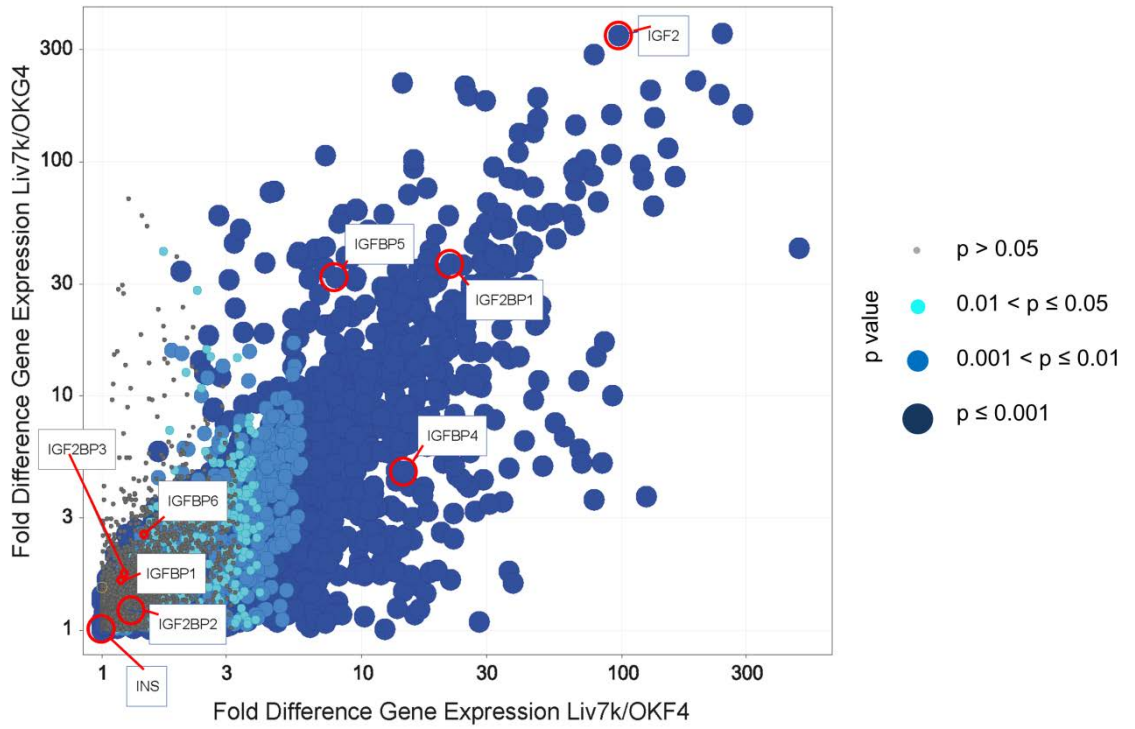


Figure 5.3 RNA sequencing reveals fold change gene expression of insulin signalling genes between Liv7k and OKF/OKG4 cell lines. Scatter plot showing fold change of gene expression between Liv7k oral SCC cell line and two immortalised keratinocyte cell lines (OKF4, OKG4). Circle size and colour depicts significance according to unpaired t-test (p value). Insulin pathway genes are labelled.

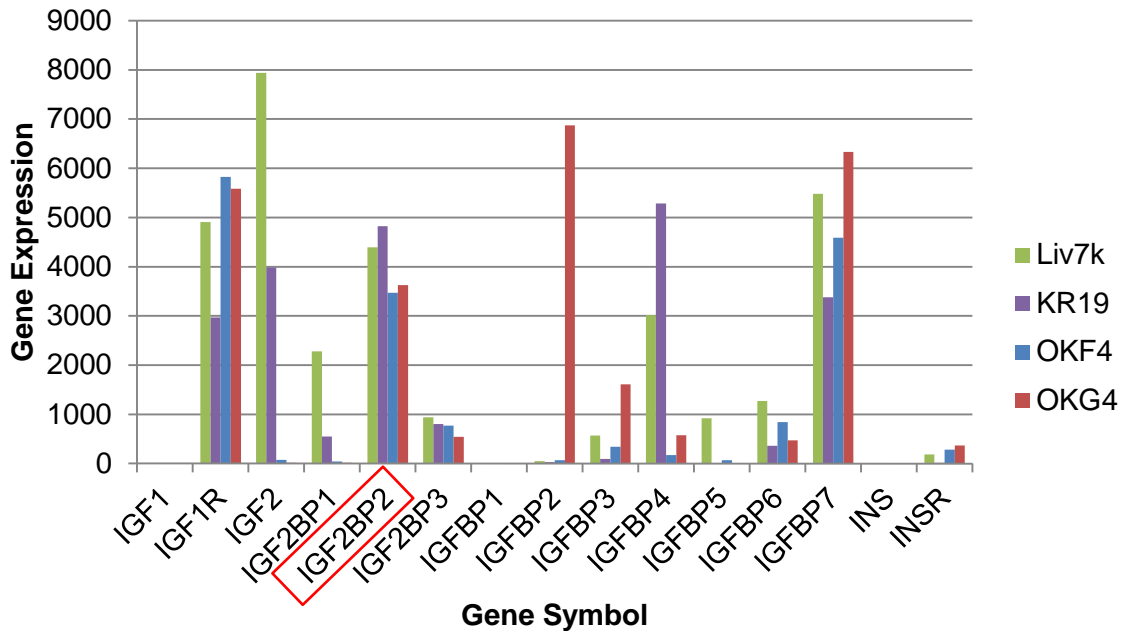


Figure 5.4 RNA sequencing reveals gene expression of insulin signalling genes. Mean normalised read count of insulin signalling genes in two oral SCC cell lines (Liv7k, KR19) and two immortalised keratinocyte cell lines (OKF4, OKG4). IGF2BP2 is highlighted.

5.5 Knockdown of insulin signalling genes results in suppression of fitness in Liv7k cell line

RNA expression of *IGF2BP2* and other insulin pathway signalling genes was analysed in order to identify components of the pathway, which were upregulated in oral cancer cell lines versus immortalised keratinocyte lines. In addition, percentage growth inhibition (GI) data from the siRNA screen revealed variable dependencies on IGF signalling genes, with knockdown of *IGF2BP2* causing approximately 30% GI (Figure 5.5 and Figure 5.6). Applying a minimum cut-off value of 20% GI, genes that are important for survival in the Liv7k oral SCC cell line include *IGF1*, *IGF2*, *IGF2BP2*, *IGFBP2*, *IGFBP4*, *IGFBP6*, *IGFBP7* and *INSR*.

The mRNA expression of *IGF2BP2* does not change significantly between tumour and keratinocyte cell lines. However, it is possible that *IGF2BP2* acts on a different set of target transcripts in cancer cells compared to normal, or exhibits different activities. Interestingly, silencing of *IGF2* results in a similar percentage growth inhibition as *IGF2BP2*; possibly suggesting that *IGF2BP2* is exerting its phenotypic effect through the IGF2 growth factor.

Despite the negligible expression of *IGF1*, *INS* and *INSR* (shown in Figure 5.4), knockdown of these genes using pooled siRNAs resulted in a high percentage growth inhibition (Figure 5.6). This suggests that the siRNAs used in the screen are having off-target effects.



Figure 5.5 Scatter plot showing percentage growth inhibition in the Liv7k (median) cell line versus fold change of gene expression between Liv7k and OKF4 cell line. Thick lines represent fold change ≥ 2 for fold change and minimum growth inhibition of 30%, relative to siNTC control; colour is percentage growth inhibition upon gene knockdown in Liv7k cell line (green = low, red = high). *IGF2BP2* is highlighted.

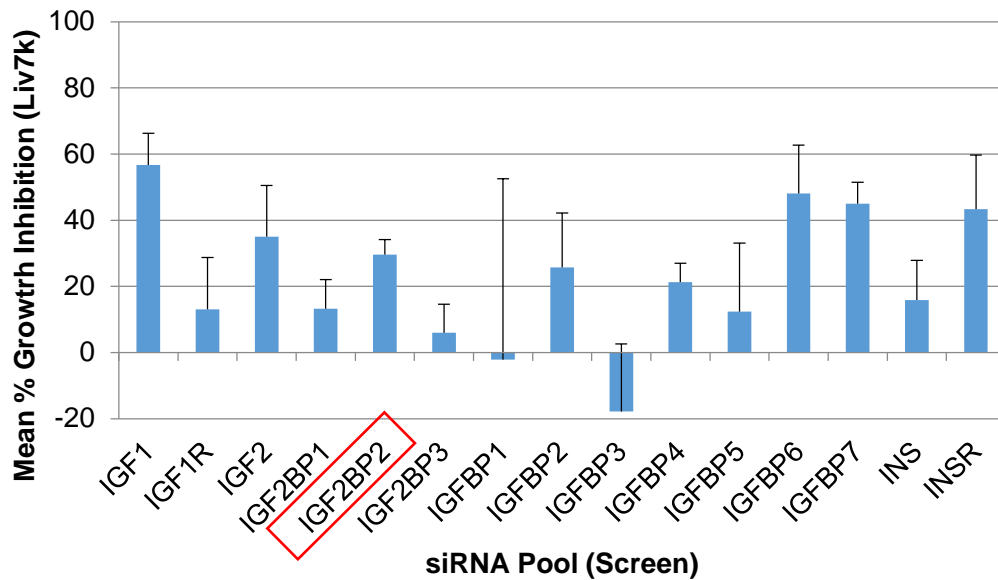


Figure 5.6 The effect on Liv7k growth of knockdown of insulin pathway genes in siRNA screen. Results are normalised to non-targeting control (NTC) and presented as mean \pm SD. *IGF2BP2* is highlighted.

5.6 Quantification of IGF2BP2 levels in patient tumour vs matched normal tissue

IGF2BP2 is overexpressed in ~22% of patients with HNSCC, according to the TCGA dataset. To determine *IGF2BP2* expression in patient derived tumours versus normal matched tissue, RNA was isolated from four tumour/normal paired samples and converted to cDNA for qRT-PCR analysis (Figure 5.7). Two out of four showed increased expression of *IGF2BP2* (fold change > 2) while a decrease was observed in one sample. Normal as described here refers to a sample taken from outside the tumour boundary, and was not histologically defined. *IGF2BP2* copy number was not measured in these tumour samples, but analysis of HNSCC (and oral SCC) datasets in Oncomine (www.oncomine.org) reveals consistent over-expression of the gene in tumours compared to normal matched tissue[459-463].

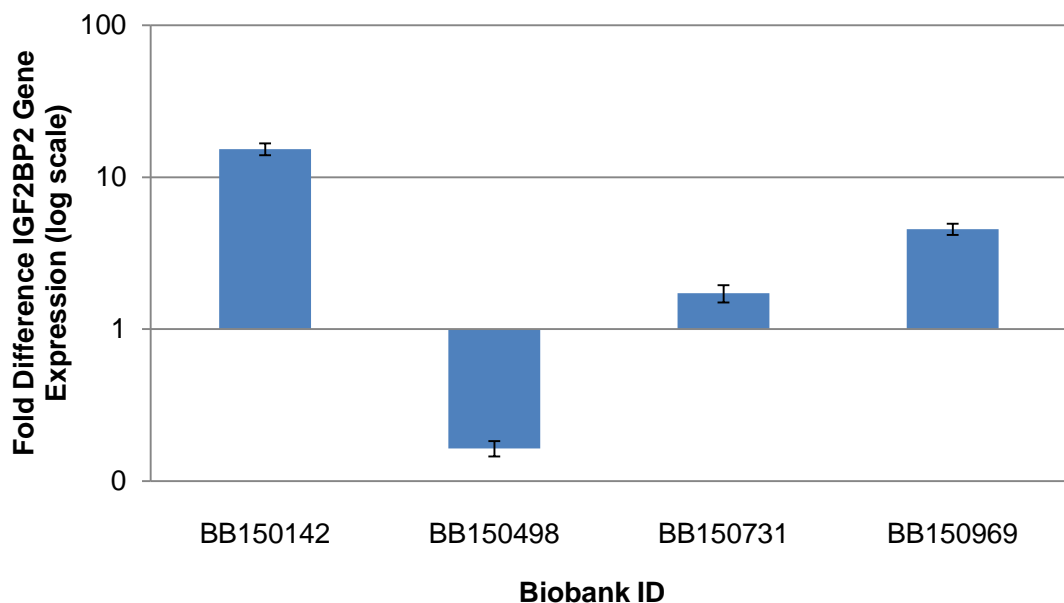


Figure 5.7 *IGF2BP2* mRNA expression was measured in patient tumour and matched normal samples. qRT-PCR showing *IGF2BP2* gene expression in patient samples. *IGF2BP2* expression was normalised to ACTB and given as tumour/normal. Data is mean \pm SD of three technical replicates from the same samples.

5.7 Generation of an shIGF2BP2 knockdown model

In order to further assess the role of IGF2BP2 in HNSCC, Liv7k and Liv37k cells were infected with an inducible shRNA plasmid, which also contained an RFP reporter for visual confirmation of induction. After selection, cells were further selected by fluorescence-activated cell sorting. Cells were treated for 72 hours with doxycycline to induce maximum RFP expression and cells with high RFP expression were isolated and cultured independently (Figure 5.8).

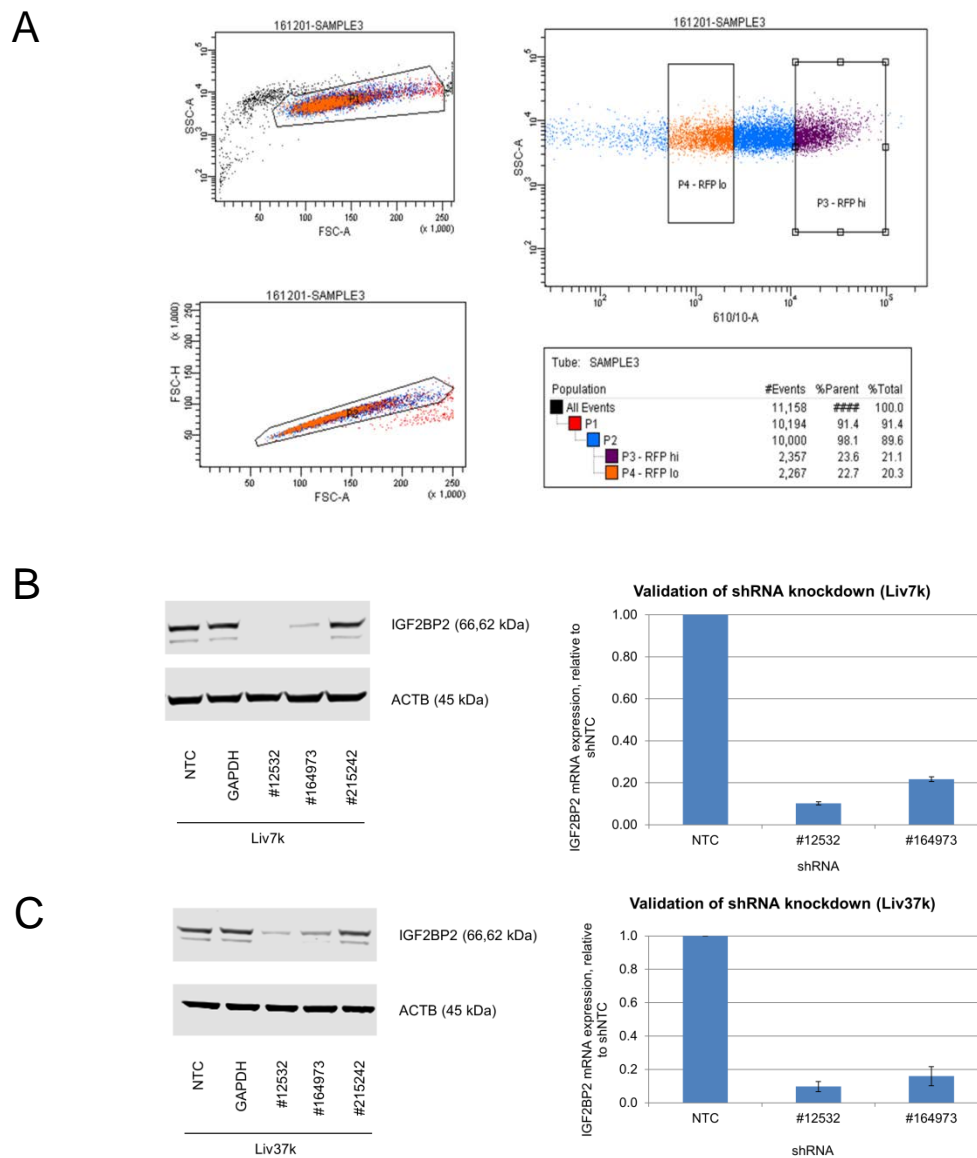


Figure 5.8 Generation of an inducible shRNA knockdown model. (A) FACS of Liv7k cells into high RFP expressing sub-population. (B, C) The efficiency of shRNA knockdown was assessed by western blot and RTq-PCR in Liv7k and Liv37k cells. For western blots, cells were treated with 1 μ g/mL doxycycline for 72 hours prior to cell lysis. 20 μ g of protein was loaded per lane. ACTB was used as a loading control. RTq-PCR results are the mean \pm SD of three biological replicates. IGF2BP2 expression was normalised to ACTB reference gene and presented relative to shNTC negative control.

5.8 IGF2BP2 knockdown does not significantly affect oral cell line propagation

Evidence in the literature has suggested that IGF2BP2 can enhance growth and survival of cancer cells[177]. To determine the role of IGF2BP2 in promoting an aggressive phenotype in oral SCC (based on TNM stage), a series of phenotypic assays were performed upon shRNA-mediated knockdown of the gene. The Incucyte ZOOM[®] (Essen BioScience) was used to measure cell propagation, migration and invasion, which were quantified using ZOOM software. Two unique shRNA sequences (#12532, #164973) were tested in each assay, with identical results. Hence, the result for one shRNA only is shown here.

The result of each knockdown was normalised to a non-targeting control cell line. 1µg/mL doxycycline was added 72 hours prior to starting assays to ensure complete knockdown at experimental start point. Two cell lines were tested in each assay (Liv7k and Liv37k) because of their high and low expression of IGF2BP2, respectively. In addition, the Liv37k cell line exhibited a loss of the 3q26-29 region (Figure 4.1).

Cell propagation analysis (percentage confluence) revealed no impairment of propagation in either cell line. A representative result of shRNA-mediated knockdown is shown below (Figure 5.9). Non-doxycycline treated cells serve as an additional control showing changes in proliferation rates are not due to silencing of IGF2BP2.

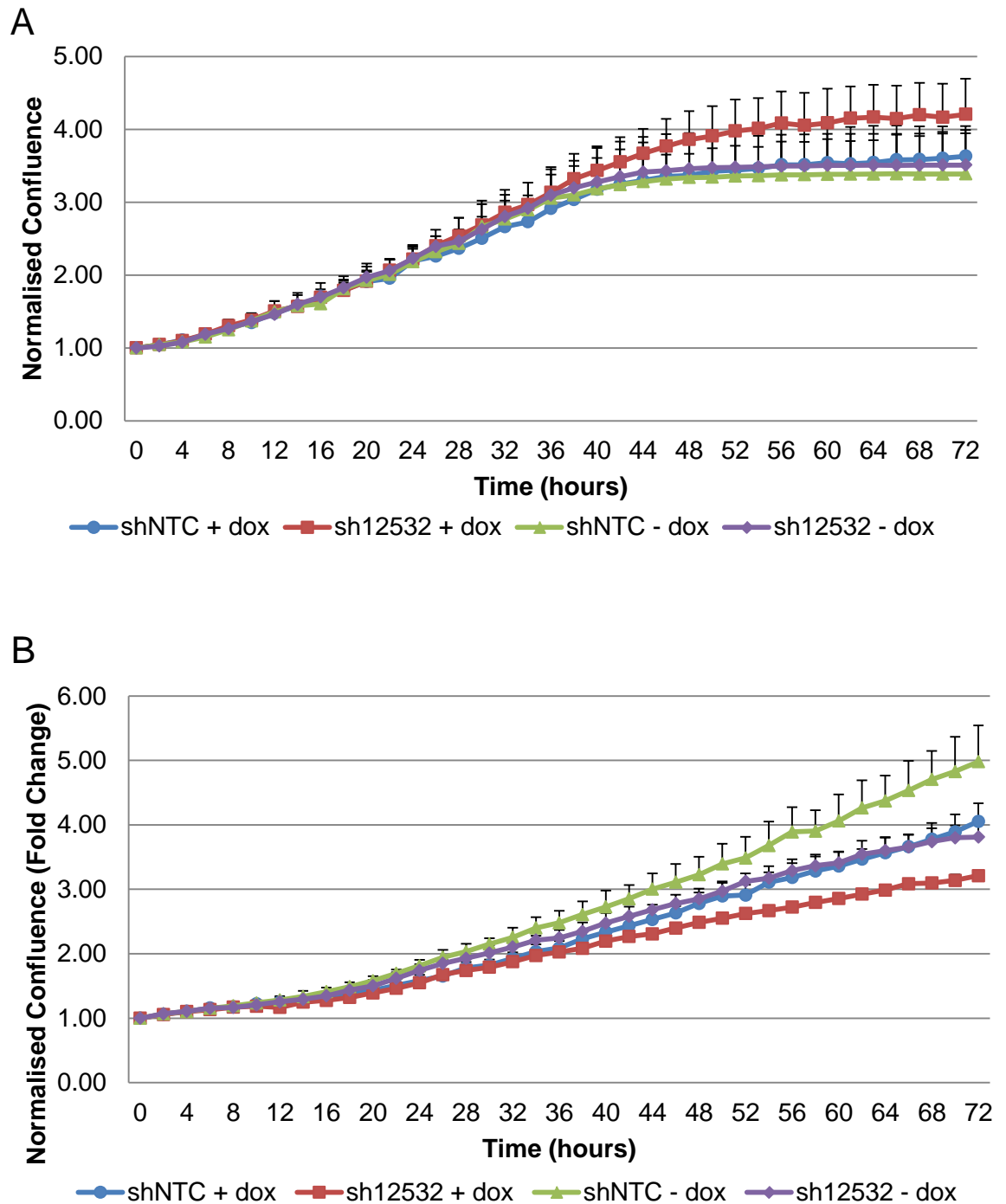


Figure 5.9 Cell propagation quantification following silencing of IGF2BP2 in (A) Liv7k and (B) Liv37k. Percentage confluence is shown for a non-targeting negative control cell line (shNTC) and a stable IGF2BP2 knockdown cell line (sh#12532) for each cell line. Results are plotted as the mean \pm SD of one representative experiment, $n=3-6$ wells.

5.9 IGF2BP2 knockdown does not significantly affect oral cell line migration

The effect of IGF2BP2 knockdown on cell migration (wound healing assay) was measured and normalised to the shNTC negative control cell line. The result for one representative experiment is shown below (Figure 5.10). Knockdown of IGF2BP2 did not significantly impair cell migration following wounding of the monolayer. Follow up experiments in which human recombinant insulin and IGF-I growth factor were added in addition to knockdown yielded a similar result (data not shown).

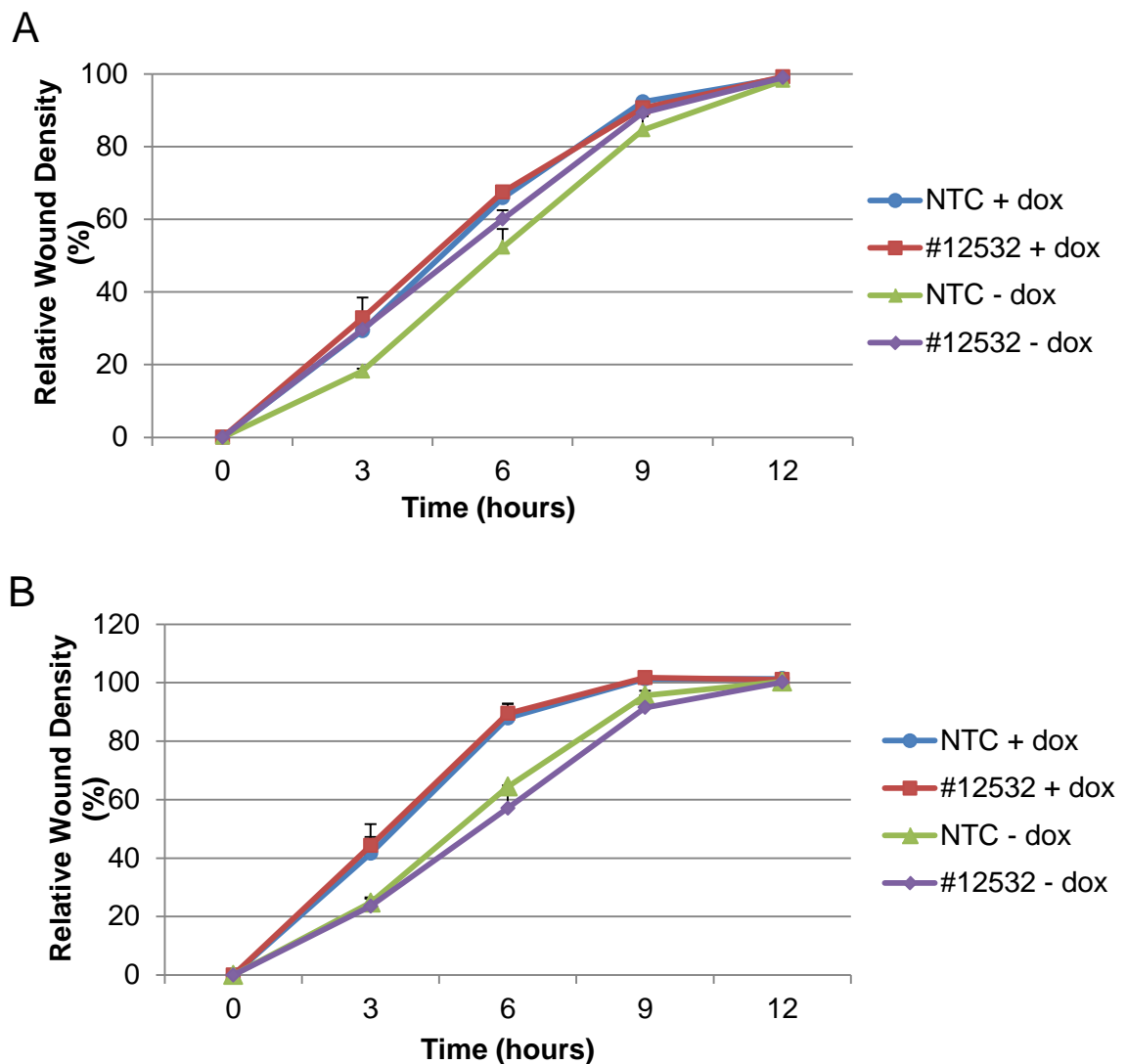


Figure 5.10 Measurement of cell migration following silencing of IGF2BP2 in (A) Liv7k and (B) Liv37k cells. Cells were pre-treated with 1 μ g/mL doxycycline and grown to a confluent monolayer over 24h. Following this, a scratch was made. The wound was imaged every two hours until complete closure. Relative wound density was calculated by the Incucyte ZOOM software and represents the density of the wound at the indicated time points compared to the initial wound. Graph shows results from one representative experiment, mean \pm SD, n=3–6 wells per condition.

5.10 IGF2BP2 knockdown does not impair oral cell line invasion

The rate of invasion through matrigel extracellular matrix was measured in Liv7k and Liv37k cell lines after IGF2BP2 knockdown. A schematic of the scratch assay is shown in Figure 5.11. However, silencing of the gene did not significantly slow the rate of invasion in the scratch assay over a 72-hour period (Figure 5.12). Induction of the shRNA was confirmed by imaging in both brightfield and the red channel (representative result shown in Figure 5.13).

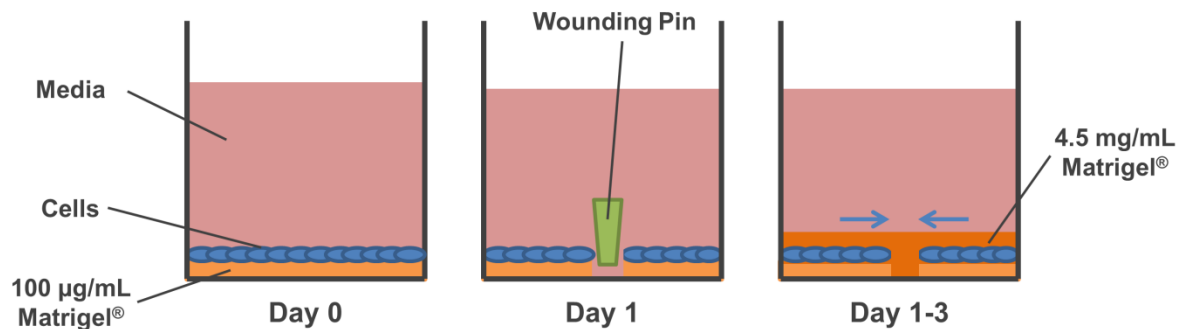


Figure 5.11 Schematic representation of scratch assay used to assess oral SCC invasion. Briefly, diluted matrigel was used to coat each well of a 96-well plate and incubated overnight. The next day, 30,000 cells per well were seeded on top of the matrix layer and allowed to adhere overnight at 37°C / 5% CO₂. A scratch was made using a Woundmaker™ (Essen Bioscience) and concentrated matrigel was added on top of the cell layer. Images were acquired every 2-3 hours for 72 hours on the Incucyte Zoom 3™ (Essen Bioscience).

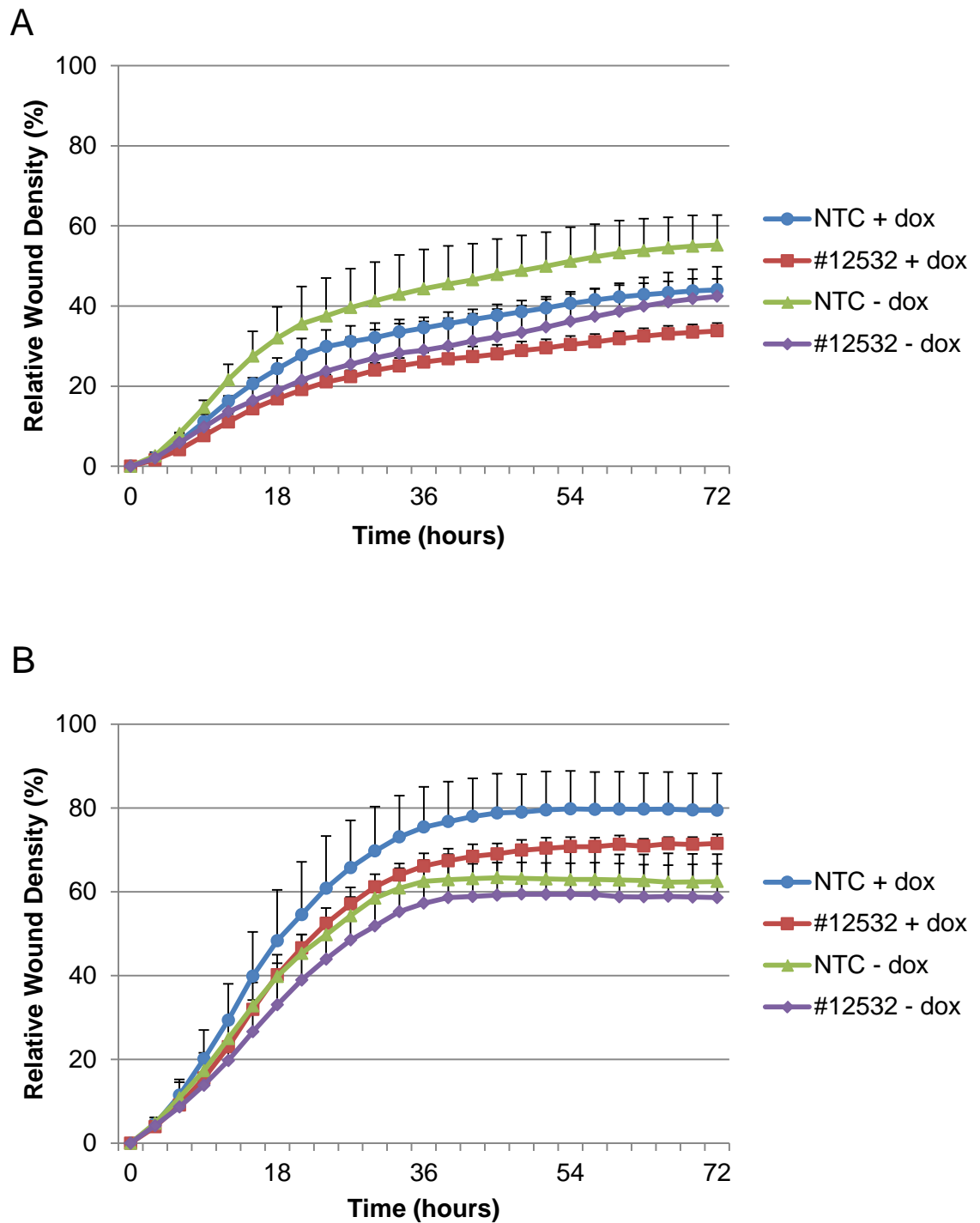


Figure 5.12 Cell invasion analysis following IGF2BP2 knockdown in (A) Liv7k and (B) Liv37k cells. Knockdown of IGF2BP2 does not impair wound healing through matrigel. Cells were pre-treated with doxycycline and grown to a monolayer over 24 h. Following this, a scratch was made and images were taken every 2 hours for 72 h. Relative wound density was calculated by the Incucyte ZOOM software and represents the density of the wound at the indicated time points compared to the initial wound. Graph shows results from one representative experiment, mean \pm SD, n=3–6 wells per condition.

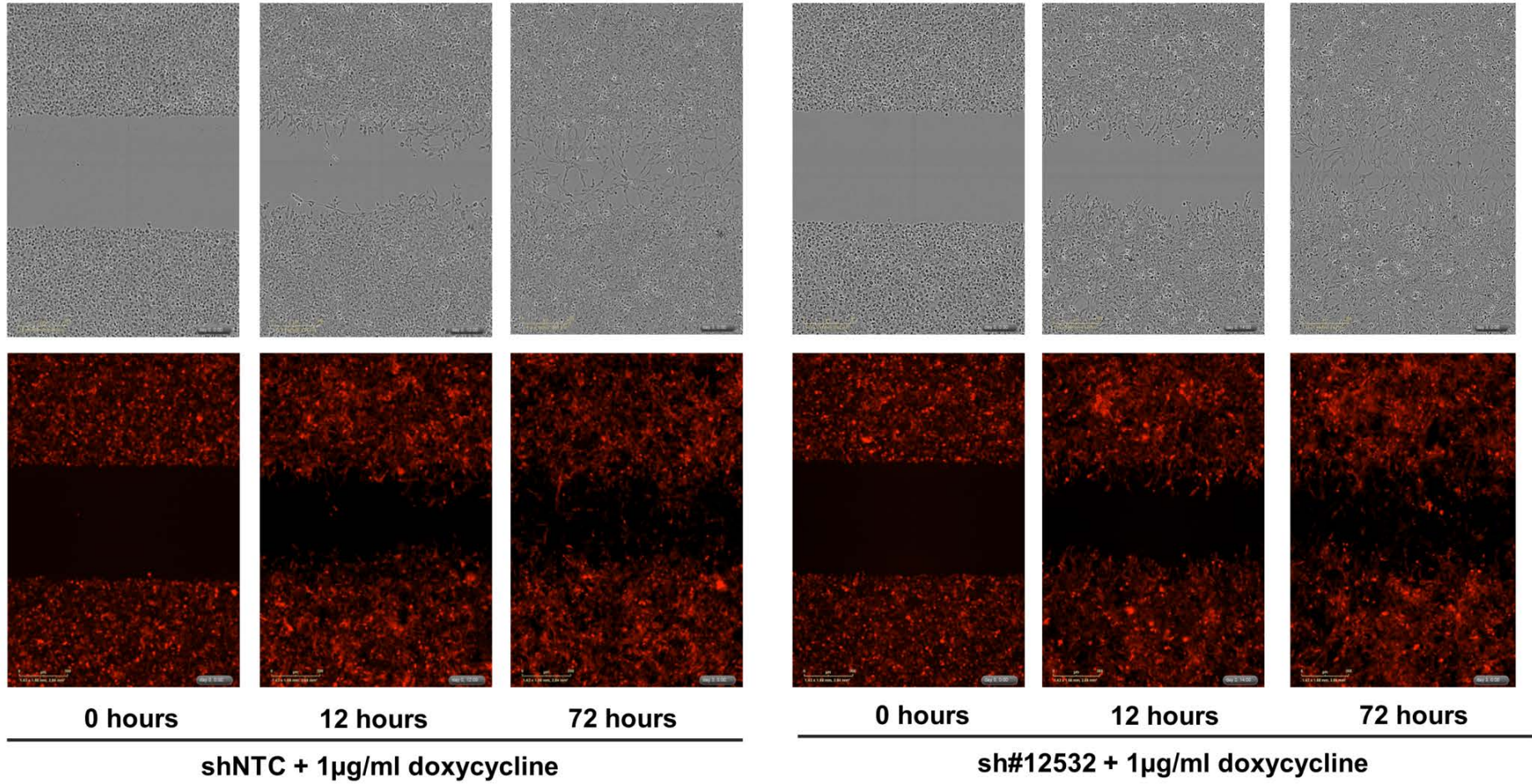


Figure 5.13 Confirmation of RFP induction in Liv37k cells stably expressing the plasmid.

5.11 The role of IGF2BP2 in epithelial to mesenchymal transition (EMT)

Metastasis to local lymph node is a multistep process involving the detachment of transformed cells from tumour tissue and invasion through the extracellular membrane. Loss of E-cadherin leads to reduced intracellular adhesion of tumour cells and a more mesenchymal phenotype. In addition to directly assessing the role of IGF2BP2 in invasion, evidence suggests that IGF2BP2 may promote invasion indirectly through its modulation of epithelial to mesenchymal transition (EMT)[177].

Different invasive phenotypes were observed in the Liv7k and Liv37k cell lines, which were dyscohesive and non-cohesive, respectively. Expression of common markers of EMT (Slug, Snail and E-cadherin) was measured by western blot in the Liv7k and Liv37k cell lines. Complete loss of E-cadherin and high expression of Slug and Snail were observed in the Liv37ks, suggesting a more invasive phenotype in this low-expressing *IGF2BP2* cell line. Silencing of *IGF2BP2* led to a decrease in the expression of Snail, but not Slug in the Liv37k cell line (Figure 5.14).

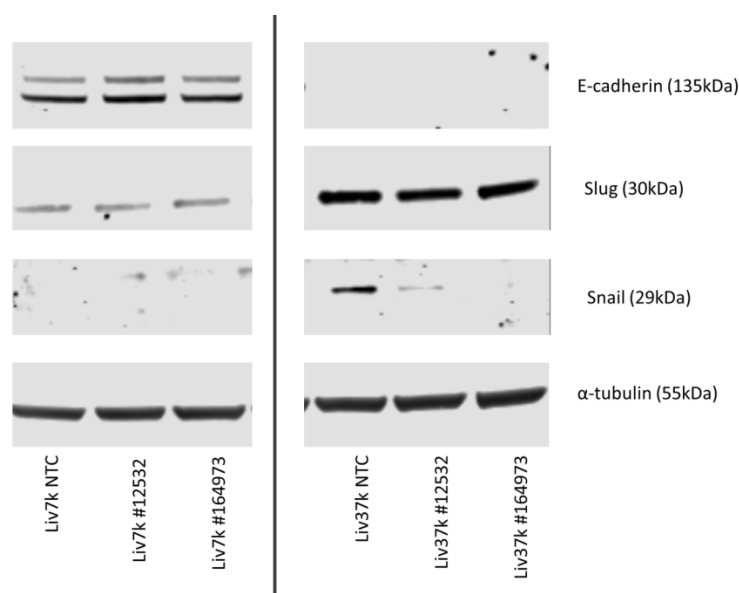


Figure 5.14 IGF2BP2 knockdown leads to decreased Snail expression in Liv37k cell line. Western blot showing expression of E-cadherin, Slug and Snail in IGF2BP2-knockdown cell lines. 20 μ g protein was loaded per well and α -tubulin was used as a loading control.

5.12 IGF2BP2 depletion did not significantly impair chemotactic invasion in Liv37k cells

Based on their enhanced invasiveness and EMT, Liv37k cells were selected for another invasion assay, this time involving a chemoattractant. These results suggest that IGF2BP2 is not required for chemotactic invasion in oral SCC cells as no difference in invasion was observed in a matrigel-containing transwell membrane (Figure 5.15).

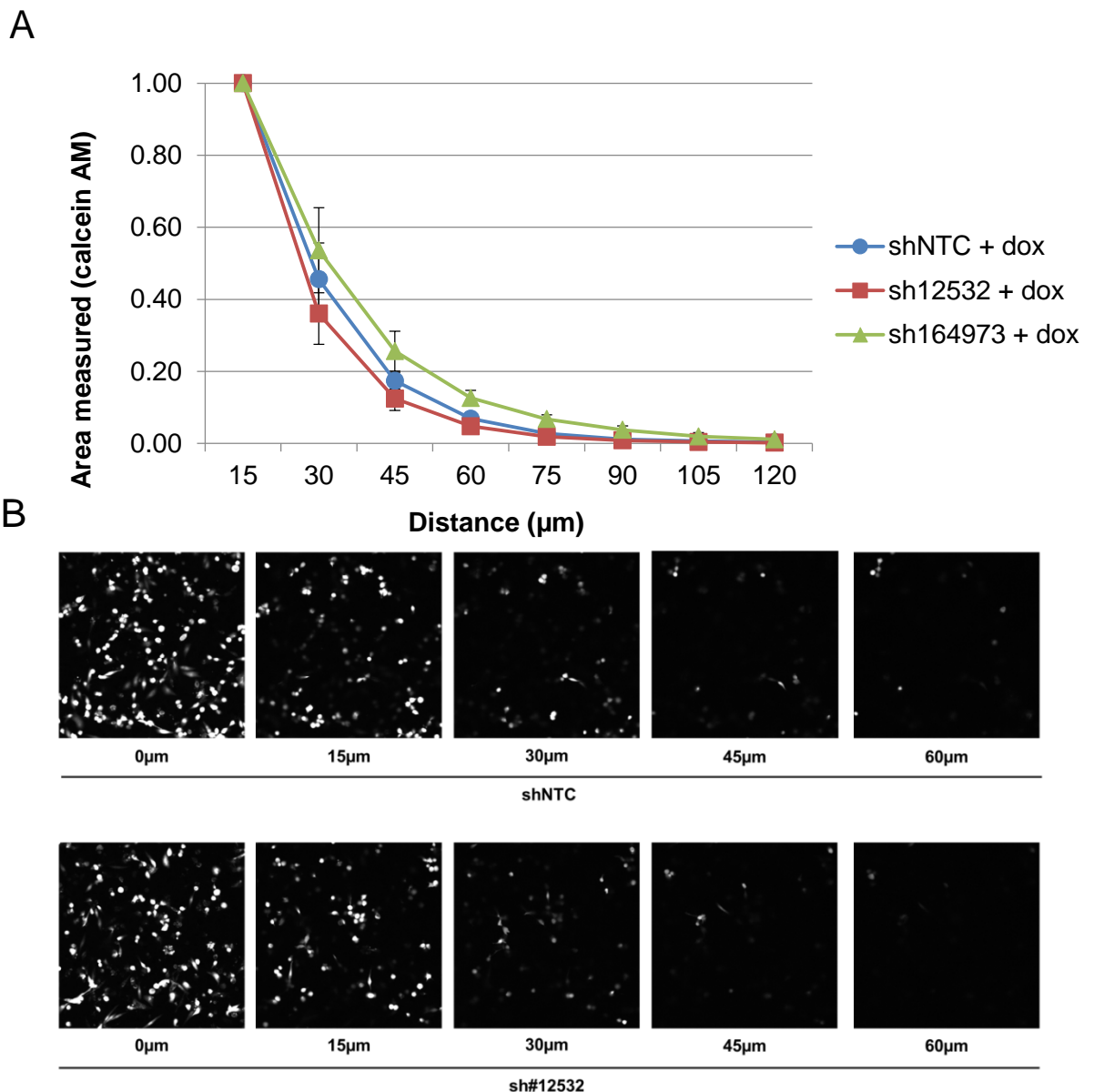


Figure 5.15 Inverse invasion assays were performed on shIGFBP2-induced Liv37k cell line. Cells were seeded in media (- EGF) and left to invade upwards toward media (+EGF and 20% FBS) for 5 days, when cells were live-cell stained with calcein AM and imaged using confocal microscope. Graph shows quantification of calcein AM area as measured by Fiji (ImageJ), mean \pm SD, n = 3 independent experiments.

5.13 IGF2BP2 knockdown did not affect spheroid growth

This project has mainly used *in vitro* 2D phenotypic assays to assess the role of IGF2BP2 in oral cancer progression. However, a 2D monolayer does not reproduce the complex architecture of a tumour *in vivo*, and often creates discrepancies in the efficacy of anti-cancer compounds. 3D culturing of cells creates a more physiologically relevant environment and represents the early, avascular stage of tumour formation. Additional factors such as tumour heterogeneity, hypoxia, cell-cell interaction and the remodelling of extracellular matrix are recapitulated in a 3D context[464].

In order to provide a more accurate depiction of the role of IGF2BP2 *in vivo*, 3D spheroid models were formed using three oral SCC cell lines (Liv7k, Liv37k and Liv72k) with and without IGF2BP2 knockdown. Silencing of IGF2BP2 did not affect spheroid growth in any cell line tested. The results for one experiment carried out on the Liv7k cell line is shown in **Figure 5.16**.

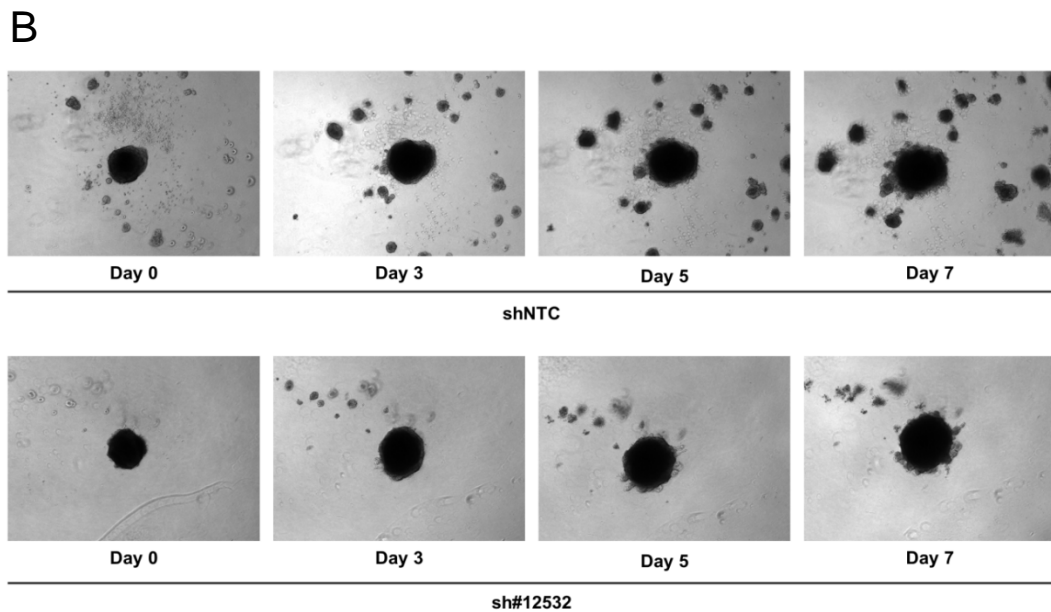
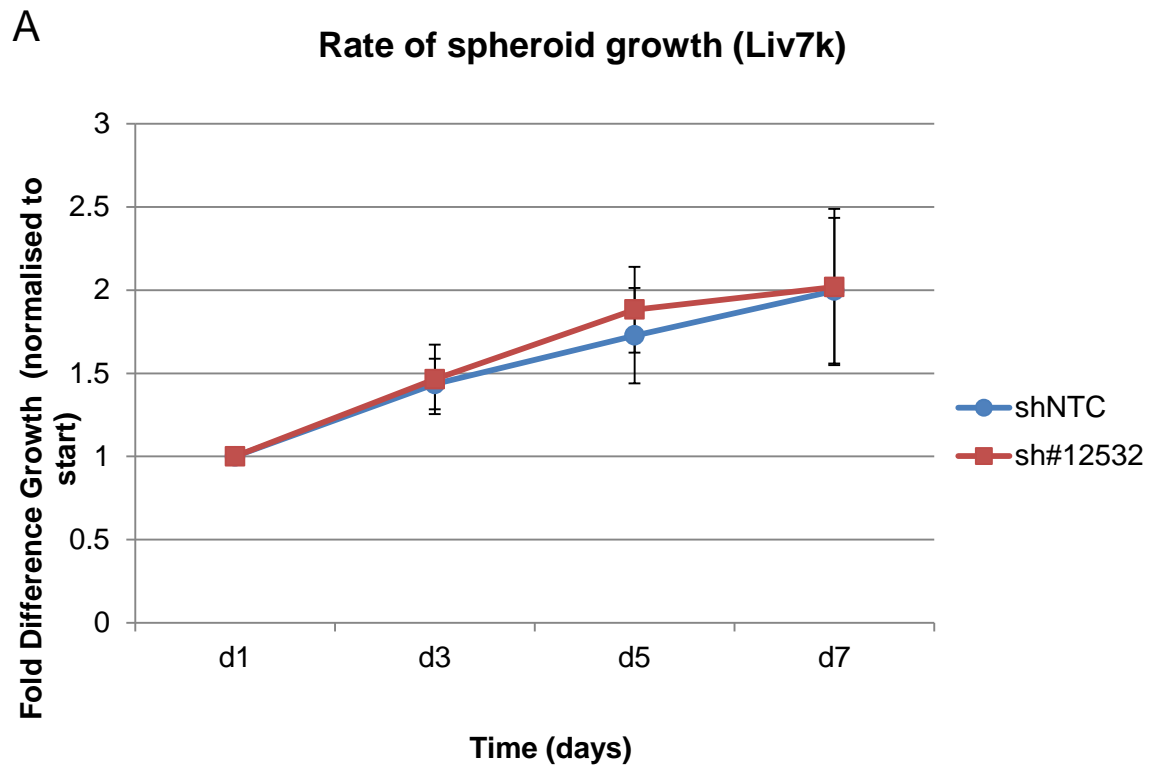


Figure 5.16 Spheroid formation assay, showing the effect of IGF2BP2 knockdown in the Liv7k cell line. 5000 cells/well were seeded in ultra-low attachment round bottomed plates in ECM matrix and spun down to form a sphere. After 3 days, concentrated invasion matrix gel was added and images of spheroids were taken with 4x objective lens. Image quantification was carried out using ImageJ. Results are presented as mean \pm SD (n = 6) based on one experiment.

5.14 The role of IGF2BP2 in mitochondrial metabolism

Based on previous results published by Janiszewska *et al.*[179], measurements reflecting mitochondrial activity were made in the Liv7k and Liv37k (not shown) cell lines. Following stable knockdown of IGF2BP2, oxygen consumption rate (OCR) and extracellular acidification rate (ECAR), which are indicative of levels of oxidative phosphorylation and glycolysis, respectively, were measured (Figure 5.17). No significant change was detected in either metabolic readout.

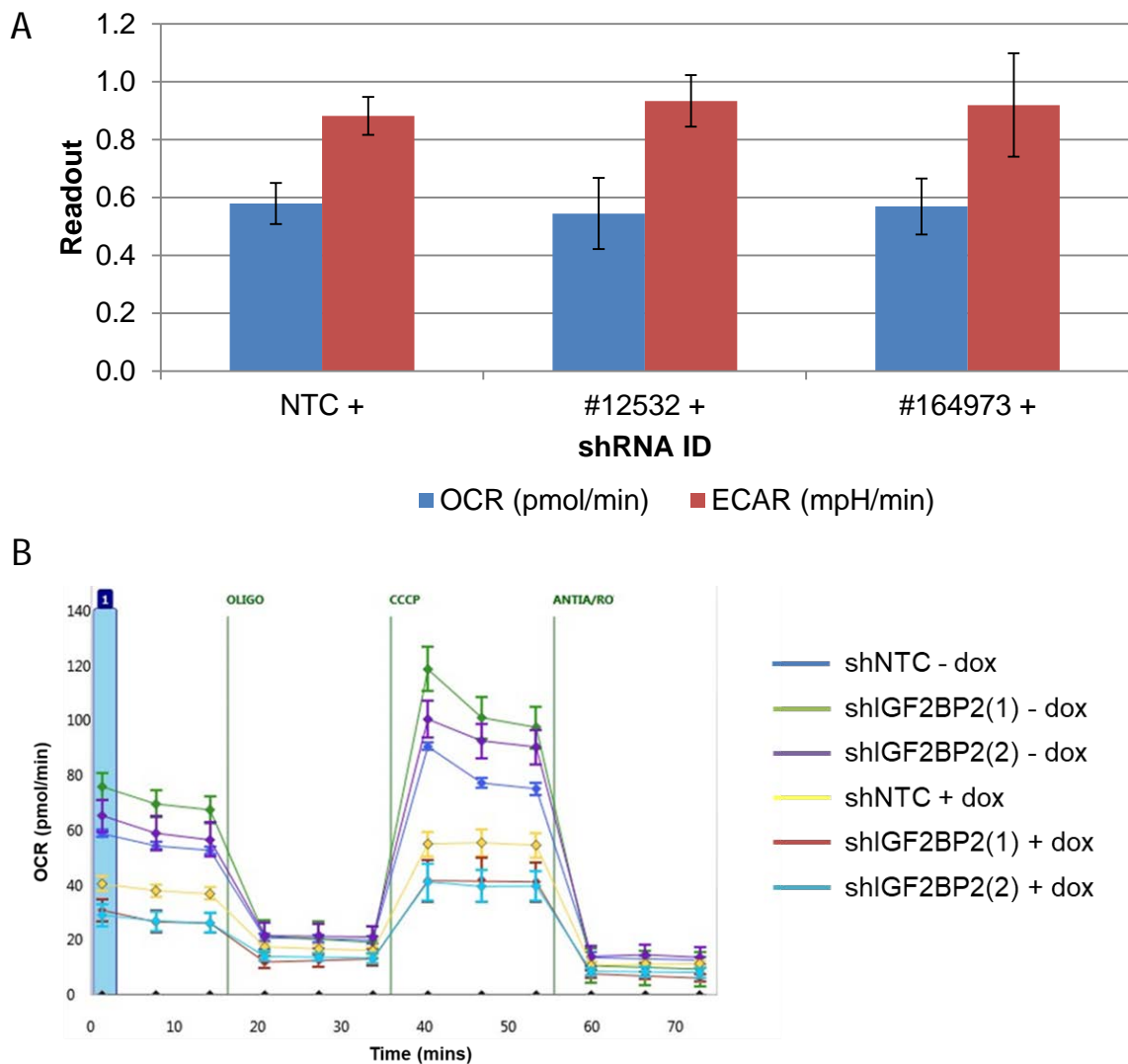


Figure 5.17 The effect of IGF2BP2 depletion on OCR and ECAR in Liv7k cell line. (A) Bar chart showing OCR and ECAR normalised to number of nuclei. Values were normalised to post-measurement nuclei counts (DAPI stained cells read on Operetta) and presented as mean \pm SD, $n=20$ wells. One representative experiment of three biological replicates. (B) Extracellular flux analysis in Liv7k cell line. OCR was measured under basal conditions followed by the sequential addition of oligomycin ($1\mu\text{M}$), FCCP ($1\mu\text{M}$), rotenone ($1\mu\text{M}$) and antimycin A ($1\mu\text{M}$). Each data point represents an OCR measurement. OCR, oxygen consumption rate; ECAR, extracellular acidification rate.

5.15 The role of IGF2BP2 in the regulation of oncogenic signalling

In order to determine if IGF2BP2 is an upstream activator of oncogenic signalling pathways, western blots were performed following shRNA-mediated knockdown. The results for the Liv7k cell line are shown in Figure 5.18. Human recombinant insulin was added to stimulate IGF-1R activation. However, no decrease in the phosphorylation of AKT, MAPK or p70 S6 kinase was observed. Similar results were obtained for the Liv37k and Liv72k cell lines and for cells treated with IGF1 growth factor (data not shown). Knockdown of IGF-1R did not decrease IGF2BP2 expression and silencing of IGF2BP2 did not decrease IGF-1R phosphorylation in Liv7k or Liv37k cell lines (data not shown). Given that knockdown of IGF-1R did reduce the expression of phospho AKT and MAPK, it appears that IGF2BP2 is not acting via this receptor, at least in oral cancer (Figure 5.19).

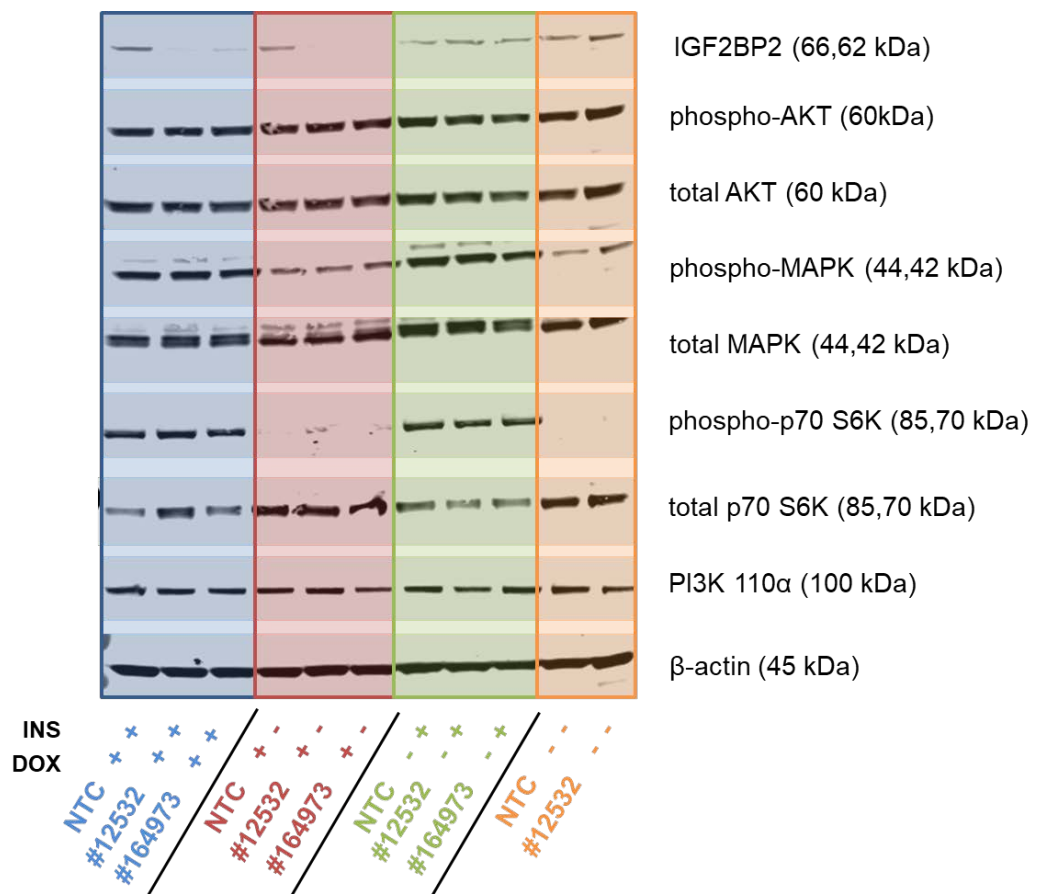


Figure 5.18 The effect of IGF2BP2 knockdown on oncogenic signalling in the Liv7k cell line. Western blot shows expression of phospho and total AKT, phospho and total MAPK, phospho and total p70 S6 kinase and PI3K upon IGF2BP2 knockdown. 20µg protein was loaded per well and β-actin was used as a loading control. Insulin was added to cells for 5 minutes prior to cell lysis.

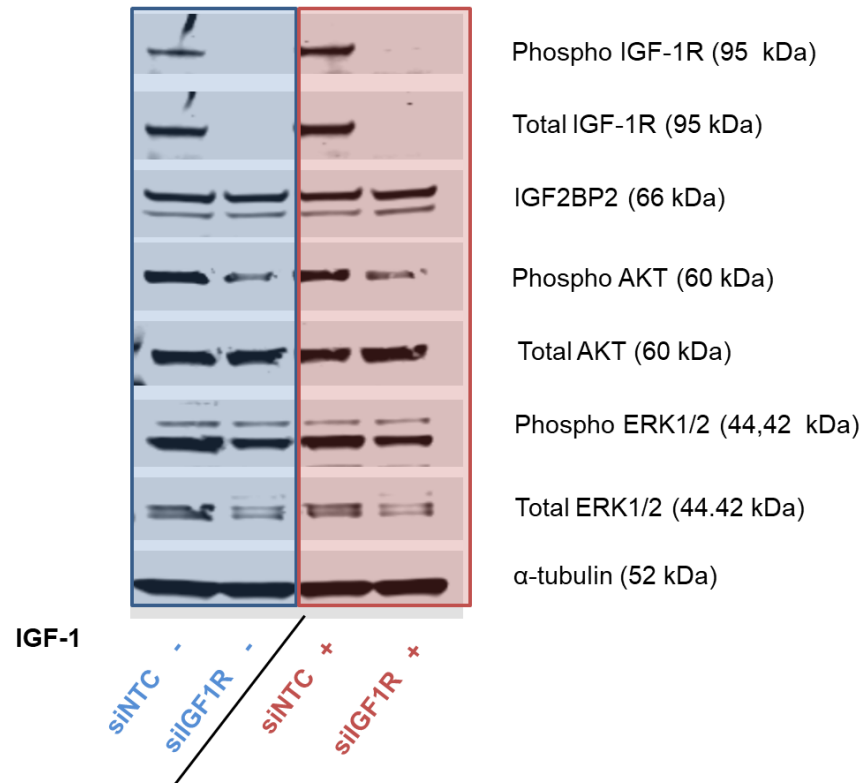


Figure 5.19 Western blot showing expression of phospho and total IGF1R, IGF2BP2, phospho and total AKT and phospho and total MAPK upon IGF1R knockdown in Liv7k cell line. Results include cells treated with 100ng/mL IGF-1 for 15 minutes. 20 μ g protein was loaded per well and α -tubulin was used as a loading control.

5.16 Discussion

In this chapter, the role of IGF2BP2 in HNSCC was assessed in a variety of phenotypic assays. There was a strong rationale in selecting the gene as a potential oncogenic driver in the diseases, based on genomic data and its correlation with patient survival. RNA-binding proteins, like IGF2BP2, interact with a large number of RNA transcripts throughout the cell and thus have the potential to influence a wide range of cellular processes[465]. RNA-immunoprecipitation experiments have uncovered a host of new binding targets, further expanding the possible roles of IGF2BP2[173]. Previous studies have shown how IGF2BP2 can control oxidative phosphorylation in primary glioblastoma spheroids, and regulate the translation of EMT proteins[179, 213].

TCGA patient data reveals *IGF2BP2* upregulation in ~22% of HNSCC tumour samples. However, the same is true of many of genes in the 3q26-29 amplicon. It is likely that the majority of genes contained within this region are passengers of larger amplification events and have no effect on cell phenotype. For this reason, it was necessary to factor in additional selection criteria, such as patient survival, to refine the list of genes down to a more manageable set of 10 genes. In this set, *IGF2BP2* had the highest individual significance on patient survival and pathway analysis revealed putative interactions with known oncogenic drivers in the disease. Knockdown of the gene also resulted in a high percentage loss of viability in the siRNA screen. This stepwise process of elimination allowed for the selection of the most likely driver gene candidates in HNSCC progression.

Insulin signalling represents a key mechanism of HNSCC cell growth and survival[466]. IGF1R expression is higher in advanced TNM staged oral SCC tumours and is predictive of clinical outcome[120]. Moreover, the receptor can be trans-activated with EGFR[467], which also promotes cancer progression, metastasis and therapeutic resistance in the disease[468]. A number of small molecule inhibitors and monoclonal antibodies to IGF1R have entered clinical trials in recent years. Yet, despite a strong rationale, they have failed to show significant benefit to patients because of development of resistance and receptor crosstalk[153].

Knockdown of IGF2BP2 was achieved by siRNA, shRNA and CRISPR knockout, and each system was tested in phenotypic assays. CRISPR knockout cell lines yielded similar results to the shRNA models and thus results are not shown. In this study, knockdown of IGF2BP2, by any means, did not have a significant effect on the proliferation, migration or invasion in a set of oral SCC cell lines. Silencing of IGF2BP2 did not impair the growth rate of 3D spheroid models or result in a change in oxygen consumption rate. Importantly, knockdown of the gene did appear to decrease SNAIL expression in one cell line (Liv37k), but it did not translate to a reduced capacity to invade. Moreover, silencing of IGF2BP2 did not significantly influence major oncogenic signalling networks in HNSCC. The decreased expression of SNAIL in Liv37k cells (which display loss of 3q26-29 and have the lowest gene expression of *IGF2BP2*) is surprising, and may suggest that a minimal level of IGF2BP2 activity is required to maintain an aggressive phenotype in oral cancer. Overexpression of the gene in this cell line would perhaps provide more insight into its cellular function.

Overall, despite a solid rationale for characterising the role of IGF2BP2 overexpression, the results here show that it is most likely not a major player in HNSCC progression. To date, this is the first functional assessment of IGF2BP2 in a head and neck cancer setting. Studies demonstrating an oncogenic role for the gene thus far have been performed in other cancer models with potentially very different genetic backgrounds. Moreover, the heterogeneity of HNSCC itself may explain the inconsistencies in response to IGF2BP2 knockdown in this study. The Liv7k and Liv37k cell lines were primarily chosen for their high and low expression of IGF2BP2, respectively, and it was hypothesised that these cell lines would respond differently to the silencing of the gene. Despite originating from primary tumours with nodal involvement, the Liv7k and Liv37k cells displayed different invasive phenotypes (dyscohesive and non-cohesive, respectively) which may also have influenced their response to IGF2BP2 knockdown. I have recently completed an RNA-immunoprecipitation experiment with the Liv7k cell line, which is due to be sequenced in the near future. I hope that this will reveal novel binding partners of IGF2BP2 and provide further insight into its role in a head and neck cancer.

Chapter 6 Results – Validation of *PSMD2* as a driver gene in oral squamous cell carcinoma

6.1 Introduction

PSMD2 was the second gene selected for phenotypic validation based on the analysis of the 3q26-29 amplicon. The gene, which encodes a subunit of the 26S proteasome, is overexpressed in 34% of patients with HNSCC and is significantly correlated with reduced overall survival in these patients (Figure 4.3).

Moreover, silencing of the gene resulted in ~40% growth inhibition of Liv7k cells (Figure 4.5). Investigation of the proteasome as a therapeutic target also led to the identification of proteasomal subunit genes, which are downregulated in patients with HNSCC (compared to normal tissue), such as *PSMD6*. As proteasome activity is essential for cellular function, it was hypothesized that targeting genes with partial copy number loss would result in greater loss of viability in cancer cells than normal cells. In this chapter, copy number loss of *PSMD6* is confirmed using Taqman® assays in a series of oral cell lines and the effect of siRNA knockdown on cell viability is measured. Dysregulation of the proteasome complex is clinically significant in a number of disease pathologies, and can be therapeutically exploited in the clinic.

PSMD2 encodes a non-ATPase subunit (RPN1) of the 19S regulatory cap, which exists bound to a 20S catalytic core to form the 26S proteasome (Figure 6.1). RPN1 is the largest proteasomal subunit at 110 kDa and coordinates ubiquitin processing factors at the boundary between the regulatory and catalytic domains[469, 470]. Like *PSMD2*, *PSMD6* encodes a protein in the 19S regulatory cap (RPN7) (Figure 6.1). In *S. cerevisiae*, the protein is essential in the maintenance of proteasomal integrity[471], and in human cells it has been shown to co-localise with DNA damage foci where it promotes cellular senescence following genotoxic insult[472]. Evidence for RPN7's role in DNA damage repair has been strengthened by the finding that it interacts with BRCA2[473]. Two other proteasomal subunits, *PSMC2* and *PSME4*, are investigated in this chapter based on their copy number alteration status. The former encodes RPT1, another essential subunit of the 19S regulatory cap while the latter encodes PA200, a regulator of proteasomal activity that stimulates the

hydrolysis of small peptides without using ATP[474]. The protein, which is primarily localised in the nucleus[475], is required for normal spermatogenesis in mice and plays an important role in DNA repair by recruiting proteasomes to sites of double stranded breaks[476, 477]. A putative role for PA200 has been discovered in a cancer setting where it was shown to regulate tumour cell responsiveness to glutamine after exposure to ionising radiation, by enhancing postglutamyl proteolytic activity[478, 479].

The proteasome represents the end stage of ubiquitin-mediated protein degradation and is essential for the maintenance of cellular homeostasis. Bortezomib (Velcade®; Millennium Pharmaceuticals Inc., Takeda Oncology, Cambridge, MA, USA) specifically targets the $\beta 5$ subunit of the 20S core, inhibiting the chymotrypsin-like activity of the proteasome[480]. Evidence suggests that individual subunits play distinct roles in cancer, for example, *PSMD9* expression has been shown to predict radioresistance in breast cancer whereas *PSMD10* overexpression can promote cell survival in hepatocellular carcinoma[481, 482].

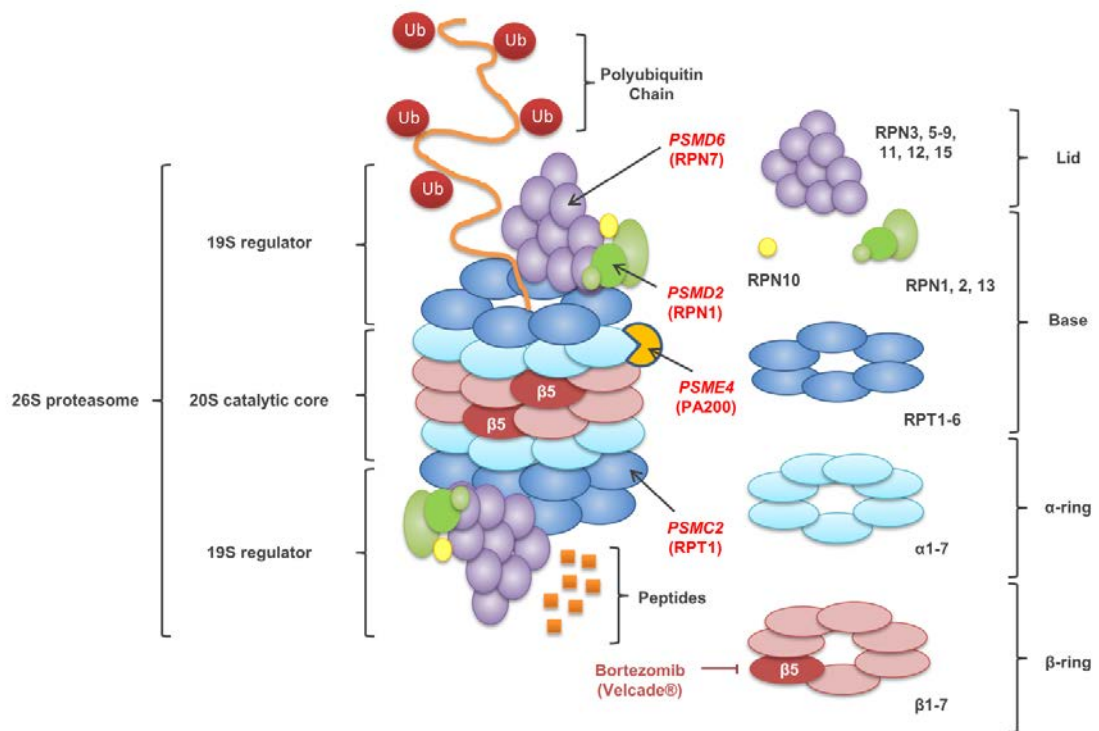


Figure 6.1 Structure of the 26S proteasome. The 20S catalytic core consists of a barrel of four stacked rings (two outer α rings and two inner β rings) and is capped on both ends by 19S regulatory particles. RPN1 (*PSMD2*) is highlighted in red. Bortezomib specifically inhibits the $\beta 5$ subunit of the 19S regulatory particle, which is responsible for chymotrypsin-like activity.

In addition to residing in a commonly amplified region of chromosome 3 (q26-29), *PSMD2* was identified as part of a metastatic gene signature in lung cancer where high expression of the gene correlates with poor prognosis[425]. Furthermore, knockdown of the gene significantly reduced proteasomal activity and proliferation in a panel of lung adenocarcinoma cell lines[426]. Interestingly, the authors of this study observed an increase in the expression of p21 (as well as a modest increase in p53 expression) upon silencing of *PSMD2*. Interestingly, a recent study found that a modest reduction of *PSMD2* expression induced a shift in 20/26S proteasome complex ratios and protected cells against proteasomal inhibition by bortezomib[483].

Dependence on proteasomal turnover can leave cancer cells vulnerable to the silencing of subunit genes. Indeed, Nijhawan *et al.* recently showed that tumour cells harbouring partial loss of the *PSMC2* gene are more sensitive to its silencing by siRNA/shRNA than non-tumour cells with normal copy number[484]. In a similar manner, this study aims to determine if oral cancer cells harbouring partial copy number loss of *PSMD6* are more sensitive to knockdown of the gene. Collectively, these observations highlight the diverse and dynamic roles of proteasomal subunit genes in cancer progression. The current project seeks to investigate this reliance in two ways: firstly, to determine if overexpression of *PSMD2* in oral SCC cell lines confers enhanced sensitivity to bortezomib; and secondly, to investigate the sensitivity of oral SCC cell lines exhibiting loss of copy number of proteasomal subunit genes to further suppression.

Tumour cells are heavily reliant on proteasomal machinery in order to support high rates of proliferation. Since the FDA's approval of bortezomib for the treatment of multiple myeloma in 2003[480], a number of next generation proteasome inhibitors have been developed[485]. However, the success of these inhibitors in blood-borne cancers has not extended to solid tumours. Bortezomib has been trialled in HNSCC in combination with existing chemotherapies, but the response rate in patients has been low[422]. The primary aim of this chapter is to determine whether targeting specific proteasomal subunit genes, such as *PSMD2* or *PSMD6* could represent a viable therapeutic strategy in HNSCC, or improve the efficacy of existing drugs.

6.2 *PSMD2* is frequently overexpressed in HNSCC patient samples

Using TCGA's cBioPortal, the mRNA expression of 43 genes encoding proteasomal subunits were queried in the HNSCC dataset (n = 522), revealing upregulation of *PSMD2* gene expression (z score > 2) in 34% of tumour samples (Figure 6.2).

Moreover, silencing of the gene caused ~40% growth inhibition in the Liv7k cell line, possibly because of incomplete knockdown owing to extra gene copies.

PSMD2 copy number amplification was present in ~20% of these tumour samples, a value consistent with other 3q26-29 genes.

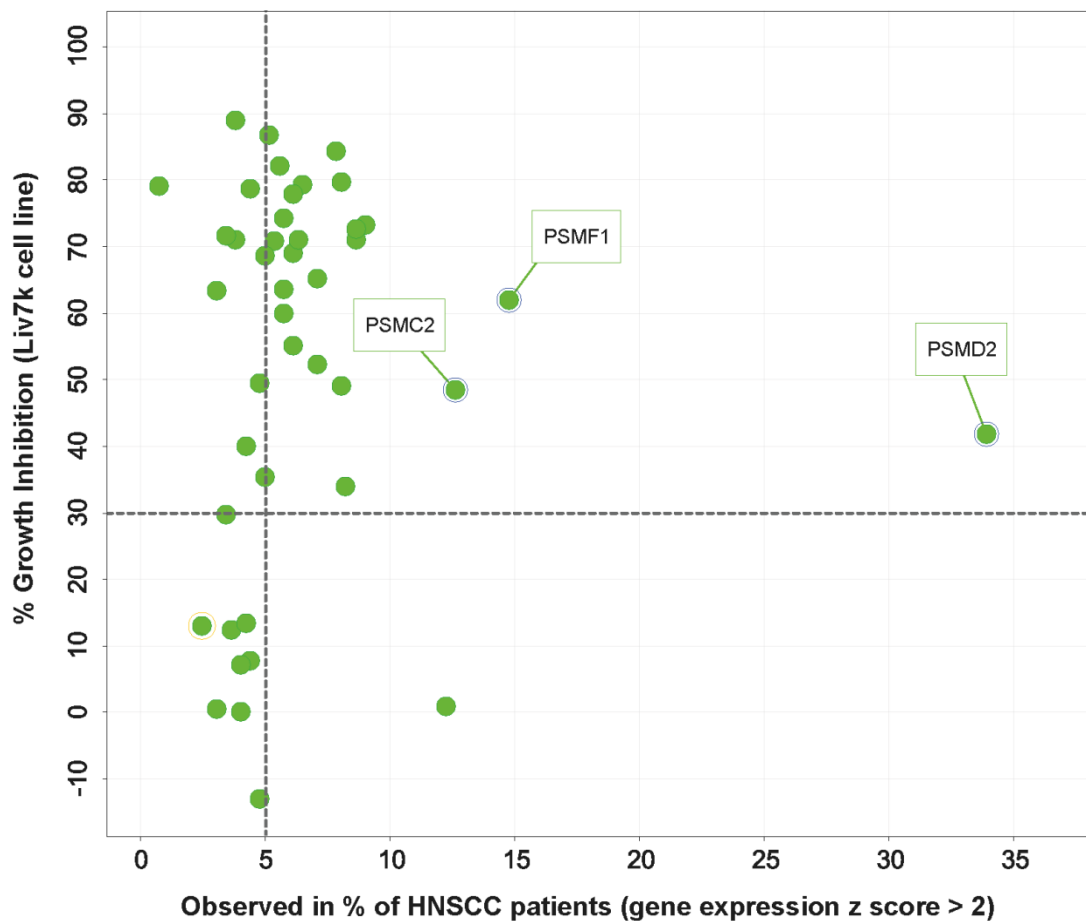


Figure 6.2 Genomic profiling of upregulated genes encoding proteasomal subunits. 43 genes encoding proteasomal subunits were queried in TCGA's cBioPortal (n = 522 samples). The percentage of patients with gene overexpression (z score ≥ 2) is plotted against the percentage growth inhibition resulting from gene knockdown in the Liv7k cell line, normalised to a non-targeting control siRNA. Dashed lines indicate a minimum cut-off of 30% growth inhibition and overexpression in $\geq 5\%$ of patient samples.

6.3 Concurrent downregulation of *PSMD6* is a common event in HNSCC patient samples

In addition to upregulation of *PSMD2*, gene expression and viability analysis for related proteasomal subunits identified concurrent downregulation of *PSMD6*. Approximately 60% of patient samples with upregulation of *PSMD2* gene expression (z score > 2) also exhibited downregulation of *PSMD6* gene expression (z score < -2) (Figure 6.4). *PSMD6* is encoded within 3p14.1, a commonly deleted region in HNSCC tumours, which is also observed in the Liv7k cell line[117].

Based on a recent study by William Hahn's group[484], which identified specific vulnerabilities as a result of copy number loss, it was hypothesized that partial copy number loss of *PSMD6* observed in Liv7k cells would render them highly dependent on the expression of the remaining copies. Thus, suppression with RNAi would have a greater effect in the Liv7k cell line than in other cancer cell lines that have diploid *PSMD6* copy number.

RNAi screening revealed a high dependence on genes with frequent copy number loss, including *PSMD6*, where knockdown in the Liv7k cell line caused ~80% growth inhibition (Figure 6.3). Furthermore, loss of *PSMD6* copy number is correlated with decreased mRNA expression in patient samples (Figure 6.4).

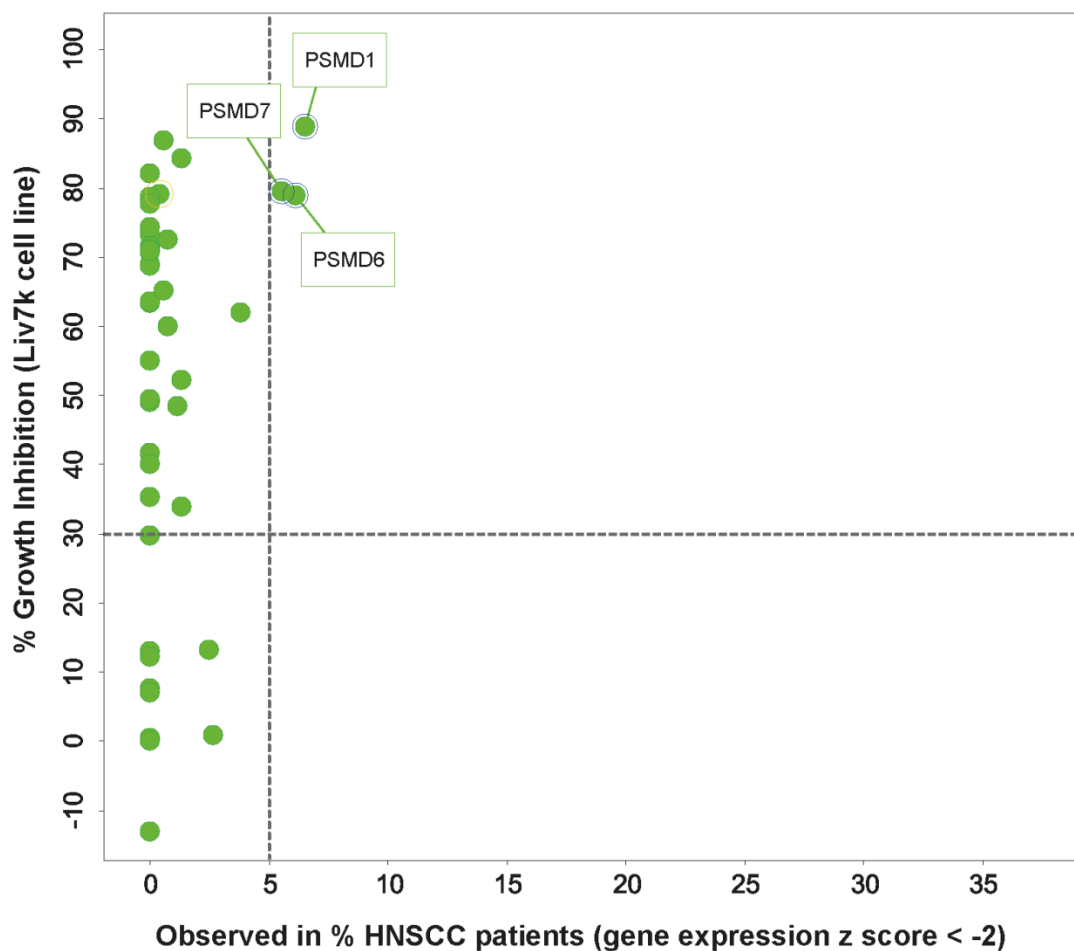


Figure 6.3 Genomic profiling of downregulated genes encoding proteasomal subunits. 43 genes encoding proteasomal subunits were queried in TCGA's cBioPortal (n = 522 samples). The percentage of patients with downregulation of gene expression (z score ≤ -2) is plotted against the percentage growth inhibition resulting from gene knockdown in the Liv7k cell line, normalised to a non-targeting control siRNA. Dashed lines indicate a minimum cut-off of 30% growth inhibition and overexpression in $\geq 5\%$ of patient samples.

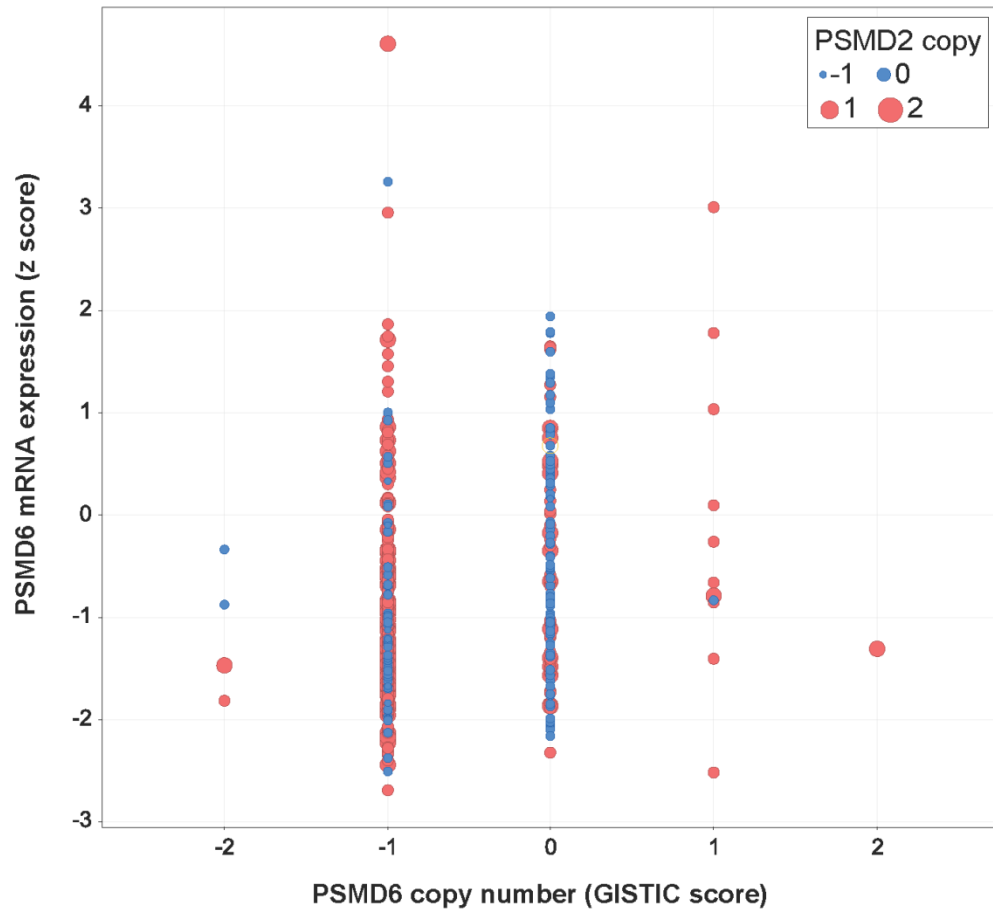


Figure 6.4 Genomic profile of *PSMD6* expression in TCGA patient samples. Copy number status is given as GISTIC score (-2, deep deletion; -1, shallow deletion; 0, equal to matched normal sample; 1, gain; 2, amplification) alongside mRNA expression z score. *PSMD6* copy number loss is frequently accompanied by downregulation at mRNA level (TCGA, n=522 samples). Red circles represent samples with *PSMD2* copy number amplification (GISTIC +2).

6.4 *PSMD6* gene copy number loss renders tumour cells more vulnerable to suppression of remaining copies

RNA sequencing of two oral SCC and two oral keratinocyte cell lines revealed a differential expression of proteasomal subunit genes. *PSMD2* and *PSMD6* expression sit at opposite ends of this spectrum. Subtracting the mean gene expression in the keratinocyte cell lines from the mean gene expression in the oral SCC cell lines revealed: (1) overexpression of *PSMD2* and (2) downregulation of *PSMD6* in carcinoma cells versus keratinocytes (Figure 6.5).

To validate this, mRNA expression and copy number profiles of four differentially expressed genes were generated for a panel of cell lines using qRT-PCR (Figure 6.6 and Figure 6.7). The genes were selected in order to provide a gradient of expression, from highly amplified *PSMD2* > moderately amplified *PSMC2* > moderately deleted *PSME4* > highly deleted *PSMD6*. Copy number measurements revealed gain of *PSMD2* in Liv7k and KR19 OSCC lines and loss of *PSMD6* and *PSME4*, compared to normal control lines. Regardless of gene copy number status or mRNA expression, protein expression was similar in all tested cell lines (Figure 6.8).

Percentage loss of viability was measured in two cancer and two non-cancer cell lines after siRNA knockdown of PSM genes (Figure 6.9A). This revealed a greater sensitivity of Liv7k/KR19 to loss of *PSME4* and *PSMD6* compared to OKG4, but not OKF4. Silencing of *PSMD6* is particularly caused major growth inhibition in three out of four cell lines tested. Validation of *PSMD2* knockdown was validated using qRT-PCR (Figure 6.9B). Validation of protein knockdown also showed on-target effect (data not shown). *PSMD6* knockdown could not be assessed owing to very high growth inhibitory effect on cells.

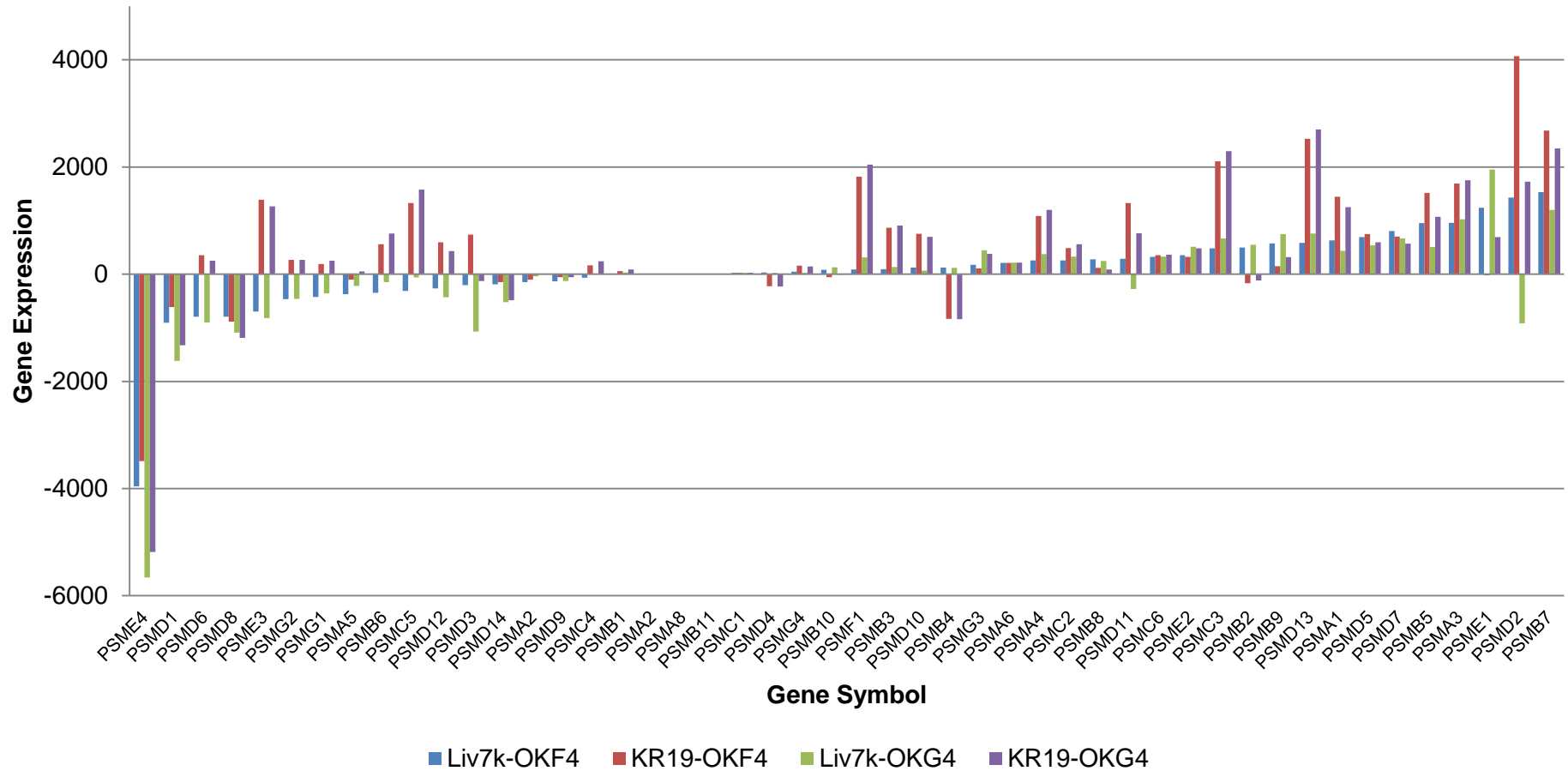


Figure 6.5 RNA sequencing analysis reveals differential expression of proteasomal subunit genes in oral SCC cells versus immortalised keratinocytes. Each bar represents the difference in expression between oral SCC cells and immortalised keratinocyte cells as denoted in the legend. Expression is given as the mean of three biological replicate samples.

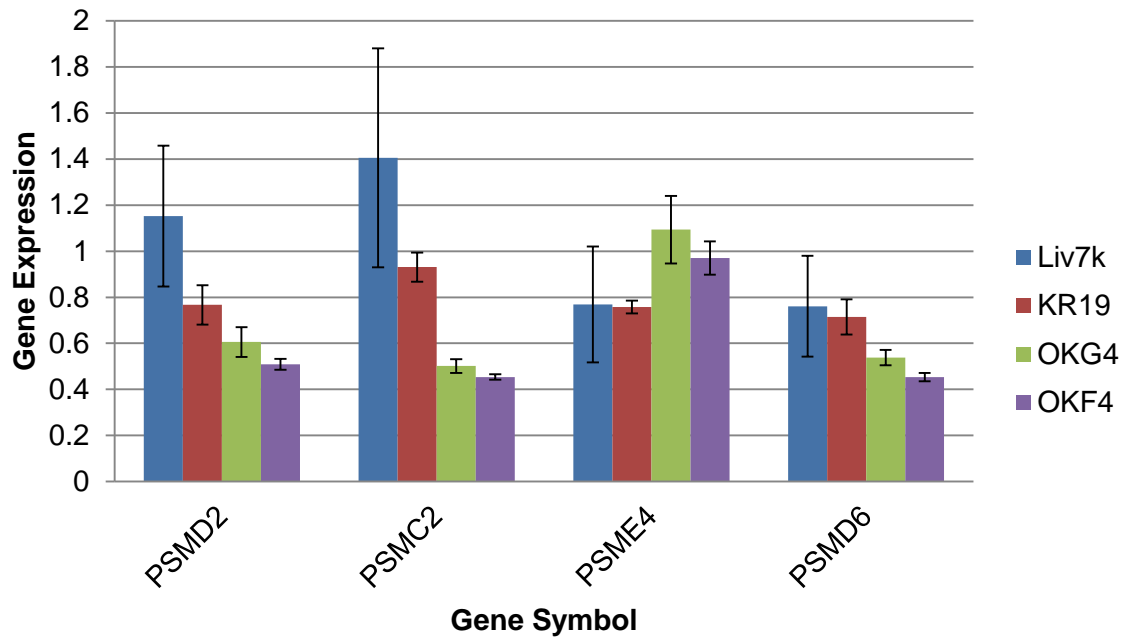


Figure 6.6 Proteasomal subunit RNA expression profile. RTq-PCR was used to confirm proteasomal subunit mRNA expression in oral SCC cells and immortalised keratinocytes. Gene expression was normalised to β -actin and presented as mean \pm SD of three biological replicates.

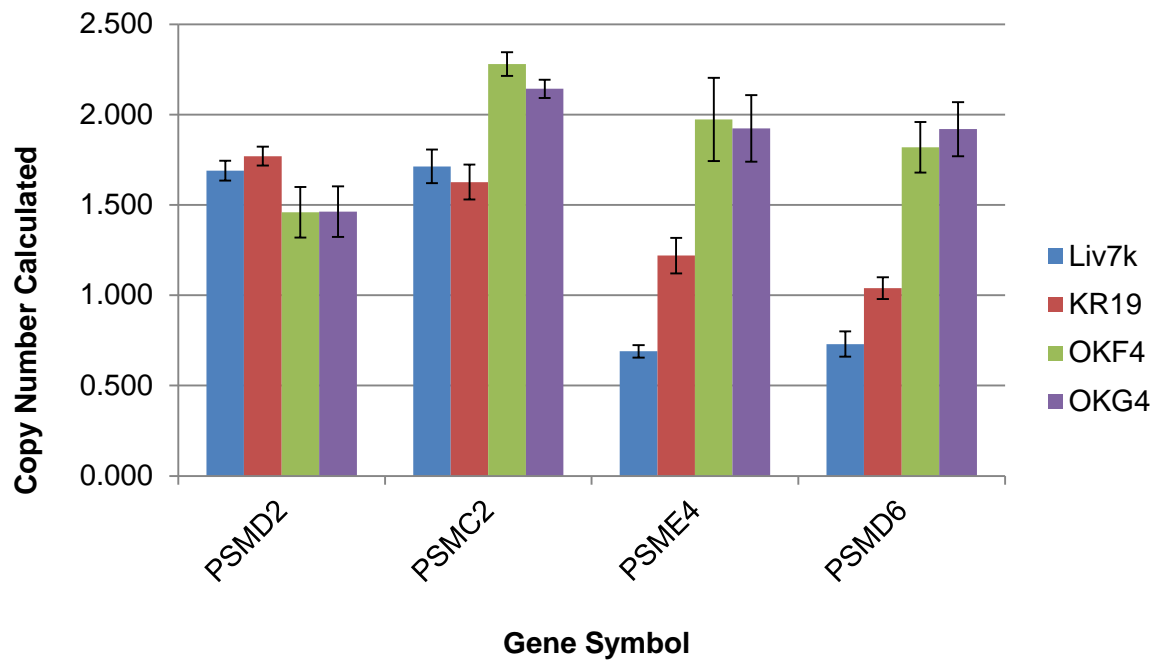


Figure 6.7 Copy number analysis of *PSMD2*, *PSMC2*, *PSME4* and *PSMD6* using Taqman RTq-PCR assays in oral SCC/keratinocyte cell lines. RNaseP was used to normalise genomic DNA concentrations and DNA from a cell line known to be diploid (copy number = 2) for each gene was used as a reference control. Copy number is presented as the mean \pm SD of three biological replicates.

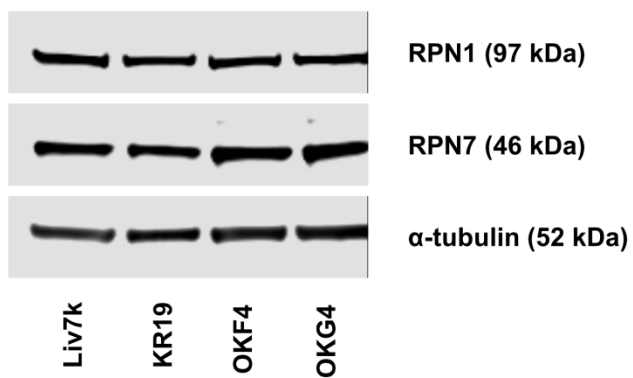


Figure 6.8 Western blot analysis of the expression of the proteins encoded by *PSMD2* and *PSMD6*, RPN1 and RPN7 respectively, in two oral SCC and two oral keratinocyte cell lines. 20 μ g of whole-cell lysate was loaded per lane. Extracts were quantified and normalised using BSA assay and alpha-tubulin was used as a loading control.

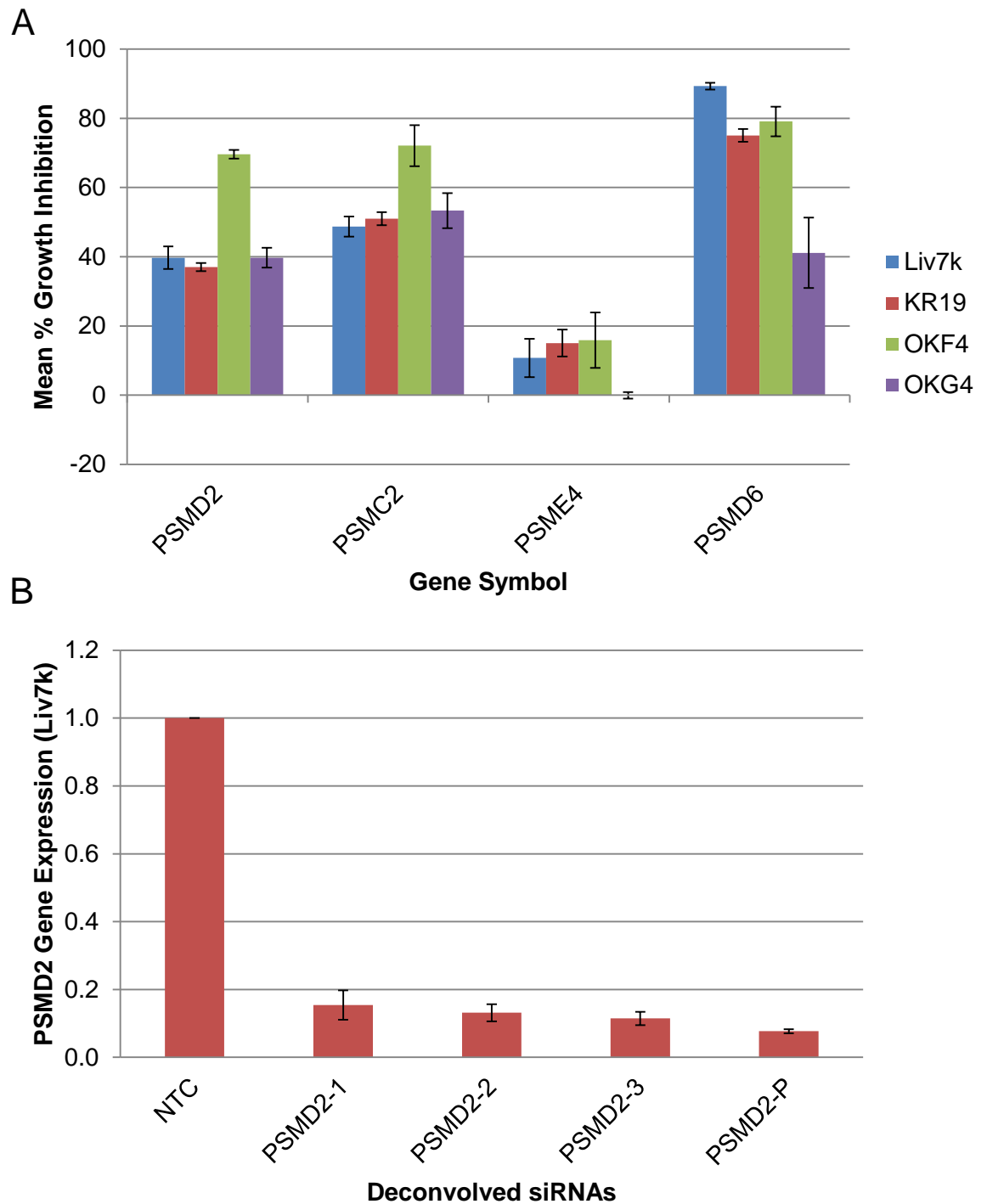


Figure 6.9 Mean growth inhibition after knockdown of proteasomal subunit genes. (A) Pooled siRNA targeting selected proteasomal subunit genes were transfected into two oral SCC cell lines and two oral keratinocyte cell lines. 72h post-transfection, cells were fixed and stained with DAPI for imaging on the Operetta. Results are normalised to non-targeting control siRNA and represent the mean \pm SD of three technical replicates. (B) RTq-PCR showing reduction in PSMD2 gene expression after siRNA knockdown in Liv7k cells. PSMD2 expression was normalised to ACTB and presented relative to NTC. Data is mean \pm SD of three biological replicates. siRNA #4 was too lethal to get enough genetic material for analysis by RTq-PCR.

6.5 Copy number amplification of proteasomal subunit genes does not predict sensitivity to bortezomib

Using compound screening data from the Sanger Institute[486], the sensitivity of 427 authenticated cancer cell lines to bortezomib was plotted (Figure 6.10). Based on this, the relative sensitivity of the oral cancer cell lines used in this project was ascertained. A bortezomib-resistant breast cancer cell line (BT-474) was subjected to a dose response experiment alongside four oral cell lines. This cell line was used, as it was the only resistant cell line in frozen storage. The results are shown in Figure 6.11. All four oral cell lines had an IC₅₀ value of between 0.002-0.006 μM , suggesting that the copy number status of PSM genes does not predict bortezomib sensitivity.

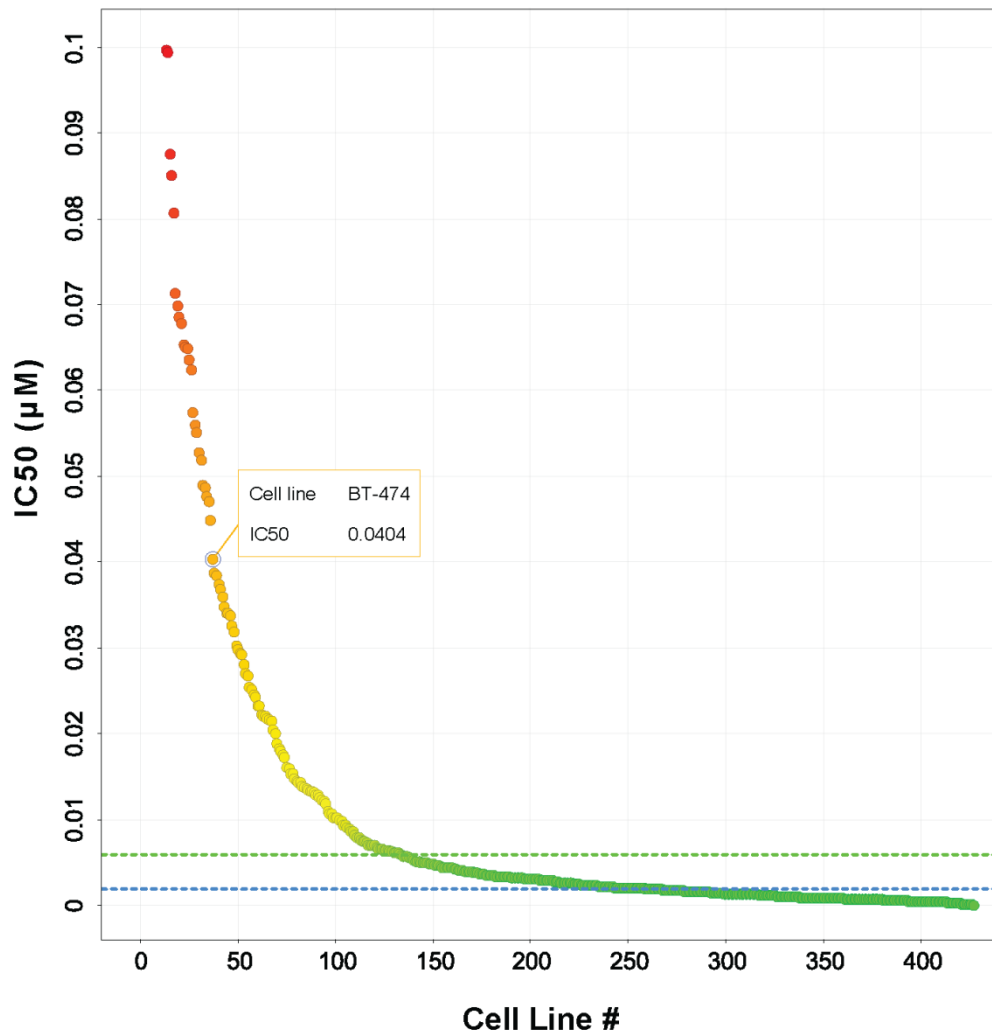


Figure 6.10 Bortezomib IC₅₀ values from the Genomics of Drug Sensitivity in Cancer Screen (Sanger Institute). IC₅₀ values are presented for cell lines < 0.1 μM , with BT-474 cell line labelled. Blue dotted line, 0.002 μM ; green dotted line, 0.006 μM). Data adapted from [486].

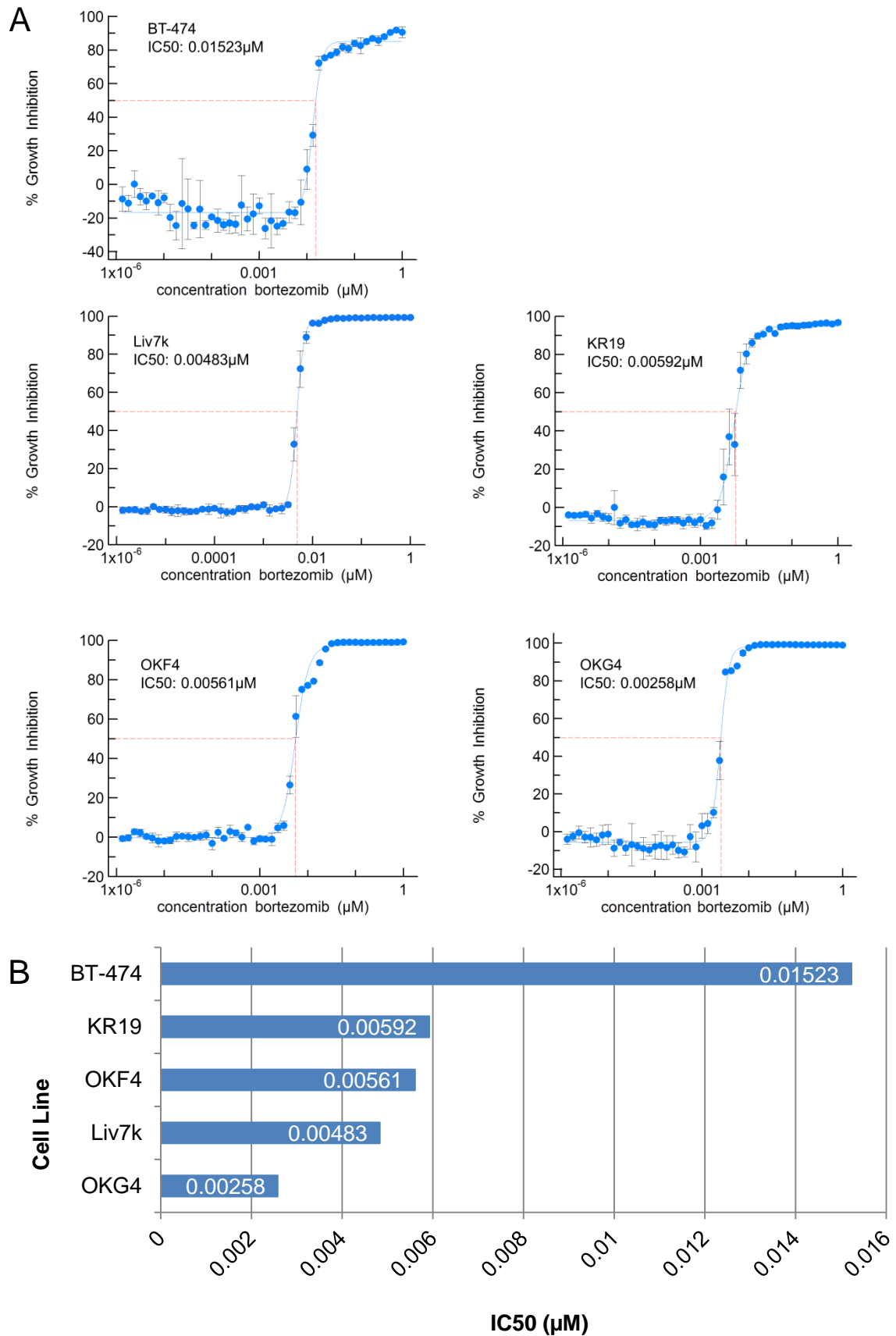


Figure 6.11 Bortezomib dose response curves in BT-474, oral SCC and immortalised keratinocyte cell lines. (A) Dose response curves and (B) IC₅₀ values. Bortezomib concentration ranges from 0.00001-1µM. Results are normalised to DMSO vehicle control treatment and represent the mean ± SD of three technical replicates.

6.6 Silencing of *PSMD2* does not alter the response of oral cancer cells to proteasomal inhibition by bortezomib

Based on a recent study by Tsvetkov *et al.*, which showed that reducing the expression of 19S subunits protected cancer cells from bortezomib-mediated proteasomal inhibition[483], it was hypothesized that knockdown of *PSMD2* in oral SCC cells may alter their response to bortezomib. To determine if this was the case, siRNA targeting the *PSMD2* gene was transfected into Liv7k cells 24 hours prior to the addition of bortezomib. However, no significant difference was observed in cells +/- *PSMD2* in response to bortezomib (Figure 6.12).

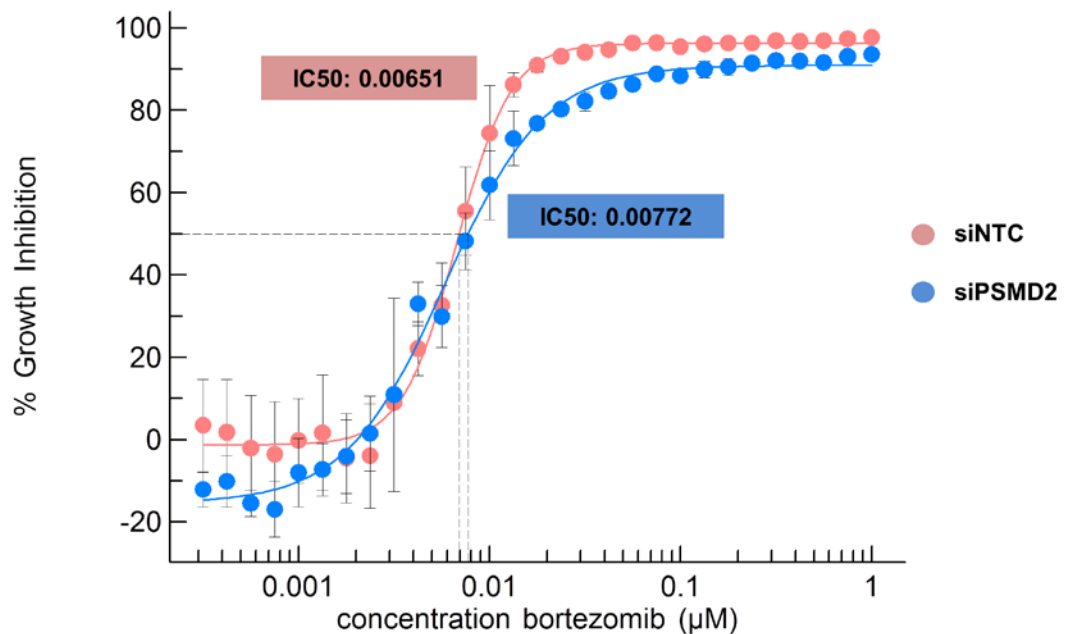


Figure 6.12 Bortezomib dose response curve +/- *PSMD2* in Liv7k cell line. Pooled *PSMD2* siRNA was transfected into cells 24 hour prior to addition of bortezomib (concentration range 0.0003 - 1 µM). Results are presented relative to DMSO vehicle control and are representative of the mean \pm SD of three technical replicates.

6.7 Proteasomal activity is not altered by gene expression of PSMD2 (preliminary data)

In order to determine if different gene expression profiles affected proteasomal function, basal proteasomal activity was measured in a panel of oral cell lines using the Proteasome-Glo™ chymotrypsin-like assay (Promega #G8660). Relative Light Units (RLU) was normalised to the number of nuclei per well and plotted in Figure 6.13. In this experiment, Liv7k and OKF4 cell lines had a lower basal proteasomal activity than KR19 and OKG4 cells. The effect of bortezomib on proteasome activity was also measured in the Liv7k, Liv37k and OKF4 cell lines, but no significant difference in IC₅₀ was observed (Figure 6.14).

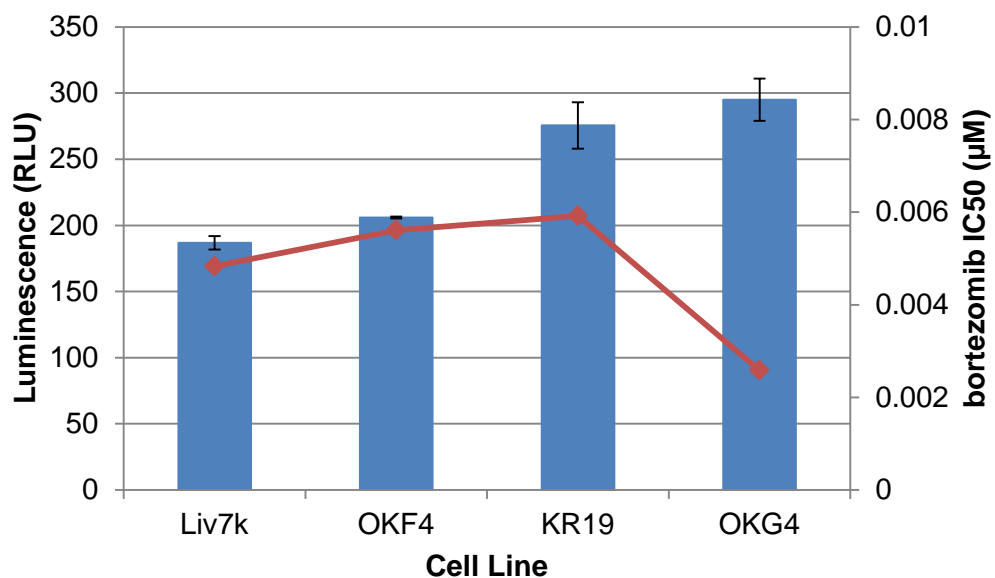


Figure 6.13 Basal proteasomal activity measured in oral SCC and immortalised keratinocyte cell lines. Chymotrypsin-like activity of oral cell lines is ranked from lowest to highest. RLU is normalised to cell number. Bortezomib IC₅₀ values are overlaid. Results are mean±SD of three biological replicates.

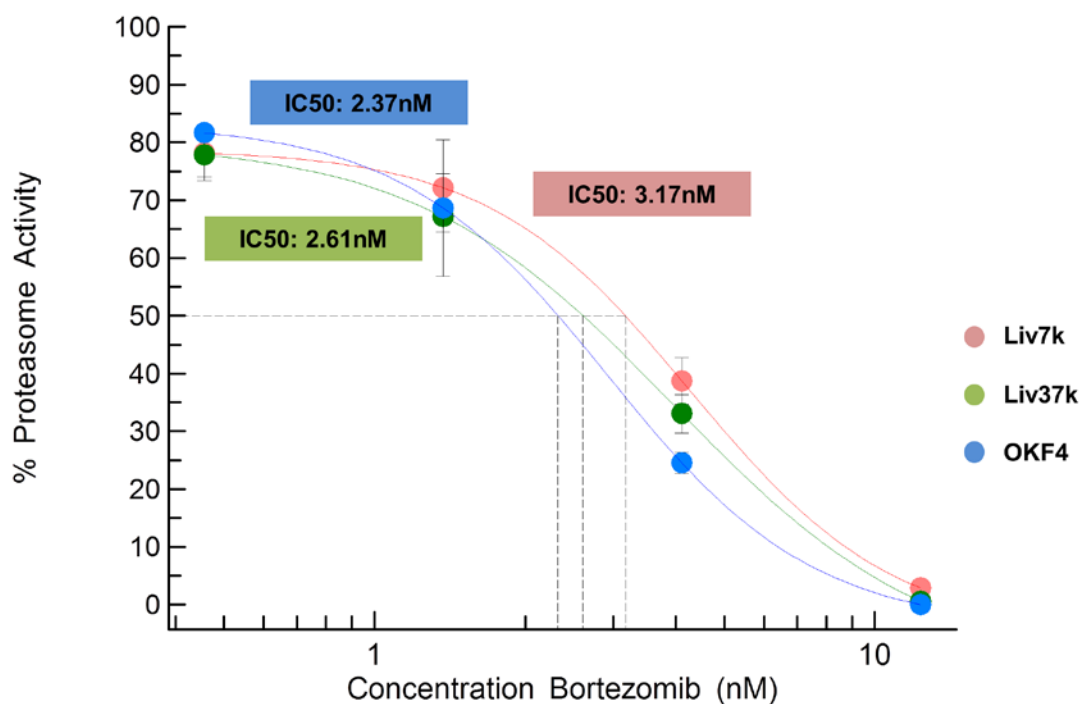


Figure 6.14 The effect of bortezomib treatment on proteasome activity. Bortezomib dose response curves in Liv7k, Liv37k and OKF4 cell lines showing concentration required to inhibit proteasomal activity by 50%. Results are normalised to negative control and represent the mean \pm SD of three technical replicates.

6.8 Discussion

PSMD2 encodes a regulatory subunit of the 26S proteasome, which is responsible for ATP-dependent degradation of ubiquitinated proteins. Similar to *IGF2BP2*, *PSMD2* was shown to be highly upregulated in patient tumour samples and amplification of the gene was significantly correlated with reduced survival. Highly proliferative cells have a higher proteasomal activity and are thus more vulnerable to its depletion than normal cells. Thus, it was hypothesized that knockdown of *PSMD2* would have a greater effect on the survival of cancer cell lines than normal controls.

Publically available data from the Sanger Institute (Wellcome Trust) presented a number of useful control cell lines, previously shown to be sensitive/resistant to bortezomib. In a pan-cancer analysis, resistance to bortezomib in these cell lines is significantly correlated with a number of genetic alterations (including mutation in *SOS2*), but no alterations in proteasomal subunit genes was detected in bortezomib resistant cell lines[486]. To test this theory, I carried out real time qPCR on a panel of oral SCC cell lines in order to rank them from highest to lowest expression of *PSMD2*, which I could then relate with their sensitivity to bortezomib. To support the mRNA expression, I carried out western blots to assess basal protein expression in selected cell lines. No significant difference in protein expression was observed. I also generated IC50 curves for bortezomib; however, there was no correlation between a higher transcription of the *PSMD2* gene and enhanced sensitivity to bortezomib. A second-generation proteasomal inhibitor, carfilzomib, was also tested, but similar results were observed (data not shown). However, other factors can also contribute to bortezomib sensitivity, including AKT activation status.

Although there was a higher mRNA expression of the gene in Liv7k cells compared to immortalised oral keratinocyte cell lines, protein expression was similar in all cell lines tested. In addition, silencing of *PSMD2* resulted in a similar or greater loss of viability in the normal control cell lines, and did not alter the response of Liv7k cells to bortezomib. This, combined with the high proteasomal activity in these cell lines, suggests that the immortalised keratinocyte cell lines have adapted to growth on a 2D monolayer. This

highlights a weakness of this project, which is the lack of control cells that accurately represent the situation in normal tissue. Moreover, the tumour cell lines may respond differently to loss of proteasomal subunit expression *in vivo* where nutrients and oxygen are limited.

In addition to upregulation of *PSMD2*, gene expression and viability analysis for related proteasomal subunits identified concurrent downregulation of *PSMD6* in oral cancer cell lines. Genomic instability of tumours often promotes loss of chromosomal regions, which contain tumour suppressor genes, accompanied by collateral loss of other genes. Based on a recent study by William Hahn's group[484], which identified specific vulnerabilities resulting from gene copy number loss, it was hypothesized that the partial copy number loss of *PSMD6* would render Liv7k cells highly dependent on expression of the remaining copy. Thus, suppression with siRNA would have a greater effect in the Liv7k cell line than in normal cell lines with diploid copy number. The gene, which is deleted in ~6% of HNSCCs, is important for cell viability as knockdown of the gene resulted in >80% growth inhibition in Liv7k cells. In addition, RNA sequencing revealed downregulation of the gene in cancer cell lines compared to oral keratinocytes. Knockdown of the gene was only half as effective in the OKG4 cell line. However, OKF4 cells did not follow this trend. This inconsistency cannot be explained by the expression of *PSMD6* in the cell lines, as both OKF4 and OKG4 showed a relative copy number loss of the gene compared to Liv7k.

Protein expression of RPN1 (*PSMD2*) and RPN7 (*PSMD6*) was equal in all cell lines, which might explain the similar response to bortezomib. Gene expression does not always correlate with protein expression[487] as many levels of regulation exist between gene transcription and production of the final protein[488]. RNA-binding proteins, such as IGF2BP2, exert a major influence on the stability and the rate of translation[489]. However, as previously stated, the environment *in situ* may alter the dynamics of this relationship in such a way as to render the expression of *PSMD2* or *PSMD6* relevant for survival.

In conclusion, overexpression of *PSMD2* could not be correlated to an increased dependence on proteasomal machinery in an oral SCC model. Partial copy loss of *PSMD6* does not appear to render cells more vulnerable to its suppression, and

the gene appears to be critical for survival in oral keratinocyte cell lines. The activity of the proteasome, and hence its importance in cancer progression, relies on a regulatory system more complex than expression of its individual components. Based on these results, there is nothing to support that PSMD2 amplification or PSMD6 deletion supports patient stratification for bortezomib alone.

Chapter 7 Results – The Role of Lipid Metabolism Genes in Hypoxia

7.1 Triglyceride Metabolism

The mainstay treatment for resectable oral SCC is surgery; however, chemo/radiotherapy is used as a primary means of treatment in patients who are unable to tolerate such a procedure[490]. External beam radiotherapy (EBRT) and conventional chemotherapy can also be used as adjuvants. Hypoxia is a defining feature of oral SCC and tumours with poor oxygenation are more resistant to chemo/radiotherapy[491, 492]. Hypoxia elicits a range of cellular responses, including changes in metabolism, increased angiogenesis and enhanced growth and survival. The master regulator of the hypoxic response is HIF-1 α , which is overexpressed in up to 70% of oral SCCs and is significantly correlated with poor survival[493]. Moreover, increased expression of HIF-1 α is associated with increased rates of metastasis through increased expression of matrix metalloproteases and chemokines[494, 495].

An increased rate of lipid synthesis is recognised as an important aspect of altered metabolism in tumour cells. However, the role that lipids play in cancer progression is not clear. Under normal conditions, *de novo* biosynthesis of fatty acids is restricted to particular tissues such as the liver. However, tumours can autonomously produce fatty acids and lipid components required for growth[272]. Fatty acids are the essential building blocks of lipids and are used to build many classes of lipids, which perform a range of functions within the cell. A family of transcription factors called sterol regulatory element-binding proteins (SREBPS) are master regulators of lipid biosynthesis[496]. Dysregulation of SREBPs can stimulate a network of oncogenic signals and promote an aggressive phenotype in oral cancer cells[275].

7.1.1 Lipid metabolism genes are upregulated in hypoxia

The aim of this project was to identify genes that provide a growth advantage to cells in hypoxia (defined here as 0.1% O₂). A data multiplexing approach was taken which combined results from a whole genome siRNA screen with RNA sequencing analysis. The siRNA screen, which was carried out on the aggressive

oral SCC cell line (Liv7k), involved the knockdown of 18,175 genes in normoxic (21% O₂) and hypoxic (0.1% O₂) conditions. In addition, RNA sequencing (RNAseq) was carried out to identify changes in gene expression in hypoxia.

A threshold window of 20% growth inhibition was set between hypoxia and normoxia, with a 10% minimum growth inhibition in hypoxia. Of 18,175 genes screened, 11% (n=1990) met this criteria (**Figure 7.1**). However, only 813 genes in this subset were deemed significant when a Mann-Whitney t-test was applied (p<0.05). Of this filtered set, 127 genes (22%) were also significantly upregulated at mRNA level (p<0.05) by ≥ 2 -fold. Gene Ontology analysis of this refined gene set revealed significant over-representation of genes involved in lipid metabolism.

Enrichment analysis was carried out using Metacore GeneGo™ software in order to narrow down specific canonical pathways, which are upregulated in hypoxia (**Figure 7.2**). In this analysis, control of cholesterol and fatty acid biosynthesis by SREBP ranked as the second most significant biological pathway (**Figure 7.3**). Sterol regulatory element binding proteins (SREBPs) are a family of transcription factors that regulate various aspects of lipid metabolism. SREBP cleavage-activating protein (SCAP) acts as a chaperone for SREBPs, mediating their transport from the endoplasmic reticulum to the Golgi apparatus where they are cleaved into active forms. Three isoforms (SREBP1a, SREBP1c and SREBP2) exist in mammalian cells and regulate expression of different target genes. SREBP1c preferentially regulates genes involved in fatty acid and triglyceride metabolism (e.g. *FASN*), while SREBP2 activates cholesterol synthesis (e.g. *HMGCS1*). SREBP1 is a potent activator of all genes containing the sterol regulatory element DNA sequence.

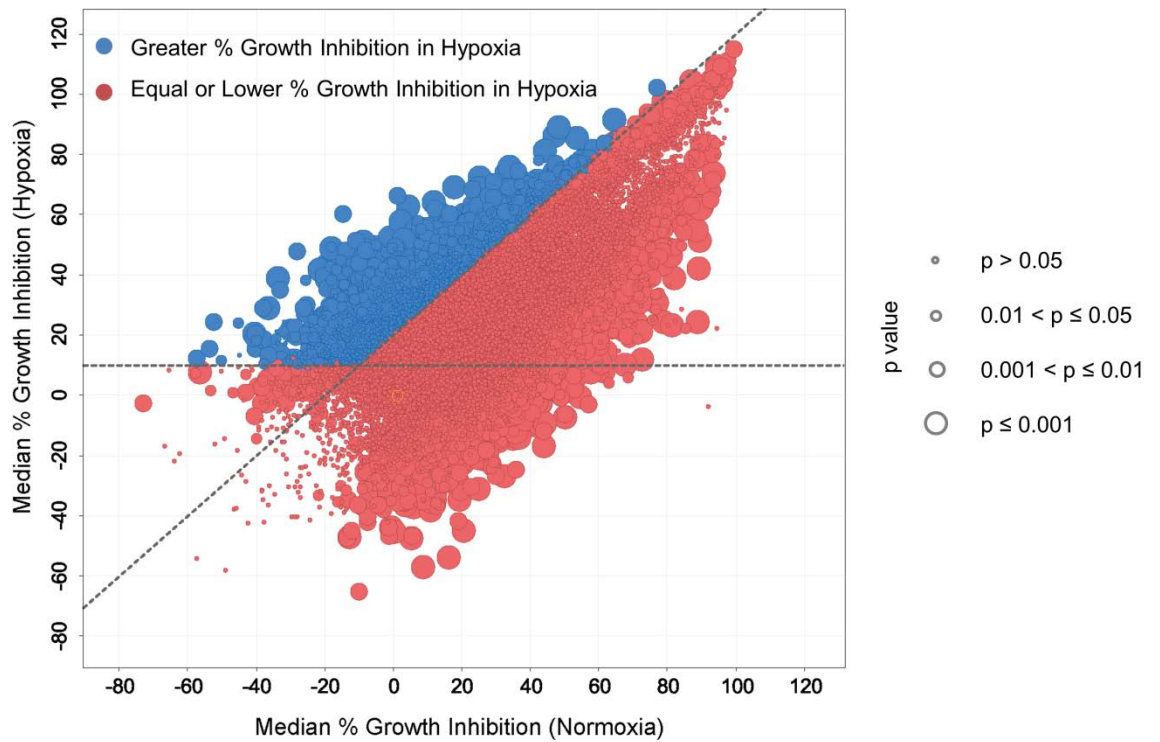


Figure 7.1 Primary siRNA screen results showing median percentage growth inhibition relative to non-targeting control in normoxic and hypoxic conditions. Gene knockdowns that are selectively lethal in hypoxia are highlighted in blue. Growth inhibition is normalised to non-targeting control siRNA. Cut-off was set at 20% difference between hypoxia and normoxia (diagonal line) with a minimum growth inhibition of 10% in hypoxia (horizontal line). Circle size is indicative of significance according to Mann-Whitney u-test (p value).

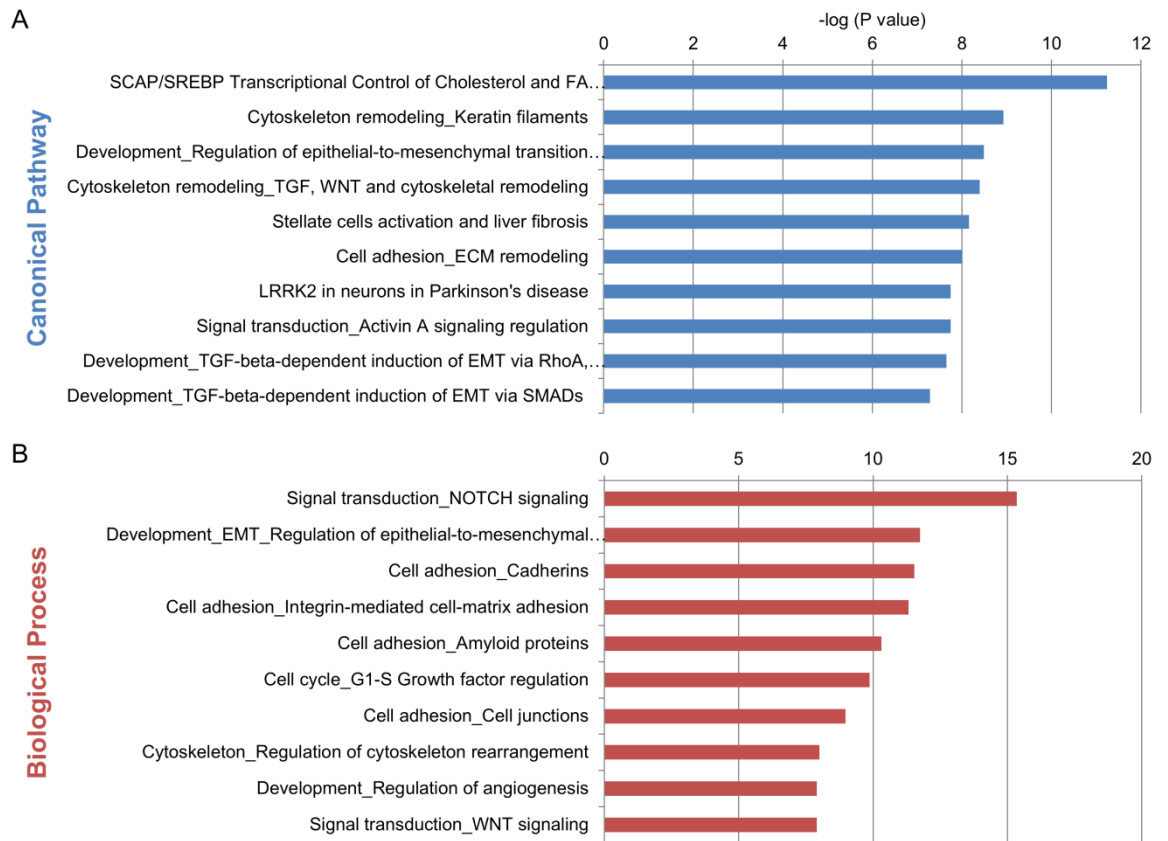


Figure 7.2 Metacore GeneGo™ analysis of the hypoxic gene set. Enrichment analysis of RNAseq data reveals top 10 upregulated (A) canonical pathways and (B) biological processes in hypoxia. Results are ranked in order of significance.

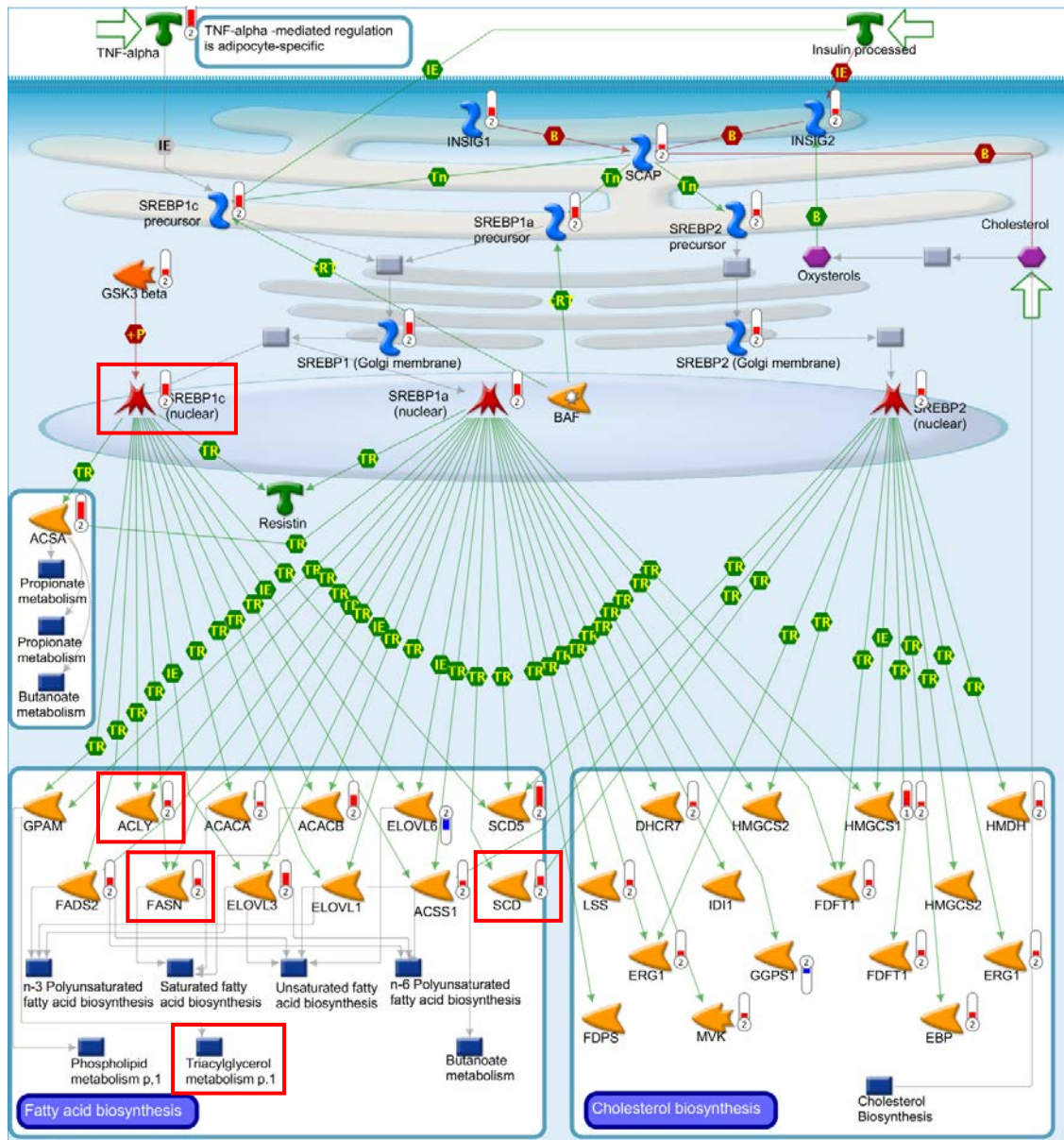


Figure 7.3 SREBP-mediated regulation of cholesterol/fatty acid biosynthesis. Pathway mapping of “SCAP/SREBP Transcriptional Control of Cholesterol and FA Biosynthesis”, highlighting up (red) and downregulated (blue) genes. Image generated by Metacore GeneGo™ software. Highlighted genes are discussed further in this chapter and/or the main introduction.

7.1.2 A subset of triglyceride metabolism genes are important for cell survival in hypoxia

Based on this analysis, a subset of genes that mediate triglyceride metabolism (*DAGLA*, *DGAT1*, *DGAT2*, *LIPE*, *MGLL*, *PNPLA2*, *SCD*) was selected for further study based on the differential effect observed upon their knockdown in hypoxia. Six of these genes (*DGAT1*, *DGAT2*, *LIPE*, *MGLL*, *PNPLA2*, *SCD*) demonstrated an increase in gene expression in hypoxic conditions (Figure 7.4). *DAGLA* gene expression was reduced by > 2 fold in hypoxia (data not shown).

In addition, data from the siRNA screen indicated that knockdown of monoacylglycerol lipase (*MGLL*) and diacylglyceride acyltransferase 2 (*DGAT2*) resulted in a significantly greater percentage growth inhibition in hypoxia compared to normoxia (Figure 7.5). The proteins encoded by these genes work in opposing ways, with *DGAT2* building triglycerides from fatty acids and *MGLL* breaking them down. This highlights the importance the two genes play in terms of energy release vs storage, a vital process for highly proliferative oral cancer cells.

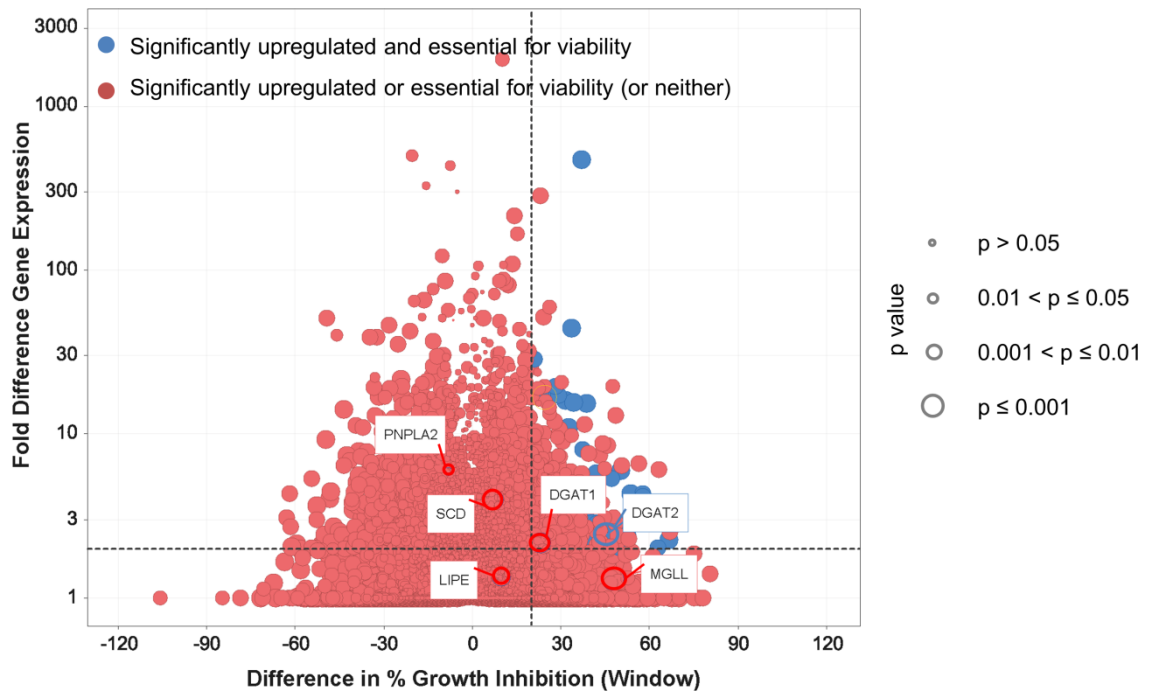


Figure 7.4 Window of percentage growth inhibition versus fold change in gene expression between hypoxic and normoxic conditions. Blue circles represent statistical significance in both the siRNA screen and the RNAseq dataset, including a window of growth inhibition between hypoxia and normoxia of $\geq 20\%$, a minimum growth inhibition of 10% in the normoxic condition ($p < 0.05$) and a fold change in gene expression of > 2 ($p < 0.05$). Circle size denotes growth inhibition significance according to Mann-Whitney u-test (p value). Triglyceride metabolism genes are labelled.

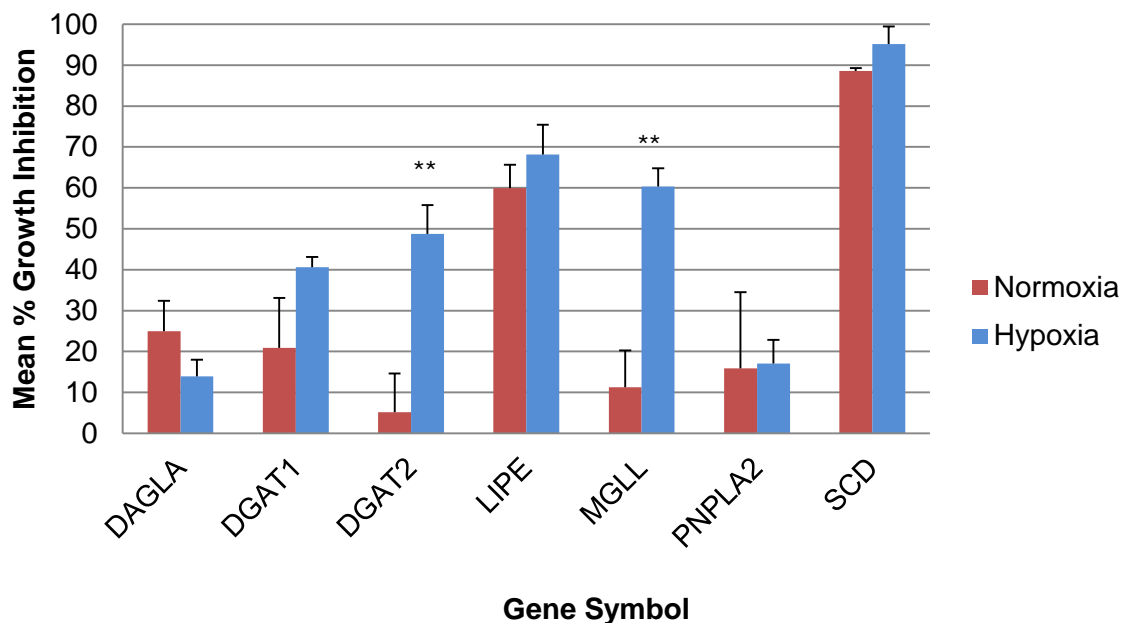


Figure 7.5 Mean percentage growth inhibition after knockdown of triglyceride metabolism genes (data from siRNA screen). Results are presented as mean \pm SD. *DGAT2* and *MGLL* were significantly different according to Mann-Whitney u-test (** $p < 0.01$).

7.1.3 Validation of differential growth inhibition did not confirm screen findings

In order to validate the differential growth inhibition observed in the siRNA screen siRNAs from a different supplier targeting genes of interest were transfected into two oral SCC (Liv7k, Liv37k) and two immortalised keratinocyte cell lines (OKF4, OKG4). However, under these conditions, *MGLL* and *DGAT2* knockdown resulted in a similar percentage growth inhibition in both normoxia and hypoxia (Figure 7.6). Interestingly, silencing of *PNPLA2*, which encodes adipose triglyceride lipase (ATGL), resulted in a greater differential than that measured in the siRNA screen.

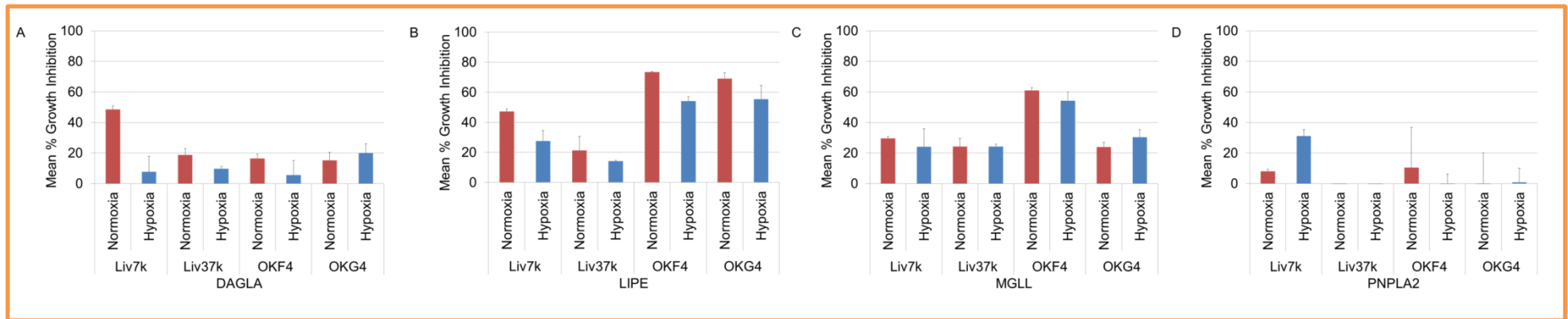
| Mean Percentage Growth Inhibition | | | | |
|-----------------------------------|------------|------------|----------------|----------------|
| Gene | Screen (N) | Screen (H) | Validation (N) | Validation (H) |
| DAGLA | 25.0 | 13.9 | 48.54 | 7.75 |
| DGAT1 | 20.9 | 40.6 | 68.44 | 39.55 |
| DGAT2 | 5.1 | 48.8 | 16.33 | -14.90 |
| LIPE | 61.8 | 68.2 | 47.24 | 27.63 |
| MGLL | 13.8 | 60.3 | 29.59 | 24.10 |
| PNPLA2 | 24.9 | 17.0 | 8.04 | 31.23 |
| SCD | 88.9 | 95.1 | 92.49 | 55.29 |

Table 7.1 Mean percentage growth inhibition after knockdown of triglyceride metabolism genes (comparison of data from siRNA screen with validation experiments). Results are presented as mean \pm SD.

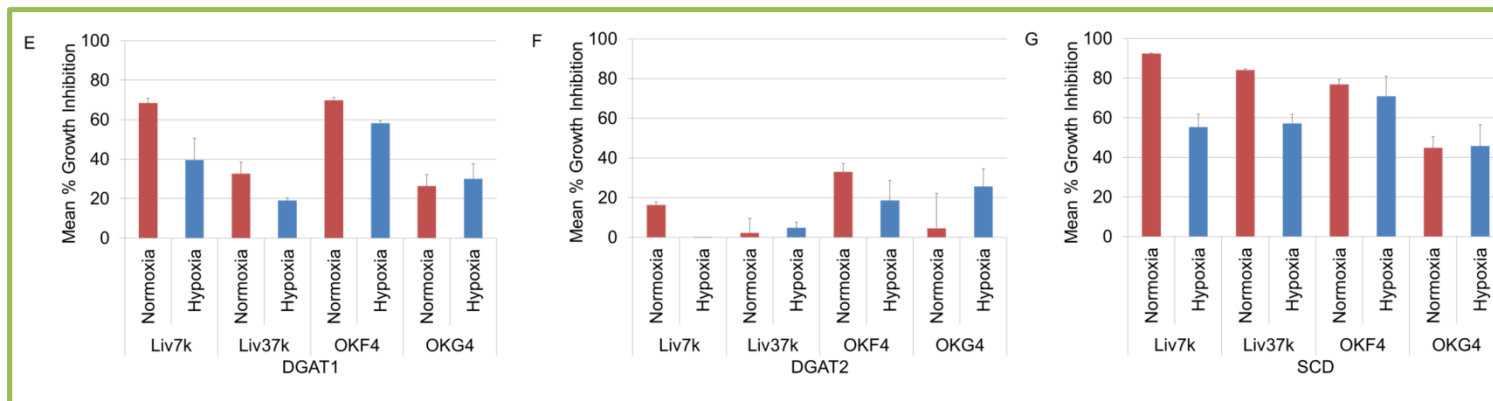
The ATGL enzyme works alongside hormone sensitive lipase (LIPE) to mobilise triglycerides and provide cells with energy. A series of recent papers document a role for ATGL in cancer. Inhibition of ATGL by the small molecule inhibitor atglistatin attenuates the growth of non-small cell lung adenocarcinomas, suggesting it enables an aggressive phenotype in tumours[497]. Increased expression of the protein was also associated with higher rates of stromal proliferation in pancreatic ductal adenocarcinoma, possibly contributing to a more invasion phenotype[498]. It has been established that ATGL catalyses the rate-limiting step in triglyceride metabolism in adipose tissue, and that its

activity increases in parallel with tumour growth[499, 500]. ATGL has also been implicated in cachexia in cancer patients, confirming *in vivo* studies which show *ATGL* null mice to be protected from tumour-induced lipolysis[501].

The most lethal knockdown observed in these validation studies was that of stearoyl-CoA Desaturase (*SCD*), possibly reflecting its unique importance in fatty acid chain modification. While a degree of redundancy exists in the triglyceride storage system with more than one enzyme catalysing similar steps, *SCD* is the only enzyme that can create a double bond in long-chain fatty acids. Interestingly, silencing of the gene caused greater growth inhibition in the Liv7k cell line compared to the OKG4 keratinocyte cell line. This could possibly suggest a vulnerability of highly proliferative cells on the modification of fatty acid chains, which are synthesized in greater numbers. However, OKF4 cells were as sensitive to *SCD* silencing as the oral cancer cell lines.



Catabolic



Anabolic

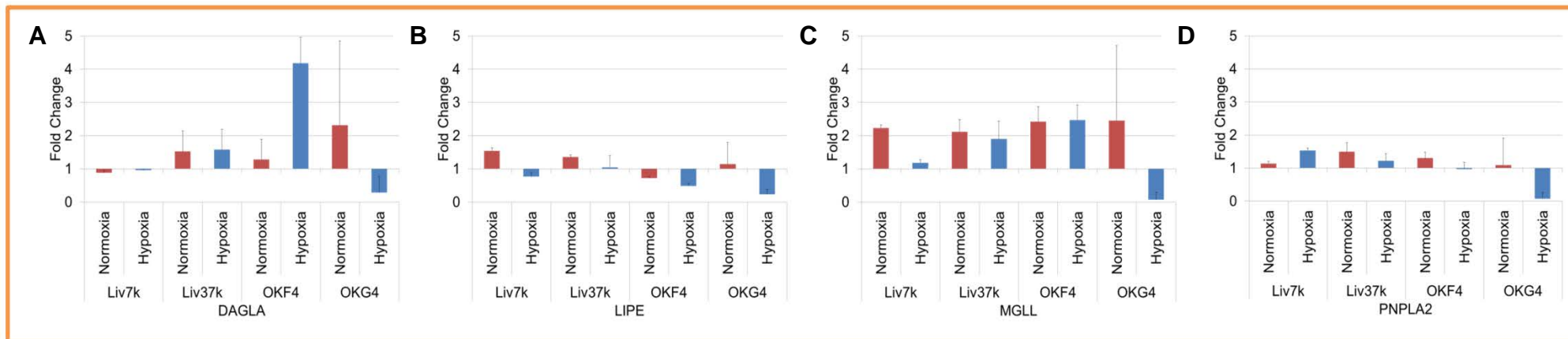
Figure 7.6 Knockdown of triglyceride metabolism genes leads to growth inhibition in oral cancer cells and immortalised keratinocytes. (A-G) Mean growth inhibition was measured in response to gene knockdown and normalised to non-targeting control siRNA in normoxic (red) and hypoxic (blue) conditions. The results from pooled siRNA are shown and results are presented as the mean \pm SD of three experiments.

7.1.4 Silencing of MGLL leads to a build-up of triglycerides in tumour cells

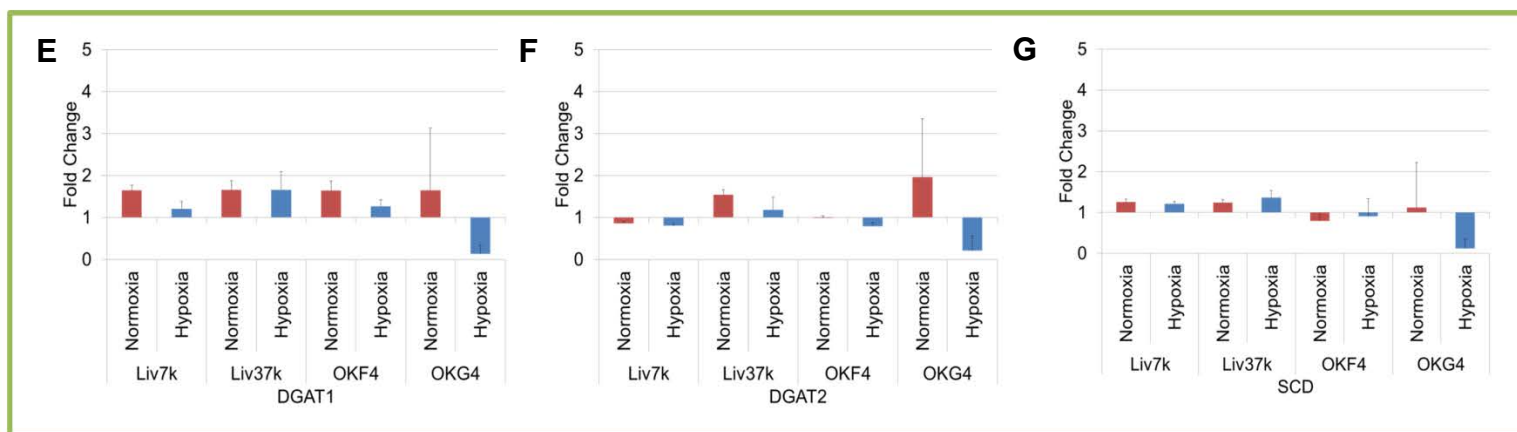
In order to confirm the mechanism by which silencing of triglyceride metabolism genes causes a reduction in cell growth, neutral lipid staining with BODIPY 493/503 was performed. After treatment with siRNA, cells were fixed and stained with DAPI (nuclei), whole cell stain red (cell boundaries) and BODIPY 493/503 (neutral lipid droplets). Lipid droplet quantifications were generated alongside percentage growth inhibition for four cell lines (Liv7k and OKF4 shown in Figure 7.7).

Silencing of *MGLL* led to a build-up of lipid droplets in both normoxic and hypoxic conditions, consistent with its role in breaking down triglycerides into fatty acids. Interestingly, knockdown of *LIPE* resulted in a marked difference in the levels of lipid droplets between hypoxia and normoxia. Silencing of *DGAT2* led to a small reduction numbers of lipid droplets in the Liv7k cell line. While the effect of *MGLL* knockdown was consistent in all cell lines tested, knockdown of *LIPE* and *DGAT2* also caused an increase in the number of droplets in other lines. It is possible a degree of overlap exists between *DGAT2* and its family gene, *DGAT1*, which could be elucidated by dual knockdown.

If oral cancer cells are more dependent on fatty acids for energy in hypoxia, it would be expected that knockdown of triglyceride lipase genes (*DAGLA*, *MGLL*, *PNPLA2*, *LIPE*) would have a greater effect on cell growth in this condition. In the Liv7k cell line, knockdown of *MGLL* and *LIPE* led to a build-up of lipid droplets in normoxia only (> 1.5 fold). This may suggest a greater activity of other lipases in hypoxia, which are able to compensate for the silencing of one gene. Interestingly, *PNPLA2* knockdown had the opposite effect, showing a hypoxia-specific increase in lipid droplets.



Catabolic



Anabolic

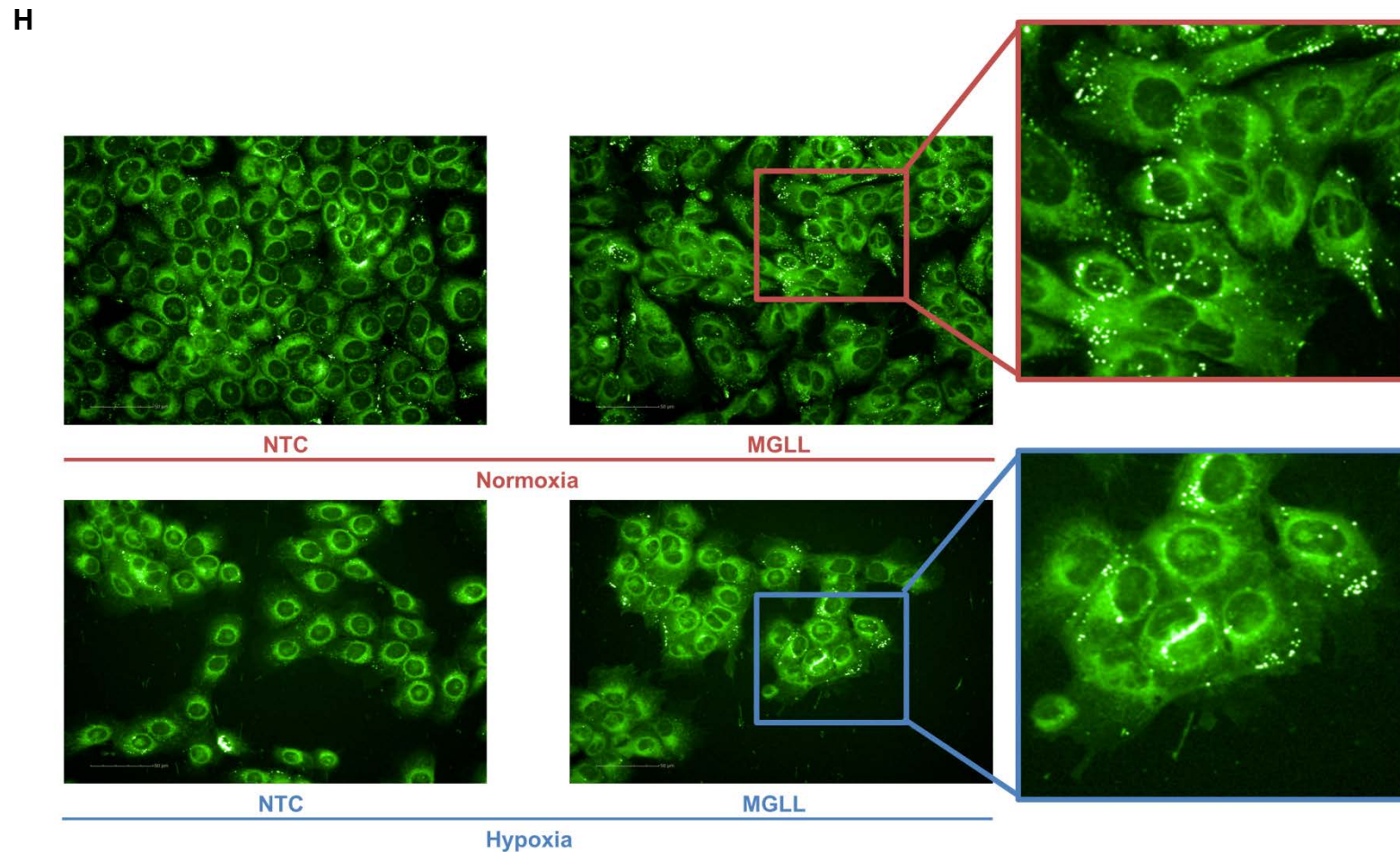


Figure 7.7 Quantification of neutral lipid droplets in oral cell lines. (A-G) BODIPY 493/503 neutral lipid stain was used to stain neutral lipid droplets (mostly triglycerides) in normoxia (red) and hypoxia (blue) upon knockdown of triglyceride metabolism genes. Lipid droplets were counted using Harmony software (Perkin Elmer) and normalised to non-targeting control siRNA. Fold change is the mean \pm SD of three experiments. (H) Representative image of Liv7k cells treated with non-targeting control and MGLL siRNA, with magnified inset.

7.2 Ether Lipid Metabolism

Reprogramming of metabolism is an important hallmark of cancer and dysregulated lipid metabolism plays a major role in tumour development[502, 503]. Fatty acids support the rapid proliferation of tumour cells by acting as a substrate for energy production, building blocks for cell membranes and lipid signalling molecules. Ether lipids make up approximately 20% of total phospholipid mass[504], and data from the siRNA screen, in combination with pathway analysis suggests that ether lipid metabolism can selectively support cell viability in a hypoxic environment.

Tumour cells possess elevated levels of ether lipids (such as plasmalogens), which are characterised by one or more ether linkages on the glycerol backbone, in place of the more common ester linkage[505-507]. This alternative structure has important implications for the roles of ether lipids within the cell, including membrane fusion, vesicle formation and lipid-mediated signalling. A key enzyme involved in ether lipid biosynthesis, alkylglycerone phosphate synthase (AGPS), is overexpressed in a number of aggressive cancer types, including breast and melanoma[268]. By mobilising free fatty acids from neutral lipid stores, AGPS intensifies *de novo* generation of lipid signalling molecules such as lysophosphatidic acid (LPA), and enhances tumourigenicity[508]. However, the specific role of AGPS and ether lipids in a low oxygen setting is unknown. An overview of ether lipid synthesis is shown in **Figure 7.8**.

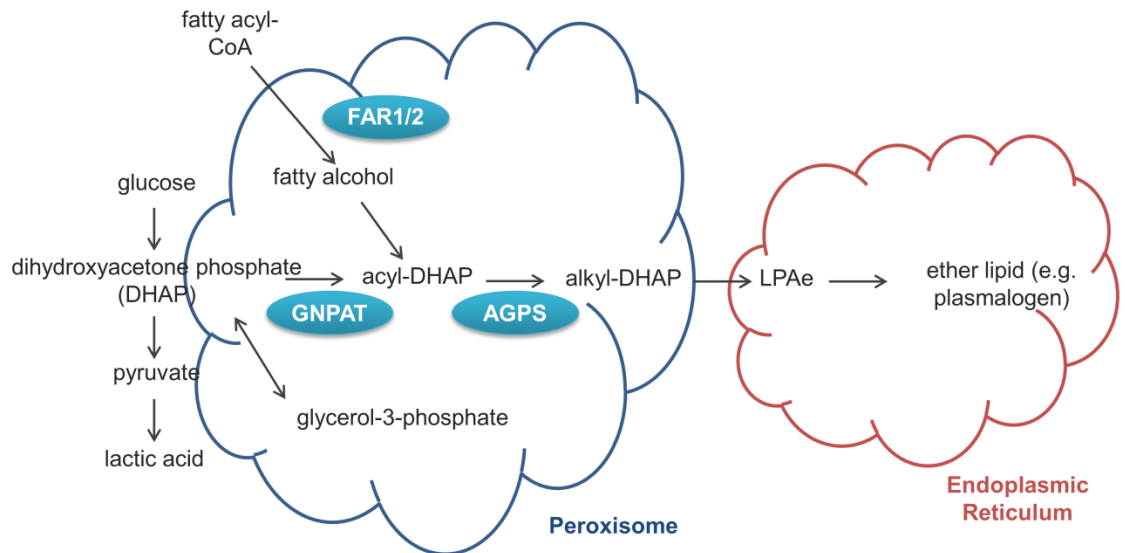


Figure 7.8 Overview of Ether Lipid Synthesis. AGPS, alkylglycerone phosphate synthase; FAR, fatty Acyl-CoA Reductase; GNPAT, glycerone-phosphate O-Acyltransferase; e: lysophosphatidic acid-ether.

AGPS catalyses the rate limiting step in ether lipid synthesis but the process also involves Fatty Acyl-CoA Reductase 1 and 2 (FAR1/2) and Glycerone-phosphate O-Acyltransferase (GNPAT)[509]. All three enzymes reside and act within peroxisomes where FAR1 and FAR2 provide substrate for GNPAT and AGPS to synthesize ether lipids by reducing fatty acids to fatty alcohols. GNPAT catalyses the acylation of dihydroxyacetonephosphate (DHAP) to acyl-DHAP, which is subsequently acted on by AGPS to exchange the acyl for an alkyl group[510]. Genetic deficiencies in AGPS, GNPAT or FAR1 severely impair the formation of etherphospholipids, and have been linked to cataract formation in humans and mice[511-514]. At the time of writing, only AGPS has been shown to have a role in cancer progression[268].

7.2.1 A subset of genes involved in ether lipid synthesis are essential for cell viability in hypoxia

Analysis of the ether lipid synthesis pathway revealed a number of ether lipid-related genes that when silenced in the Liv7k cell line had an effect on viability in hypoxia (Table 7.2). Analysis of the TCGA HNSCC dataset reveals altered gene expression of ether lipid biosynthesis genes in 5-10% of cases, confirming the importance of this pathway (Figure 7.9). Alterations in the expression of *AGPS* tend toward a reduction in patient survival, according to the TCGA HNSCC dataset (not significant). A small percentage of patient samples contain mutually exclusive alterations in ether lipid biosynthesis genes, but no further reduction in patient survival is observed.

Mean % Growth Inhibition

| Gene | Normoxia | Hypoxia | Fold Change | P value |
|--------------|----------|---------|-------------|---------|
| AGPS | 19.22 | 69.06 | 3.59 | 0.006 |
| FAR1 | 24.27 | 32.41 | 1.34 | 0.619 |
| FAR2 | 3.52 | 34.56 | 9.80 | 0.015 |
| GNPAT | 14.74 | 24.02 | 1.63 | 0.398 |

Table 7.2 siRNA screen results showing percentage growth inhibition for ether lipid biosynthesis genes in Liv7k cell line. Fold change values are given for hypoxia and normoxia samples. Significance was assessed using Mann-Whitney u test ($p < 0.05$).

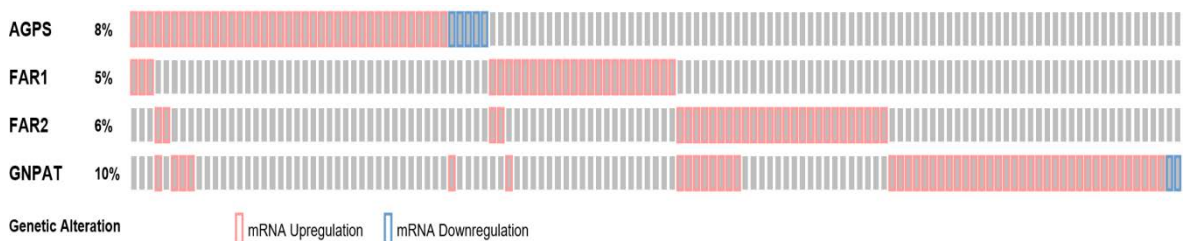


Figure 7.9 Gene expression of major ether lipid pathway components from TCGA HNSCC dataset. Box plot shows the percentage of 522 patients with altered expression (red, z score > 2; blue, z score < -2).

7.2.2 Validation of AGPS knockdown in oral SCC cell lines

Knockdown with deconvolved siRNAs (same sequence as in screen) to ether lipid genes validated the high percentage growth inhibition from the siRNA screen; however, the differential between hypoxia and normoxia could not be repeated in 3/4 oligos (Figure 7.10). The efficiency of *AGPS* knockdown was assessed by qRT-PCR showed $\geq 90\%$ loss of gene expression compared to non-targeting control (data not shown). A significant reduction in protein expression was also observed in response to *AGPS* knockdown (Figure 7.11). However, *AGPS* is also essential for the viability of normal cell lines, as evidenced by the high percentage growth inhibition in OKF4 (data not shown).

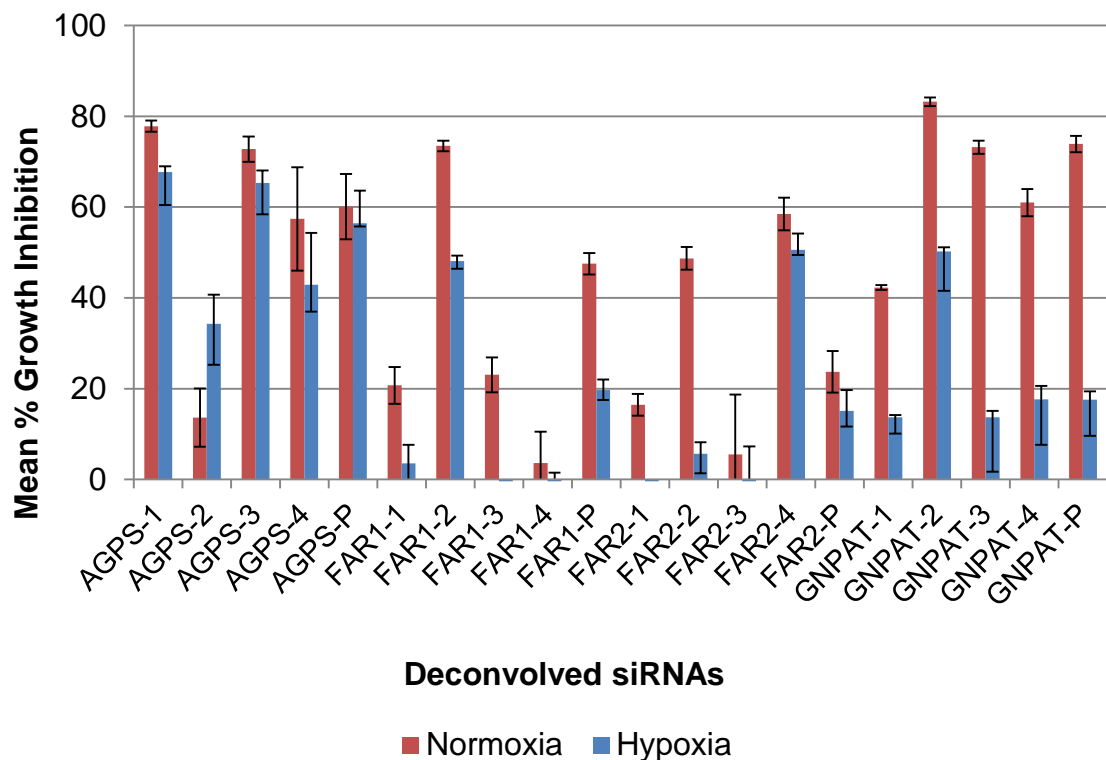


Figure 7.10 Validation of growth inhibition upon silencing of ether lipid genes in Liv7k cell line. Cells transfected with four individual and pooled siRNA sequences were normalised to non-targeting control. Results are mean \pm SD of three independent experiments.

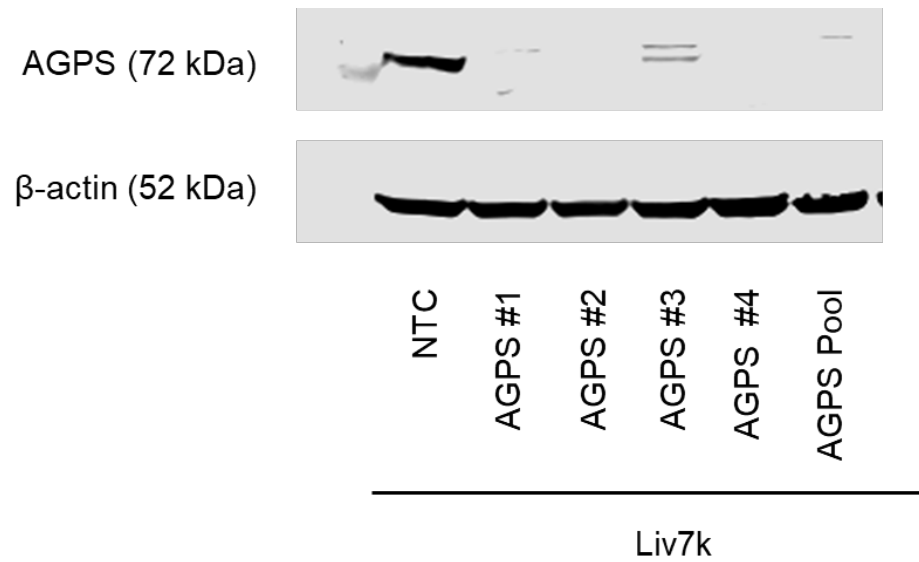


Figure 7.11 Validation of AGPS knockdown in Liv7k cell line. Western blotting of treated cells confirmed reduction in AGPS protein expression in response to silencing with siRNA targeting the gene. Knockdown was observed in all deconvolved sequences (#1-4). 20 μ g of protein was loaded per lane and β -actin was used as a loading control.

7.2.3 Lipid profiling of AGPS knockdown cells in hypoxia

Ether lipids are present at higher levels in tumour cells, but their function therein is unclear. AGPS catalyses a critical step in the production of ether lipids and is upregulated in HNSCC. So far, I have shown that AGPS and other related pathway components are required for oral cell viability under both normoxia and hypoxia. To unravel the dependence of oral cells on ether lipid species, a series of LCMS experiments were performed. In addition, the impact of low oxygen on levels of ether lipid species was assessed.

LCMS profiling of Liv7k cells following *AGPS* knockdown in normoxia and hypoxia revealed alterations in multiple ether lipid metabolites, including phosphocholines (PC), phosphoethanolamines (PE), phosphoinositols (PI), phosphoserines (PS) and lysophosphatidylcholines (LPC) (diacylglycerols and triacylglycerols were not included in this analysis). These lipids carry out a range of functions, including formation of the cell membrane, energy storage, and cell signalling.

Gillian Mackay (CRUK Beatson Institute) carried out LC-MS analysis in which Liv7k cells were treated with a non-targeting control siRNA and compared to four unique siRNAs targeting *AGPS* in normoxia and hypoxia. In addition to internal standards (pos, PC 170/170; neg, PE 170/170), the concentration of lipid species was measured and normalised to cellular RNA content. In total, 68 ether lipid species were detected. Species detected by positive (n=29) and negative (n=39) ion mode were combined for this analysis. MetaboAnalyst 3.0 software (<http://www.metaboanalyst.ca>) was used to analyse mass spectrometry data in this project[515]. The first step was to normalise and transform the data (Figure 7.12). Data was mean-centred and divided by the standard deviation in order to make individual species more comparable. Following this, the data was logged in order to handle zero values in the dataset.

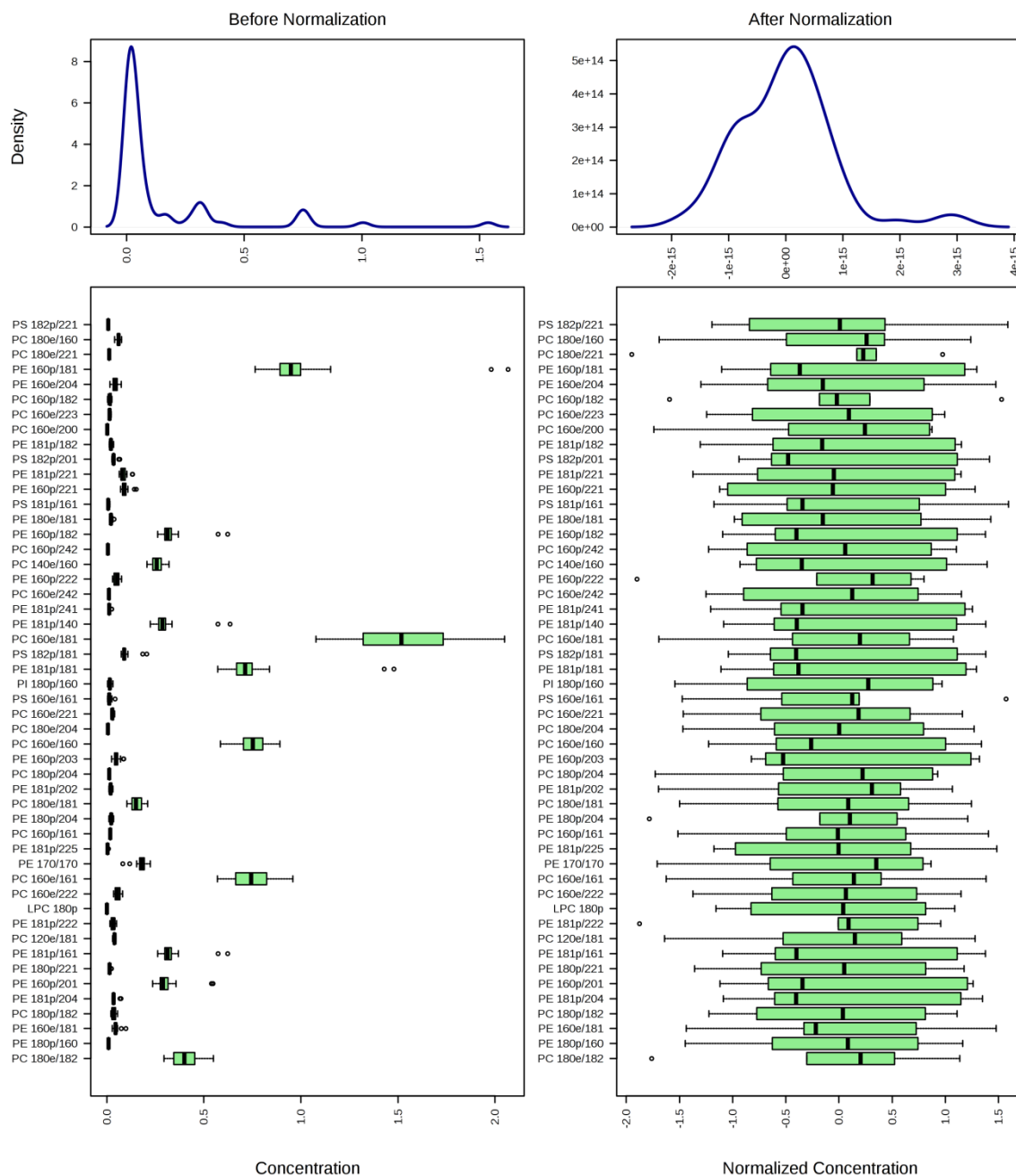


Figure 7.12 Pre-processing of LC-MS Data. Data was pre-normalised to internal lipid control species (pos, PC 170/170; neg, PE 170/170). Prior to analysis, normalised data was log transformed and mean-centred in order to make individual values comparable in magnitude to each other. The left panel shows a box and whisker plot of the data before normalisation while the right panel shows the data after normalisation.

7.2.4 Hypoxia alters levels of ether lipid species

Unsupervised principal component analysis (PCA) was performed on the non-targeting groups only to assess the changes in the lipid profile in hypoxic conditions. A 2D PCA scores plot describes a set of observations based on a large number of variables in a two dimensional graph. PC1 and PC2 represent the principal components, which in this case, describe the concentration of lipid species spanning the most and the second most variation between hypoxia and normoxia, respectively. The levels of lipid metabolites varied depending on oxygen condition (Figure 7.13). The expression of 36 metabolites decreased in hypoxia while 32 increased (Figure 7.14). However, significant downregulation of ether lipids ($\log_2FC > 1.5$, $p < 0.05$) was observed for 5/36 lipids, and only 1/32 metabolites significantly increased.

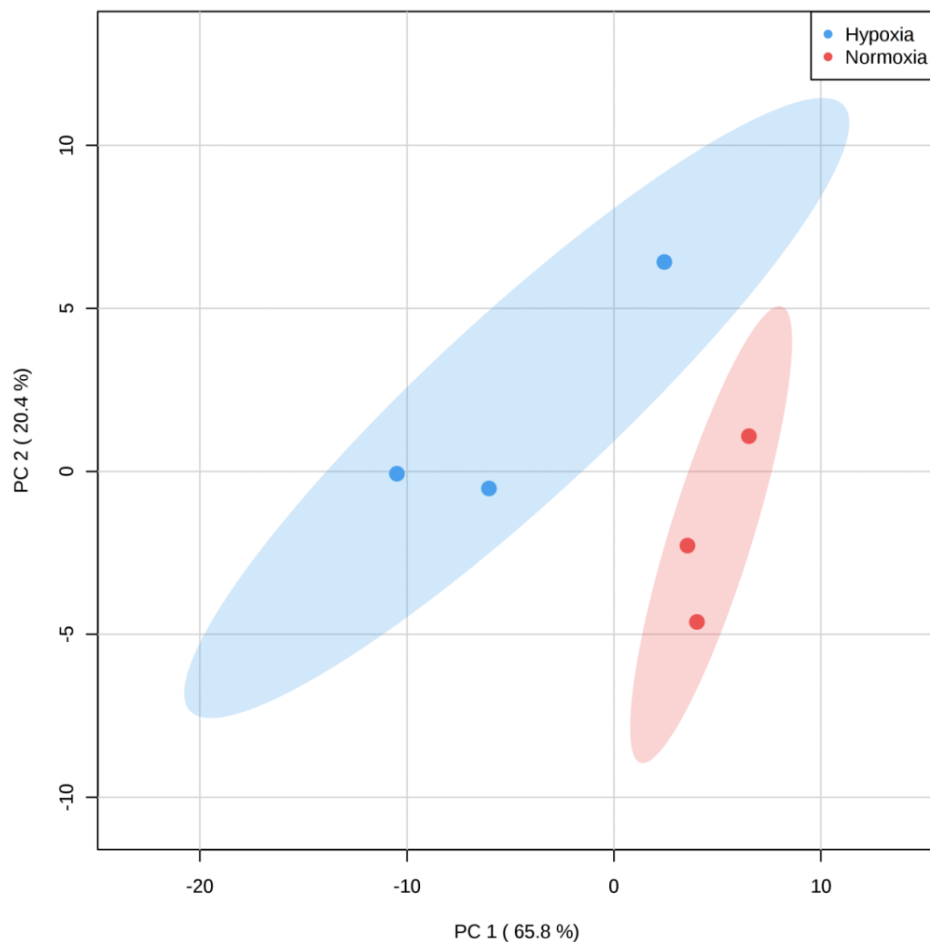
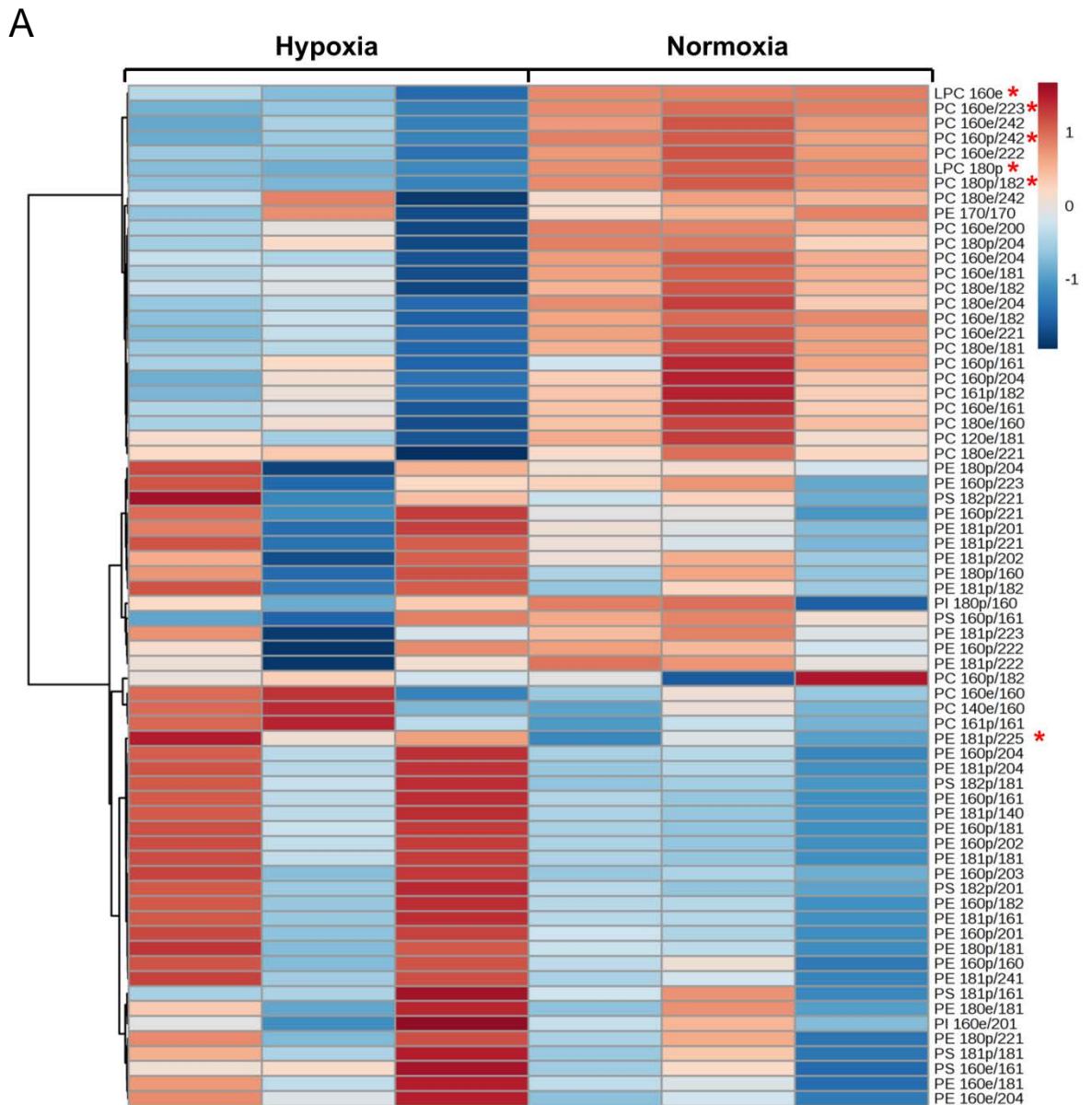


Figure 7.13 Principal Component Analysis (PCA) plot of ether lipid species in hypoxia and normoxia. PC1 explains 65.8% of variation in the concentration of ether lipid species, while PC2 explains 20.4%; together PC1 and PC2 account for 86.2% of variation. Non-targeting control groups only are shown. Lipid concentrations were normalised and auto-scaled prior to analysis, which was performed using MetaboAnalyst 3.0.



B

| Lipid Species | FC (Hyp/Nor) | log2(FC) | raw.pval | -log10(p) |
|---------------|--------------|----------|----------|-----------|
| LPC 180p | 0.32866 | -1.6053 | 0.000687 | 3.1629 |
| PC 180p/182 | 0.62508 | -0.67788 | 0.00169 | 2.7722 |
| PC 160p/242 | 0.51452 | -0.9587 | 0.00275 | 2.5607 |
| PC 160e/223 | 0.55899 | -0.8391 | 0.006529 | 2.1852 |
| LPC 160e | 0.3975 | -1.331 | 0.032412 | 1.4893 |
| PE 181p/225 | 1.7586 | 0.81446 | 0.047359 | 1.3246 |

Figure 7.14 Hypoxia significantly altered levels of certain ether lipids. (A) Heat map showing differential lipid profiles in hypoxia and normoxia (siNTC); (B) Significantly altered lipids in the dataset ($\log_2\text{FC} > 1.5$, $p < 0.05$). PE, phosphatidylethanolamine; PI, phosphatidylinositol; PS, phosphatidylserine; LPC, lysophosphatidylcholines; ether linkage; p, plasmalogen.

7.2.5 AGPS knockdown selectively decreases ether lipid species in hypoxia

Principal component analysis of all tested groups shows the distribution of expression changes. The NTC condition in hypoxia is distant from other groups, but an outlier replicate (hypoxia replicate #2) maintains a connection with them (Figure 7.15). Knockdown of *AGPS* in hypoxia decreases ether lipid production in the Liv7k cell line (Figure 7.16A). Decreases were observed in the levels of ether lipids upon pooled knockdown of the gene in hypoxia (Figure 7.16B). Three ether lipids were significantly downregulated: PE(160p/203), PE(160p/223), PE(181p/225).

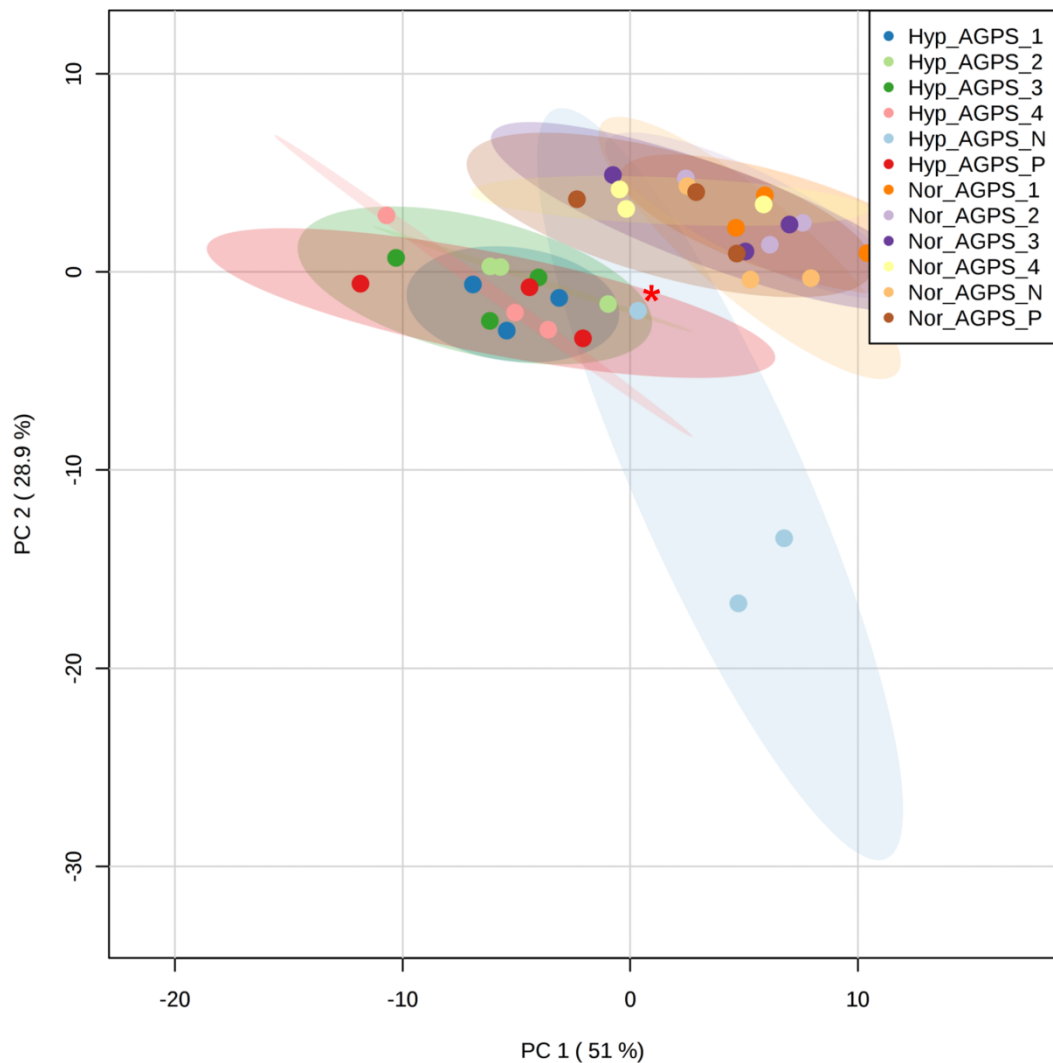


Figure 7.15 PCA plot showing distribution of correlations between groups. The Hyp_AGPS_N group has an outlying data point (red asterisk), which affects the significance of expression changes.

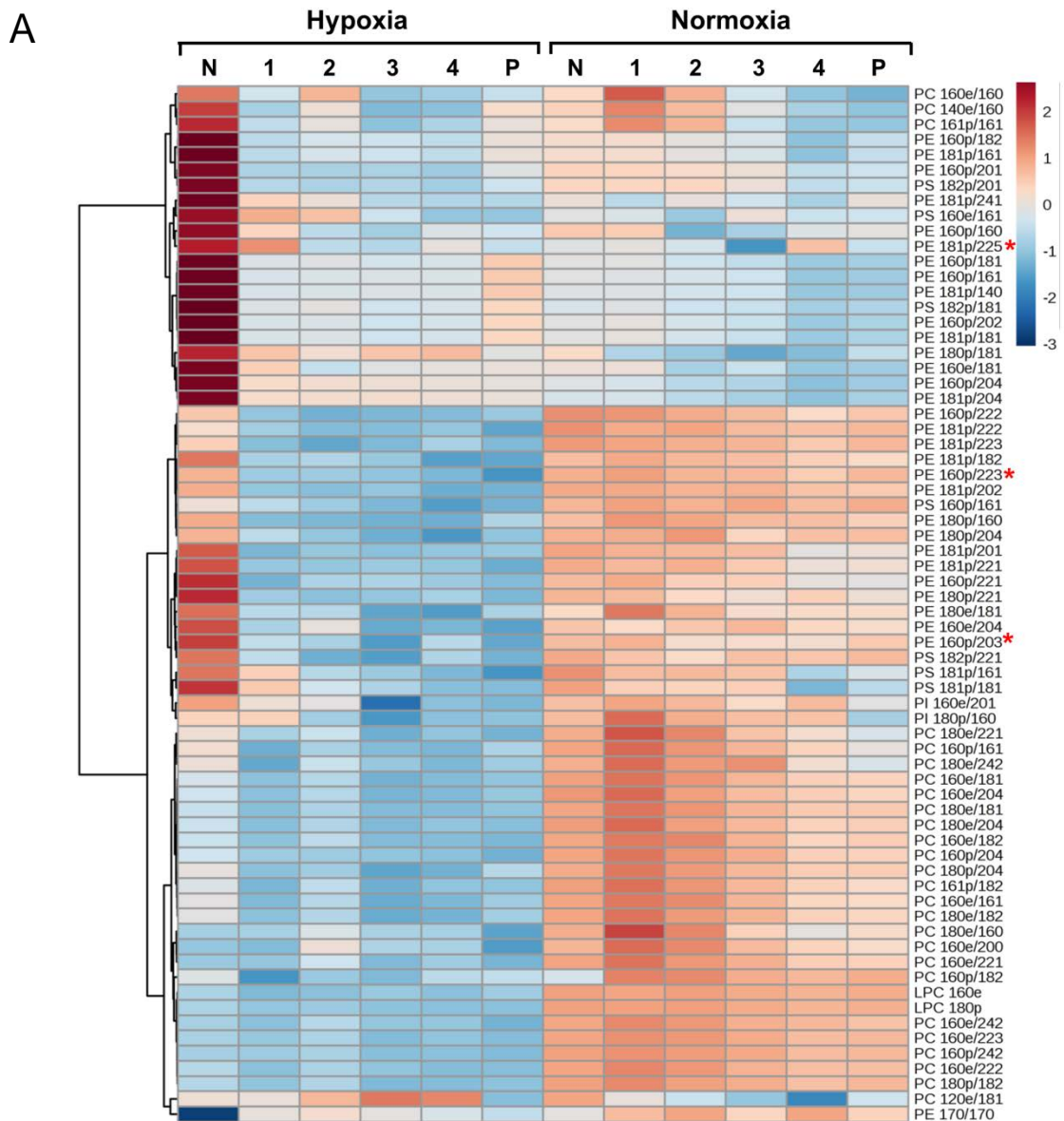


Figure 7.16 Heat map and hierarchical clustering of ether lipid metabolites upon knockdown of AGPS in hypoxia and normoxia. (A) Expression of lipid metabolites in Liv7k cells in normoxia and hypoxia, after transfection with four unique AGPS siRNAs, compared to non-targeting control siRNA (n=3). (B) Significant changes in levels of ether lipid metabolites were assessed by unpaired t-test upon AGPS knockdown in hypoxia ($FC_{\log 2} < 1.5$, $p < 0.05$). PE, phosphatidylethanolamine; PI, phosphatidylinositol; PS, phosphatidylserine; LPC, lysophosphatidylcholines; ether linkage; p, plasmalogen.

7.3 Discussion

Hypoxia is a critical modulator of gene expression in solid tumour cells and promotes a resistant phenotype associated with reduced survival[250]. However, the mechanism of hypoxic tumour progression is not fully understood. The extent of hypoxia fluctuates throughout the tumour mass, giving rise to a heterogeneous population of cells with varying physiological characteristics[516]. Nutrient and oxygen stress leads to the activation of a hypoxic transcriptome, which stimulates a network of signalling pathways involved in cell growth and survival. This hostile environment also necessitates changes to cellular metabolism to utilise limited resources more efficiently[517]. Whole genome siRNA screening was combined with RNA sequencing of patient-derived oral SCC cell lines to identify genes that are equally essential for cell growth and viability in hypoxia and normoxia. As a result, lipid metabolism pathways pertaining to fatty acid/triglyceride metabolism and ether lipid synthesis were selected for follow up.

SREBP-mediated fatty acid metabolism was identified as a selectively essential process in hypoxic conditions. Activation of SREBP1 has been also shown to promote survival through an EGFR-AKT signalling axis in glioblastoma, which, like HNSCC exhibits a high percentage of EGFR amplification[518, 519]. It has previously been shown that loss of SREBP activity leads to growth inhibition in cancer cells by preventing SCD1-mediated fatty acid desaturation[520]. *SCD1* was identified in the siRNA screen as being upregulated in hypoxia (Figure 7.3) and knockdown of the gene led to a significant inhibition of growth in oral SCC cell lines (Figure 7.6). However, in validation experiments, no difference in growth inhibition was observed between normoxic and hypoxic conditions. Further investigation is merited to confirm the decreased effect of *SCD1* knockdown in OKG4 keratinocyte cell line, in order to see if tumour and normal cells rely on the activity of the enzyme to different extents.

MGLL and *DGAT2*, which control the catabolism and anabolism of triglycerides to fatty acids, respectively, were identified as selectively essential for cell viability in the siRNA screen ($p < 0.01$). However, this differential could not be reproduced in validation experiments. The enzymes encoded by these genes

catalyse the breakdown and build-up of triglyceride molecules into neutral lipid droplets, respectively (Figure 1.8). Despite the inconsistency of results between hypoxia and normoxia, the effect on growth inhibition pointed toward the importance of dynamic lipid storage for oral SCC growth and survival. To this end, the abundance of lipid droplets was measured in response to gene knockdown in hypoxia. This revealed a build-up of lipid droplets in MGLL knockdown cells, confirming its role in the breakdown of triglyceride molecules to free fatty acids. In contrast, silencing of *DGAT2* led to a reduction in lipid droplet number. The average number of lipid droplets per cell was similar in normoxic and hypoxic conditions (data not shown). However, upon silencing of *MGLL* in the Liv7k cell line, a greater increase in the number of lipid droplets was observed in the normoxic condition, suggesting that under hypoxic conditions, other enzymes may have a more active role in the breakdown of triglycerides. Alternatively, it may suggest that under hypoxia, *DGAT2* does not act to generate triglycerides as efficiently. Cells with knockdown of LIPE (which cooperates with MGLL to hydrolyse triglyceride stores) displayed a similar change in lipid droplet levels.

Tumours favour *de novo* lipid synthesis and it is well documented that hypoxia leads to triglyceride accumulation in cancer cells[521]. However, in this study, similar levels of LDs were observed under both oxygen conditions. It is possible that this is a result of using serum-free media, as it has been shown that lipid droplet accumulation in hypoxia is mainly due to fatty acid uptake from serum[328]. Bensaad *et al.* reported that lipid droplet accumulation was due to induction of the membrane-associated protein adipophilin (*PLIN2*) [328] in contrast to the SREBP mechanism reported in other cancer models[522]. However, *PLIN2* gene expression was barely detectable in RNA sequencing of the Liv7k cell line in either oxygen condition (data not shown). The size of lipid droplets was not analysed in this study, but could perhaps shed more light on the impact of hypoxia on lipid storage.

The greater impact of *MGLL* knockdown on lipid droplet number in normoxia was also unexpected, given that the gene was upregulated (albeit not significantly) in hypoxia. In addition, treatment of Liv7k cells with the MGLL inhibitor, JZL-184, resulted in ~30% growth inhibition in normoxia but had no effect in hypoxia

(data not shown). The function of MGLL extends beyond that of lipid metabolism - in addition to its role in lipid mobilisation, MGLL is the major enzyme responsible for the hydrolysis of 2-arachidonoylglycerol (2-AG), an endogenous ligand of the endocannabinoid system[523]. This system is involved in a number of physiological responses, including pain, appetite, mood and memory[524]. The product of 2-AG hydrolysis, arachidonic acid, is the precursor molecule for eicosanoid biosynthesis, which act to promote inflammation (see also chapter 8)[525]. Blockage of MGLL reduces the available pool of arachidonic acid, thus diminishing the damaging inflammatory response that occurs in hepatic ischemia reperfusion (I/R) injury[526]. The pleiotropic actions of *MGLL* may explain the inconsistencies observed in response to its knockdown in this project.

On the other hand, *PNPLA2* (which encodes adipose triglyceride lipase, ATGL[527]) was not identified as selectively essential in hypoxia in the siRNA screen but caused greater growth inhibition in follow up experiments (Figure 7.6). Moreover, the gene was ~6-fold upregulated in hypoxia and siRNA-mediated knockdown led to a build-up of lipid droplets in hypoxia in Liv7k cells (Figure 7.7). The efficacy of a small molecule ATGL inhibitor, atglistatin, was tested in high and low oxygen, but failed to result in loss of viability in either condition at concentrations up to 10 μ M (Liv7k cells, data not shown). Increased ATGL activity has been observed in obese breast cancer patients[528] and has been implicated in cancer-associated cachexia[500]. Moreover, high ATGL expression led to increased rates of tumour stromal proliferation in pancreatic ductal adenocarcinoma[498], whereas inhibition of the protein was shown to attenuate the growth of lung cancer cells[497].

In addition to genes involved in fatty acid and triglyceride metabolism, a subset of genes involved in the synthesis of ether lipids was identified as essential in oral cells. The finding here reflects that of another study which showed hypoxia increasing levels of ether phosphatidylethanolamines (ePEs) in a leukaemia cell line, independently of HIF-1 α [529]. Ether lipids constitute ~15-20% of phospholipids in cell membranes[504].

Plasmalogens are a lesser-studied species of phospholipid which contain a *cis* double bond adjacent to this ether-linked alkyl chain at the first carbon of glycerol[530]. This “vinyl-ether” linkage renders plasmalogens uniquely sensitive to reactive oxygen species and as such, they act as effective scavengers of ROS[531]. Indeed, plasmalogens have repeatedly been shown to act as endogenous antioxidants in mammalian cells[532, 533]. Accordingly, plasmalogens have been shown to protect pulmonary artery endothelial cells from mitochondrial-derived ROS generated in the initial period of hypoxia, as cells adjust their rate of respiration[534].

TCGA analysis revealed upregulation of genes involved in ether lipid synthesis in ~5-10% of HNSCC patients. The rate-limited step of ether lipid biosynthesis is catalysed by alkylglyceronephosphate synthase (AGPS), which was recently shown to be upregulated in aggressive human cancer and drive an oncogenic lipid-signalling network[268]. Moreover, small molecule inhibition of the protein impaired cancer migration and invasion[535].

At the time of writing, a direct role of AGPS in hypoxia had not been studied. In this project, RNA sequencing of Liv7k cells revealed a slight downregulation of all four ether-lipid synthesizing genes (*AGPS*, *FAR1*, *FAR2* and *GNPAT*) in hypoxia (**data not shown**). This project was discontinued after a failure to reproduce the hypoxia differential observed in the siRNA screen upon *AGPS* knockdown (**Figure 7.10**), despite showing an efficient reduction of protein expression (**Figure 7.11**).

A direct assessment of the role of AGPS in oral SCC came from the measurement of ether lipids upon gene knockdown. As shown in **Figure 7.14**, hypoxia significantly altered ether lipid/plasmalogen levels in Liv7k cells. Knockdown of AGPS appeared to reduce ether lipids in the hypoxic condition; however, an outlier in the NTC condition meant that only three phosphatidyl ethanolamine-plasmalogen (PEp) species were significantly downregulated according to unpaired t-test ($p < 0.05$). Further work is required to determine the functional impact of AGPS-induced ether lipid reduction in an oral cancer setting. CRISPR knockout cell lines have been generated, but a phenotypic assessment has yet to

be completed. Until then, it is difficult to speculate on a role for the gene in oral SCC progression or in fact, what the downstream lipids do.

The absence of clinically applicable methods for measuring tumour oxygenation has fuelled the development of hypoxic gene signatures, with the potential to predict therapeutic response[536], and the ability to accurately reproduce tumour hypoxia *in vivo* using xenograft models has facilitated this goal[537]. This study sought to improve on gene expression studies by identifying genes, which are essential for viability in hypoxic conditions. However, the differential effect observed between hypoxia and normoxia in the siRNA screen could not be reproduced in small scale validation studies. A follow up siRNA screen targeting the ~10% of genes which were selectively essential in the hypoxic condition has since been completed. This second screen used On-Target Plus siRNA instead of the siGENOME set used in the primary screen, which should provide a greater knockdown specificity and thus a more robust result. It will be interesting to compare the two and identify additional targets to investigate.

Lipid metabolism is a complex system that is highly dependent on cellular context and the surrounding microenvironment. Blocking individual processes in a 2D setting is of questionable relevance when it comes to addressing the situation *in vivo*[538]. To this end, the development of high-throughput 3D screening methods may help bridge the gap between *in vitro* and *in vivo* success. Moreover, different tools to tease out the effect of individual lipids in cells and the phenotypic effects resulting from fluctuations in lipid biosynthesis would shed more light on the situation.

Chapter 8 Results – *In vivo* significance of cysteinyl leukotrienes in oral SCC

8.1 Introduction

The tumour microenvironment is a dynamic structure that influences tumour cell survival and mobility. It consists of a variety of cell types, including those of the immune system, tumour vasculature, and the extracellular matrix[539].

Cysteinyl leukotrienes are a class of inflammatory mediators, which are produced mainly by white blood cells in response to inflammatory stimuli[540]. They exert their effect through two G-coupled protein receptors, CysLT₁R and CysLT₂R. The former is the main receptor subtype in the inflammatory response and is expressed on the surface of nasal mucosa interstitial cells, endothelial and smooth muscle cells, and a variety of inflammatory cells[541-543]. Although the receptor is not normally expressed on the surface of epithelial cells (such as those in the oral cavity), some epithelial cells are capable of producing CysLT ligands[544]. Moreover, overexpression of CysLT₁R has been detected in various tumours[378, 379].

Leukotrienes are a class of biologically active lipids called eicosanoids, which have previously been implicated in tumour progression. The leukotriene pathway branches off at LTRA₄ to generate either LTB₄ or LTC₄, via LTRA₄ hydrolase and LTC₄ synthase, respectively (**Figure 8.1**). LTB₄ which is elevated in colorectal and prostate cancer[545, 546], stimulates a distinct pair of receptors and is not discussed here. LTC₄ is exported to the extracellular environment and further metabolised to LTD₄ and LTE₄[354]. LTD₄ binds the CysLT₁R with the highest affinity, making it the most potent stimulator of receptor activity[368]. In the intestine, LTD₄ has been shown to promote proliferation, survival and migration through PKC-Raf-Erk, GSK3B-βcatenin and PI3K-Akt-Rac pathways, respectively[362-364]. Moreover, CysLT₁R is overexpressed in colorectal cancer and is associated with a poor prognosis in patients[377].

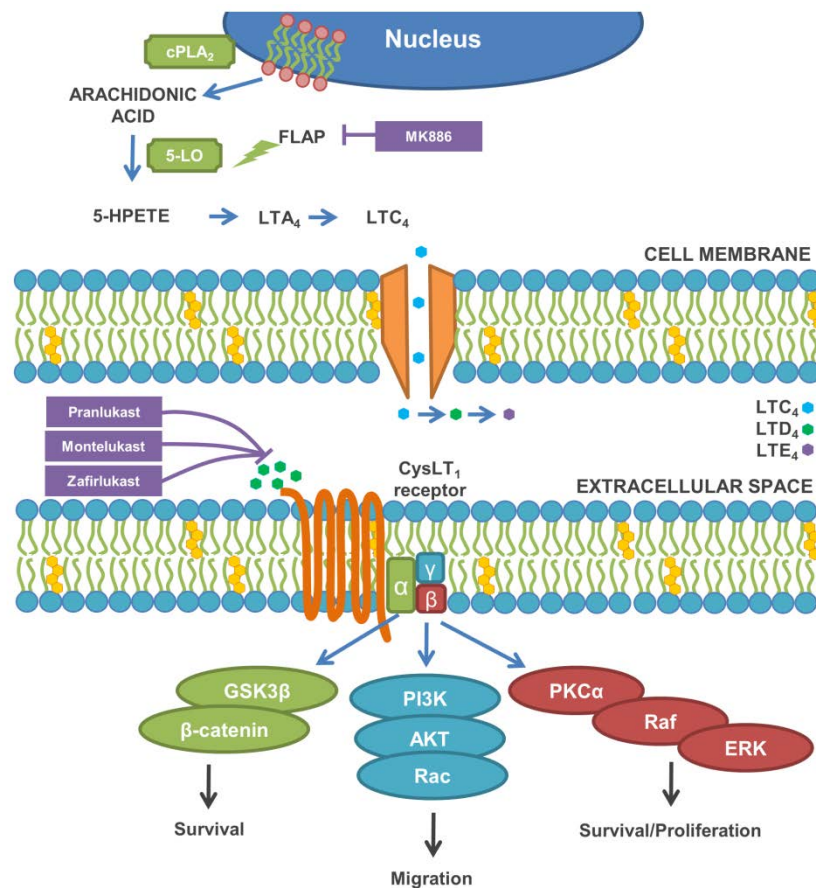


Figure 8.1 Overview of cysteinyl leukotriene metabolism. CysLT₁R has been shown to activate downstream pathways including PI3K[362], ERK[363] and GSK3β[364]. Inhibitors act on various points in this pathway (purple boxes). LTRA₄, C₄, D₄, leukotriene A₄, C₄, D₄; FLAP, 5-lipoxygenase-activating protein; 5-LO, 5-lipoxygenase; 5-HPETE, 5-hydroperoxyeicosatetraenoic acid; GSK3β, glycogen synthase kinase 3 beta; PI3K, phosphoinositide 3-kinase; PKCα, protein kinase C α; ERK, extracellular signal-related kinase; MEK, mitogen-activated protein kinase kinase; cPLA₂, cytosolic phospholipase A₂.

Non-steroidal anti-inflammatory drugs are significantly associated with a reduced risk of metastasis development[547]. Montelukast, zafirlukast and pranlukast belong to a family of NSAIDs that selectively antagonise CysLT₁R, and evidence suggests they may be effective in a cancer setting[548]. Zafirlukast was found to slow the progression of lung adenomas induced by treatment with vinyl carbamate[549]. Similarly, montelukast reduced tumour growth in a colorectal xenograft model by slowing proliferation and inducing apoptosis[394]. This chapter presents data from experiments designed to assess the effect of montelukast in aggressive oral cancer cell lines. This project was performed in collaboration with Karen Blyth's lab (CRUK Beatson Institute) and *in vivo* experiments were carried out by Susan Mason.

8.2 Cysteinyl leukotriene pathway inhibitors inhibit growth of oral SCC cells in a drug screen

To complement the results of the siRNA screen, Liv7k cells were treated with 1,351 FDA-approved drugs for cancer and non-cancer indications. This revealed a striking dependence on a subset of genes involved in the cysteinyl leukotriene inflammatory pathway (Figure 8.2). Given the resistance often seen in hypoxic tumours in response to drug treatment, a 90% growth inhibition minimum was set in both normoxic and hypoxic conditions, in order to ensure selection of drugs effective in cells in a hypoxic environment.

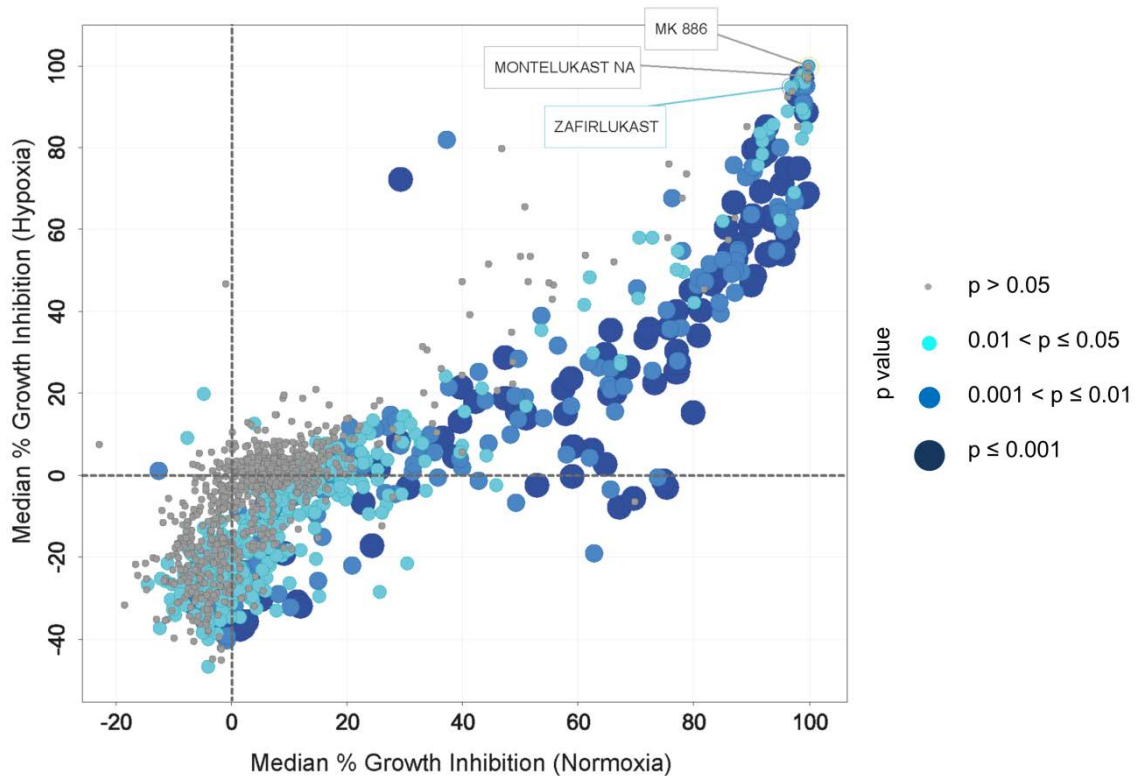


Figure 8.2 Scatter plot showing percentage growth inhibition of the Liv7k cell line in a drug-repurposing screen. 1,351 compounds were added to Liv7k cells at a fixed concentration of 10 μ M for 72h. Results are normalised to DMSO control and represent the median of three screening replicates in normoxic and hypoxic conditions. Dashed lines represent 0% growth inhibition cut-off in normoxia and hypoxia. Circle size and colour is indicative of significance according to unpaired t test (p value).

Three compounds (montelukast, zafirlukast and MK-886) used for the treatment of asthma and inflammatory conditions, caused >90% growth inhibition of Liv7k cells, while having little or no effect on non-oral cancer cell lines previously tested within the BICR screening facility (Figure 8.3). All three target components of the CysLT pathway: MK-886 is an inhibitor of 5-lipoxygenase-activating protein (FLAP), while montelukast and zafirlukast are CysLT₁R antagonists (Figure 8.1).

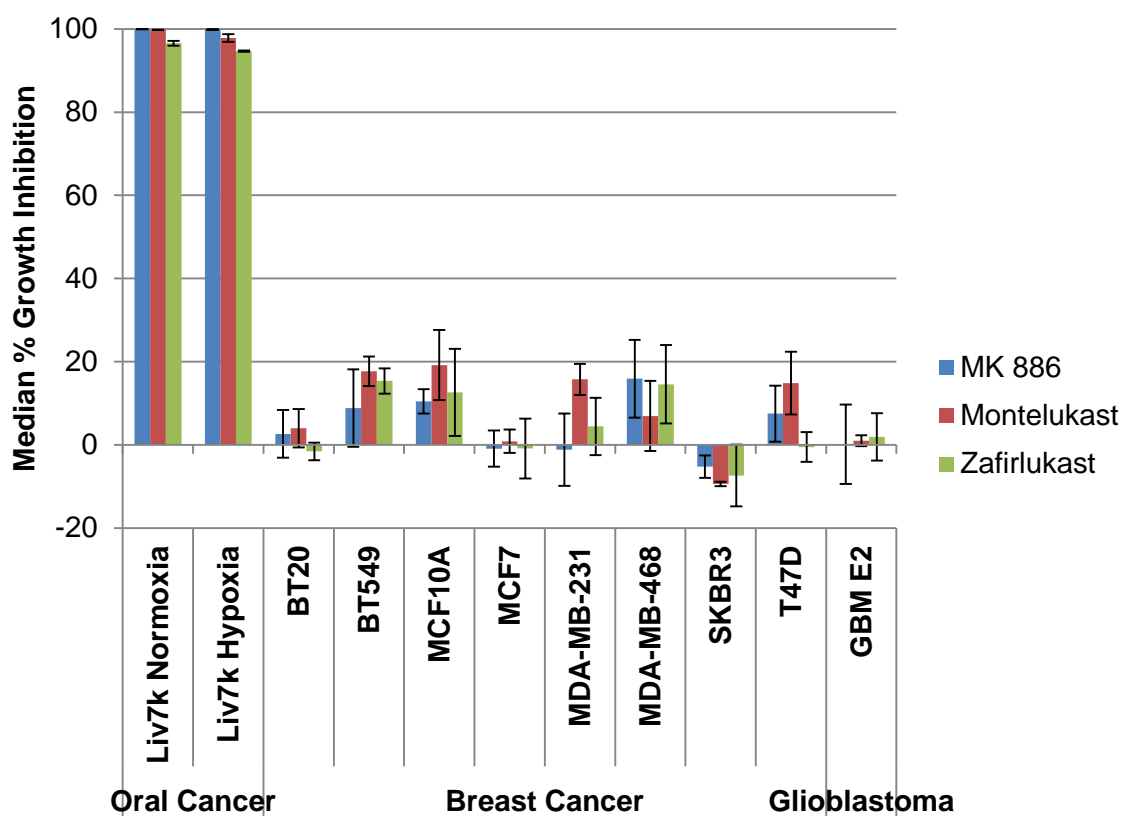


Figure 8.3 Bar chart showing percentage growth inhibition in a panel of cancer cell lines treated with CysLT₁R antagonists. A fixed concentration of at 10 μ M was used and the experiment end point was 72h post drug-addition. Results are normalised to DMSO control and represent the median \pm SD of three screening replicates.

8.3 Serum-containing media protects cells from leukotriene pathway inhibition

By testing a panel of oral cell lines, it was found that serum-containing media negated the growth inhibition caused by leukotriene receptor antagonists (LTRAs) and an upstream FLAP inhibitor. Figure 8.4A shows the effect of LTRAs in cell lines grown in keratinocyte serum-free media, but testing of seven additional oral cancer cell lines grown in serum-containing media showed no effect up to 10 μ M (not shown). However, it is unclear how serum provides a survival benefit to cells treated with LTRAs. To validate this effect, Liv7k cells were adapted to grow in DMEM containing 10% serum and treated with montelukast (Figure 8.4B). The growth inhibition observed in cells grown in serum-free media was lost. Comparable IC₅₀ values were observed for two immortalised keratinocyte cell lines (OKF4, OKG4) in this analysis.

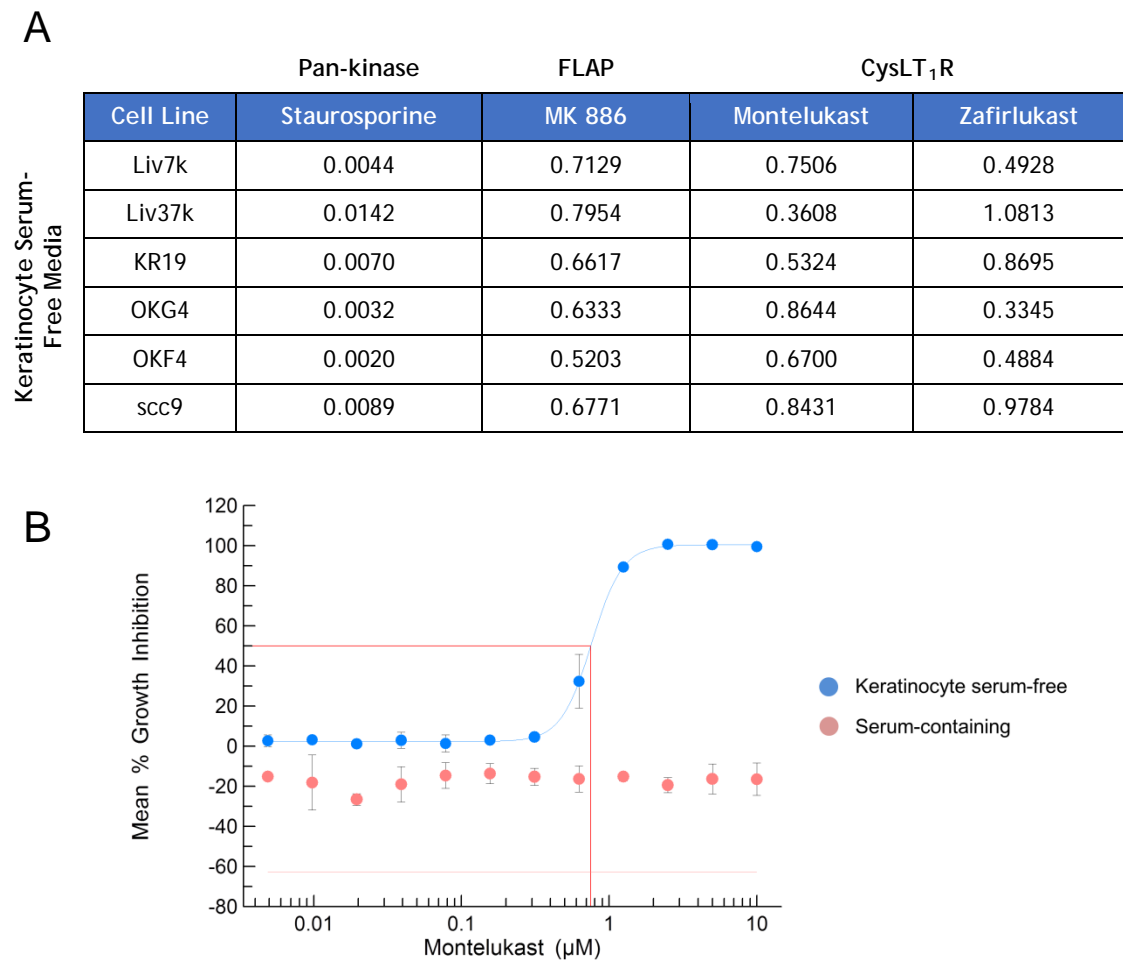


Figure 8.4 Percentage growth inhibition (IC₅₀ values) of leukotriene pathway antagonists in a series of oral cell lines. (A) IC₅₀ values (μ M) in a series of oral cell lines, grown in keratinocyte serum-free media. OKF4 and OKG4 are immortalised keratinocytes. MK 886, montelukast and zafirlukast were tested. (B) Montelukast dose-response curve in the Liv7k cell line with a concentration range of 0.005-10 μ M. Results are normalised to DMSO control and represent the mean \pm SD of three experiments. Liv7k IC₅₀ minus FBS = 0.7506 μ M.

8.4 Montelukast is a selective antagonist of CysLT₁R

Despite the lack of effect in serum-containing media, it was reasoned that keratinocyte serum free media contained growth factors at more physiologically relevant concentrations than that of serum containing media. STITCH 'Search Tool for Interactions of Chemicals' [550] reveals known interactors of montelukast (Figure 8.5). The strongest interaction occurs between montelukast and CysLT₁R, the primary binding partner of LTD₄. Confidence scores are presented in the table, with interacting proteins ranked from highest to lowest probability. Montelukast binds to CysLT₁R with an IC₅₀ of less than 5nM in human HEK-293 cells stably expressing the receptor[551].

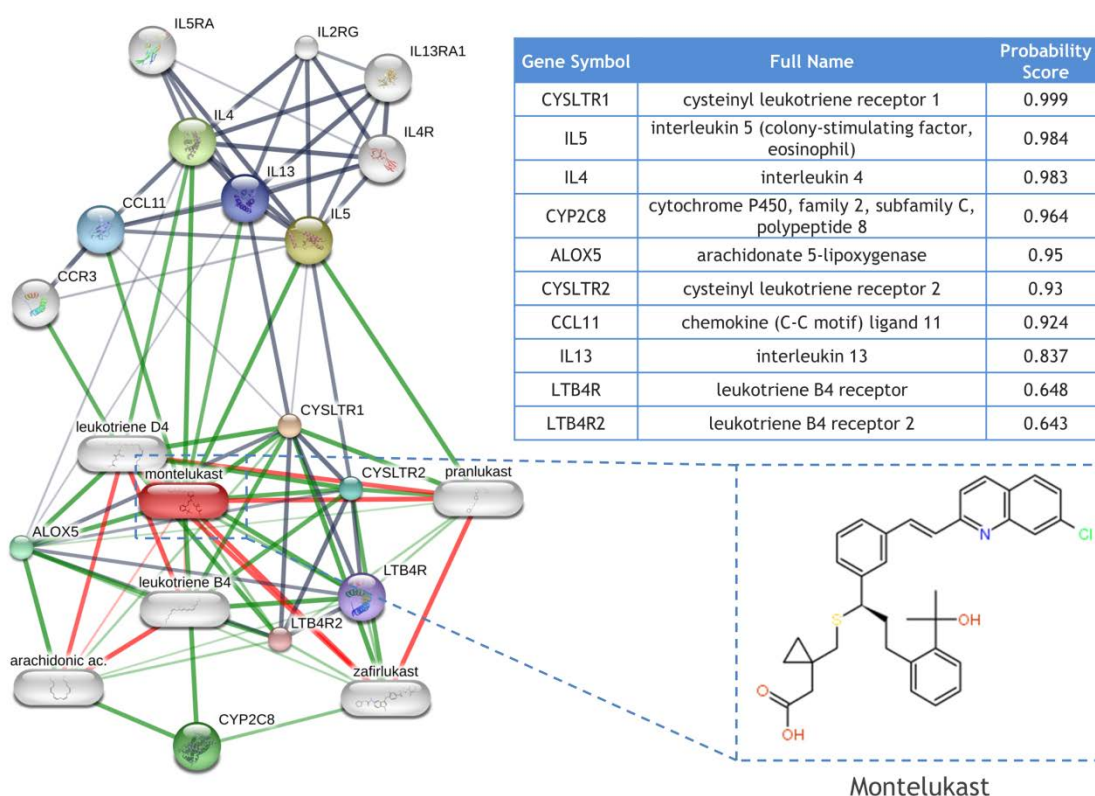


Figure 8.5 Molecular structure of montelukast and its known interactions. Thick lines represent stronger associations, which are based on the probability of the interaction being non-random. Protein-protein interactions are shown in grey, chemical-protein interactions in green and interactions between chemicals in red. Small nodes depict proteins of unknown 3D structure; large nodes depict proteins where some 3D structure is known. Table shows association probability scores. Image was generated using STITCH software[550].

8.5 Knockdown of CysLT₁R causes growth inhibition in Liv7k cell line

The efficacy of leukotriene inhibitors is paralleled by the knockdown of CysLT₁R, which results in > 60% growth inhibition in both normoxic and hypoxic conditions in Liv7k cells (Figure 8.6). Screening data also shows a high percentage growth inhibition in response to knockdown of genes that are predicted to interact with montelukast (Figure 8.5): *ALOX5*, *IL13*, *CYSLTR2R*, *LTB4R* and *LTB4R2*. This data validated the importance of leukotriene signalling pathways, centred around CysLT₁R, in oral SCC.

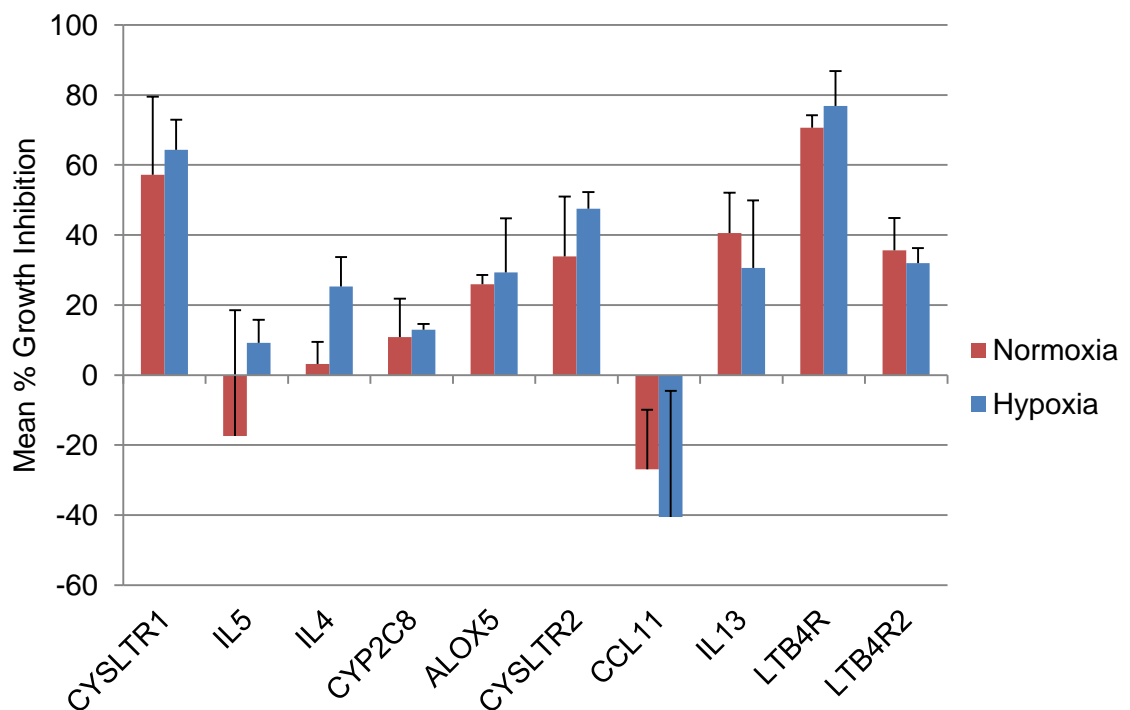


Figure 8.6 Bar chart showing percentage growth inhibition upon knockdown of montelukast target genes in the Liv7k cell line. Results are normalised to non-targeting control and represent the mean \pm SD of three screening replicates. Keratinocyte serum-free media was used in the siRNA screen.

8.6 Montelukast induces cell death in the Liv7k cell line

To determine if montelukast was cytostatic or cytotoxic, Liv7k cells were treated with a range of montelukast concentrations in the presence of Sytox Green™ (Thermo Fisher). Higher concentrations ($> 1\mu\text{M}$) of montelukast resulted in cell death after 16 hours, while DMSO control cells remained viable (Figure 8.7). Lower concentrations of montelukast ($\leq 1\mu\text{M}$) did not appear to induce cell death, but still reduced total cell number.

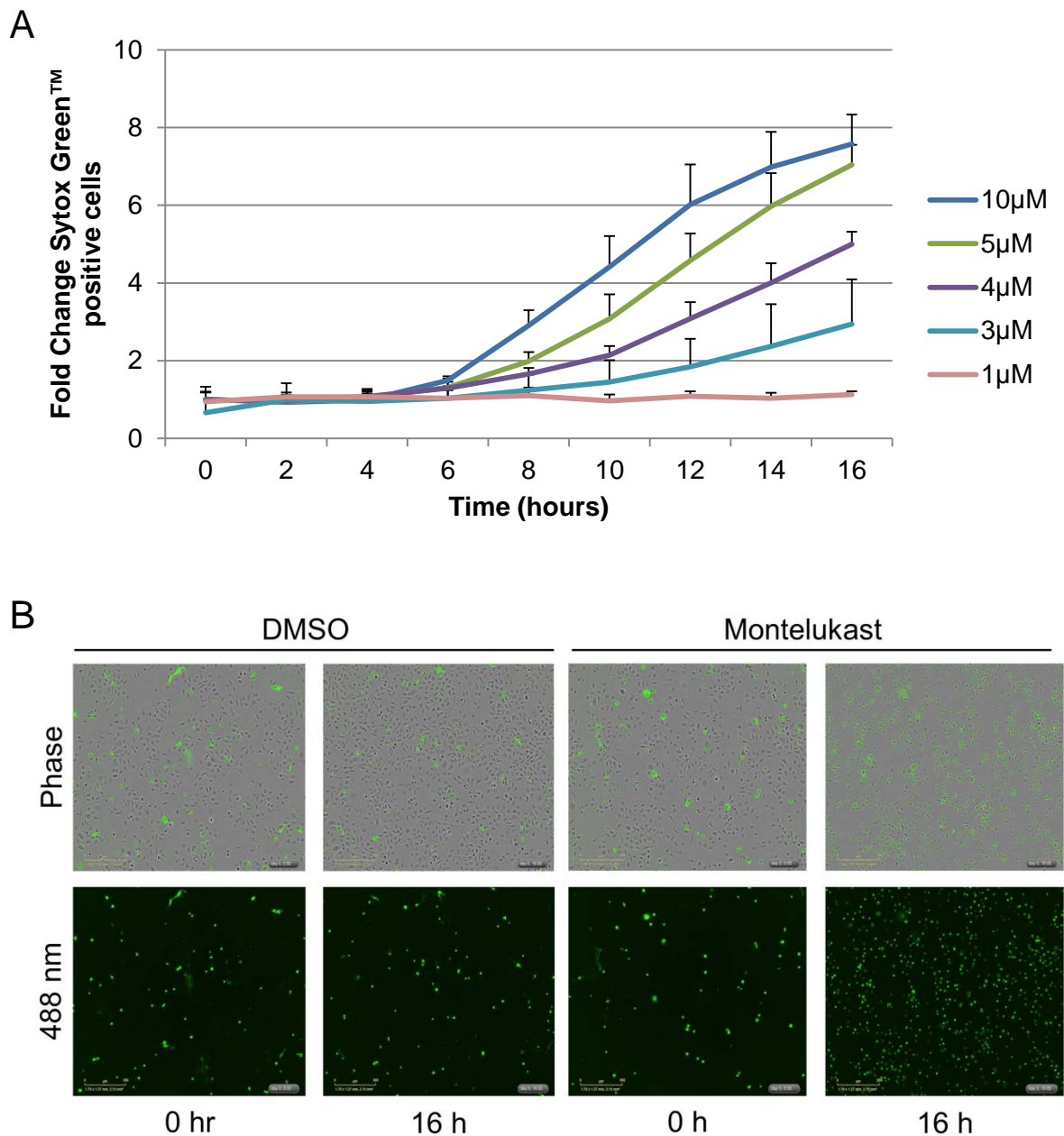


Figure 8.7 Liv7k cells were treated for 16 h with montelukast (0.75-10µM). (A) Cell death was quantified using an Incucyte Zoom imager, measuring SYTOX Green uptake. Green cell count was normalised to total confluency and is presented relative to DMSO negative control. Results are mean \pm SD of three experiments. (B) Representative phase and fluorescent images taken of 10µM montelukast treated cells at 16 h time point.

8.7 Preliminary data shows montelukast slows growth in a 3D culture model

The effect of montelukast was assessed in a 3D spheroid model as a proof of principle experiment for *in vivo* efficacy. 3D culturing of cells creates a more physiologically relevant environment in which additional factors such as tumour heterogeneity, hypoxia, cell-cell interaction and extracellular matrix remodelling are recapitulated. Results from the single experiment performed showed a slight decrease in the rate of spheroid growth in cells treated with montelukast at 1 and 10 μ M (Figure 8.8).

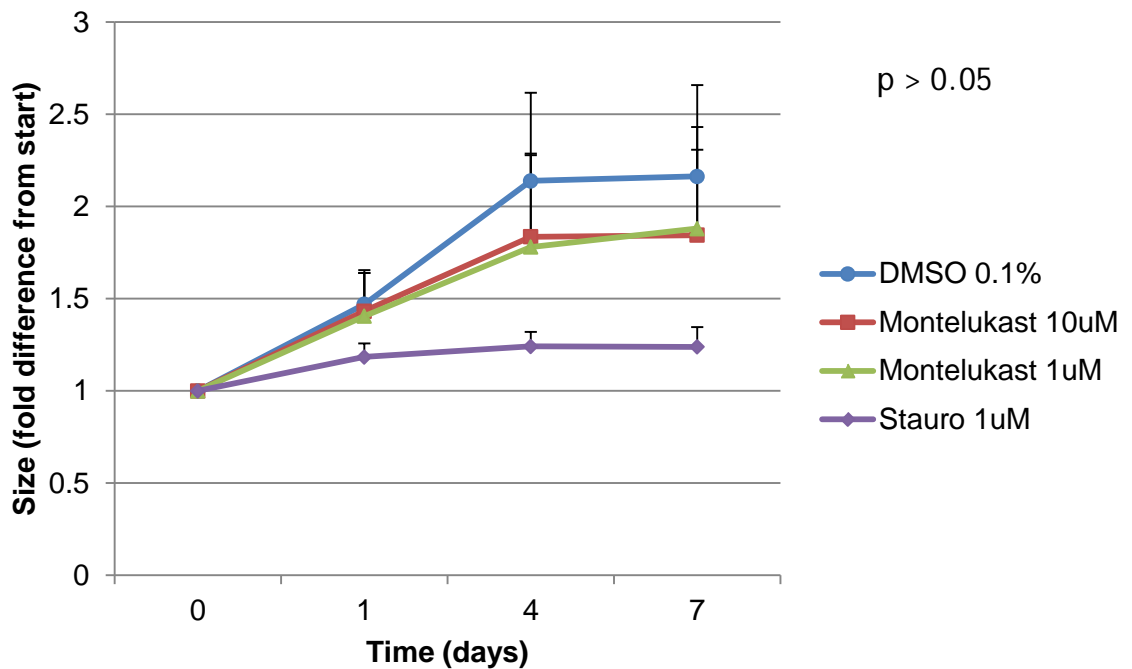


Figure 8.8 Rate of spheroid growth in a 3D spheroid model (preliminary data). Liv7k cells were cultured into 3D spheroids and treated with montelukast at 1 μ M and 10 μ M. 1 μ M staurosporine and 0.1% DMSO were used as positive and negative controls, respectively. Results are normalised to start volume and represent mean \pm SD of five technical replicates only.

8.8 Montelukast tends toward reduced tumour volume in Liv7k xenograft model

Given the success of montelukast in other xenograft models and the results of *in vitro* experiments in this project, its efficacy *in vivo* was assessed. Prior to drug treatment, the ability of Liv7k cells to form tumours in mice was evaluated, and showed that tumours formed in 5/5 mice injected (data not shown). Following this, twenty NOD/SCID mice were subcutaneously injected with 5×10^6 Liv7k cells. Mice were split into treatment or control groups by cage assignment (n=10 per group). Montelukast (5 mg/kg) or vehicle control were administered daily by oral gavage once tumours were palpable and had reached a predetermined size (5mm x 5mm). Thereafter, measurements were taken using calipers three times weekly until tumour endpoint had been reached, as per licence conditions (15mm x 15mm). Results show that average tumour volume in the control group began to separate from the treated group as the experiment progressed. An unpaired t-test revealed statistical significance at day 61 post-treatment; however, fewer control mice were alive at this point having reached clinical endpoint before this time (Figure 8.9). A breakdown of measured tumour volumes for each mouse is shown in Figure 8.10.

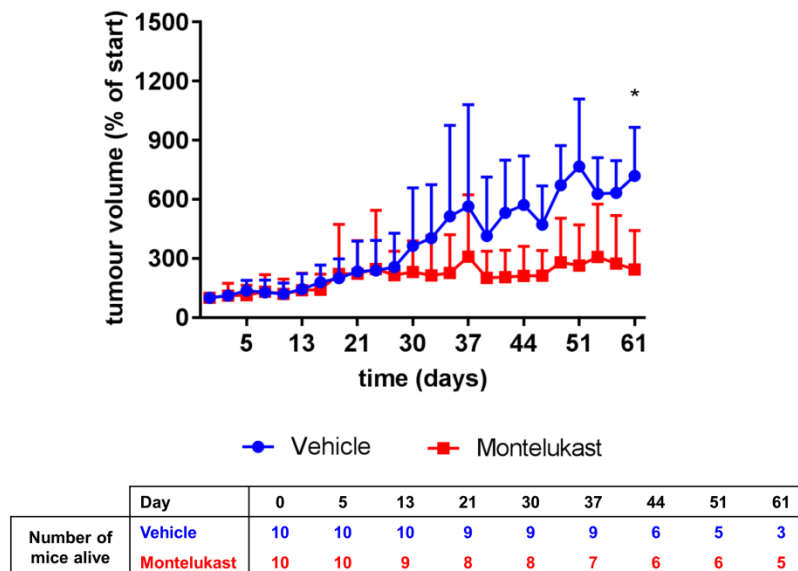


Figure 8.9 Tumour size as a percentage of start volume for montelukast (n=10) and vehicle control groups (n=10). Average tumour volume was normalised to start volume and is presented as the mean \pm SD of each treatment group. Significance was assessed by unpaired t-test at each time point. At day 61, five treated mice were being compared to three control mice. The lower table shows number of mice alive at each time point.

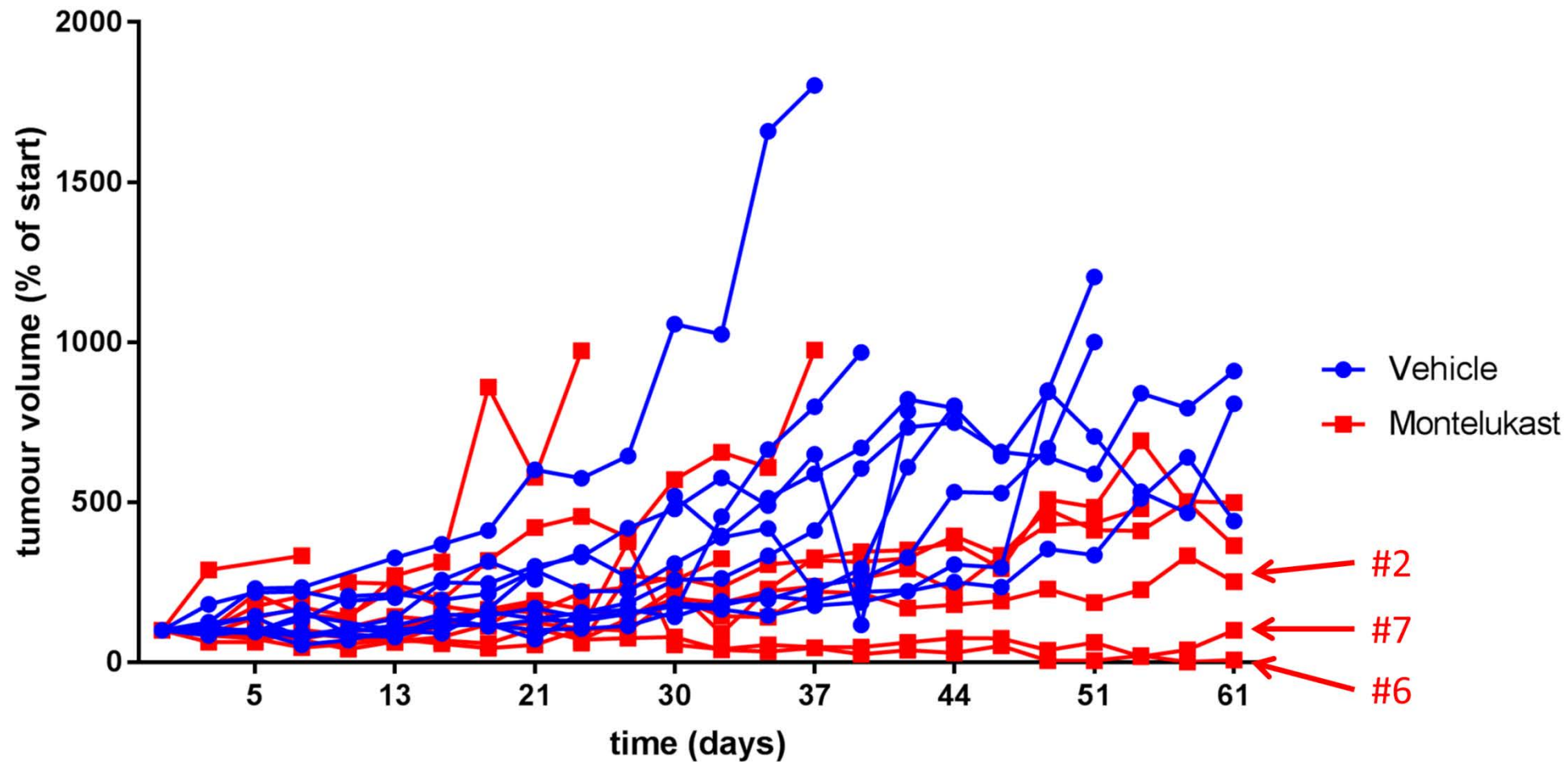
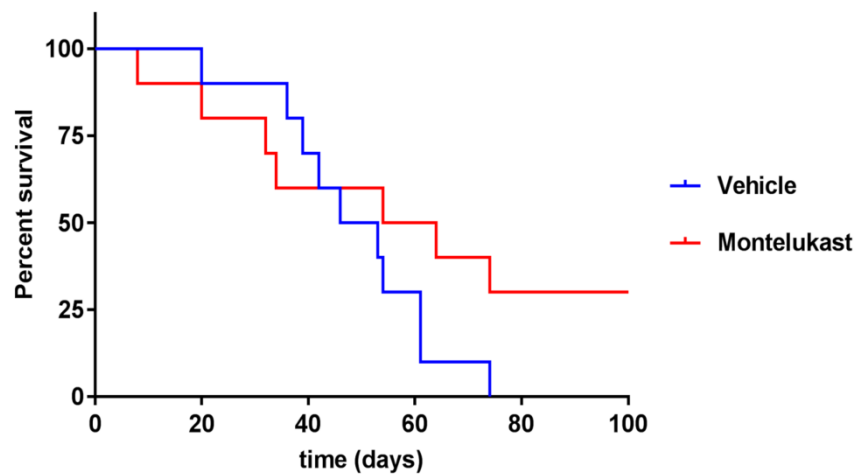


Figure 8.10 Tumour size as a percentage of start volume for individual montelukast and vehicle control mice. 0 days is the start of treatment at which time all mice had palpable tumours. Vehicle (blue) and montelukast treated (red) cohorts are shown. Mice still alive at 100 days are labelled with unique IDs.

8.9 Montelukast does not significantly delay time to tumour endpoint

Mice were taken when tumour size reached 15mm in any direction (as per licence conditions) and survival curves were plotted. However, treatment with montelukast did not significantly delay time to tumour endpoint (Figure 8.11). Moreover, the survival curves crossed, indicating that the hazard ratio was not proportional in the two groups. Three mice in the montelukast group survived beyond 100 days, at which point treatment was stopped (# 2, #6 and #7, see Figure 8.10). The tumour in one of these mice had regressed by this point (#6, while the other two tumours (#2 and #7) gradually increased in size after treatment cessation, suggesting that treatment had constrained tumour growth.



| | Day | 0 | 20 | 40 | 60 | 80 | 100 |
|----------------------|-------------|----|----|----|----|----|-----|
| Number of mice alive | Vehicle | 10 | 9 | 6 | 3 | 0 | 0 |
| | Montelukast | 10 | 8 | 6 | 5 | 3 | 3 |

Figure 8.11 Survival curve of montelukast (n=10) versus vehicle control (n=10) mice, up to 100 days since the start of treatment. The difference in survival is not statistically significant, according to log-rank test ($p > 0.05$). The lower panel shows the number of mice alive at each time point.

8.10 Montelukast does not affect the proliferation of Liv7k xenograft cells

Xenograft sections were stained with Ki67 to determine if montelukast treatment had an effect on proliferation. Human lymphocyte antigen staining was used to confirm the presence of human cells (data not shown). Halo[®] software (Indica Labs) was used to quantify staining intensity of Ki67 in human squamous epithelial cells only (Figure 8.12). However, there was no significant difference in staining intensity between the two groups (unpaired t-test, $p > 0.05$). The intensity of phospho AKT, phospho MTOR, phospho ERK and total ERK was also quantified but no significant differences were observed (data not shown).

Given that mice were taken after tumours reached end point, it is perhaps not surprising that there was little difference in proliferation. A cross sectional study measuring markers of proliferation and survival at a number of earlier time points, when tumours are actively expanding, may yield a more significant difference in staining intensity. LTD₄ is the most potent activator of CysLT₁R but free LTD₄ is rapidly metabolised into LTE₄, which is rapidly eliminated from blood plasma (plasma half-life ~7 minutes)[552]. However, LTE₄ can be readily detected in urine at a concentration of between 10-60 pg/ml in humans (higher in asthma sufferers)[552]. The level of LTE₄ was measured in mouse urine but no meaningful difference was found between control and treated mice, owing to inconsistencies in urine collection.

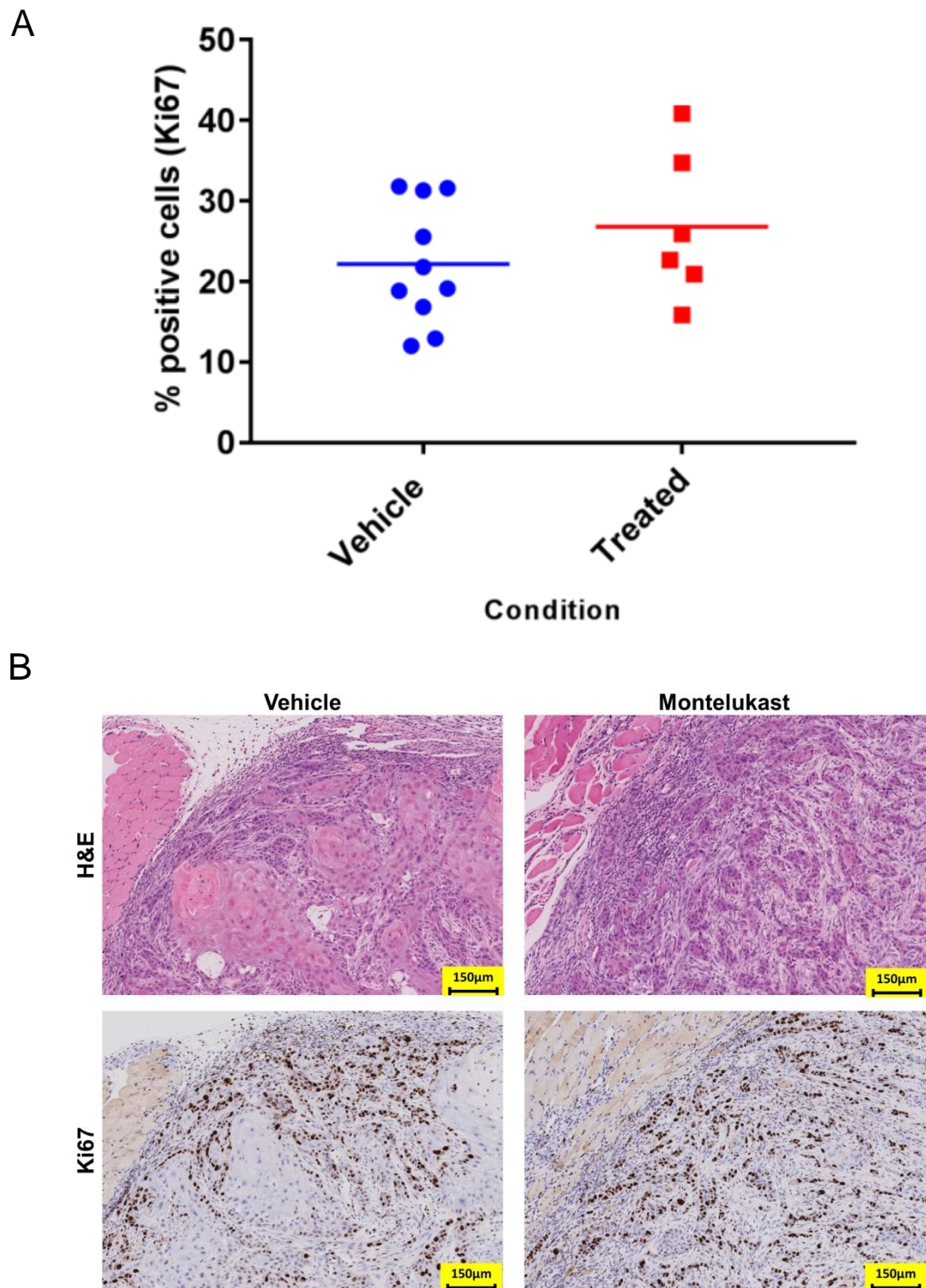


Figure 8.12 Ki67 histological staining. (A) Scatter plot showing percentage Ki67 positive cells in Liv7k xenograft sections. The differences in the treated (n=6) and control (n=10) groups was shown not to be statistically significant when assessed by unpaired t-test. (B) Representative images of stained sections are shown.

8.11 Montelukast treatment did not significantly alter the innate immune response to tumour cells

Given that montelukast is an anti-inflammatory drug, it was hypothesized that it may reduce the inflammatory immune response in treated mice. Neutrophils are one of the first responders to inflammatory insult, migrating through dilated blood vessels to phagocytose foreign cells and release pro-inflammatory cytokines[553]. Similarly, monocytes flood to the site of inflammation and differentiate into mature macrophages. The levels of neutrophils (NIMP) and macrophages (F4/80) were determined histologically in Liv7k xenograft sections, but revealed no obvious difference in the intensity of staining between the treated and control groups (Figure 8.13).

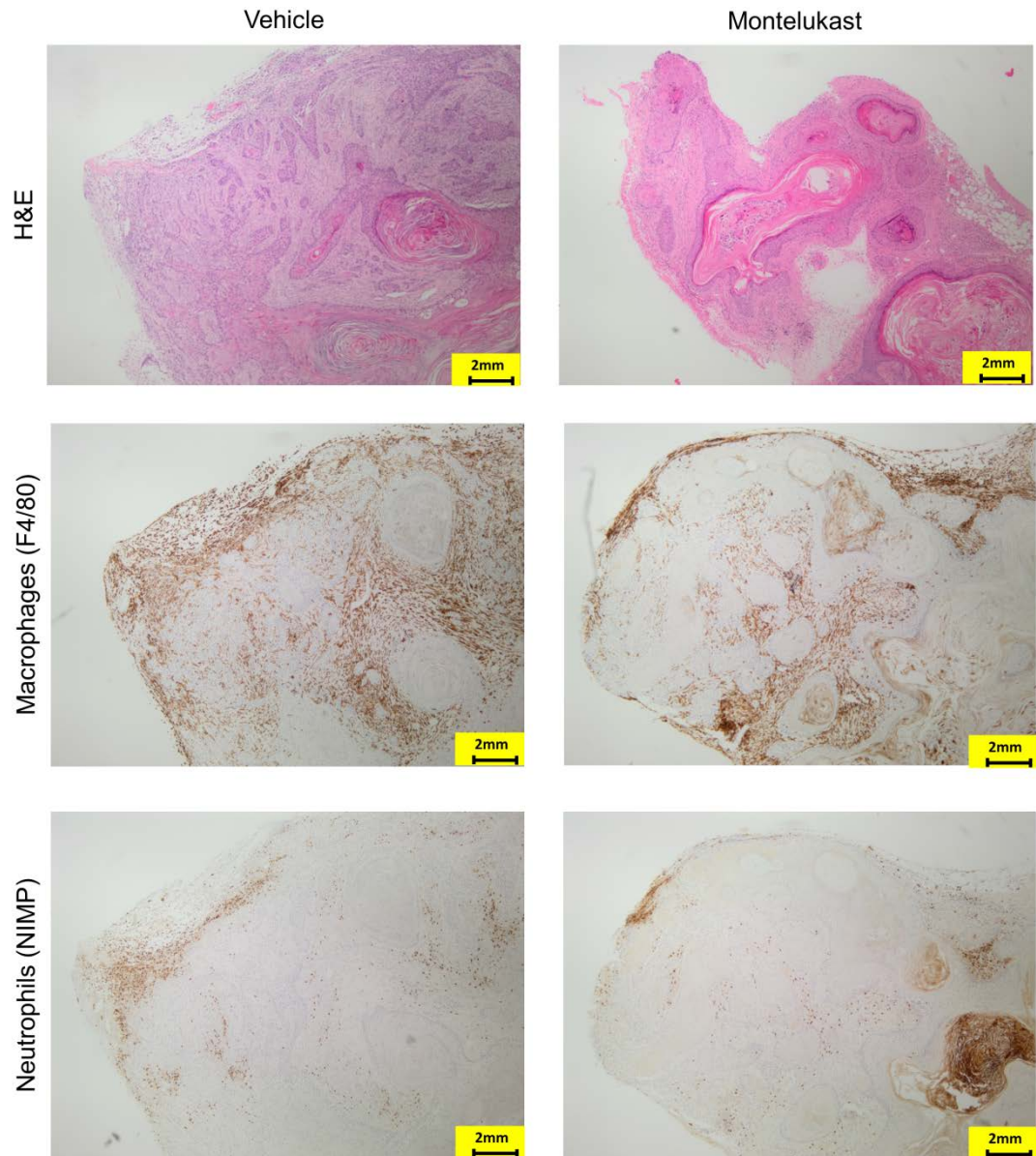


Figure 8.13 H&E, macrophage (F4/80) and neutrophil (NIMP) histological staining. Representative images of stained sections are shown. Ten control tumours and six treated tumours were stained in total.

8.12 Discussion

In this chapter, the role of cysteinyl leukotrienes in oral SCC has been addressed in a series of *in vitro* and *in vivo* experiments. Treatment with the FLAP inhibitor, MK-886 and two leukotriene receptor antagonists (LTRAs), montelukast and zafirlukast, resulted in near-complete growth inhibition of a patient-derived oral SCC cell line in a drug-repurposing screen. In terms of growth inhibition in normoxia, the compounds ranked 2nd, 10th and 41st, respectively. LTRAs are approved for the maintenance treatment of asthma, where they block the action of CysLT₁R, thus relaxing airway constriction and reduce inflammation and mucus build-up in the lungs[554]. Encouragingly, use of LTRAs was shown to decrease cancer risk in a meta-analysis of ~25,000 adults with asthma diagnosed between 2001 and 2011[555].

Moreover, the effect appeared to be specific to the oral cancer cell line, as no effect of montelukast was shown in previous drug screens, carried out on cell lines derived from other cancer types by the screening facility. It was later discovered that the effect was dependent on the presence of foetal bovine serum (FBS) in the culture media, as was the case for the eight breast cancer lines and one glioblastoma line screened previously. Many cell lines require FBS supplementation for proper growth and proliferation. FBS contains a multitude of growth factors, transport proteins, essential amino acids and other small molecules such as sugars and lipids[556].

A possible explanation for this unusual finding is that LTRAs are bound by serum proteins such as human serum albumin (HSA) and alpha-1 acid glycoprotein (AGP). In humans, montelukast is rapidly absorbed following administration, and has a half-life of 2.7-5.5 hours[557]. Importantly, montelukast has a highly lipophilic structure that causes 99% of the molecule to become bound to plasma proteins, leaving a limited unbound fraction to have a biological effect[558]. A drug-drug interaction study found that montelukast possessed the strongest AGP binding affinity in a series of cystic fibrosis drugs[559]. Another possibility is that FBS supplementation maintains the activity of oncogenic signalling pathways in the absence of CysLT₁R activation, through the stimulation of other receptors such as IGF1R[560]. However, it is reasonable to assume that keratinocyte serum

free media contains more physiologically relevant concentrations of growth factors and nutrients than serum-containing media.

Previous *in vitro* data supports the potential anti-cancer role of montelukast. The major mediator of leukotriene action, LTD₄, has been shown to increase cell proliferation and survival in intestinal epithelial cells[383]. In addition, LTD₄ significantly reduced apoptosis by preventing the activation of caspase-8[561]. Addition of LTD₄ to intestinal epithelial cells activated PI3K signalling and increased translocation of β -catenin to the nucleus[396].

To date, three *in vivo* studies have shown efficacy of LTRAs as cancer therapeutics[393, 394, 549], however their potential role in oral SCC had yet to be evaluated. In this study, daily treatment of mice with 5 mg/kg montelukast did not significantly reduce tumour volume compared to the control group; however, there was a trend for smaller tumour size. No significant difference in time to tumour endpoint was observed; albeit a tantalising tail of responders was seen in the survival graph (Figure 8.11). In light of these results, it was not unexpected to find no significant difference in Ki67 staining intensity between the two groups. This is in contrast to findings by Savari *et al.*, who found that average tumour weight was significantly reduced in the montelukast group in a colorectal xenograft model[394].

However, there were some important differences between the two studies. This study used immunocompromised NOD/SCID mice, while Savari's study was performed on athymic balb/c nude mice in which HCT-116 colorectal cells were pre-treated with montelukast prior to injection. In addition, montelukast was given by intraperitoneal injection in their study. Reassuringly, no significant reduction in Ki67 positive cells was observed in Savari's study, which suggests that the drug may be exerting its anti-tumour effects through other pathways (cell death was observed in Figure 8.7). To this end, the authors showed montelukast treatment led to significantly increased expression of p21^{WAF/Cip1} and decreased levels of VEGF in xenograft samples, indicating roles in cell cycle arrest and suppression of angiogenesis. Additional studies performed by the group showed montelukast treatment promoted apoptosis through cleavage of

caspase-3. The preliminary results in our study have not merited investigation of these pathways, although cross-sectional studies in the future may be pursued.

Future *in vivo* experiments should have increased numbers of mice to provide greater confidence in the results. Moreover, a more thorough characterisation of cell lines used in these experiments would likely elucidate the differential response to montelukast. This would allow for the categorisation into high and low CysLT₁R-expressing cell lines, which could be compared in further studies. Given that montelukast induced cell death in Liv7k cells, the mode of cell death needs to be determined. Cell cycle analysis by flow cytometry will reveal the effect of montelukast on cell growth, while western blotting for cleaved caspase 3 and cleaved PARP will determine if montelukast induces apoptosis in oral SCC cell lines. It was hypothesized that blocking the CysLT₁R would lead to a build-up of leukotrienes in the extracellular space. Given that excess leukotriene metabolites are excreted in the urine, the concentration of these metabolites was measured in treated and control mice by ELISA. However, the results of this experiment were extremely variable. Another approach would have been to measure the concentration of excreted drug in the urine to provide an idea of its bioavailability in this *in vivo* model.

In summary, although previous evidence has shown that LTRAs such as montelukast can prevent cancer progression, no significant reduction in tumour growth was observed in this study, albeit this may be due to limitations in the current study design. It is clear from *in vitro* data that inhibition of CysLT₁R is effective at inhibiting the growth of oral SCC cells, but this did not translate into success *in vivo*. It is likely that tumour heterogeneity plays an important role in the efficacy of leukotriene inhibitors. The patient-derived Liv7k cell line was used in these experiments at a low passage, and possibly more heterogeneous than the established HCT-116 cell line used in the Savari study. Moreover, the basal expression of CysLT₁R in the primary tumour may be predictive of LTRA response. High expression of the parallel COX pathway is also predictive of a poor prognosis, and may negate the benefit of LTRAs. Therefore, dual inhibition of the COX and LOX pathways would be a logical avenue of investigation in further studies.

Chapter 9 Concluding Remarks

For many years, the standard treatment options for patients diagnosed with oral cancer have been surgery and radio-therapy, and it was only in 2006 that the FDA approved chemotherapeutic agents for use in treating HNSCC. The first of these, cetuximab, targets the EGF Receptor, which is expressed in >90% of HNSCC tumours[562]. However, recent clinical trials have shown disappointing results, and failure to prolong patient survival[563]. The failure of the humanised monoclonal antibody to significantly prolong patient survival is primarily due to the heterogeneity of the disease, which contributes to intrinsic and acquired resistance[564]. While cetuximab undoubtedly has a place in HNSCC treatment, it does not provide benefit to a substantial proportion of the patient population[565], and indeed, despite the availability of chemotherapeutics approved for HNSCC, only one in two patients diagnosed with advanced oral cancer in the UK survive for five years after diagnosis[2]. Resistance to currently available therapeutics will continue to contribute to high rates of recurrence and metastases, necessitating the pursuit of novel therapeutic strategies which are based on the identification of driver genes with key roles in HNSCC progression.

Recent advances in the genomic characterisation of cancer have allowed tumours to be classified based on molecular subtype[35], which in turn has opened the door to personalised treatment strategies with maximal patient benefit. This body of work sought to identify novel driver genes in oral SCC, which may have potential clinical relevance. In doing so, three major themes emerged: (1) the clinical relevance of an amplicon found on chromosome three; (2) the role of hypoxia in lipid metabolism; and (3) tumour promoting inflammation.

Analysis of a commonly amplified region of chromosome 3 led to the selection of two genes for further investigation, *IGF2BP2* and *PSMD2*, both of which displayed amplified copy number, overexpression at mRNA level and significant correlation with HNSCC patient survival, in addition to being required for Liv7k cell line viability. Potential mechanisms of oncogenic progression in oral SCC were explored based on putative roles in the literature. *IGF2BP2* was hypothesized to

contribute to a more aggressive phenotype through its modulation of the insulin signalling pathway. However, silencing of *IGF2BP2* did not lead to significant abrogation of IGF1R phosphorylation or downstream signalling nodes, such as AKT and ERK. Moreover, knockdown of *IGF2BP2* did not significantly impair proliferation, migration, or invasion, in oral SCC cell lines. This does not necessarily rule out a role for the gene in HNSCC/oral cancer, but a better understanding of its targets in HNSCC cancer cells, as are expected imminently from the results of an RNA immunoprecipitation experiment, will help guide further investigations of this molecule and the phenotypic effects of amplification and over expression.

The second gene investigated was *PSMD2*, which encodes a subunit of the proteasome. *PSMD2* was found to be over-expressed in >30% of HNSCC tumours, with over-expression correlated with reduced overall survival of patients. Silencing of the gene resulted in ~40% growth inhibition in the Liv7k cell line. The fact that *PSMD2* silencing led to the selective induction of p21 in lung adenocarcinoma cell lines (but not human dermal fibroblasts) suggested that modulation of individual proteasomal subunits could lower the apoptotic threshold in cancer cells[426]. However, this did not appear to be the case for oral cancer, as equal or greater growth inhibition was observed in response to *PSMD2* knockdown in immortalised keratinocyte cell lines.

PSMD6, another proteasomal subunit, was found to be down-regulated in ~6% of tumours in the TCGA HNSCC dataset, leading to the hypothesis that the affected cancer cells may exhibit a greater dependence on *PSMD6* activity than diploid oral keratinocytes. This was borne out by the silencing of the gene, which resulted in reduced growth inhibition in a keratinocyte cell line compared to two oral SCC cell lines. The resistance to *PSMD6* silencing needs to be confirmed in a wider range of non-cancer cell lines in order to establish its selectivity in HNSCC.

A number of proteasomal subunits were identified as being altered in these studies and others, giving credence to the use of proteasomal inhibitors in the treatment of HNSCC. *In vitro* experiments have demonstrated that proteasomal inhibition is an effective method of killing HNSCC cells *in vitro* through the stimulation of apoptosis, inhibition of the NF- κ B pathway and generation of

reactive oxygen species[423, 566, 567]. In clinical trials however, bortezomib (which targets the $\beta 5$ subunit of the 20S proteolytic core), has resulted in high rates of resistance and toxicity[422]. Second-generation proteasomal inhibitors such as carfilzomib, which exhibit greater specificity than bortezomib, have been effective at overcoming resistance to proteasomal inhibitors *in vitro* and inhibiting the growth of HNSCC xenografts[568, 569]. However, the efficacy of these agents is limited by the fact that proteasomal inhibitors also stimulate survival signals in HNSCC cells[570, 571]. Bortezomib was demonstrated to antagonise the action of the EGFR inhibitor cetuximab in a phase I clinical trial, resulting in unexpected early progression of HNSCC tumours[572]. This highlights the need for a more targeted strategy to inhibit proteasomal activity with enhanced specificity and higher tolerability.

A major aim of this project was to uncover novel processes through which hypoxia influences the progression of oral SCC. To this end, an oxygen differential was employed in both the siRNA screen and RNA sequencing experiments in order to select for genes which, when silenced, resulted in a greater percentage growth inhibition in hypoxia than normoxia. Tumour hypoxia is an important prognostic factor in HNSCC, and is associated with therapeutic resistance and reduced overall survival[47]. A hypoxic tumour microenvironment drives phenotypic diversity within the tumour and selects for cells that best adapt to nutrient stress[573]. This includes alterations in energy metabolism such as increased glycolysis, reduced oxidative phosphorylation and increased *de novo* fatty acid synthesis. In this study, pathway analysis carried out on genes upregulated and essential for survival in hypoxia identified a subset of genes involved in triglyceride metabolism.

One of these genes, *MGLL*, had previously been shown to regulate a fatty acid network that promotes cancer pathogenesis[312]. Although the triglyceride hydrolysis aspect of MGLL action was confirmed in this study, the selective growth inhibition observed in our initial screen could not be reproduced in follow up experiments. The gene is involved in additional catalytic processes and has even been purported as a tumour suppressor gene in colorectal cancer[319]. The pleiotropic roles of MGLL in different cancer types may have contributed to the inconsistencies observed upon its silencing, but more work is needed to

investigate its relevance in HNSCC. Knockdown of another gene responsible for triglyceride breakdown, *PNPLA2*, did show a hypoxia specific effect in follow up experiments, but treatment with a small molecule inhibitor of the protein did not result in a loss of viability in high or low oxygen. Analysis of data from a re-screen carried out as part of this project with stricter statistical thresholds, and utilising a more specific set of siRNAs, may uncover targets with greater significance in hypoxia.

Similarly, a subset of genes involved in the synthesis of a structural class of lipid known as ether lipids were initially found to be essential for viability in hypoxia, but this could not be validated upon further experimentation. *AGPS*, which catalyses the rate limiting step in this process, has previously been shown to fuel an aggressive phenotype in cancer cells through its modulation of ether lipid signalling molecules[268]. This study found that silencing of *AGPS* in the Liv7k cell line resulted in a hypoxia-selective reduction of ether lipids, supporting the original hypothesis. This may suggest the *AGPS* is required in this condition to maintain the structural integrity of rapidly proliferating oral cancer cells. Although an outlying replicate affected the overall significance of the result, a small number of ether lipid species were altered upon knockdown of *AGPS*. It is possible that these lipids are involved in oncogenic signalling pathways in oral cancer, thus contributing to enhanced proliferation and survival. Additional work is required to determine if the gene can modulate oncogenic signalling networks in HNSCC and effect phenotypic change.

Finally, a drug-repurposing experiment, carried out to complement the results of the siRNA screen, revealed a selective sensitivity of oral cells grown in serum-free media to a family of leukotriene pathway antagonists. Leukotrienes are important pro-inflammatory mediators, which have been identified in a number of disease processes, including cancer[574]. Montelukast, an antagonist of the primary cysteinyl leukotriene receptor, CysLT1R, resulted in an IC_{50} of 670 nM in oral cancer cells, but showed no effect up to 10 μ M in cell lines grown in serum-containing media. Serum-free media likely recapitulates the limited nutrient environment available to tumour cells lacking adequate vasculature, making it more physiologically relevant. However, immortalised keratinocyte cells were

equally sensitive to montelukast treatment, indicating a process not specific to cancer cells is being targeted.

Treatment of nude mice with montelukast did tend toward reduced tumour volume of Liv7k xenografts, but did not significantly delay time to tumour endpoint, although there was a tendency toward prolonged survival. Histological staining of xenograft sections revealed no decrease in proliferation as measured by Ki67 staining intensity, perhaps not unexpectedly given that tissues were only collected at end-point. Interestingly, one tumour did begin to grow slowly upon treatment cessation at 100 days, after remaining static while on treatment. Staining of these sections may shed some light on its apparent sensitivity to montelukast.

In addition, treatment of cells within an extracellular matrix containing cancer-associated fibroblasts may elicit a more realistic response to montelukast treatment, which better reproduces the cross-talk between oral SCC cells and the microenvironment, indicating that patient-derived xenografts, or xenografts with and without co-cultured fibroblasts may be required to better tease out the potential benefits of montelukast or similar cysteinyl leukotriene receptor inhibitors. Similarly, performing cross-sectional studies, and taking animals at particular time points post treatment initiation may reveal differences in tumour dynamics, immune cell infiltration, and stromal response.

Survival rates for patients with advanced HNSCC have not improved since the licensing of cisplatin as an antineoplastic agent in the late 1970s[575]. Cetuximab represented the first targeted therapeutic agent to be employed in the disease, and yet has failed to provide a survival benefit commensurate with the extent of EGFR expression in HNSCCs[576]. Equally as important as better therapeutic options are the development of biomarkers to predict disease behaviour and allow for the stratification of patients into personalised therapeutic regimes, because, at present, no such biomarker exists to stratify patients into likely effective treatment groups.

The work described herein sought to combine both the comprehensive genomic characterization of cancer genomes available in publicly available datasets such

as the TCGA and ICGC, and the power of high-throughput screening, to identify potential novel therapeutic targets in HNSCC. Furthermore, by utilising physiologically relevant criteria, such as differential efficacy between hypoxic and normoxic conditions, we hoped to generate a set of targets which could be used to benefit a substantial portion of the population diagnosed with HNSCC. In summary, this study has provided an analysis of potential driver genes in oral squamous cell carcinoma, and insights into their role in the pathobiology of the disease.

List of References

1. Torre, L. A., Bray, F., Siegel, R. L., Ferlay, J., Lortet-Tieulent, J. & Jemal, A. (2015) Global cancer statistics, 2012, *CA Cancer J Clin.* **65**, 87-108.
2. CRUK (2017) Oral Cancer Statistics in
3. Sanderson, R. J. & Ironside, J. A. (2002) Squamous cell carcinomas of the head and neck, *BMJ.* **325**, 822-7.
4. Myers, J. N., Greenberg, J. S., Mo, V. & Roberts, D. (2001) Extracapsular spread. A significant predictor of treatment failure in patients with squamous cell carcinoma of the tongue, *Cancer.* **92**, 3030-6.
5. Leemans, C. R., Tiwari, R., Nauta, J. J., van der Waal, I. & Snow, G. B. (1993) Regional lymph node involvement and its significance in the development of distant metastases in head and neck carcinoma, *Cancer.* **71**, 452-6.
6. Dutton, J. M., Graham, S. M. & Hoffman, H. T. (2002) Metastatic cancer to the floor of mouth: the lingual lymph nodes, *Head Neck.* **24**, 401-5.
7. Snow, G. B., Patel, P., Leemans, C. R. & Tiwari, R. (1992) Management of cervical lymph nodes in patients with head and neck cancer, *Eur Arch Otorhinolaryngol.* **249**, 187-94.
8. Suh, Y., Amelio, I., Urbano, T. G. & Tavassoli, M. (2014) Clinical update on cancer: molecular oncology of head and neck cancer, *Cell Death Dis.* **5**.
9. Bonner, J. A., Harari, P. M., Giralt, J., Azarnia, N., Shin, D. M., Cohen, R. B., Jones, C. U., Sur, R., Raben, D., Jassem, J., Ove, R., Kies, M. S., Baselga, J., Yousoufian, H., Amellal, N., Rowinsky, E. K. & Ang, K. K. (2006) Radiotherapy plus cetuximab for squamous-cell carcinoma of the head and neck, *New Engl J Med.* **354**, 567-578.
10. Magrini, S. M., Buglione, M., Corvo, R., Pirtoli, L., Paiar, F., Ponticelli, P., Petrucci, A., Bacigalupo, A., Crociani, M., Lastrucci, L., Vecchio, S., Bonomo, P., Pasinetti, N., Triggiani, L., Cavagnini, R., Costa, L., Tonoli, S., Maddalo, M. & Grisanti, S. (2016) Cetuximab and Radiotherapy Versus Cisplatin and Radiotherapy for Locally Advanced Head and Neck Cancer: A Randomized Phase II Trial, *J Clin Oncol.* **34**, 427-+.
11. Husain, Z. A., Burtness, B. A. & Decker, R. H. (2016) Cisplatin Versus Cetuximab With Radiotherapy in Locally Advanced Squamous Cell Carcinoma of the Head and Neck, *J Clin Oncol.* **34**, 396-+.
12. Raedler, L. A. (2015) Keytruda (Pembrolizumab): First PD-1 Inhibitor Approved for Previously Treated Unresectable or Metastatic Melanoma, *Am Health Drug Benefits.* **8**, 96-100.
13. Reck, M., Rodriguez-Abreu, D., Robinson, A. G., Hui, R., Czoszi, T., Fulop, A., Gottfried, M., Peled, N., Tafreshi, A., Cuffe, S., O'Brien, M., Rao, S., Hotta, K., Leiby, M. A., Lubiniecki, G. M., Shentu, Y., Rangwala, R., Brahmer, J. R. & Investigators, K.-. (2016) Pembrolizumab versus Chemotherapy for PD-L1-Positive Non-Small-Cell Lung Cancer, *N Engl J Med.* **375**, 1823-1833.
14. Seiwert, T. Y., Burtness, B., Mehra, R., Weiss, J., Berger, R., Eder, J. P., Heath, K., McClanahan, T., Lunceford, J., Gause, C., Cheng, J. D. & Chow, L. Q. (2016) Safety and clinical activity of pembrolizumab for treatment of recurrent or metastatic squamous cell carcinoma of the head and neck (KEYNOTE-012): an open-label, multicentre, phase 1b trial, *Lancet Oncol.* **17**, 956-65.
15. Bauml, J., Seiwert, T. Y., Pfister, D. G., Worden, F., Liu, S. V., Gilbert, J., Saba, N. F., Weiss, J., Wirth, L., Sukari, A., Kang, H., Gibson, M. K., Massarelli, E., Powell, S., Meister, A., Shu, X., Cheng, J. D. & Haddad, R. (2017) Pembrolizumab for Platinum- and Cetuximab-Refractory Head and Neck Cancer: Results From a Single-Arm, Phase II Study, *J Clin Oncol.* **35**, 1542-1549.
16. Le, D. T., Durham, J. N., Smith, K. N., Wang, H., Bartlett, B. R., Aulakh, L. K., Lu, S., Kemberling, H., Wilt, C., Luber, B. S., Wong, F., Azad, N. S., Rucki, A. A., Laheru, D., Donehower, R., Zaheer, A., Fisher, G. A., Crocenzi, T. S., Lee, J. J., Greten, T. F., Duffy, A. G., Ciombor, K. K., Eyring, A. D., Lam, B. H., Joe, A., Kang, S. P., Holdhoff, M., Danilova, L., Cope, L., Meyer, C., Zhou, S., Goldberg, R. M., Armstrong, D. K., Bever, K. M., Fader, A. N., Taube, J., Housseau, F., Spetzler, D., Xiao, N., Pardoll, D. M., Papadopoulos, N., Kinzler, K. W., Eshleman, J. R., Vogelstein, B., Anders, R. A. & Diaz, L. A., Jr. (2017) Mismatch repair deficiency predicts response of solid tumors to PD-1 blockade, *Science.* **357**, 409-413.

17. Ferris, R. L., Blumenschein, G., Fayette, J., Guigay, J., Colevas, A. D., Licitra, L., Harrington, K., Kasper, S., Vokes, E. E., Even, C., Worden, F., Saba, N. F., Docampo, L. C. I., Haddad, R., Rordorf, T., Kiyota, N., Tahara, M., Monga, M., Lynch, M., Geese, W. J., Kopit, J., Shaw, J. W. & Gillison, M. L. (2016) Nivolumab for Recurrent Squamous-Cell Carcinoma of the Head and Neck, *New Engl J Med.* **375**, 1856-1867.
18. Warnakulasuriya, S. (2009) Global epidemiology of oral and oropharyngeal cancer, *Oral Oncol.* **45**, 309-16.
19. Young, D., Xiao, C. C., Murphy, B., Moore, M., Fakhry, C. & Day, T. A. (2015) Increase in head and neck cancer in younger patients due to human papillomavirus (HPV), *Oral Oncol.* **51**, 727-30.
20. Hashibe, M., Brennan, P., Chuang, S. C., Boccia, S., Castellsague, X., Chen, C., Curado, M. P., Dal Maso, L., Daudt, A. W., Fabianova, E., Fernandez, L., Wunsch-Filho, V., Franceschi, S., Hayes, R. B., Herrero, R., Kelsey, K., Koifman, S., La Vecchia, C., Lazarus, P., Levi, F., Lence, J. J., Mates, D., Matos, E., Menezes, A., McClean, M. D., Muscat, J., Eluf-Neto, J., Olshan, A. F., Purdue, M., Rudnai, P., Schwartz, S. M., Smith, E., Sturgis, E. M., Szeszenia-Dabrowska, N., Talamini, R., Wei, Q., Winn, D. M., Shangina, O., Pilarska, A., Zhang, Z. F., Ferro, G., Berthiller, J. & Boffetta, P. (2009) Interaction between tobacco and alcohol use and the risk of head and neck cancer: pooled analysis in the International Head and Neck Cancer Epidemiology Consortium, *Cancer Epidemiol Biomarkers Prev.* **18**, 541-50.
21. Majchrzak, E., Szybiak, B., Wegner, A., Pienkowski, P., Pazdrowski, J., Luczewski, L., Sowka, M., Golusinski, P., Malicki, J. & Golusinski, W. (2014) Oral cavity and oropharyngeal squamous cell carcinoma in young adults: a review of the literature, *Radiol Oncol.* **48**, 1-10.
22. Llewellyn, C. D., Johnson, N. W. & Warnakulasuriya, K. A. (2001) Risk factors for squamous cell carcinoma of the oral cavity in young people--a comprehensive literature review, *Oral Oncol.* **37**, 401-18.
23. Kuriakose, M., Sankaranarayanan, M., Nair, M. K., Cherian, T., Sugar, A. W., Scully, C. & Prime, S. S. (1992) Comparison of oral squamous cell carcinoma in younger and older patients in India, *Eur J Cancer B Oral Oncol.* **28B**, 113-20.
24. Llewellyn, C. D., Linklater, K., Bell, J., Johnson, N. W. & Warnakulasuriya, S. (2004) An analysis of risk factors for oral cancer in young people: a case-control study, *Oral Oncol.* **40**, 304-13.
25. Chaturvedi, A. K., Engels, E. A., Pfeiffer, R. M., Hernandez, B. Y., Xiao, W., Kim, E., Jiang, B., Goodman, M. T., Sibug-Saber, M., Cozen, W., Liu, L., Lynch, C. F., Wentzensen, N., Jordan, R. C., Altekruze, S., Anderson, W. F., Rosenberg, P. S. & Gillison, M. L. (2011) Human papillomavirus and rising oropharyngeal cancer incidence in the United States, *J Clin Oncol.* **29**, 4294-301.
26. Mehanna, H., Beech, T., Nicholson, T., El-Hariry, I., McConkey, C., Paleri, V. & Roberts, S. (2013) Prevalence of human papillomavirus in oropharyngeal and nonoropharyngeal head and neck cancer--systematic review and meta-analysis of trends by time and region, *Head Neck.* **35**, 747-55.
27. Ang, K. K., Harris, J., Wheeler, R., Weber, R., Rosenthal, D. I., Nguyen-Tan, P. F., Westra, W. H., Chung, C. H., Jordan, R. C., Lu, C., Kim, H., Axelrod, R., Silverman, C. C., Redmond, K. P. & Gillison, M. L. (2010) Human papillomavirus and survival of patients with oropharyngeal cancer, *N Engl J Med.* **363**, 24-35.
28. Gillison, M. L., Koch, W. M., Capone, R. B., Spafford, M., Westra, W. H., Wu, L., Zahurak, M. L., Daniel, R. W., Viglione, M., Symer, D. E., Shah, K. V. & Sidransky, D. (2000) Evidence for a causal association between human papillomavirus and a subset of head and neck cancers, *J Natl Cancer Inst.* **92**, 709-20.
29. Ringstrom, E., Peters, E., Hasegawa, M., Posner, M., Liu, M. & Kelsey, K. T. (2002) Human papillomavirus type 16 and squamous cell carcinoma of the head and neck, *Clin Cancer Res.* **8**, 3187-92.
30. Bonner, J. A., Mesia, R., Giralt, J., Psyrris, A., Keilholz, U., Rosenthal, D. I., Beier, F., Schulten, J. & Vermorken, J. B. (2017) p16, HPV, and Cetuximab: What Is the Evidence?, *Oncologist.*
31. Jin, C., Jin, Y., Wennerberg, J., Akervall, J., Dictor, M. & Mertens, F. (2002) Karyotypic heterogeneity and clonal evolution in squamous cell carcinomas of the head and neck, *Cancer Genet Cytogenet.* **132**, 85-96.

32. Jeon, G. A., Lee, J. S., Patel, V., Gutkind, J. S., Thorgeirsson, S. S., Kim, E. C., Chu, I. S., Amornphimoltham, P. & Park, M. H. (2004) Global gene expression profiles of human head and neck squamous carcinoma cell lines, *Int J Cancer*. **112**, 249-58.
33. Zhang, X. C., Xu, C., Mitchell, R. M., Zhang, B., Zhao, D., Li, Y., Huang, X., Fan, W., Wang, H., Lerma, L. A., Upton, M. P., Hay, A., Mendez, E. & Zhao, L. P. (2013) Tumor evolution and intratumor heterogeneity of an oropharyngeal squamous cell carcinoma revealed by whole-genome sequencing, *Neoplasia*. **15**, 1371-8.
34. Mroz, E. A., Tward, A. M., Hammon, R. J., Ren, Y. & Rocco, J. W. (2015) Intra-tumor Genetic Heterogeneity and Mortality in Head and Neck Cancer: Analysis of Data from The Cancer Genome Atlas, *Plos Med*. **12**.
35. Biankin, A. V., Piantadosi, S. & Hollingsworth, S. J. (2015) Patient-centric trials for therapeutic development in precision oncology, *Nature*. **526**, 361-70.
36. Dai, X., Li, T., Bai, Z., Yang, Y., Liu, X., Zhan, J. & Shi, B. (2015) Breast cancer intrinsic subtype classification, clinical use and future trends, *Am J Cancer Res*. **5**, 2929-43.
37. Andreadis, C., Vahtsevanos, K., Sidiras, T., Thomaidis, I., Antoniadis, K. & Mouratidou, D. (2003) 5-Fluorouracil and cisplatin in the treatment of advanced oral cancer, *Oral Oncol*. **39**, 380-5.
38. Noguti, J., De Moura, C. F., De Jesus, G. P., Da Silva, V. H., Hossaka, T. A., Oshima, C. T. & Ribeiro, D. A. (2012) Metastasis from oral cancer: an overview, *Cancer Genomics Proteomics*. **9**, 329-35.
39. Nithya, C., Pandey, M., Naik, B. & Ahamed, I. M. (2003) Patterns of cervical metastasis from carcinoma of the oral tongue, *World J Surg Oncol*. **1**, 10.
40. Shaw, R. J., Lowe, D., Woolgar, J. A., Brown, J. S., Vaughan, E. D., Evans, C., Lewis-Jones, H., Hanlon, R., Hall, G. L. & Rogers, S. N. (2010) Extracapsular spread in oral squamous cell carcinoma, *Head Neck*. **32**, 714-22.
41. Maxwell, J. H., Ferris, R. L., Gooding, W., Cunningham, D., Mehta, V., Kim, S., Myers, E. N., Johnson, J. & Chiosea, S. (2013) Extracapsular spread in head and neck carcinoma: impact of site and human papillomavirus status, *Cancer*. **119**, 3302-8.
42. Mack, M. G., Rieger, J., Baghi, M., Bisdas, S. & Vogl, T. J. (2008) Cervical lymph nodes, *Eur J Radiol*. **66**, 493-500.
43. Hanahan, D. & Weinberg, R. A. (2011) Hallmarks of cancer: the next generation, *Cell*. **144**, 646-74.
44. Stransky, N., Egloff, A. M., Tward, A. D., Kostic, A. D., Cibulskis, K., Sivachenko, A., Kryukov, G. V., Lawrence, M. S., Sougnez, C., McKenna, A., Shefler, E., Ramos, A. H., Stojanov, P., Carter, S. L., Voet, D., Cortes, M. L., Auclair, D., Berger, M. F., Saksena, G., Guiducci, C., Onofrio, R. C., Parkin, M., Romkes, M., Weissfeld, J. L., Seethala, R. R., Wang, L., Rangel-Escareno, C., Fernandez-Lopez, J. C., Hidalgo-Miranda, A., Melendez-Zajgla, J., Winckler, W., Ardlie, K., Gabriel, S. B., Meyerson, M., Lander, E. S., Getz, G., Golub, T. R., Garraway, L. A. & Grandis, J. R. (2011) The Mutational Landscape of Head and Neck Squamous Cell Carcinoma, *Science*. **333**, 1157-1160.
45. Riaz, N., Morris, L. G., Lee, W. & Chan, T. A. (2014) Unraveling the molecular genetics of head and neck cancer through genome-wide approaches, *Genes Dis*. **1**, 75-86.
46. Janssen, H. L., Haustermans, K. M., Balm, A. J. & Begg, A. C. (2005) Hypoxia in head and neck cancer: how much, how important?, *Head Neck*. **27**, 622-38.
47. Bittner, M. I. & Grosu, A. L. (2013) Hypoxia in Head and Neck Tumors: Characteristics and Development during Therapy, *Front Oncol*. **3**, 223.
48. Masson, N. & Ratcliffe, P. J. (2014) Hypoxia signaling pathways in cancer metabolism: the importance of co-selecting interconnected physiological pathways, *Cancer Metab*. **2**, 3.
49. Luo, X., Cheng, C., Tan, Z., Li, N., Tang, M., Yang, L. & Cao, Y. (2017) Emerging roles of lipid metabolism in cancer metastasis, *Mol Cancer*. **16**, 76.
50. Bonomi, M., Patsias, A., Posner, M. & Sikora, A. (2014) The role of inflammation in head and neck cancer, *Adv Exp Med Biol*. **816**, 107-27.
51. Pries, R., Nitsch, S. & Wollenberg, B. (2006) Role of cytokines in head and neck squamous cell carcinoma, *Expert Rev Anticancer Ther*. **6**, 1195-203.

52. Papadimitrakopoulou, V. A., William, W. N., Jr., Dannenberg, A. J., Lippman, S. M., Lee, J. J., Ondrey, F. G., Peterson, D. E., Feng, L., Atwell, A., El-Naggar, A. K., Nathan, C. O., Helman, J. I., Du, B., Yueh, B. & Boyle, J. O. (2008) Pilot randomized phase II study of celecoxib in oral premalignant lesions, *Clin Cancer Res.* **14**, 2095-101.
53. Global Burden of Disease Cancer, C.Fitzmaurice, C.Allen, C.Barber, R. M.Barregard, L.Bhutta, Z. A.Brenner, H.Dicker, D. J.Chimed-Orchir, O.Dandona, R.Dandona, L.Fleming, T.Forouzanfar, M. H.Hancock, J.Hay, R. J.Hunter-Merrill, R.Huynh, C.Hosgood, H. D.Johnson, C. O.Jonas, J. B.Khubchandani, J.Kumar, G. A.Kutz, M.Lan, Q.Larson, H. J.Liang, X.Lim, S. S.Lopez, A. D.MacIntyre, M. F.Marczak, L.Marquez, N.Mokdad, A. H.Pinho, C.Pourmalek, F.Salomon, J. A.Sanabria, J. R.Sandar, L.Sartorius, B.Schwartz, S. M.Shackelford, K. A.Shibuya, K.Stanaway, J.Steiner, C.Sun, J.Takahashi, K.Vollset, S. E.Vos, T.Wagner, J. A.Wang, H.Westerman, R.Zeeb, H.Zoeckler, L.Abd-Allah, F.Ahmed, M. B.Alabed, S.Alam, N. K.Aldahri, S. F.Alem, G.Alemayohu, M. A.Ali, R.Al-Raddadi, R.Amare, A.Amoako, Y.Artaman, A.Asayesh, H.Atnafu, N.Awasthi, A.Saleem, H. B.Barac, A.Bedi, N.Bensenor, I.Berhane, A.Bernabe, E.Betsu, B.Binagwaho, A.Boneya, D.Campos-Nonato, I.Castaneda-Orjuela, C.Catala-Lopez, F.Chiang, P.Chibueze, C.Chitheer, A.Choi, J. Y.Cowie, B.Damtew, S.das Neves, J.Dey, S.Dharmaratne, S.Dhillon, P.Ding, E.Driscoll, T.Ekwueme, D.Endries, A. Y.Farvid, M.Farzadfar, F.Fernandes, J.Fischer, F.TT, G. H.Gebru, A.Gopalani, S., et al. (2017) Global, Regional, and National Cancer Incidence, Mortality, Years of Life Lost, Years Lived With Disability, and Disability-Adjusted Life-years for 32 Cancer Groups, 1990 to 2015: A Systematic Analysis for the Global Burden of Disease Study, *JAMA Oncol.* **3**, 524-548.
54. Cancer Genome Atlas, N. (2015) Comprehensive genomic characterization of head and neck squamous cell carcinomas, *Nature.* **517**, 576-82.
55. Demokan, S., Chuang, A., Suoglu, Y., Uluhan, M., Yalniz, Z., Califano, J. A. & Dalay, N. (2012) Promoter methylation and loss of p16(INK4a) gene expression in head and neck cancer, *Head Neck.* **34**, 1470-5.
56. Hanken, H., Grobe, A., Cachovan, G., Smeets, R., Simon, R., Sauter, G., Heiland, M. & Blessmann, M. (2014) CCND1 amplification and cyclin D1 immunohistochemical expression in head and neck squamous cell carcinomas, *Clin Oral Investig.* **18**, 269-76.
57. Lui, V. W., Hedberg, M. L., Li, H., Vangara, B. S., Pendleton, K., Zeng, Y., Lu, Y., Zhang, Q., Du, Y., Gilbert, B. R., Freilino, M., Sauerwein, S., Peyser, N. D., Xiao, D., Diergaard, B., Wang, L., Chiosea, S., Seethala, R., Johnson, J. T., Kim, S., Duvvuri, U., Ferris, R. L., Romkes, M., Nukui, T., Kwok-Shing Ng, P., Garraway, L. A., Hammerman, P. S., Mills, G. B. & Grandis, J. R. (2013) Frequent mutation of the PI3K pathway in head and neck cancer defines predictive biomarkers, *Cancer Discov.* **3**, 761-9.
58. Squarize, C. H., Castilho, R. M., Abrahao, A. C., Molinolo, A., Lingen, M. W. & Gutkind, J. S. (2013) PTEN deficiency contributes to the development and progression of head and neck cancer, *Neoplasia.* **15**, 461-71.
59. Bian, Y., Hall, B., Sun, Z. J., Molinolo, A., Chen, W., Gutkind, J. S., Waes, C. V. & Kulkarni, A. B. (2012) Loss of TGF-beta signaling and PTEN promotes head and neck squamous cell carcinoma through cellular senescence evasion and cancer-related inflammation, *Oncogene.* **31**, 3322-32.
60. Agrawal, N., Frederick, M. J., Pickering, C. R., Bettegowda, C., Chang, K., Li, R. J., Fakhry, C., Xie, T. X., Zhang, J., Wang, J., Zhang, N., El-Naggar, A. K., Jasser, S. A., Weinstein, J. N., Trevino, L., Drummond, J. A., Muzny, D. M., Wu, Y., Wood, L. D., Hruban, R. H., Westra, W. H., Koch, W. M., Califano, J. A., Gibbs, R. A., Sidransky, D., Vogelstein, B., Velculescu, V. E., Papadopoulos, N., Wheeler, D. A., Kinzler, K. W. & Myers, J. N. (2011) Exome sequencing of head and neck squamous cell carcinoma reveals inactivating mutations in NOTCH1, *Science.* **333**, 1154-7.
61. Kandoth, C., McLellan, M. D., Vandin, F., Ye, K., Niu, B., Lu, C., Xie, M., Zhang, Q., McMichael, J. F., Wyczalkowski, M. A., Leiserson, M. D., Miller, C. A., Welch, J. S., Walter, M. J., Wendl, M. C., Ley, T. J., Wilson, R. K., Raphael, B. J. & Ding, L. (2013) Mutational landscape and significance across 12 major cancer types, *Nature.* **502**, 333-9.
62. Pickering, C. R., Zhang, J., Yoo, S. Y., Bengtsson, L., Moorthy, S., Neskey, D. M., Zhao, M., Ortega Alves, M. V., Chang, K., Drummond, J., Cortez, E., Xie, T. X., Zhang, D., Chung, W., Issa, J. P., Zweidler-McKay, P. A., Wu, X., El-Naggar, A. K., Weinstein, J. N., Wang, J., Muzny, D. M., Gibbs, R.

- A., Wheeler, D. A., Myers, J. N. & Frederick, M. J. (2013) Integrative genomic characterization of oral squamous cell carcinoma identifies frequent somatic drivers, *Cancer Discov.* **3**, 770-81.
63. Sakamoto, K., Fujii, T., Kawachi, H., Miki, Y., Omura, K., Morita, K., Kayamori, K., Katsube, K. & Yamaguchi, A. (2012) Reduction of NOTCH1 expression pertains to maturation abnormalities of keratinocytes in squamous neoplasms, *Lab Invest.* **92**, 688-702.
64. Duan, L., Yao, J., Wu, X. & Fan, M. (2006) Growth suppression induced by Notch1 activation involves Wnt-beta-catenin down-regulation in human tongue carcinoma cells, *Biol Cell.* **98**, 479-90.
65. Sun, W., Gaykalova, D. A., Ochs, M. F., Mambo, E., Arnaoutakis, D., Liu, Y., Loyo, M., Agrawal, N., Howard, J., Li, R., Ahn, S., Fertig, E., Sidransky, D., Houghton, J., Buddavarapu, K., Sanford, T., Choudhary, A., Darden, W., Adai, A., Latham, G., Bishop, J., Sharma, R., Westra, W. H., Hennessey, P., Chung, C. H. & Califano, J. A. (2014) Activation of the NOTCH pathway in head and neck cancer, *Cancer Res.* **74**, 1091-104.
66. Hijioka, H., Setoguchi, T., Miyawaki, A., Gao, H., Ishida, T., Komiya, S. & Nakamura, N. (2010) Upregulation of Notch pathway molecules in oral squamous cell carcinoma, *Int J Oncol.* **36**, 817-22.
67. Lee, S. H., Hong, H. S., Liu, Z. X., Kim, R. H., Kang, M. K., Park, N. H. & Shin, K. H. (2012) TNFalpha enhances cancer stem cell-like phenotype via Notch-Hes1 activation in oral squamous cell carcinoma cells, *Biochem Biophys Res Commun.* **424**, 58-64.
68. Lee, S. H., Do, S. I., Lee, H. J., Kang, H. J., Koo, B. S. & Lim, Y. C. (2016) Notch1 signaling contributes to stemness in head and neck squamous cell carcinoma, *Lab Invest.* **96**, 508-16.
69. Yoshida, R., Nagata, M., Nakayama, H., Niimori-Kita, K., Hassan, W., Tanaka, T., Shinohara, M. & Ito, T. (2013) The pathological significance of Notch1 in oral squamous cell carcinoma, *Lab Invest.* **93**, 1068-81.
70. Joo, Y. H., Jung, C. K., Kim, M. S. & Sun, D. I. (2009) Relationship between vascular endothelial growth factor and Notch1 expression and lymphatic metastasis in tongue cancer, *Otolaryngol Head Neck Surg.* **140**, 512-8.
71. Zhang, T. H., Liu, H. C., Zhu, L. J., Chu, M., Liang, Y. J., Liang, L. Z. & Liao, G. Q. (2011) Activation of Notch signaling in human tongue carcinoma, *J Oral Pathol Med.* **40**, 37-45.
72. Yao, J., Duan, L., Fan, M. & Wu, X. (2007) Gamma-secretase inhibitors exerts antitumor activity via down-regulation of Notch and Nuclear factor kappa B in human tongue carcinoma cells, *Oral Dis.* **13**, 555-63.
73. Yap, L. F., Lee, D., Khairuddin, A., Pairan, M. F., Puspita, B., Siar, C. H. & Paterson, I. C. (2015) The opposing roles of NOTCH signalling in head and neck cancer: a mini review, *Oral Dis.* **21**, 850-7.
74. Zhang, M., Biswas, S., Qin, X., Gong, W., Deng, W. & Yu, H. (2016) Does Notch play a tumor suppressor role across diverse squamous cell carcinomas?, *Cancer Med.* **5**, 2048-60.
75. Carvalho, C. M. & Lupski, J. R. (2016) Mechanisms underlying structural variant formation in genomic disorders, *Nat Rev Genet.* **17**, 224-38.
76. Alkan, C., Coe, B. P. & Eichler, E. E. (2011) Genome structural variation discovery and genotyping, *Nat Rev Genet.* **12**, 363-76.
77. Ciriello, G., Miller, M. L., Aksoy, B. A., Senbabaoglu, Y., Schultz, N. & Sander, C. (2013) Emerging landscape of oncogenic signatures across human cancers, *Nat Genet.* **45**, 1127-33.
78. Ah-See, K. W., Cooke, T. G., Pickford, I. R., Soutar, D. & Balmain, A. (1994) An allelotype of squamous carcinoma of the head and neck using microsatellite markers, *Cancer Res.* **54**, 1617-21.
79. Li, X., Lee, N. K., Ye, Y. W., Waber, P. G., Schweitzer, C., Cheng, Q. C. & Nisen, P. D. (1994) Allelic loss at chromosomes 3p, 8p, 13q, and 17p associated with poor prognosis in head and neck cancer, *J Natl Cancer Inst.* **86**, 1524-9.
80. Van Dyke, D. L., Worsham, M. J., Benninger, M. S., Krause, C. J., Baker, S. R., Wolf, G. T., Drumheller, T., Tilley, B. C. & Carey, T. E. (1994) Recurrent cytogenetic abnormalities in squamous cell carcinomas of the head and neck region, *Genes Chromosomes Cancer.* **9**, 192-206.
81. Sheu, J. J., Hua, C. H., Wan, L., Lin, Y. J., Lai, M. T., Tseng, H. C., Jinawath, N., Tsai, M. H., Chang, N. W., Lin, C. F., Lin, C. C., Hsieh, L. J., Wang, T. L., Shih Ie, M. & Tsai, F. J. (2009) Functional

- genomic analysis identified epidermal growth factor receptor activation as the most common genetic event in oral squamous cell carcinoma, *Cancer Res.* **69**, 2568-76.
82. Grandis, J. R. & Tweardy, D. J. (1993) Elevated levels of transforming growth factor alpha and epidermal growth factor receptor messenger RNA are early markers of carcinogenesis in head and neck cancer, *Cancer Res.* **53**, 3579-84.
83. Rubin Grandis, J., Melhem, M. F., Barnes, E. L. & Tweardy, D. J. (1996) Quantitative immunohistochemical analysis of transforming growth factor-alpha and epidermal growth factor receptor in patients with squamous cell carcinoma of the head and neck, *Cancer.* **78**, 1284-92.
84. Sarkis, S. A., Abdullah, B. H., Abdul Majeed, B. A. & Talabani, N. G. (2010) Immunohistochemical expression of epidermal growth factor receptor (EGFR) in oral squamous cell carcinoma in relation to proliferation, apoptosis, angiogenesis and lymphangiogenesis, *Head Neck Oncol.* **2**, 13.
85. Christensen, M. E., Therkildsen, M. H., Hansen, B. L., Albeck, H., Hansen, G. N. & Bretlau, P. (1992) Epidermal growth factor receptor expression on oral mucosa dysplastic epithelia and squamous cell carcinomas, *Eur Arch Otorhinolaryngol.* **249**, 243-7.
86. Hiraishi, Y., Wada, T., Nakatani, K., Negoro, K. & Fujita, S. (2006) Immunohistochemical expression of EGFR and p-EGFR in oral squamous cell carcinomas, *Pathol Oncol Res.* **12**, 87-91.
87. Ang, K. K., Berkey, B. A., Tu, X., Zhang, H. Z., Katz, R., Hammond, E. H., Fu, K. K. & Milas, L. (2002) Impact of epidermal growth factor receptor expression on survival and pattern of relapse in patients with advanced head and neck carcinoma, *Cancer Res.* **62**, 7350-6.
88. Chung, C. H., Ely, K., McGavran, L., Varella-Garcia, M., Parker, J., Parker, N., Jarrett, C., Carter, J., Murphy, B. A., Nettekville, J., Burkey, B. B., Sinard, R., Cmelak, A., Levy, S., Yarbrough, W. G., Slebos, R. J. & Hirsch, F. R. (2006) Increased epidermal growth factor receptor gene copy number is associated with poor prognosis in head and neck squamous cell carcinomas, *J Clin Oncol.* **24**, 4170-6.
89. Temam, S., Kawaguchi, H., El-Naggar, A. K., Jelinek, J., Tang, H., Liu, D. D., Lang, W., Issa, J. P., Lee, J. J. & Mao, L. (2007) Epidermal growth factor receptor copy number alterations correlate with poor clinical outcome in patients with head and neck squamous cancer, *J Clin Oncol.* **25**, 2164-70.
90. Modjtahedi, H. & Essapen, S. (2009) Epidermal growth factor receptor inhibitors in cancer treatment: advances, challenges and opportunities, *Anticancer Drugs.* **20**, 851-5.
91. Albanell, J., Codony-Servat, J., Rojo, F., Del Campo, J. M., Sauleda, S., Anido, J., Raspall, G., Giralt, J., Rosello, J., Nicholson, R. I., Mendelsohn, J. & Baselga, J. (2001) Activated extracellular signal-regulated kinases: association with epidermal growth factor receptor/transforming growth factor alpha expression in head and neck squamous carcinoma and inhibition by anti-epidermal growth factor receptor treatments, *Cancer Res.* **61**, 6500-10.
92. Grandis, J. R., Drenning, S. D., Chakraborty, A., Zhou, M. Y., Zeng, Q., Pitt, A. S. & Tweardy, D. J. (1998) Requirement of Stat3 but not Stat1 activation for epidermal growth factor receptor-mediated cell growth In vitro, *J Clin Invest.* **102**, 1385-92.
93. Hambek, M., Baghi, M., Baumaun, H., Strebhardt, K., Adunka, O., Gstottner, W. & Knecht, R. (2005) Iressa (ZD 1839) inhibits phosphorylation of three different downstream signal transducers in head and neck cancer (SCCHN), *Anticancer Res.* **25**, 1871-5.
94. Chang, K. Y., Tsai, S. Y., Chen, S. H., Tsou, H. H., Yen, C. J., Liu, K. J., Fang, H. L., Wu, H. C., Chuang, B. F., Chou, S. W., Tang, C. K., Liu, S. Y., Lu, P. J., Yen, C. Y. & Chang, J. Y. (2013) Dissecting the EGFR-PI3K-AKT pathway in oral cancer highlights the role of the EGFR variant III and its clinical relevance, *J Biomed Sci.* **20**, 43.
95. Chen, Y. & Chen, C. (2008) DNA copy number variation and loss of heterozygosity in relation to recurrence of and survival from head and neck squamous cell carcinoma: a review, *Head Neck.* **30**, 1361-83.
96. Rothenberg, S. M. & Ellisen, L. W. (2012) The molecular pathogenesis of head and neck squamous cell carcinoma, *J Clin Invest.* **122**, 1951-7.
97. Tokheim, C. J., Papadopoulos, N., Kinzler, K. W., Vogelstein, B. & Karchin, R. (2016) Evaluating the evaluation of cancer driver genes, *Proc Natl Acad Sci U S A.* **113**, 14330-14335.

98. Vogelstein, B., Papadopoulos, N., Velculescu, V. E., Zhou, S., Diaz, L. A., Jr. & Kinzler, K. W. (2013) Cancer genome landscapes, *Science*. **339**, 1546-58.
99. Petti, S. (2003) Pooled estimate of world leukoplakia prevalence: a systematic review, *Oral Oncol.* **39**, 770-80.
100. Tabor, M. P., Braakhuis, B. J., van der Wal, J. E., van Diest, P. J., Leemans, C. R., Brakenhoff, R. H. & Kummer, J. A. (2003) Comparative molecular and histological grading of epithelial dysplasia of the oral cavity and the oropharynx, *J Pathol.* **199**, 354-60.
101. Braakhuis, B. J., Tabor, M. P., Kummer, J. A., Leemans, C. R. & Brakenhoff, R. H. (2003) A genetic explanation of Slaughter's concept of field cancerization: evidence and clinical implications, *Cancer Res.* **63**, 1727-30.
102. Leemans, C. R., Braakhuis, B. J. & Brakenhoff, R. H. (2011) The molecular biology of head and neck cancer, *Nat Rev Cancer.* **11**, 9-22.
103. Califano, J., van der Riet, P., Westra, W., Nawroz, H., Clayman, G., Piantadosi, S., Corio, R., Lee, D., Greenberg, B., Koch, W. & Sidransky, D. (1996) Genetic progression model for head and neck cancer: implications for field cancerization, *Cancer Res.* **56**, 2488-92.
104. Slaughter, D. P., Southwick, H. W. & Smejkal, W. (1953) Field cancerization in oral stratified squamous epithelium; clinical implications of multicentric origin, *Cancer.* **6**, 963-8.
105. Tabor, M. P., Brakenhoff, R. H., van Houten, V. M., Kummer, J. A., Snel, M. H., Snijders, P. J., Snow, G. B., Leemans, C. R. & Braakhuis, B. J. (2001) Persistence of genetically altered fields in head and neck cancer patients: biological and clinical implications, *Clin Cancer Res.* **7**, 1523-32.
106. Hayat, M. J., Howlander, N., Reichman, M. E. & Edwards, B. K. (2007) Cancer statistics, trends, and multiple primary cancer analyses from the Surveillance, Epidemiology, and End Results (SEER) Program, *The oncologist.* **12**, 20-37.
107. Califano, J., vanderRiet, P., Westra, W., Nawroz, H., Clayman, G., Piantadosi, S., Corio, R., Lee, D., Greenberg, B., Koch, W. & Sidransky, D. (1996) Genetic progression model for head and neck cancer: Implications for field cancerization, *Cancer Research.* **56**, 2488-2492.
108. Beroukhi, R., Mermel, C. H., Porter, D., Wei, G., Raychaudhuri, S., Donovan, J., Barretina, J., Boehm, J. S., Dobson, J., Urashima, M., Mc Henry, K. T., Pinchback, R. M., Ligon, A. H., Cho, Y. J., Haery, L., Greulich, H., Reich, M., Winckler, W., Lawrence, M. S., Weir, B. A., Tanaka, K. E., Chiang, D. Y., Bass, A. J., Loo, A., Hoffman, C., Prensner, J., Liefeld, T., Gao, Q., Yecies, D., Signoretti, S., Maher, E., Kaye, F. J., Sasaki, H., Tepper, J. E., Fletcher, J. A., Taberner, J., Baselga, J., Tsao, M. S., Demicheli, F., Rubin, M. A., Janne, P. A., Daly, M. J., Nucera, C., Levine, R. L., Ebert, B. L., Gabriel, S., Rustgi, A. K., Antonescu, C. R., Ladanyi, M., Letai, A., Garraway, L. A., Loda, M., Beer, D. G., True, L. D., Okamoto, A., Pomeroy, S. L., Singer, S., Golub, T. R., Lander, E. S., Getz, G., Sellers, W. R. & Meyerson, M. (2010) The landscape of somatic copy-number alteration across human cancers, *Nature.* **463**, 899-905.
109. Taylor, B. S., Barretina, J., Socci, N. D., Decarolis, P., Ladanyi, M., Meyerson, M., Singer, S. & Sander, C. (2008) Functional copy-number alterations in cancer, *PLoS One.* **3**, e3179.
110. Zack, T. I., Schumacher, S. E., Carter, S. L., Cherniack, A. D., Saksena, G., Tabak, B., Lawrence, M. S., Zhsng, C. Z., Wala, J., Mermel, C. H., Sougnez, C., Gabriel, S. B., Hernandez, B., Shen, H., Laird, P. W., Getz, G., Meyerson, M. & Beroukhi, R. (2013) Pan-cancer patterns of somatic copy number alteration, *Nat Genet.* **45**, 1134-40.
111. Mermel, C. H., Schumacher, S. E., Hill, B., Meyerson, M. L., Beroukhi, R. & Getz, G. (2011) GISTIC2.0 facilitates sensitive and confident localization of the targets of focal somatic copy-number alteration in human cancers, *Genome Biol.* **12**, R41.
112. Harvard., B. I. o. M. a. (2015) Broad Institute TCGA Genome Data Analysis Center. (2015). SNP6 Copy number analysis (GISTIC2). .
113. Fields, A. P., Justilien, V. & Murray, N. R. (2016) The chromosome 3q26 OncCassette: A multigenic driver of human cancer, *Adv Biol Regul.* **60**, 47-63.
114. Qiu, W., Schonleben, F., Li, X., Ho, D. J., Close, L. G., Manolidis, S., Bennett, B. P. & Su, G. H. (2006) PIK3CA mutations in head and neck squamous cell carcinoma, *Clin Cancer Res.* **12**, 1441-6.
115. Rocco, J. W., Leong, C. O., Kuperwasser, N., DeYoung, M. P. & Ellisen, L. W. (2006) p63 mediates survival in squamous cell carcinoma by suppression of p73-dependent apoptosis, *Cancer Cell.* **9**, 45-56.

116. Lee, S. H., Oh, S. Y., Do, S. I., Lee, H. J., Kang, H. J., Rho, Y. S., Bae, W. J. & Lim, Y. C. (2014) SOX2 regulates self-renewal and tumorigenicity of stem-like cells of head and neck squamous cell carcinoma, *Br J Cancer*. **111**, 2122-30.
117. Hashimoto, Y., Oga, A., Kawachi, S., Furuya, T., Shimizu, N., Nakano, T., Imate, Y., Yamashita, H. & Sasaki, K. (2001) Amplification of 3q26 approximately qter correlates with tumor progression in head and neck squamous cell carcinomas, *Cancer Genet Cytogenet*. **129**, 52-6.
118. Singh, B., Stoffel, A., Gogineni, S., Poluri, A., Pfister, D. G., Shaha, A. R., Pathak, A., Bosl, G., Cordon-Cardo, C., Shah, J. P. & Rao, P. H. (2002) Amplification of the 3q26.3 locus is associated with progression to invasive cancer and is a negative prognostic factor in head and neck squamous cell carcinomas, *Am J Pathol*. **161**, 365-71.
119. Woenckhaus, J., Steger, K., Werner, E., Fenic, I., Gamedinger, U., Dreyer, T. & Stahl, U. (2002) Genomic gain of PIK3CA and increased expression of p110alpha are associated with progression of dysplasia into invasive squamous cell carcinoma, *J Pathol*. **198**, 335-42.
120. Lara, P. C., Bordon, E., Rey, A., Moreno, M., Lloret, M. & Henriquez-Hernandez, L. A. (2011) IGF-1R expression predicts clinical outcome in patients with locally advanced oral squamous cell carcinoma, *Oral Oncol*. **47**, 615-9.
121. Dale, O. T., Aleksic, T., Shah, K. A., Han, C., Mehanna, H., Rapozo, D. C., Sheard, J. D., Goodyear, P., Upile, N. S., Robinson, M., Jones, T. M., Winter, S. & Macaulay, V. M. (2015) IGF-1R expression is associated with HPV-negative status and adverse survival in head and neck squamous cell cancer, *Carcinogenesis*. **36**, 648-55.
122. Perisanidis, C., Wrba, F., Brandstetter, A., Kornek, G., Mitchell, D., Seemann, R., Selzer, E., Ewers, R. & Filipits, M. (2013) Impact of epidermal growth factor receptor, mesenchymal-epithelial transition factor, and insulin-like growth factor receptor 1 expression on survival of patients with oral and oropharyngeal cancer, *Br J Oral Maxillofac Surg*. **51**, 234-40.
123. Sun, J. M., Jun, H. J., Ko, Y. H., Park, Y. H., Ahn, Y. C., Son, Y. I., Baek, J. H., Park, K. & Ahn, M. J. (2011) Insulin-like growth factor binding protein-3, in association with IGF-1 receptor, can predict prognosis in squamous cell carcinoma of the head and neck, *Oral Oncol*. **47**, 714-9.
124. Carboni, J. M., Lee, A. V., Hadsell, D. L., Rowley, B. R., Lee, F. Y., Bol, D. K., Camuso, A. E., Gottardis, M., Greer, A. F., Ho, C. P., Hurlburt, W., Li, A., Saulnier, M., Velaparthy, U., Wang, C., Wen, M. L., Westhouse, R. A., Wittman, M., Zimmermann, K., Rupnow, B. A. & Wong, T. W. (2005) Tumor development by transgenic expression of a constitutively active insulin-like growth factor I receptor, *Cancer Res*. **65**, 3781-7.
125. Olivo-Marston, S. E., Hursting, S. D., Lavigne, J., Perkins, S. N., Maarouf, R. S., Yakar, S. & Harris, C. C. (2009) Genetic reduction of circulating insulin-like growth factor-1 inhibits azoxymethane-induced colon tumorigenesis in mice, *Mol Carcinog*. **48**, 1071-6.
126. Sutherland, B. W., Knoblauch, S. E., Kaplan-Lefko, P. J., Wang, F., Holzenberger, M. & Greenberg, N. M. (2008) Conditional deletion of insulin-like growth factor-I receptor in prostate epithelium, *Cancer Res*. **68**, 3495-504.
127. Favelyukis, S., Till, J. H., Hubbard, S. R. & Miller, W. T. (2001) Structure and autoregulation of the insulin-like growth factor 1 receptor kinase, *Nat Struct Biol*. **8**, 1058-63.
128. Ullrich, A., Gray, A., Tam, A. W., Yang-Feng, T., Tsubokawa, M., Collins, C., Henzel, W., Le Bon, T., Kathuria, S., Chen, E. & et al. (1986) Insulin-like growth factor I receptor primary structure: comparison with insulin receptor suggests structural determinants that define functional specificity, *EMBO J*. **5**, 2503-12.
129. Frattali, A. L., Treadway, J. L. & Pessin, J. E. (1992) Insulin/IGF-1 hybrid receptors: implications for the dominant-negative phenotype in syndromes of insulin resistance, *J Cell Biochem*. **48**, 43-50.
130. Le Roith, D. (2003) The insulin-like growth factor system, *Exp Diabetes Res*. **4**, 205-12.
131. Giovannone, B., Scaldaferri, M. L., Federici, M., Porzio, O., Lauro, D., Fusco, A., Sbraccia, P., Borboni, P., Lauro, R. & Sesti, G. (2000) Insulin receptor substrate (IRS) transduction system: distinct and overlapping signaling potential, *Diabetes Metab Res Rev*. **16**, 434-41.
132. Backer, J. M., Myers, M. G., Jr., Shoelson, S. E., Chin, D. J., Sun, X. J., Miralpeix, M., Hu, P., Margolis, B., Skolnik, E. Y., Schlessinger, J. & et al. (1992) Phosphatidylinositol 3'-kinase is activated by association with IRS-1 during insulin stimulation, *EMBO J*. **11**, 3469-79.

133. Alessi, D. R., Andjelkovic, M., Caudwell, B., Cron, P., Morrice, N., Cohen, P. & Hemmings, B. A. (1996) Mechanism of activation of protein kinase B by insulin and IGF-1, *EMBO J.* **15**, 6541-51.
134. Takada, T., Matozaki, T., Takeda, H., Fukunaga, K., Noguchi, T., Fujioka, Y., Okazaki, I., Tsuda, M., Yamao, T., Ochi, F. & Kasuga, M. (1998) Roles of the complex formation of SHPS-1 with SHP-2 in insulin-stimulated mitogen-activated protein kinase activation, *J Biol Chem.* **273**, 9234-42.
135. Inoki, K., Li, Y., Zhu, T., Wu, J. & Guan, K. L. (2002) TSC2 is phosphorylated and inhibited by Akt and suppresses mTOR signalling, *Nat Cell Biol.* **4**, 648-57.
136. Maehama, T. & Dixon, J. E. (1998) The tumor suppressor, PTEN/MMAC1, dephosphorylates the lipid second messenger, phosphatidylinositol 3,4,5-trisphosphate, *J Biol Chem.* **273**, 13375-8.
137. Poetsch, M., Lorenz, G. & Kleist, B. (2002) Detection of new PTEN/MMAC1 mutations in head and neck squamous cell carcinomas with loss of chromosome 10, *Cancer Genet Cytogenet.* **132**, 20-4.
138. Schmitz, S., Kaminsky-Forrett, M. C., Henry, S., Zanetta, S., Geoffrois, L., Bompas, E., Moxhon, A., Mignon, L., Guigay, J., Knoop, L., Hamoir, M. & Machiels, J. P. (2012) Phase II study of figitumumab in patients with recurrent and/or metastatic squamous cell carcinoma of the head and neck: clinical activity and molecular response (GORTEC 2008-02), *Ann Oncol.* **23**, 2153-61.
139. Reidy, D. L., Vakiani, E., Fakih, M. G., Saif, M. W., Hecht, J. R., Goodman-Davis, N., Hollywood, E., Shia, J., Schwartz, J., Chandrawansa, K., Dontabhaktuni, A., Youssoufian, H., Solit, D. B. & Saltz, L. B. (2010) Randomized, phase II study of the insulin-like growth factor-1 receptor inhibitor IMC-A12, with or without cetuximab, in patients with cetuximab- or panitumumab-refractory metastatic colorectal cancer, *J Clin Oncol.* **28**, 4240-6.
140. Ulanet, D. B., Ludwig, D. L., Kahn, C. R. & Hanahan, D. (2010) Insulin receptor functionally enhances multistage tumor progression and conveys intrinsic resistance to IGF-1R targeted therapy, *Proc Natl Acad Sci U S A.* **107**, 10791-8.
141. Thariat, J., Bensadoun, R. J., Etienne-Grimaldi, M. C., Grall, D., Penault-Llorca, F., Dassonville, O., Bertucci, F., Cayre, A., De Raucourt, D., Geoffrois, L., Finetti, P., Giraud, P., Racadot, S., Moriniere, S., Sudaka, A., Van Obberghen-Schilling, E. & Milano, G. (2012) Contrasted outcomes to gefitinib on tumoral IGF1R expression in head and neck cancer patients receiving postoperative chemoradiation (GORTEC trial 2004-02), *Clin Cancer Res.* **18**, 5123-33.
142. Weinstein, D., Sarfstein, R., Laron, Z. & Werner, H. (2014) Insulin receptor compensates for IGF1R inhibition and directly induces mitogenic activity in prostate cancer cells, *Endocr Connect.* **3**, 24-35.
143. Zhang, H., Fagan, D. H., Zeng, X., Freeman, K. T., Sachdev, D. & Yee, D. (2010) Inhibition of cancer cell proliferation and metastasis by insulin receptor downregulation, *Oncogene.* **29**, 2517-27.
144. Carboni, J. M., Wittman, M., Yang, Z., Lee, F., Greer, A., Hurlburt, W., Hillerman, S., Cao, C., Cantor, G. H., Dell-John, J., Chen, C., Discenza, L., Menard, K., Li, A., Trainor, G., Vyas, D., Kramer, R., Attar, R. M. & Gottardis, M. M. (2009) BMS-754807, a small molecule inhibitor of insulin-like growth factor-1R/IR, *Mol Cancer Ther.* **8**, 3341-9.
145. Hou, X., Huang, F., Macedo, L. F., Harrington, S. C., Reeves, K. A., Greer, A., Finckenstein, F. G., Brodie, A., Gottardis, M. M., Carboni, J. M. & Haluska, P. (2011) Dual IGF-1R/InsR inhibitor BMS-754807 synergizes with hormonal agents in treatment of estrogen-dependent breast cancer, *Cancer Res.* **71**, 7597-607.
146. Axelrod, M. J., Mendez, R. E., Khalil, A., Leimgruber, S. S., Sharlow, E. R., Capaldo, B., Conaway, M., Gioeli, D. G., Weber, M. J. & Jameson, M. J. (2015) Synergistic apoptosis in head and neck squamous cell carcinoma cells by co-inhibition of insulin-like growth factor-1 receptor signaling and compensatory signaling pathways, *Head Neck.* **37**, 1722-32.
147. Awasthi, N., Zhang, C., Ruan, W., Schwarz, M. A. & Schwarz, R. E. (2012) BMS-754807, a small-molecule inhibitor of insulin-like growth factor-1 receptor/insulin receptor, enhances gemcitabine response in pancreatic cancer, *Mol Cancer Ther.* **11**, 2644-53.
148. Huang, F., Greer, A., Hurlburt, W., Han, X., Hafezi, R., Wittenberg, G. M., Reeves, K., Chen, J., Robinson, D., Li, A., Lee, F. Y., Gottardis, M. M., Clark, E., Helman, L., Attar, R. M., Dongre, A. & Carboni, J. M. (2009) The mechanisms of differential sensitivity to an insulin-like growth factor-1

- receptor inhibitor (BMS-536924) and rationale for combining with EGFR/HER2 inhibitors, *Cancer Res.* **69**, 161-70.
149. Chakravarti, A., Loeffler, J. S. & Dyson, N. J. (2002) Insulin-like growth factor receptor I mediates resistance to anti-epidermal growth factor receptor therapy in primary human glioblastoma cells through continued activation of phosphoinositide 3-kinase signaling, *Cancer Res.* **62**, 200-7.
150. Barnes, C. J., Ohshiro, K., Rayala, S. K., El-Naggar, A. K. & Kumar, R. (2007) Insulin-like growth factor receptor as a therapeutic target in head and neck cancer, *Clin Cancer Res.* **13**, 4291-9.
151. Knowlden, J. M., Jones, H. E., Barrow, D., Gee, J. M., Nicholson, R. I. & Hutcheson, I. R. (2008) Insulin receptor substrate-1 involvement in epidermal growth factor receptor and insulin-like growth factor receptor signalling: implication for Gefitinib ('Iressa') response and resistance, *Breast Cancer Res Treat.* **111**, 79-91.
152. Raju, U., Molkenkine, D. P., Valdecanas, D. R., Deorukhkar, A., Mason, K. A., Buchholz, T. A., Meyn, R. E., Ang, K. K. & Skinner, H. (2015) Inhibition of EGFR or IGF-1R signaling enhances radiation response in head and neck cancer models but concurrent inhibition has no added benefit, *Cancer Med.* **4**, 65-74.
153. Matsumoto, F., Valdecanas, D. N., Mason, K. A., Milas, L., Ang, K. K. & Raju, U. (2012) The impact of timing of EGFR and IGF-1R inhibition for sensitizing head and neck cancer to radiation, *Anticancer Res.* **32**, 3029-35.
154. Yaniv, K. & Yisraeli, J. K. (2002) The involvement of a conserved family of RNA binding proteins in embryonic development and carcinogenesis, *Gene.* **287**, 49-54.
155. Bell, J. L., Wachter, K., Muhleck, B., Pazaitis, N., Kohn, M., Lederer, M. & Huttelmaier, S. (2013) Insulin-like growth factor 2 mRNA-binding proteins (IGF2BPs): post-transcriptional drivers of cancer progression?, *Cell Mol Life Sci.* **70**, 2657-75.
156. Hammer, N. A., Hansen, T., Byskov, A. G., Rajpert-De Meyts, E., Grondahl, M. L., Bredkjaer, H. E., Wewer, U. M., Christiansen, J. & Nielsen, F. C. (2005) Expression of IGF-II mRNA-binding proteins (IMPs) in gonads and testicular cancer, *Reproduction.* **130**, 203-12.
157. Le, H. T., Sorrell, A. M. & Siddle, K. (2012) Two isoforms of the mRNA binding protein IGF2BP2 are generated by alternative translational initiation, *PLoS One.* **7**, e33140.
158. Farina, K. L., Huttelmaier, S., Musunuru, K., Darnell, R. & Singer, R. H. (2003) Two ZBP1 KH domains facilitate beta-actin mRNA localization, granule formation, and cytoskeletal attachment, *J Cell Biol.* **160**, 77-87.
159. Nielsen, J., Kristensen, M. A., Willemoes, M., Nielsen, F. C. & Christiansen, J. (2004) Sequential dimerization of human zipcode-binding protein IMP1 on RNA: a cooperative mechanism providing RNP stability, *Nucleic Acids Res.* **32**, 4368-76.
160. Dreyfuss, G., Kim, V. N. & Kataoka, N. (2002) Messenger-RNA-binding proteins and the messages they carry, *Nat Rev Mol Cell Bio.* **3**, 195-205.
161. Miyazawa, J., Mitoro, A., Kawashiri, S., Chada, K. K. & Imai, K. (2004) Expression of mesenchyme-specific gene HMGA2 in squamous cell carcinomas of the oral cavity, *Cancer Res.* **64**, 2024-9.
162. Brants, J. R., Ayoubi, T. A., Chada, K., Marchal, K., Van de Ven, W. J. & Petit, M. M. (2004) Differential regulation of the insulin-like growth factor II mRNA-binding protein genes by architectural transcription factor HMGA2, *FEBS Lett.* **569**, 277-83.
163. Cleyne, I., Brants, J. R., Peeters, K., Deckers, R., Debiec-Rychter, M., Sciot, R., Van de Ven, W. J. & Petit, M. M. (2007) HMGA2 regulates transcription of the Imp2 gene via an intronic regulatory element in cooperation with nuclear factor-kappaB, *Mol Cancer Res.* **5**, 363-72.
164. Li, Z., Gilbert, J. A., Zhang, Y., Zhang, M., Qiu, Q., Ramanujan, K., Shavlakadze, T., Eash, J. K., Scaramozza, A., Goddeeris, M. M., Kirsch, D. G., Campbell, K. P., Brack, A. S. & Glass, D. J. (2012) An HMGA2-IGF2BP2 axis regulates myoblast proliferation and myogenesis, *Dev Cell.* **23**, 1176-88.
165. Summerer, I., Unger, K., Braselmann, H., Schuettrumpf, L., Maihoefer, C., Baumeister, P., Kirchner, T., Niyazi, M., Sage, E., Specht, H. M., Multhoff, G., Moertl, S., Belka, C. & Zitzelsberger, H. (2015) Circulating microRNAs as prognostic therapy biomarkers in head and neck cancer patients, *Br J Cancer.* **113**, 76-82.

166. Li, X., Li, Y. & Lu, H. (2017) miR-1193 Suppresses Proliferation and Invasion of Human Breast Cancer Cells Through Directly Targeting IGF2BP2, *Oncol Res.* **25**, 579-585.
167. Hui, A. B., Lenarduzzi, M., Krushel, T., Waldron, L., Pintilie, M., Shi, W., Perez-Ordóñez, B., Jurisica, I., O'Sullivan, B., Waldron, J., Gullane, P., Cummings, B. & Liu, F. F. (2010) Comprehensive MicroRNA profiling for head and neck squamous cell carcinomas, *Clin Cancer Res.* **16**, 1129-39.
168. Alajez, N. M., Shi, W., Wong, D., Lenarduzzi, M., Waldron, J., Weinreb, I. & Liu, F. F. (2012) Lin28b promotes head and neck cancer progression via modulation of the insulin-like growth factor survival pathway, *Oncotarget.* **3**, 1641-52.
169. Chien, C. S., Wang, M. L., Chu, P. Y., Chang, Y. L., Liu, W. H., Yu, C. C., Lan, Y. T., Huang, P. I., Lee, Y. Y., Chen, Y. W., Lo, W. L. & Chiou, S. H. (2015) Lin28B/Let-7 Regulates Expression of Oct4 and Sox2 and Reprograms Oral Squamous Cell Carcinoma Cells to a Stem-like State, *Cancer Res.* **75**, 2553-65.
170. Fu, T. Y., Hsieh, I. C., Cheng, J. T., Tsai, M. H., Hou, Y. Y., Lee, J. H., Liou, H. H., Huang, S. F., Chen, H. C., Yen, L. M., Tseng, H. H. & Ger, L. P. (2016) Association of OCT4, SOX2, and NANOG expression with oral squamous cell carcinoma progression, *J Oral Pathol Med.* **45**, 89-95.
171. Shrivastava, S., Steele, R., Sowadski, M., Crawford, S. E., Varvares, M. & Ray, R. B. (2015) Identification of molecular signature of head and neck cancer stem-like cells, *Sci Rep.* **5**, 7819.
172. Yu, C. C., Chen, Y. W., Chiou, G. Y., Tsai, L. L., Huang, P. I., Chang, C. Y., Tseng, L. M., Chiou, S. H., Yen, S. H., Chou, M. Y., Chu, P. Y. & Lo, W. L. (2011) MicroRNA let-7a represses chemoresistance and tumorigenicity in head and neck cancer via stem-like properties ablation, *Oral Oncol.* **47**, 202-10.
173. Degrauwe, N., Schlumpf, T. B., Janiszewska, M., Martin, P., Cauderay, A., Provero, P., Riggi, N., Suva, M. L., Paro, R. & Stamenkovic, I. (2016) The RNA Binding Protein IMP2 Preserves Glioblastoma Stem Cells by Preventing let-7 Target Gene Silencing, *Cell Rep.* **15**, 1634-47.
174. Lee, Y. S. & Dutta, A. (2007) The tumor suppressor microRNA let-7 represses the HMGA2 oncogene, *Genes Dev.* **21**, 1025-30.
175. Hayes, T. F., Benaich, N., Goldie, S. J., Sipila, K., Ames-Draycott, A., Cai, W. J., Yin, G. L. & Watt, F. M. (2016) Integrative genomic and functional analysis of human oral squamous cell carcinoma cell lines reveals synergistic effects of FAT1 and CASP8 inactivation, *Cancer Lett.* **383**, 106-114.
176. Barghash, A., Golob-Schwarzl, N., Helms, V., Haybaeck, J. & Kessler, S. M. (2016) Elevated expression of the IGF2 mRNA binding protein 2 (IGF2BP2/IMP2) is linked to short survival and metastasis in esophageal adenocarcinoma, *Oncotarget.* **7**, 49743-49750.
177. Mu, Q., Wang, L., Yu, F., Gao, H., Lei, T., Li, P., Liu, P., Zheng, X., Hu, X., Chen, Y., Jiang, Z., Sayari, A. J., Shen, J. & Huang, H. (2015) Imp2 regulates GBM progression by activating IGF2/PI3K/Akt pathway, *Cancer Biol Ther.* **16**, 623-33.
178. Cook, K. B., Kazan, H., Zuberi, K., Morris, Q. & Hughes, T. R. (2011) RBPDB: a database of RNA-binding specificities, *Nucleic Acids Res.* **39**, D301-8.
179. Janiszewska, M., Suva, M. L., Riggi, N., Houtkooper, R. H., Auwerx, J., Clement-Schatlo, V., Radovanovic, I., Rheinbay, E., Provero, P. & Stamenkovic, I. (2012) Imp2 controls oxidative phosphorylation and is crucial for preserving glioblastoma cancer stem cells, *Genes Dev.* **26**, 1926-44.
180. Dai, N., Rapley, J., Angel, M., Yanik, M. F., Blower, M. D. & Avruch, J. (2011) mTOR phosphorylates IMP2 to promote IGF2 mRNA translation by internal ribosomal entry, *Genes Dev.* **25**, 1159-72.
181. DeChiara, T. M., Efstratiadis, A. & Robertson, E. J. (1990) A growth-deficiency phenotype in heterozygous mice carrying an insulin-like growth factor II gene disrupted by targeting, *Nature.* **345**, 78-80.
182. Engstrom, W., Shokrai, A., Otte, K., Granerus, M., Gessbo, A., Bierke, P., Madej, A., Sjolund, M. & Ward, A. (1998) Transcriptional regulation and biological significance of the insulin like growth factor II gene, *Cell Prolif.* **31**, 173-89.
183. Liu, L., Greenberg, S., Russell, S. M. & Nicoll, C. S. (1989) Effects of insulin-like growth factors I and II on growth and differentiation of transplanted rat embryos and fetal tissues, *Endocrinology.* **124**, 3077-82.

184. Anisimov, V. N. & Bartke, A. (2013) The key role of growth hormone-insulin-IGF-1 signaling in aging and cancer, *Crit Rev Oncol Hematol.* **87**, 201-23.
185. Frasca, F., Pandini, G., Scalia, P., Sciacca, L., Mineo, R., Costantino, A., Goldfine, I. D., Belfiore, A. & Vigneri, R. (1999) Insulin receptor isoform A, a newly recognized, high-affinity insulin-like growth factor II receptor in fetal and cancer cells, *Mol Cell Biol.* **19**, 3278-88.
186. Pandini, G., Frasca, F., Mineo, R., Sciacca, L., Vigneri, R. & Belfiore, A. (2002) Insulin/insulin-like growth factor I hybrid receptors have different biological characteristics depending on the insulin receptor isoform involved, *J Biol Chem.* **277**, 39684-95.
187. Oka, Y., Rozek, L. M. & Czech, M. P. (1985) Direct demonstration of rapid insulin-like growth factor II Receptor internalization and recycling in rat adipocytes. Insulin stimulates 125I-insulin-like growth factor II degradation by modulating the IGF-II receptor recycling process, *J Biol Chem.* **260**, 9435-42.
188. Kornfeld, S. (1992) Structure and function of the mannose 6-phosphate/insulinlike growth factor II receptors, *Annu Rev Biochem.* **61**, 307-30.
189. O'Gorman, D. B., Weiss, J., Hettiaratchi, A., Firth, S. M. & Scott, C. D. (2002) Insulin-like growth factor-II/mannose 6-phosphate receptor overexpression reduces growth of choriocarcinoma cells in vitro and in vivo, *Endocrinology.* **143**, 4287-94.
190. Baxter, R. C. (1993) Circulating binding proteins for the insulinlike growth factors, *Trends Endocrinol Metab.* **4**, 91-6.
191. Rajaram, S., Baylink, D. J. & Mohan, S. (1997) Insulin-like growth factor-binding proteins in serum and other biological fluids: regulation and functions, *Endocr Rev.* **18**, 801-31.
192. Juul, A., Dalgaard, P., Blum, W. F., Bang, P., Hall, K., Michaelsen, K. F., Muller, J. & Skakkebaek, N. E. (1995) Serum levels of insulin-like growth factor (IGF)-binding protein-3 (IGFBP-3) in healthy infants, children, and adolescents: the relation to IGF-I, IGF-II, IGFBP-1, IGFBP-2, age, sex, body mass index, and pubertal maturation, *J Clin Endocrinol Metab.* **80**, 2534-42.
193. Twigg, S. M. & Baxter, R. C. (1998) Insulin-like growth factor (IGF)-binding protein 5 forms an alternative ternary complex with IGFs and the acid-labile subunit, *J Biol Chem.* **273**, 6074-9.
194. Baxter, R. C. (2014) IGF binding proteins in cancer: mechanistic and clinical insights, *Nat Rev Cancer.* **14**, 329-41.
195. Dimitriadis, E., Trangas, T., Milatos, S., Foukas, P. G., Gioulbasanis, I., Courtis, N., Nielsen, F. C., Pandis, N., Dafni, U., Bardi, G. & Ioannidis, P. (2007) Expression of oncofetal RNA-binding protein CRD-BP/IMP1 predicts clinical outcome in colon cancer, *Int J Cancer.* **121**, 486-94.
196. Kobel, M., Weidensdorfer, D., Reinke, C., Lederer, M., Schmitt, W. D., Zeng, K., Thomssen, C., Hauptmann, S. & Huttelmaier, S. (2007) Expression of the RNA-binding protein IMP1 correlates with poor prognosis in ovarian carcinoma, *Oncogene.* **26**, 7584-9.
197. Liao, B., Hu, Y., Herrick, D. J. & Brewer, G. (2005) The RNA-binding protein IMP-3 is a translational activator of insulin-like growth factor II leader-3 mRNA during proliferation of human K562 leukemia cells, *J Biol Chem.* **280**, 18517-24.
198. Christiansen, J., Kolte, A. M., Hansen, T. & Nielsen, F. C. (2009) IGF2 mRNA-binding protein 2: biological function and putative role in type 2 diabetes, *J Mol Endocrinol.* **43**, 187-95.
199. Diabetes Genetics Initiative of Broad Institute of, H., Mit, L. U., Novartis Institutes of BioMedical, R., Saxena, R., Voight, B. F., Lyssenko, V., Burt, N. P., de Bakker, P. I., Chen, H., Roix, J. J., Kathiresan, S., Hirschhorn, J. N., Daly, M. J., Hughes, T. E., Groop, L., Altshuler, D., Almgren, P., Florez, J. C., Meyer, J., Ardlie, K., Bengtsson Bostrom, K., Isomaa, B., Lettre, G., Lindblad, U., Lyon, H. N., Melander, O., Newton-Cheh, C., Nilsson, P., Orho-Melander, M., Rastam, L., Speliotes, E. K., Taskinen, M. R., Tuomi, T., Guiducci, C., Berglund, A., Carlson, J., Gianniny, L., Hackett, R., Hall, L., Holmkvist, J., Laurila, E., Sjogren, M., Sterner, M., Surti, A., Svensson, M., Svensson, M., Tewhey, R., Blumenstiel, B., Parkin, M., Defelice, M., Barry, R., Brodeur, W., Camarata, J., Chia, N., Fava, M., Gibbons, J., Handsaker, B., Healy, C., Nguyen, K., Gates, C., Sougnez, C., Gage, D., Nizzari, M., Gabriel, S. B., Chirn, G. W., Ma, Q., Parikh, H., Richardson, D., Ricke, D. & Purcell, S. (2007) Genome-wide association analysis identifies loci for type 2 diabetes and triglyceride levels, *Science.* **316**, 1331-6.
200. Boudoukha, S., Cuvellier, S. & Polesskaya, A. (2010) Role of the RNA-binding protein IMP-2 in muscle cell motility, *Mol Cell Biol.* **30**, 5710-25.

201. Zhang, J. Y., Chan, E. K., Peng, X. X. & Tan, E. M. (1999) A novel cytoplasmic protein with RNA-binding motifs is an autoantigen in human hepatocellular carcinoma, *J Exp Med.* **189**, 1101-10.
202. Zhou, S. L., Yue, W. B., Fan, Z. M., Du, F., Liu, B. C., Li, B., Han, X. N., Ku, J. W., Zhao, X. K., Zhang, P., Cui, J., Zhou, F. Y., Zhang, L. Q., Fan, X. P., Zhou, Y. F., Zhu, L. L., Liu, H. Y. & Wang, L. D. (2014) Autoantibody detection to tumor-associated antigens of P53, IMP1, P16, cyclin B1, P62, C-myc, Survivin, and Koc for the screening of high-risk subjects and early detection of esophageal squamous cell carcinoma, *Dis Esophagus.* **27**, 790-7.
203. Liu, W., Li, Y., Wang, B., Dai, L., Qian, W. & Zhang, J. Y. (2015) Autoimmune Response to IGF2 mRNA-Binding Protein 2 (IMP2/p62) in Breast Cancer, *Scand J Immunol.* **81**, 502-7.
204. Chong, H., Vikis, H. G. & Guan, K. L. (2003) Mechanisms of regulating the Raf kinase family, *Cell Signal.* **15**, 463-9.
205. Dhillon, A. S., Hagan, S., Rath, O. & Kolch, W. (2007) MAP kinase signalling pathways in cancer, *Oncogene.* **26**, 3279-90.
206. Tso, C. L., Shintaku, P., Chen, J., Liu, Q., Liu, J., Chen, Z., Yoshimoto, K., Mischel, P. S., Cloughesy, T. F., Liau, L. M. & Nelson, S. F. (2006) Primary glioblastomas express mesenchymal stem-like properties, *Mol Cancer Res.* **4**, 607-19.
207. Suvasini, R., Shruti, B., Thota, B., Shinde, S. V., Friedmann-Morvinski, D., Nawaz, Z., Prasanna, K. V., Thennarasu, K., Hegde, A. S., Arivazhagan, A., Chandramouli, B. A., Santosh, V. & Somasundaram, K. (2011) Insulin growth factor-2 binding protein 3 (IGF2BP3) is a glioblastoma-specific marker that activates phosphatidylinositol 3-kinase/mitogen-activated protein kinase (PI3K/MAPK) pathways by modulating IGF-2, *J Biol Chem.* **286**, 25882-90.
208. Sanchez-Alvarez, R., Martinez-Outschoorn, U. E., Lamb, R., Hulit, J., Howell, A., Gandara, R., Sartini, M., Rubin, E., Lisanti, M. P. & Sotgia, F. (2013) Mitochondrial dysfunction in breast cancer cells prevents tumor growth: understanding chemoprevention with metformin, *Cell Cycle.* **12**, 172-82.
209. Dai, N., Zhao, L., Wrighting, D., Kramer, D., Majithia, A., Wang, Y., Cracan, V., Borges-Rivera, D., Mootha, V. K., Nahrendorf, M., Thorburn, D. R., Minichiello, L., Altshuler, D. & Avruch, J. (2015) IGF2BP2/IMP2-Deficient mice resist obesity through enhanced translation of Ucp1 mRNA and Other mRNAs encoding mitochondrial proteins, *Cell Metab.* **21**, 609-21.
210. Thiery, J. P. & Sleeman, J. P. (2006) Complex networks orchestrate epithelial-mesenchymal transitions, *Nat Rev Mol Cell Biol.* **7**, 131-42.
211. Batlle, E., Sancho, E., Franci, C., Dominguez, D., Monfar, M., Baulida, J. & Garcia De Herreros, A. (2000) The transcription factor snail is a repressor of E-cadherin gene expression in epithelial tumour cells, *Nat Cell Biol.* **2**, 84-9.
212. Bolos, V., Peinado, H., Perez-Moreno, M. A., Fraga, M. F., Esteller, M. & Cano, A. (2003) The transcription factor Slug represses E-cadherin expression and induces epithelial to mesenchymal transitions: a comparison with Snail and E47 repressors, *J Cell Sci.* **116**, 499-511.
213. Lien, H. C., Hsiao, Y. H., Lin, Y. S., Yao, Y. T., Juan, H. F., Kuo, W. H., Hung, M. C., Chang, K. J. & Hsieh, F. J. (2007) Molecular signatures of metaplastic carcinoma of the breast by large-scale transcriptional profiling: identification of genes potentially related to epithelial-mesenchymal transition, *Oncogene.* **26**, 7859-71.
214. Morishita, A., Zaidi, M. R., Mitoro, A., Sankarasharma, D., Szabolcs, M., Okada, Y., D'Armiento, J. & Chada, K. (2013) HMGA2 is a driver of tumor metastasis, *Cancer Res.* **73**, 4289-99.
215. Thuault, S., Tan, E. J., Peinado, H., Cano, A., Heldin, C. H. & Moustakas, A. (2008) HMGA2 and Smads co-regulate SNAIL1 expression during induction of epithelial-to-mesenchymal transition, *J Biol Chem.* **283**, 33437-46.
216. Zhao, X. P., Zhang, H., Jiao, J. Y., Tang, D. X., Wu, Y. L. & Pan, C. B. (2016) Overexpression of HMGA2 promotes tongue cancer metastasis through EMT pathway, *J Transl Med.* **14**, 26.
217. Bussink, J., Kaanders, J. H. & van der Kogel, A. J. (2003) Tumor hypoxia at the micro-regional level: clinical relevance and predictive value of exogenous and endogenous hypoxic cell markers, *Radiother Oncol.* **67**, 3-15.

218. Vaupel, P., Kallinowski, F. & Okunieff, P. (1989) Blood flow, oxygen and nutrient supply, and metabolic microenvironment of human tumors: a review, *Cancer research*. **49**, 6449-65.
219. Adam, M. F., Gabalski, E. C., Bloch, D. A., Oehlert, J. W., Brown, J. M., Elsaid, A. A., Pinto, H. A. & Terris, D. J. (1999) Tissue oxygen distribution in head and neck cancer patients, *Head Neck*. **21**, 146-53.
220. Winter, S. C., Buffa, F. M., Silva, P., Miller, C., Valentine, H. R., Turley, H., Shah, K. A., Cox, G. J., Corbridge, R. J., Homer, J. J., Musgrove, B., Slevin, N., Sloan, P., Price, P., West, C. M. & Harris, A. L. (2007) Relation of a hypoxia metagene derived from head and neck cancer to prognosis of multiple cancers, *Cancer research*. **67**, 3441-9.
221. Dunst, J., Stadler, P., Becker, A., Lautenschlager, C., Pelz, T., Hansgen, G., Molls, M. & Kuhnt, T. (2003) Tumor volume and tumor hypoxia in head and neck cancers. The amount of the hypoxic volume is important, *Strahlenther Onkol*. **179**, 521-6.
222. Nordsmark, M., Bentzen, S. M. & Overgaard, J. (1994) Measurement of human tumour oxygenation status by a polarographic needle electrode. An analysis of inter- and intratumour heterogeneity, *Acta Oncol*. **33**, 383-9.
223. McKeown, S. R. (2014) Defining normoxia, physoxia and hypoxia in tumours-implications for treatment response, *Br J Radiol*. **87**, 20130676.
224. Tredan, O., Galmarini, C. M., Patel, K. & Tannock, I. F. (2007) Drug resistance and the solid tumor microenvironment, *J Natl Cancer Inst*. **99**, 1441-54.
225. Graeber, T. G., Osmanian, C., Jacks, T., Housman, D. E., Koch, C. J., Lowe, S. W. & Giaccia, A. J. (1996) Hypoxia-mediated selection of cells with diminished apoptotic potential in solid tumours, *Nature*. **379**, 88-91.
226. Dachs, G. U. & Chaplin, D. J. (1998) Microenvironmental control of gene expression: implications for tumor angiogenesis, progression, and metastasis, *Semin Radiat Oncol*. **8**, 208-16.
227. Denko, N. C., Fontana, L. A., Hudson, K. M., Sutphin, P. D., Raychaudhuri, S., Altman, R. & Giaccia, A. J. (2003) Investigating hypoxic tumor physiology through gene expression patterns, *Oncogene*. **22**, 5907-5914.
228. Semenza, G. L. (1998) Hypoxia-inducible factor 1: master regulator of O₂ homeostasis, *Curr Opin Genet Dev*. **8**, 588-94.
229. Ivan, M., Kondo, K., Yang, H., Kim, W., Valiando, J., Ohh, M., Salic, A., Asara, J. M., Lane, W. S. & Kaelin, W. G., Jr. (2001) HIF α targeted for VHL-mediated destruction by proline hydroxylation: implications for O₂ sensing, *Science*. **292**, 464-8.
230. Jaakkola, P., Mole, D. R., Tian, Y. M., Wilson, M. I., Gielbert, J., Gaskell, S. J., von Kriegsheim, A., Hebestreit, H. F., Mukherji, M., Schofield, C. J., Maxwell, P. H., Pugh, C. W. & Ratcliffe, P. J. (2001) Targeting of HIF- α to the von Hippel-Lindau ubiquitylation complex by O₂-regulated prolyl hydroxylation, *Science*. **292**, 468-72.
231. Zundel, W., Schindler, C., Haas-Kogan, D., Koong, A., Kaper, F., Chen, E., Gottschalk, A. R., Ryan, H. E., Johnson, R. S., Jefferson, A. B., Stokoe, D. & Giaccia, A. J. (2000) Loss of PTEN facilitates HIF-1-mediated gene expression, *Genes Dev*. **14**, 391-6.
232. Yu, T., Tang, B. & Sun, X. (2017) Development of Inhibitors Targeting Hypoxia-Inducible Factor 1 and 2 for Cancer Therapy, *Yonsei Med J*. **58**, 489-496.
233. Denko, N. C. (2008) Hypoxia, HIF1 and glucose metabolism in the solid tumour, *Nature Reviews Cancer*. **8**, 705-713.
234. Hockel, M. & Vaupel, P. (2001) Tumor hypoxia: Definitions and current clinical, biologic, and molecular aspects, *J Natl Cancer I*. **93**, 266-276.
235. Warburg, O. (1956) On respiratory impairment in cancer cells, *Science*. **124**, 269-70.
236. Gatenby, R. A. & Gillies, R. J. (2004) Why do cancers have high aerobic glycolysis?, *Nature Reviews Cancer*. **4**, 891-899.
237. Powis, G. & Kirkpatrick, L. (2004) Hypoxia inducible factor-1 α as a cancer drug target, *Molecular cancer therapeutics*. **3**, 647-54.
238. Gatenby, R. A. & Vincent, T. L. (2003) An evolutionary model of carcinogenesis, *Cancer Research*. **63**, 6212-6220.

239. Martinez-Zaguilan, R., Lynch, R. M., Martinez, G. M. & Gillies, R. J. (1993) Vacuolar-type H(+)-ATPases are functionally expressed in plasma membranes of human tumor cells, *Am J Physiol.* **265**, C1015-29.
240. Harshani, J. M., Yeluri, S. & Guttikonda, V. R. (2014) Glut-1 as a prognostic biomarker in oral squamous cell carcinoma, *J Oral Maxillofac Pathol.* **18**, 372-8.
241. Estrella, V., Chen, T., Lloyd, M., Wojtkowiak, J., Cornell, H. H., Ibrahim-Hashim, A., Bailey, K., Balagurunathan, Y., Rothberg, J. M., Sloane, B. F., Johnson, J., Gatenby, R. A. & Gillies, R. J. (2013) Acidity generated by the tumor microenvironment drives local invasion, *Cancer Res.* **73**, 1524-35.
242. Colegio, O. R., Chu, N. Q., Szabo, A. L., Chu, T., Rhebergen, A. M., Jairam, V., Cyrus, N., Brokowski, C. E., Eisenbarth, S. C., Phillips, G. M., Cline, G. W., Phillips, A. J. & Medzhitov, R. (2014) Functional polarization of tumour-associated macrophages by tumour-derived lactic acid, *Nature.* **513**, 559-63.
243. Winter, S. C., Buffa, F. M., Silva, P., Miller, C., Valentine, H. R., Turley, H., Shah, K. A., Cox, G. J., Corbridge, R. J., Homer, J. J., Musgrove, B., Slevin, N., Sloan, P., Price, P., West, C. M. & Harris, A. L. (2007) Relation of a hypoxia metagene derived from head and neck cancer to prognosis of multiple cancers, *Cancer Res.* **67**, 3441-9.
244. Toustrup, K., Sorensen, B. S., Nordmark, M., Busk, M., Wiuf, C., Alsner, J. & Overgaard, J. (2011) Development of a hypoxia gene expression classifier with predictive impact for hypoxic modification of radiotherapy in head and neck cancer, *Cancer Res.* **71**, 5923-31.
245. Sorensen, B. S., Toustrup, K., Horsman, M. R., Overgaard, J. & Alsner, J. (2010) Identifying pH independent hypoxia induced genes in human squamous cell carcinomas in vitro, *Acta Oncol.* **49**, 895-905.
246. Lessa, R. C., Campos, A. H., Freitas, C. E., Silva, F. R., Kowalski, L. P., Carvalho, A. L. & Vettore, A. L. (2013) Identification of upregulated genes in oral squamous cell carcinomas, *Head Neck.* **35**, 1475-81.
247. Li, S., Yang, X., Wang, P. & Ran, X. (2013) The effects of GLUT1 on the survival of head and neck squamous cell carcinoma, *Cell Physiol Biochem.* **32**, 624-34.
248. Wang, Y. D., Li, S. J. & Liao, J. X. (2013) Inhibition of glucose transporter 1 (GLUT1) chemosensitized head and neck cancer cells to cisplatin, *Technol Cancer Res Treat.* **12**, 525-35.
249. Nakajima, E. C., Laymon, C., Oborski, M., Hou, W. Z., Wang, L., Grandis, J. R., Ferris, R. L., Mountz, J. M. & Van Houten, B. (2014) Quantifying Metabolic Heterogeneity in Head and Neck Tumors in Real Time: 2-DG Uptake Is Highest in Hypoxic Tumor Regions, *Plos One.* **9**.
250. Nordmark, M., Bentzen, S. M., Rudat, V., Brizel, D., Lartigau, E., Stadler, P., Becker, A., Adam, M., Molls, M., Dunst, J., Terriis, D. J. & Overgaard, J. (2005) Prognostic value of tumor oxygenation in 397 head and neck tumors after primary radiation therapy. An international multi-center study, *Radiotherapy and Oncology.* **77**, 18-24.
251. Pignon, J. P., le Maitre, A. & Bourhis, J. (2007) Meta-Analyses of Chemotherapy in Head and Neck Cancer (MACH-NC): an update, *Int J Radiat Oncol Biol Phys.* **69**, S112-4.
252. Vermorken, J. B. & Specenier, P. (2010) Optimal treatment for recurrent/metastatic head and neck cancer, *Annals of oncology : official journal of the European Society for Medical Oncology / ESMO.* **21 Suppl 7**, vii252-61.
253. Overgaard, J. (2007) Hypoxic radiosensitization: adored and ignored, *Journal of clinical oncology : official journal of the American Society of Clinical Oncology.* **25**, 4066-74.
254. Bristow, R. G. & Hill, R. P. (2008) Hypoxia and metabolism. Hypoxia, DNA repair and genetic instability, *Nature reviews Cancer.* **8**, 180-92.
255. Chan, D. A. & Giaccia, A. J. (2007) Hypoxia, gene expression, and metastasis, *Cancer Metastasis Rev.* **26**, 333-9.
256. Harris, A. L. (2002) Hypoxia--a key regulatory factor in tumour growth, *Nature reviews Cancer.* **2**, 38-47.
257. Wardman, P. (2007) Chemical radiosensitizers for use in radiotherapy, *Clin Oncol (R Coll Radiol).* **19**, 397-417.
258. Kaanders, J. H., Pop, L. A., Marres, H. A., Bruaset, I., van den Hoogen, F. J., Merks, M. A. & van der Kogel, A. J. (2002) ARCON: experience in 215 patients with advanced head-and-neck cancer, *Int J Radiat Oncol Biol Phys.* **52**, 769-78.

259. Brown, J. M. (1984) Clinical trials of radiosensitizers: what should we expect?, *Int J Radiat Oncol Biol Phys.* **10**, 425-9.
260. Overgaard, J. (1994) Clinical evaluation of nitroimidazoles as modifiers of hypoxia in solid tumors, *Oncology research.* **6**, 509-18.
261. Durand, R. E. (1994) The influence of microenvironmental factors during cancer therapy, *In Vivo.* **8**, 691-702.
262. Teicher, B. A., Lazo, J. S. & Sartorelli, A. C. (1981) Classification of antineoplastic agents by their selective toxicities toward oxygenated and hypoxic tumor cells, *Cancer research.* **41**, 73-81.
263. Yoshida, S., Ito, D., Nagumo, T., Shiota, T., Hatori, M. & Shintani, S. (2009) Hypoxia induces resistance to 5-fluorouracil in oral cancer cells via G(1) phase cell cycle arrest, *Oral oncology.* **45**, 109-15.
264. Shimanishi, M., Ogi, K., Sogabe, Y., Kaneko, T., Dehari, H., Miyazaki, A. & Hiratsuka, H. (2013) Silencing of GLUT-1 inhibits sensitization of oral cancer cells to cisplatin during hypoxia, *Journal of oral pathology & medicine : official publication of the International Association of Oral Pathologists and the American Academy of Oral Pathology.* **42**, 382-8.
265. Rohwer, N. & Cramer, T. (2011) Hypoxia-mediated drug resistance: novel insights on the functional interaction of HIFs and cell death pathways, *Drug Resist Updat.* **14**, 191-201.
266. Brown, J. M. & Wilson, W. R. (2004) Exploiting tumour hypoxia in cancer treatment, *Nature reviews Cancer.* **4**, 437-47.
267. DeBerardinis, R. J., Lum, J. J., Hatzivassiliou, G. & Thompson, C. B. (2008) The biology of cancer: metabolic reprogramming fuels cell growth and proliferation, *Cell Metab.* **7**, 11-20.
268. Benjamin, D. I., Cozzo, A., Ji, X., Roberts, L. S., Louie, S. M., Mulvihill, M. M., Luo, K. & Nomura, D. K. (2013) Ether lipid generating enzyme AGPS alters the balance of structural and signaling lipids to fuel cancer pathogenicity, *Proc Natl Acad Sci U S A.* **110**, 14912-7.
269. Kroemer, G. & Pouyssegur, J. (2008) Tumor cell metabolism: cancer's Achilles' heel, *Cancer cell.* **13**, 472-82.
270. DeBerardinis, R. J., Mancuso, A., Daikhin, E., Nissim, I., Yudkoff, M., Wehrli, S. & Thompson, C. B. (2007) Beyond aerobic glycolysis: transformed cells can engage in glutamine metabolism that exceeds the requirement for protein and nucleotide synthesis, *Proceedings of the National Academy of Sciences of the United States of America.* **104**, 19345-50.
271. Menendez, J. A. & Lupu, R. (2007) Fatty acid synthase and the lipogenic phenotype in cancer pathogenesis, *Nature reviews Cancer.* **7**, 763-77.
272. Menendez, J. A. & Lupu, R. (2007) Fatty acid synthase and the lipogenic phenotype in cancer pathogenesis, *Nat Rev Cancer.* **7**, 763-77.
273. Rohrig, F. & Schulze, A. (2016) The multifaceted roles of fatty acid synthesis in cancer, *Nat Rev Cancer.* **16**, 732-749.
274. Goldstein, J. L., DeBose-Boyd, R. A. & Brown, M. S. (2006) Protein sensors for membrane sterols, *Cell.* **124**, 35-46.
275. Shao, W. & Espenshade, P. J. (2012) Expanding roles for SREBP in metabolism, *Cell Metab.* **16**, 414-9.
276. Jakobsson, A., Westerberg, R. & Jakobsson, A. (2006) Fatty acid elongases in mammals: their regulation and roles in metabolism, *Prog Lipid Res.* **45**, 237-49.
277. Watkins, P. A., Maignel, D., Jia, Z. & Pevsner, J. (2007) Evidence for 26 distinct acyl-coenzyme A synthetase genes in the human genome, *J Lipid Res.* **48**, 2736-50.
278. Enoch, H. G., Catala, A. & Strittmatter, P. (1976) Mechanism of rat liver microsomal stearyl-CoA desaturase. Studies of the substrate specificity, enzyme-substrate interactions, and the function of lipid, *J Biol Chem.* **251**, 5095-103.
279. Li, J., Ding, S. F., Habib, N. A., Fermor, B. F., Wood, C. B. & Gilmour, R. S. (1994) Partial characterization of a cDNA for human stearyl-CoA desaturase and changes in its mRNA expression in some normal and malignant tissues, *Int J Cancer.* **57**, 348-52.
280. Bauer, D. E., Hatzivassiliou, G., Zhao, F., Andreadis, C. & Thompson, C. B. (2005) ATP citrate lyase is an important component of cell growth and transformation, *Oncogene.* **24**, 6314-22.

281. Hatzivassiliou, G., Zhao, F., Bauer, D. E., Andreadis, C., Shaw, A. N., Dhanak, D., Hingorani, S. R., Tuveson, D. A. & Thompson, C. B. (2005) ATP citrate lyase inhibition can suppress tumor cell growth, *Cancer Cell*. **8**, 311-21.
282. Brusselmans, K., De Schrijver, E., Verhoeven, G. & Swinnen, J. V. (2005) RNA interference-mediated silencing of the acetyl-CoA-carboxylase-alpha gene induces growth inhibition and apoptosis of prostate cancer cells, *Cancer Res*. **65**, 6719-25.
283. Chajes, V., Cambot, M., Moreau, K., Lenoir, G. M. & Joulin, V. (2006) Acetyl-CoA carboxylase alpha is essential to breast cancer cell survival, *Cancer Res*. **66**, 5287-94.
284. Jeon, S. M., Chandel, N. S. & Hay, N. (2012) AMPK regulates NADPH homeostasis to promote tumour cell survival during energy stress, *Nature*. **485**, 661-5.
285. Silva, S. D., Cunha, I. W., Younes, R. N., Soares, F. A., Kowalski, L. P. & Graner, E. (2010) ErbB receptors and fatty acid synthase expression in aggressive head and neck squamous cell carcinomas, *Oral Dis*. **16**, 774-80.
286. Bansal, N., Mims, J., Kuremsky, J. G., Olex, A. L., Zhao, W., Yin, L., Wani, R., Qian, J., Center, B., Marrs, G. S., Porosnicu, M., Fetrow, J. S., Tsang, A. W. & Furdui, C. M. (2014) Broad phenotypic changes associated with gain of radiation resistance in head and neck squamous cell cancer, *Antioxid Redox Signal*. **21**, 221-36.
287. Kuhajda, F. P., Jenner, K., Wood, F. D., Hennigar, R. A., Jacobs, L. B., Dick, J. D. & Pasternack, G. R. (1994) Fatty acid synthesis: a potential selective target for antineoplastic therapy, *Proc Natl Acad Sci U S A*. **91**, 6379-83.
288. Su, Y. W., Lin, Y. H., Pai, M. H., Lo, A. C., Lee, Y. C., Fang, I. C., Lin, J., Hsieh, R. K., Chang, Y. F. & Chen, C. L. (2014) Association between phosphorylated AMP-activated protein kinase and acetyl-CoA carboxylase expression and outcome in patients with squamous cell carcinoma of the head and neck, *PLoS One*. **9**, e96183.
289. Vazquez, M. J., Leavens, W., Liu, R., Rodriguez, B., Read, M., Richards, S., Winegar, D. & Dominguez, J. M. (2008) Discovery of GSK837149A, an inhibitor of human fatty acid synthase targeting the beta-ketoacyl reductase reaction, *FEBS J*. **275**, 1556-67.
290. Pizer, E. S., Thupari, J., Han, W. F., Pinn, M. L., Chrest, F. J., Frehywot, G. L., Townsend, C. A. & Kuhajda, F. P. (2000) Malonyl-coenzyme-A is a potential mediator of cytotoxicity induced by fatty-acid synthase inhibition in human breast cancer cells and xenografts, *Cancer Res*. **60**, 213-8.
291. Zhou, W., Simpson, P. J., McFadden, J. M., Townsend, C. A., Medghalchi, S. M., Vadlamudi, A., Pinn, M. L., Ronnett, G. V. & Kuhajda, F. P. (2003) Fatty acid synthase inhibition triggers apoptosis during S phase in human cancer cells, *Cancer Res*. **63**, 7330-7.
292. Mims, J., Bansal, N., Bharadwaj, M. S., Chen, X., Molina, A. J., Tsang, A. W. & Furdui, C. M. (2015) Energy metabolism in a matched model of radiation resistance for head and neck squamous cell cancer, *Radiat Res*. **183**, 291-304.
293. Loftus, T. M., Jaworsky, D. E., Frehywot, G. L., Townsend, C. A., Ronnett, G. V., Lane, M. D. & Kuhajda, F. P. (2000) Reduced food intake and body weight in mice treated with fatty acid synthase inhibitors, *Science*. **288**, 2379-81.
294. Shimokawa, T., Kumar, M. V. & Lane, M. D. (2002) Effect of a fatty acid synthase inhibitor on food intake and expression of hypothalamic neuropeptides, *Proc Natl Acad Sci U S A*. **99**, 66-71.
295. Roongta, U. V., Pabalan, J. G., Wang, X., Ryseck, R. P., Fagnoli, J., Henley, B. J., Yang, W. P., Zhu, J., Madireddi, M. T., Lawrence, R. M., Wong, T. W. & Rupnow, B. A. (2011) Cancer cell dependence on unsaturated fatty acids implicates stearoyl-CoA desaturase as a target for cancer therapy, *Mol Cancer Res*. **9**, 1551-61.
296. Chen, L., Ren, J., Yang, L., Li, Y., Fu, J., Li, Y., Tian, Y., Qiu, F., Liu, Z. & Qiu, Y. (2016) Stearoyl-CoA desaturase-1 mediated cell apoptosis in colorectal cancer by promoting ceramide synthesis, *Sci Rep*. **6**, 19665.
297. Ogretmen, B. & Hannun, Y. A. (2004) Biologically active sphingolipids in cancer pathogenesis and treatment, *Nat Rev Cancer*. **4**, 604-16.
298. Hannun, Y. A. (1996) Functions of ceramide in coordinating cellular responses to stress, *Science*. **274**, 1855-9.

299. Young, M. R., Neville, B. W., Chi, A. C., Lathers, D. M., Gillespie, M. B. & Day, T. A. (2007) Autocrine motility-stimulatory pathways of oral premalignant lesion cells, *Clin Exp Metastasis*. **24**, 131-9.
300. Karahatay, S., Thomas, K., Koybasi, S., Senkal, C. E., Elojeimy, S., Liu, X., Bielawski, J., Day, T. A., Gillespie, M. B., Sinha, D., Norris, J. S., Hannun, Y. A. & Ogretmen, B. (2007) Clinical relevance of ceramide metabolism in the pathogenesis of human head and neck squamous cell carcinoma (HNSCC): attenuation of C(18)-ceramide in HNSCC tumors correlates with lymphovascular invasion and nodal metastasis, *Cancer Lett*. **256**, 101-11.
301. Mehta, S., Blackinton, D., Omar, I., Kouttab, N., Myrick, D., Klostergaard, J. & Wanebo, H. (2000) Combined cytotoxic action of paclitaxel and ceramide against the human Tu138 head and neck squamous carcinoma cell line, *Cancer Chemother Pharmacol*. **46**, 85-92.
302. Separovic, D., Breen, P., Joseph, N., Bielawski, J., Pierce, J. S., E, V. A. N. B. & Gudz, T. I. (2012) siRNA-mediated down-regulation of ceramide synthase 1 leads to apoptotic resistance in human head and neck squamous carcinoma cells after photodynamic therapy, *Anticancer Res*. **32**, 2479-2485.
303. DeBerardinis, R. J., Lum, J. J., Hatzivassiliou, G. & Thompson, C. B. (2008) The biology of cancer: metabolic reprogramming fuels cell growth and proliferation, *Cell metabolism*. **7**, 11-20.
304. Yue, S., Li, J., Lee, S. Y., Lee, H. J., Shao, T., Song, B., Cheng, L., Masterson, T. A., Liu, X., Ratliff, T. L. & Cheng, J. X. (2014) Cholesteryl ester accumulation induced by PTEN loss and PI3K/AKT activation underlies human prostate cancer aggressiveness, *Cell Metab*. **19**, 393-406.
305. Accioly, M. T., Pacheco, P., Maya-Monteiro, C. M., Carrossini, N., Robbs, B. K., Oliveira, S. S., Kaufmann, C., Morgado-Diaz, J. A., Bozza, P. T. & Viola, J. P. (2008) Lipid bodies are reservoirs of cyclooxygenase-2 and sites of prostaglandin-E2 synthesis in colon cancer cells, *Cancer Res*. **68**, 1732-40.
306. Bozza, P. T. & Viola, J. P. (2010) Lipid droplets in inflammation and cancer, *Prostaglandins Leukot Essent Fatty Acids*. **82**, 243-50.
307. Abramczyk, H., Surmacki, J., Kopec, M., Olejnik, A. K., Lubecka-Pietruszewska, K. & Fabianowska-Majewska, K. (2015) The role of lipid droplets and adipocytes in cancer. Raman imaging of cell cultures: MCF10A, MCF7, and MDA-MB-231 compared to adipocytes in cancerous human breast tissue, *Analyst*. **140**, 2224-35.
308. Cases, S., Smith, S. J., Zheng, Y. W., Myers, H. M., Lear, S. R., Sande, E., Novak, S., Collins, C., Welch, C. B., Lusis, A. J., Erickson, S. K. & Farese, R. V., Jr. (1998) Identification of a gene encoding an acyl CoA:diacylglycerol acyltransferase, a key enzyme in triacylglycerol synthesis, *Proc Natl Acad Sci U S A*. **95**, 13018-23.
309. Shi, Y. & Cheng, D. (2009) Beyond triglyceride synthesis: the dynamic functional roles of MGAT and DGAT enzymes in energy metabolism, *Am J Physiol Endocrinol Metab*. **297**, E10-8.
310. Coleman, R. A. & Lee, D. P. (2004) Enzymes of triacylglycerol synthesis and their regulation, *Prog Lipid Res*. **43**, 134-76.
311. Zimmermann, R., Strauss, J. G., Haemmerle, G., Schoiswohl, G., Birner-Gruenberger, R., Riederer, M., Lass, A., Neuberger, G., Eisenhaber, F., Hermetter, A. & Zechner, R. (2004) Fat mobilization in adipose tissue is promoted by adipose triglyceride lipase, *Science*. **306**, 1383-1386.
312. Nomura, D. K., Long, J. Z., Niessen, S., Hoover, H. S., Ng, S. W. & Cravatt, B. F. (2010) Monoacylglycerol lipase regulates a fatty acid network that promotes cancer pathogenesis, *Cell*. **140**, 49-61.
313. Nomura, D. K., Lombardi, D. P., Chang, J. W., Niessen, S., Ward, A. M., Long, J. Z., Hoover, H. H. & Cravatt, B. F. (2011) Monoacylglycerol Lipase Exerts Dual Control over Endocannabinoid and Fatty Acid Pathways to Support Prostate Cancer, *Chem Biol*. **18**, 846-856.
314. Ye, L., Zhang, B., Seyiour, E. G., Tao, K. X., Liu, X. H., Ling, Y., Chen, J. Y. & Wang, G. B. (2011) Monoacylglycerol lipase (MAGL) knockdown inhibits tumor cells growth in colorectal cancer, *Cancer Lett*. **307**, 6-17.
315. Ma, M. Y., Bai, J., Ling, Y., Chang, W. L., Xie, G. C., Li, R. D., Wang, G. B. & Tao, K. X. (2016) Monoacylglycerol lipase inhibitor JZL184 regulates apoptosis and migration of colorectal cancer cells, *Mol Med Rep*. **13**, 2850-2856.

316. Pagano, E., Borrelli, F., Orlando, P., Romano, B., Monti, M., Morbidelli, L., Aviello, G., Imperatore, R., Capasso, R., Piscitelli, F., Buono, L., Di Marzo, V. & Izzo, A. A. (2017) Pharmacological inhibition of MAGL attenuates experimental colon carcinogenesis, *Pharmacol Res.* **119**, 227-236.
317. Zhang, J. Y., Liu, Z. J., Lian, Z. R., Liao, R., Chen, Y., Qin, Y., Wang, J. L., Jiang, Q., Wang, X. B. & Gong, J. P. (2016) Monoacylglycerol Lipase: A Novel Potential Therapeutic Target and Prognostic Indicator for Hepatocellular Carcinoma, *Sci Rep-Uk.* **6**.
318. Hu, W. R., Lian, Y. F., Peng, L. X., Lei, J. J., Deng, C. C., Xu, M., Feng, Q. S., Chen, L. Z., Bei, J. X. & Zeng, Y. X. (2014) Monoacylglycerol lipase promotes metastases in nasopharyngeal carcinoma, *Int J Clin Exp Pathol.* **7**, 3704-3713.
319. Sun, H., Jiang, L., Luo, X., Jin, W., He, Q., An, J., Lui, K., Shi, J., Rong, R., Su, W., Lucchesi, C., Liu, Y., Sheikh, M. S. & Huang, Y. (2013) Potential tumor-suppressive role of monoglyceride lipase in human colorectal cancer, *Oncogene.* **32**, 234-241.
320. Michiels, C., Tellier, C. & Feron, O. (2016) Cycling hypoxia: A key feature of the tumor microenvironment, *Biochim Biophys Acta.* **1866**, 76-86.
321. Menendez, J. A. (2010) Fine-tuning the lipogenic/lipolytic balance to optimize the metabolic requirements of cancer cell growth: molecular mechanisms and therapeutic perspectives, *Biochim Biophys Acta.* **1801**, 381-91.
322. Furuta, E., Pai, S. K., Zhan, R., Bandyopadhyay, S., Watabe, M., Mo, Y. Y., Hirota, S., Hosobe, S., Tsukada, T., Miura, K., Kamada, S., Saito, K., Iizumi, M., Liu, W., Ericsson, J. & Watabe, K. (2008) Fatty acid synthase gene is up-regulated by hypoxia via activation of Akt and sterol regulatory element binding protein-1, *Cancer Research.* **68**, 1003-1011.
323. Kamphorst, J. J., Chung, M. K., Fan, J. & Rabinowitz, J. D. (2014) Quantitative analysis of acetyl-CoA production in hypoxic cancer cells reveals substantial contribution from acetate, *Cancer Metab.* **2**, 23.
324. Schug, Z. T., Vande Voorde, J. & Gottlieb, E. (2016) The metabolic fate of acetate in cancer, *Nat Rev Cancer.* **16**, 708-717.
325. Schug, Z. T., Peck, B., Jones, D. T., Zhang, Q., Grosskurth, S., Alam, I. S., Goodwin, L. M., Smethurst, E., Mason, S., Blyth, K., McGarry, L., James, D., Shanks, E., Kalna, G., Saunders, R. E., Jiang, M., Howell, M., Lassailly, F., Thin, M. Z., Spencer-Dene, B., Stamp, G., van den Broek, N. J., Mackay, G., Bulusu, V., Kamphorst, J. J., Tardito, S., Strachan, D., Harris, A. L., Aboagye, E. O., Critchlow, S. E., Wakelam, M. J., Schulze, A. & Gottlieb, E. (2015) Acetyl-CoA synthetase 2 promotes acetate utilization and maintains cancer cell growth under metabolic stress, *Cancer Cell.* **27**, 57-71.
326. Comerford, S. A., Huang, Z., Du, X., Wang, Y., Cai, L., Witkiewicz, A. K., Walters, H., Tantawy, M. N., Fu, A., Manning, H. C., Horton, J. D., Hammer, R. E., McKnight, S. L. & Tu, B. P. (2014) Acetate dependence of tumors, *Cell.* **159**, 1591-602.
327. Kamphorst, J. J., Cross, J. R., Fan, J., de Stanchina, E., Mathew, R., White, E. P., Thompson, C. B. & Rabinowitz, J. D. (2013) Hypoxic and Ras-transformed cells support growth by scavenging unsaturated fatty acids from lysophospholipids, *Proc Natl Acad Sci U S A.* **110**, 8882-7.
328. Bensaad, K., Favaro, E., Lewis, C. A., Peck, B., Lord, S., Collins, J. M., Pinnick, K. E., Wigfield, S., Buffa, F. M., Li, J. L., Zhang, Q., Wakelam, M. J., Karpe, F., Schulze, A. & Harris, A. L. (2014) Fatty acid uptake and lipid storage induced by HIF-1 α contribute to cell growth and survival after hypoxia-reoxygenation, *Cell Rep.* **9**, 349-65.
329. Currie, E., Schulze, A., Zechner, R., Walther, T. C. & Farese, R. V., Jr. (2013) Cellular fatty acid metabolism and cancer, *Cell Metab.* **18**, 153-61.
330. Farese, R. V., Jr. & Walther, T. C. (2009) Lipid droplets finally get a little R-E-S-P-E-C-T, *Cell.* **139**, 855-60.
331. Silvius, J. R. (2003) Role of cholesterol in lipid raft formation: lessons from lipid model systems, *Biochim Biophys Acta.* **1610**, 174-83.
332. Zajchowski, L. D. & Robbins, S. M. (2002) Lipid rafts and little caves. Compartmentalized signalling in membrane microdomains, *Eur J Biochem.* **269**, 737-52.
333. Simons, K. & Toomre, D. (2000) Lipid rafts and signal transduction, *Nat Rev Mol Cell Biol.* **1**, 31-9.

334. Bionda, C., Athias, A., Poncet, D., Alphonse, G., Guezguez, A., Gambert, P., Rodriguez-Lafrasse, C. & Ardail, D. (2008) Differential regulation of cell death in head and neck cell carcinoma through alteration of cholesterol levels in lipid rafts microdomains, *Biochem Pharmacol.* **75**, 761-72.
335. Lacour, S., Hammann, A., Grazide, S., Lagadic-Gossmann, D., Athias, A., Sergent, O., Laurent, G., Gambert, P., Solary, E. & Dimanche-Boitrel, M. T. (2004) Cisplatin-induced CD95 redistribution into membrane lipid rafts of HT29 human colon cancer cells, *Cancer Res.* **64**, 3593-8.
336. Kolanjiappan, K., Ramachandran, C. R. & Manoharan, S. (2003) Biochemical changes in tumor tissues of oral cancer patients, *Clin Biochem.* **36**, 61-5.
337. Tamashiro, P. M., Furuya, H., Shimizu, Y. & Kawamori, T. (2014) Sphingosine kinase 1 mediates head & neck squamous cell carcinoma invasion through sphingosine 1-phosphate receptor 1, *Cancer Cell Int.* **14**, 76.
338. Beckham, T. H., Elojeimy, S., Cheng, J. C., Turner, L. S., Hoffman, S. R., Norris, J. S. & Liu, X. (2010) Targeting sphingolipid metabolism in head and neck cancer: rational therapeutic potentials, *Expert Opin Ther Targets.* **14**, 529-39.
339. Morad, S. A. & Cabot, M. C. (2013) Ceramide-orchestrated signalling in cancer cells, *Nat Rev Cancer.* **13**, 51-65.
340. Sanchez-Martinez, R., Cruz-Gil, S., Gomez de Cedron, M., Alvarez-Fernandez, M., Vargas, T., Molina, S., Garcia, B., Herranz, J., Moreno-Rubio, J., Reglero, G., Perez-Moreno, M., Feliu, J., Malumbres, M. & Ramirez de Molina, A. (2015) A link between lipid metabolism and epithelial-mesenchymal transition provides a target for colon cancer therapy, *Oncotarget.* **6**, 38719-36.
341. Zaidi, N., Lupien, L., Kuemmerle, N. B., Kinlaw, W. B., Swinnen, J. V. & Smans, K. (2013) Lipogenesis and lipolysis: the pathways exploited by the cancer cells to acquire fatty acids, *Prog Lipid Res.* **52**, 585-9.
342. Tirinato, L., Liberale, C., Di Franco, S., Candeloro, P., Benfante, A., La Rocca, R., Potze, L., Marotta, R., Ruffilli, R., Rajamanickam, V. P., Malerba, M., De Angelis, F., Falqui, A., Carbone, E., Todaro, M., Medema, J. P., Stassi, G. & Di Fabrizio, E. (2015) Lipid droplets: a new player in colorectal cancer stem cells unveiled by spectroscopic imaging, *Stem Cells.* **33**, 35-44.
343. Li, J., Condello, S., Thomes-Pepin, J., Ma, X., Xia, Y., Hurley, T. D., Matei, D. & Cheng, J. X. (2017) Lipid Desaturation Is a Metabolic Marker and Therapeutic Target of Ovarian Cancer Stem Cells, *Cell Stem Cell.* **20**, 303-314 e5.
344. Coussens, L. M. & Werb, Z. (2002) Inflammation and cancer, *Nature.* **420**, 860-7.
345. Lee, J., Taneja, V. & Vassallo, R. (2012) Cigarette smoking and inflammation: cellular and molecular mechanisms, *J Dent Res.* **91**, 142-9.
346. Churg, A., Dai, J., Tai, H., Xie, C. & Wright, J. L. (2002) Tumor necrosis factor-alpha is central to acute cigarette smoke-induced inflammation and connective tissue breakdown, *Am J Respir Crit Care Med.* **166**, 849-54.
347. Aggarwal, B. B. (2004) Nuclear factor-kappaB: the enemy within, *Cancer Cell.* **6**, 203-8.
348. Ondrey, F. G., Dong, G., Sunwoo, J., Chen, Z., Wolf, J. S., Crawl-Bancroft, C. V., Mukaida, N. & Van Waes, C. (1999) Constitutive activation of transcription factors NF-(kappa)B, AP-1, and NF-IL6 in human head and neck squamous cell carcinoma cell lines that express pro-inflammatory and pro-angiogenic cytokines, *Mol Carcinog.* **26**, 119-29.
349. Bindhu, O. S., Ramadas, K., Sebastian, P. & Pillai, M. R. (2006) High expression levels of nuclear factor kappa B and gelatinases in the tumorigenesis of oral squamous cell carcinoma, *Head Neck.* **28**, 916-25.
350. Chung, K. F. (2005) Inflammatory mediators in chronic obstructive pulmonary disease, *Curr Drug Targets Inflamm Allergy.* **4**, 619-25.
351. Huber, M., Beutler, B. & Keppler, D. (1988) Tumor necrosis factor alpha stimulates leukotriene production in vivo, *Eur J Immunol.* **18**, 2085-8.
352. Henderson, W. R., Jr. (1994) The role of leukotrienes in inflammation, *Ann Intern Med.* **121**, 684-97.
353. Khanapure, S. P., Garvey, D. S., Janero, D. R. & Letts, L. G. (2007) Eicosanoids in inflammation: biosynthesis, pharmacology, and therapeutic frontiers, *Curr Top Med Chem.* **7**, 311-40.

354. Dennis, E. A. & Norris, P. C. (2015) Eicosanoid storm in infection and inflammation, *Nat Rev Immunol.* **15**, 511-23.
355. Greene, E. R., Huang, S., Serhan, C. N. & Panigrahy, D. (2011) Regulation of inflammation in cancer by eicosanoids, *Prostaglandins Other Lipid Mediat.* **96**, 27-36.
356. Busse, W. W. (1998) Leukotrienes and inflammation, *Am J Respir Crit Care Med.* **157**, S210-3.
357. Murphy, R. C. & Gijon, M. A. (2007) Biosynthesis and metabolism of leukotrienes, *Biochem J.* **405**, 379-95.
358. Mandal, A. K., Skoch, J., Bacskai, B. J., Hyman, B. T., Christmas, P., Miller, D., Yamin, T. T., Xu, S., Wisniewski, D., Evans, J. F. & Soberman, R. J. (2004) The membrane organization of leukotriene synthesis, *Proc Natl Acad Sci U S A.* **101**, 6587-92.
359. Ford-Hutchinson, A. W. (1990) Leukotriene B4 in inflammation, *Crit Rev Immunol.* **10**, 1-12.
360. Liu, M. & Yokomizo, T. (2015) The role of leukotrienes in allergic diseases, *Allergol Int.* **64**, 17-26.
361. Dahlen, S. E., Hansson, G., Hedqvist, P., Bjorck, T., Granstrom, E. & Dahlen, B. (1983) Allergen challenge of lung tissue from asthmatics elicits bronchial contraction that correlates with the release of leukotrienes C4, D4, and E4, *Proc Natl Acad Sci U S A.* **80**, 1712-6.
362. Paruchuri, S., Broom, O., Dib, K. & Sjolander, A. (2005) The pro-inflammatory mediator leukotriene D4 induces phosphatidylinositol 3-kinase and Rac-dependent migration of intestinal epithelial cells, *J Biol Chem.* **280**, 13538-44.
363. Paruchuri, S., Hallberg, B., Juhas, M., Larsson, C. & Sjolander, A. (2002) Leukotriene D(4) activates MAPK through a Ras-independent but PKCepsilon-dependent pathway in intestinal epithelial cells, *J Cell Sci.* **115**, 1883-93.
364. Mezhybovska, M., Wikstrom, K., Ohd, J. F. & Sjolander, A. (2006) The inflammatory mediator leukotriene D4 induces beta-catenin signaling and its association with antiapoptotic Bcl-2 in intestinal epithelial cells, *J Biol Chem.* **281**, 6776-84.
365. Yokomizo, T., Izumi, T., Chang, K., Takuwa, Y. & Shimizu, T. (1997) A G-protein-coupled receptor for leukotriene B4 that mediates chemotaxis, *Nature.* **387**, 620-4.
366. Yokomizo, T., Kato, K., Terawaki, K., Izumi, T. & Shimizu, T. (2000) A second leukotriene B(4) receptor, BLT2. A new therapeutic target in inflammation and immunological disorders, *J Exp Med.* **192**, 421-32.
367. Yokomizo, T., Izumi, T. & Shimizu, T. (2001) Leukotriene B4: metabolism and signal transduction, *Arch Biochem Biophys.* **385**, 231-41.
368. Lynch, K. R., O'Neill, G. P., Liu, Q., Im, D. S., Sawyer, N., Metters, K. M., Coulombe, N., Abramovitz, M., Figueroa, D. J., Zeng, Z., Connolly, B. M., Bai, C., Austin, C. P., Chateauneuf, A., Stocco, R., Greig, G. M., Kargman, S., Hooks, S. B., Hosfield, E., Williams, D. L., Jr., Ford-Hutchinson, A. W., Caskey, C. T. & Evans, J. F. (1999) Characterization of the human cysteinyl leukotriene CysLT1 receptor, *Nature.* **399**, 789-93.
369. Heise, C. E., O'Dowd, B. F., Figueroa, D. J., Sawyer, N., Nguyen, T., Im, D. S., Stocco, R., Bellefeuille, J. N., Abramovitz, M., Cheng, R., Williams, D. L., Jr., Zeng, Z., Liu, Q., Ma, L., Clements, M. K., Coulombe, N., Liu, Y., Austin, C. P., George, S. R., O'Neill, G. P., Metters, K. M., Lynch, K. R. & Evans, J. F. (2000) Characterization of the human cysteinyl leukotriene 2 receptor, *J Biol Chem.* **275**, 30531-6.
370. Folco, G. & Murphy, R. C. (2006) Eicosanoid transcellular biosynthesis: from cell-cell interactions to in vivo tissue responses, *Pharmacol Rev.* **58**, 375-88.
371. Zarini, S., Gijon, M. A., Ransome, A. E., Murphy, R. C. & Sala, A. (2009) Transcellular biosynthesis of cysteinyl leukotrienes in vivo during mouse peritoneal inflammation, *Proc Natl Acad Sci U S A.* **106**, 8296-301.
372. Savari, S., Vinnakota, K., Zhang, Y. & Sjolander, A. (2014) Cysteinyl leukotrienes and their receptors: bridging inflammation and colorectal cancer, *World J Gastroenterol.* **20**, 968-77.
373. (2014) Bowel cancer statistics in *Cancer Statistics*, Cancer Research UK,
374. Lutgens, M. W., van Oijen, M. G., van der Heijden, G. J., Vleggaar, F. P., Siersema, P. D. & Oldenburg, B. (2013) Declining risk of colorectal cancer in inflammatory bowel disease: an updated meta-analysis of population-based cohort studies, *Inflamm Bowel Dis.* **19**, 789-99.

375. Kim, J. H., Tagari, P., Griffiths, A. M., Ford-Hutchinson, A., Smith, C. & Sherman, P. M. (1995) Levels of peptidoleukotriene E4 are elevated in active Crohn's disease, *J Pediatr Gastroenterol Nutr.* **20**, 403-7.
376. Matsuyama, M., Funao, K., Hayama, T., Tanaka, T., Kawahito, Y., Sano, H., Takemoto, Y., Nakatani, T. & Yoshimura, R. (2009) Relationship between cysteinyl-leukotriene-1 receptor and human transitional cell carcinoma in bladder, *Urology.* **73**, 916-21.
377. Ohd, J. F., Nielsen, C. K., Campbell, J., Landberg, G., Lofberg, H. & Sjolander, A. (2003) Expression of the leukotriene D4 receptor CysLT1, COX-2, and other cell survival factors in colorectal adenocarcinomas, *Gastroenterology.* **124**, 57-70.
378. Matsuyama, M., Hayama, T., Funao, K., Kawahito, Y., Sano, H., Takemoto, Y., Nakatani, T. & Yoshimura, R. (2007) Overexpression of cysteinyl LT1 receptor in prostate cancer and CysLT1R antagonist inhibits prostate cancer cell growth through apoptosis, *Oncol Rep.* **18**, 99-104.
379. Magnusson, C., Liu, J., Ehrnstrom, R., Manjer, J., Jirstrom, K., Andersson, T. & Sjolander, A. (2011) Cysteinyl leukotriene receptor expression pattern affects migration of breast cancer cells and survival of breast cancer patients, *Int J Cancer.* **129**, 9-22.
380. Magnusson, C., Ehrnstrom, R., Olsen, J. & Sjolander, A. (2007) An increased expression of cysteinyl leukotriene 2 receptor in colorectal adenocarcinomas correlates with high differentiation, *Cancer Res.* **67**, 9190-8.
381. Magnusson, C., Mezhybovska, M., Lorinc, E., Fernebro, E., Nilbert, M. & Sjolander, A. (2010) Low expression of CysLT1R and high expression of CysLT2R mediate good prognosis in colorectal cancer, *Eur J Cancer.* **46**, 826-35.
382. Parhamifar, L., Sime, W., Yudina, Y., Vilhardt, F., Morgelin, M. & Sjolander, A. (2010) Ligand-induced tyrosine phosphorylation of cysteinyl leukotriene receptor 1 triggers internalization and signaling in intestinal epithelial cells, *PLoS One.* **5**, e14439.
383. Ohd, J. F., Wikstrom, K. & Sjolander, A. (2000) Leukotrienes induce cell-survival signaling in intestinal epithelial cells, *Gastroenterology.* **119**, 1007-18.
384. Paruchuri, S. & Sjolander, A. (2003) Leukotriene D4 mediates survival and proliferation via separate but parallel pathways in the human intestinal epithelial cell line Int 407, *J Biol Chem.* **278**, 45577-85.
385. Magnusson, C., Bengtsson, A. M., Liu, M., Liu, J., Ceder, Y., Ehrnstrom, R. & Sjolander, A. (2011) Regulation of cysteinyl leukotriene receptor 2 expression--a potential anti-tumor mechanism, *PLoS One.* **6**, e29060.
386. el-Hakim, I. E., Langdon, J. D., Zakrzewski, J. T. & Costello, J. F. (1990) Leukotriene B4 and oral cancer, *Br J Oral Maxillofac Surg.* **28**, 155-9.
387. Bateman, E. D., Hurd, S. S., Barnes, P. J., Bousquet, J., Drazen, J. M., FitzGerald, M., Gibson, P., Ohta, K., O'Byrne, P., Pedersen, S. E., Pizzichini, E., Sullivan, S. D., Wenzel, S. E. & Zar, H. J. (2008) Global strategy for asthma management and prevention: GINA executive summary, *Eur Respir J.* **31**, 143-78.
388. Matsuyama, M. & Yoshimura, R. (2010) Cysteinyl-leukotriene1 receptor is a potent target for the prevention and treatment of human urological cancer, *Mol Med Rep.* **3**, 245-51.
389. Sveinbjornsson, B., Rasmuson, A., Baryawno, N., Wan, M., Pettersen, I., Ponthan, F., Orrego, A., Haeggstrom, J. Z., Johnsen, J. I. & Kogner, P. (2008) Expression of enzymes and receptors of the leukotriene pathway in human neuroblastoma promotes tumor survival and provides a target for therapy, *FASEB J.* **22**, 3525-36.
390. Paruchuri, S., Mezhybovska, M., Juhas, M. & Sjolander, A. (2006) Endogenous production of leukotriene D4 mediates autocrine survival and proliferation via CysLT1 receptor signalling in intestinal epithelial cells, *Oncogene.* **25**, 6660-5.
391. Cianchi, F., Cortesini, C., Magnelli, L., Fanti, E., Papucci, L., Schiavone, N., Messerini, L., Vannacci, A., Capaccioli, S., Perna, F., Lulli, M., Fabbroni, V., Perigli, G., Bechi, P. & Masini, E. (2006) Inhibition of 5-lipoxygenase by MK886 augments the antitumor activity of celecoxib in human colon cancer cells, *Mol Cancer Ther.* **5**, 2716-26.
392. Lee, K. S., Kim, S. R., Park, H. S., Jin, G. Y. & Lee, Y. C. (2004) Cysteinyl leukotriene receptor antagonist regulates vascular permeability by reducing vascular endothelial growth factor expression, *J Allergy Clin Immunol.* **114**, 1093-9.

393. Nozaki, M., Yoshikawa, M., Ishitani, K., Kobayashi, H., Houkin, K., Imai, K., Ito, Y. & Muraki, T. (2010) Cysteinyl leukotriene receptor antagonists inhibit tumor metastasis by inhibiting capillary permeability, *Keio J Med.* **59**, 10-8.
394. Savari, S., Liu, M., Zhang, Y., Sime, W. & Sjolander, A. (2013) CysLT(1)R antagonists inhibit tumor growth in a xenograft model of colon cancer, *PLoS One.* **8**, e73466.
395. Ulrich, C. M., Bigler, J. & Potter, J. D. (2006) Non-steroidal anti-inflammatory drugs for cancer prevention: promise, perils and pharmacogenetics, *Nat Rev Cancer.* **6**, 130-40.
396. Mezhybovska, M., Wikstrom, K., Ohd, J. F. & Sjolander, A. (2005) Pro-inflammatory mediator leukotriene D4 induces transcriptional activity of potentially oncogenic genes, *Biochem Soc Trans.* **33**, 698-700.
397. Salim, T., Sand-Dejmek, J. & Sjolander, A. (2014) The inflammatory mediator leukotriene D(4) induces subcellular beta-catenin translocation and migration of colon cancer cells, *Exp Cell Res.* **321**, 255-66.
398. Poulin, S., Thompson, C., Thivierge, M., Veronneau, S., McMahon, S., Dubois, C. M., Stankova, J. & Rola-Pleszczynski, M. (2011) Cysteinyl-leukotrienes induce vascular endothelial growth factor production in human monocytes and bronchial smooth muscle cells, *Clin Exp Allergy.* **41**, 204-17.
399. Dickson, M. A., Hahn, W. C., Ino, Y., Ronfard, V., Wu, J. Y., Weinberg, R. A., Louis, D. N., Li, F. P. & Rheinwald, J. G. (2000) Human keratinocytes that express hTERT and also bypass a p16(INK4a)-enforced mechanism that limits life span become immortal yet retain normal growth and differentiation characteristics, *Mol Cell Biol.* **20**, 1436-47.
400. Lindberg, K. & Rheinwald, J. G. (1990) Three distinct keratinocyte subtypes identified in human oral epithelium by their patterns of keratin expression in culture and in xenografts, *Differentiation.* **45**, 230-41.
401. Fisher, S., Barry, A., Abreu, J., Minie, B., Nolan, J., Delorey, T. M., Young, G., Fennell, T. J., Allen, A., Ambrogio, L., Berlin, A. M., Blumenstiel, B., Cibulskis, K., Friedrich, D., Johnson, R., Juhn, F., Reilly, B., Shammas, R., Stalker, J., Sykes, S. M., Thompson, J., Walsh, J., Zimmer, A., Zwirko, Z., Gabriel, S., Nicol, R. & Nusbaum, C. (2011) A scalable, fully automated process for construction of sequence-ready human exome targeted capture libraries, *Genome Biol.* **12**, R1.
402. Bailey, P., Chang, D., K. Nones, K. Johns, A. L. Patch, A. M. Gingras, M. C. Miller, D. K. Christ, A. N. Bruxner, T. J. Quinn, M. C. Nourse, C. Murtaugh, L. C. Harliwong, I. Idrisoglu, S. Manning, S. Nourbakhsh, E. Wani, S. Fink, L. Holmes, O. Chin, V. Anderson, M. J. Kazakoff, S. Leonard, C. Newell, F. Waddell, N. Wood, S. Xu, Q. Wilson, P. J. Cloonan, N. Kassahn, K. S. Taylor, D. Quek, K. Robertson, A. Pantano, L. Mincarelli, L. Sanchez, L. N. Evers, L. Wu, J. Pinese, M. Cowley, M. J. Jones, M. D. Colvin, E. K. Nagrial, A. M. Humphrey, E. S. Chantrill, L. A. Mawson, A. Humphris, J. Chou, A. Pajic, M. Scarlett, C. J. Pinho, A. V. Giry-Laterriere, M. Rooman, I. Samra, J. S. Kench, J. G. Lovell, J. A. Merrett, N. D. Toon, C. W. Epari, K. Nguyen, N. Q. Barbour, A. Zeps, N. Moran-Jones, K. Jamieson, N. B. Graham, J. S. Duthie, F. Oien, K. Hair, J. Grutzmann, R. Maitra, A. Iacobuzio-Donahue, C. A. Wolfgang, C. L. Morgan, R. A. Lawlor, R. T. Corbo, V. Bassi, C. Rusev, B. Capelli, P. Salvia, R. Tortora, G. Mukhopadhyay, D. Petersen, G. M. Australian Pancreatic Cancer Genome, I. Munzy, D. M. Fisher, W. E. Karim, S. A. Eshleman, J. R. Hruban, R. H. Pilarsky, C. Morton, J. P. Sansom, O. J. Scarpa, A. Musgrove, E. A. Bailey, U. M. Hofmann, O. Sutherland, R. L. Wheeler, D. A. Gill, A. J. Gibbs, R. A. Pearson, J. V., et al. (2016) Genomic analyses identify molecular subtypes of pancreatic cancer, *Nature.* **531**, 47-52.
403. Church, D. M., Schneider, V. A., Graves, T., Auger, K., Cunningham, F., Bouk, N., Chen, H. C., Agarwala, R., McLaren, W. M., Ritchie, G. R., Albracht, D., Kremitzki, M., Rock, S., Kotkiewicz, H., Kremitzki, C., Wollam, A., Trani, L., Fulton, L., Fulton, R., Matthews, L., Whitehead, S., Chow, W., Tarrance, J., Dunn, M., Harden, G., Threadgold, G., Wood, J., Collins, J., Heath, P., Griffiths, G., Pelan, S., Grafham, D., Eichler, E. E., Weinstock, G., Mardis, E. R., Wilson, R. K., Howe, K., Flicek, P. & Hubbard, T. (2011) Modernizing reference genome assemblies, *PLoS Biol.* **9**, e1001091.
404. Kim, D., Pertea, G., Trapnell, C., Pimentel, H., Kelley, R. & Salzberg, S. L. (2013) TopHat2: accurate alignment of transcriptomes in the presence of insertions, deletions and gene fusions, *Genome Biol.* **14**, R36.
405. Langmead, B. & Salzberg, S. L. (2012) Fast gapped-read alignment with Bowtie 2, *Nat Methods.* **9**, 357-9.

406. Love, M. I., Huber, W. & Anders, S. (2014) Moderated estimation of fold change and dispersion for RNA-seq data with DESeq2, *Genome Biol.* **15**, 550.
407. Biankin, A. V. Waddell, N. Kassahn, K. S. Gingras, M. C. Muthuswamy, L. B. Johns, A. L. Miller, D. K. Wilson, P. J. Patch, A. M. Wu, J. Chang, D. K. Cowley, M. J. Gardiner, B. B. Song, S. Harliwong, I. Idrisoglu, S. Nourse, C. Nourbakhsh, E. Manning, S. Wani, S. Gongora, M. Pajic, M. Scarlett, C. J. Gill, A. J. Pinho, A. V. Rooman, I. Anderson, M. Holmes, O. Leonard, C. Taylor, D. Wood, S. Xu, Q. Nones, K. Fink, J. L. Christ, A. Bruxner, T. Cloonan, N. Kolle, G. Newell, F. Pinese, M. Mead, R. S. Humphris, J. L. Kaplan, W. Jones, M. D. Colvin, E. K. Nagrial, A. M. Humphrey, E. S. Chou, A. Chin, V. T. Chantrill, L. A. Mawson, A. Samra, J. S. Kench, J. G. Lovell, J. A. Daly, R. J. Merrett, N. D. Toon, C. Epari, K. Nguyen, N. Q. Barbour, A. Zeps, N. Australian Pancreatic Cancer Genome, I. Kakkar, N. Zhao, F. Wu, Y. Q. Wang, M. Muzny, D. M. Fisher, W. E. Brunicardi, F. C. Hodges, S. E. Reid, J. G. Drummond, J. Chang, K. Han, Y. Lewis, L. R. Dinh, H. Buhay, C. J. Beck, T. Timms, L. Sam, M. Begley, K. Brown, A. Pai, D. Panchal, A. Buchner, N. De Borja, R. Denroche, R. E. Yung, C. K. Serra, S. Onetto, N. Mukhopadhyay, D. Tsao, M. S. Shaw, P. A. Petersen, G. M. Gallinger, S. Hruban, R. H. Maitra, A. Iacobuzio-Donahue, C. A. Schulick, R. D. Wolfgang, C. L., et al. (2012) Pancreatic cancer genomes reveal aberrations in axon guidance pathway genes, *Nature*. **491**, 399-405.
408. Isa, A. Y., Ward, T. H., West, C. M., Slevin, N. J. & Homer, J. J. (2006) Hypoxia in head and neck cancer, *The British journal of radiology*. **79**, 791-8.
409. Singh, B., Stoffel, A., Gogineni, S., Poluri, A., Pfister, D. G., Shaha, A. R., Pathak, A., Bosl, G., Cordon-Cardo, C., Shah, J. P. & Rao, P. H. (2002) Amplification of the 3q26.3 locus is associated with progression to invasive cancer and is a negative prognostic factor in head and neck squamous cell carcinomas, *American Journal of Pathology*. **161**, 365-371.
410. Du, L., Chen, X., Cao, Y., Lu, L., Zhang, F., Bornstein, S., Li, Y., Owens, P., Malkoski, S., Said, S., Jin, F., Kulesz-Martin, M., Gross, N., Wang, X. J. & Lu, S. L. (2016) Overexpression of PIK3CA in murine head and neck epithelium drives tumor invasion and metastasis through PDK1 and enhanced TGFbeta signaling, *Oncogene*. **35**, 4641-52.
411. Lo Muzio, L., Santarelli, A., Caltabiano, R., Rubini, C., Pieramici, T., Trevisiol, L., Carinci, F., Leonardi, R., De Lillo, A., Lanzafame, S., Bufo, P. & Piattelli, A. (2005) p63 overexpression associates with poor prognosis in head and neck squamous cell carcinoma, *Hum Pathol*. **36**, 187-194.
412. Soder, A. I., Hoare, S. F., Muire, S., Balmain, A., Parkinson, E. K. & Keith, W. N. (1997) Mapping of the gene for the mouse telomerase RNA component, Terc, to chromosome 3 by fluorescence in situ hybridization and mouse chromosome painting, *Genomics*. **41**, 293-294.
413. Yang, Y. L., Chu, J. Y., Luo, M. L., Wu, Y. P., Zhang, Y., Feng, Y. B., Shi, Z. Z., Xu, X., Han, Y. L., Cai, Y., Dong, J. T., Zhan, Q. M., Wu, M. & Wang, M. R. (2008) Amplification of PRKCI, located in 3q26, is associated with lymph node metastasis in esophageal squamous cell carcinoma, *Gene Chromosome Canc.* **47**, 127-136.
414. Greenman, C., Stephens, P., Smith, R., Dalgliesh, G. L., Hunter, C., Bignell, G., Davies, H., Teague, J., Butler, A., Stevens, C., Edkins, S., O'Meara, S., Vastrik, I., Schmidt, E. E., Avis, T., Barthorpe, S., Bhamra, G., Buck, G., Choudhury, B., Clements, J., Cole, J., Dicks, E., Forbes, S., Gray, K., Halliday, K., Harrison, R., Hills, K., Hinton, J., Jenkinson, A., Jones, D., Menzies, A., Mironenko, T., Perry, J., Raine, K., Richardson, D., Shepherd, R., Small, A., Tofts, C., Varian, J., Webb, T., West, S., Widaa, S., Yates, A., Cahill, D. P., Louis, D. N., Goldstraw, P., Nicholson, A. G., Brasseur, F., Looijenga, L., Weber, B. L., Chiew, Y. E., DeFazio, A., Greaves, M. F., Green, A. R., Campbell, P., Birney, E., Easton, D. F., Chenevix-Trench, G., Tan, M. H., Khoo, S. K., Teh, B. T., Yuen, S. T., Leung, S. Y., Wooster, R., Futreal, P. A. & Stratton, M. R. (2007) Patterns of somatic mutation in human cancer genomes, *Nature*. **446**, 153-8.
415. Aken, B. L., Ayling, S., Barrell, D., Clarke, L., Curwen, V., Fairley, S., Fernandez Banet, J., Billis, K., Garcia Giron, C., Hourlier, T., Howe, K., Kahari, A., Kokocinski, F., Martin, F. J., Murphy, D. N., Nag, R., Ruffier, M., Schuster, M., Tang, Y. A., Vogel, J. H., White, S., Zadissa, A., Flicek, P. & Searle, S. M. (2016) The Ensembl gene annotation system, *Database : the journal of biological databases and curation*. **2016**.
416. Heselmeyer, K., Macville, M., Schrock, E., Blegen, H., Hellstrom, A. C., Shah, K., Auer, G. & Ried, T. (1997) Advanced-stage cervical carcinomas are defined by a recurrent pattern of

- chromosomal aberrations revealing high genetic instability and a consistent gain of chromosome arm 3q, *Genes Chromosomes Cancer*. **19**, 233-40.
417. Bandla, S., Pennathur, A., Luketich, J. D., Beer, D. G., Lin, L., Bass, A. J., Godfrey, T. E. & Litle, V. R. (2012) Comparative genomics of esophageal adenocarcinoma and squamous cell carcinoma, *Ann Thorac Surg*. **93**, 1101-6.
418. Pickering, C. R., Zhou, J. H., Lee, J. J., Drummond, J. A., Peng, S. A., Saade, R. E., Tsai, K. Y., Curry, J. L., Tetzlaff, M. T., Lai, S. Y., Yu, J., Muzny, D. M., Doddapaneni, H., Shinbrot, E., Covington, K. R., Zhang, J., Seth, S., Caulin, C., Clayman, G. L., El-Naggar, A. K., Gibbs, R. A., Weber, R. S., Myers, J. N., Wheeler, D. A. & Frederick, M. J. (2014) Mutational landscape of aggressive cutaneous squamous cell carcinoma, *Clin Cancer Res*. **20**, 6582-92.
419. Davidson, M. A. & Shanks, E. J. (2017) 3q26-29 Amplification in head and neck squamous cell carcinoma: a review of established and prospective oncogenes, *FEBS J*. **284**, 2705-2731.
420. Almond, J. B. & Cohen, G. M. (2002) The proteasome: a novel target for cancer chemotherapy, *Leukemia*. **16**, 433-43.
421. Field-Smith, A., Morgan, G. J. & Davies, F. E. (2006) Bortezomib (Velcade trade mark) in the Treatment of Multiple Myeloma, *Ther Clin Risk Manag*. **2**, 271-9.
422. Gilbert, J., Lee, J. W., Argiris, A., Haigentz, M., Jr., Feldman, L. E., Jang, M., Arun, P., Van Waes, C. & Forastiere, A. A. (2013) Phase II 2-arm trial of the proteasome inhibitor, PS-341 (bortezomib) in combination with irinotecan or PS-341 alone followed by the addition of irinotecan at time of progression in patients with locally recurrent or metastatic squamous cell carcinoma of the head and neck (E1304): a trial of the Eastern Cooperative Oncology Group, *Head Neck*. **35**, 942-8.
423. Li, C., Li, R., Grandis, J. R. & Johnson, D. E. (2008) Bortezomib induces apoptosis via Bim and Bik up-regulation and synergizes with cisplatin in the killing of head and neck squamous cell carcinoma cells, *Mol Cancer Ther*. **7**, 1647-55.
424. Li, C. & Johnson, D. E. (2013) Liberation of functional p53 by proteasome inhibition in human papilloma virus-positive head and neck squamous cell carcinoma cells promotes apoptosis and cell cycle arrest, *Cell Cycle*. **12**, 923-34.
425. Tomida, S., Yanagisawa, K., Koshikawa, K., Yatabe, Y., Mitsudomi, T., Osada, H. & Takahashi, T. (2007) Identification of a metastasis signature and the DLX4 homeobox protein as a regulator of metastasis by combined transcriptome approach, *Oncogene*. **26**, 4600-8.
426. Matsuyama, Y., Suzuki, M., Arima, C., Huang, Q. M., Tomida, S., Takeuchi, T., Sugiyama, R., Itoh, Y., Yatabe, Y., Goto, H. & Takahashi, T. (2011) Proteasomal non-catalytic subunit PSMD2 as a potential therapeutic target in association with various clinicopathologic features in lung adenocarcinomas, *Mol Carcinog*. **50**, 301-9.
427. Wang, J., Liu, Q. & Shyr, Y. (2015) Dysregulated transcription across diverse cancer types reveals the importance of RNA-binding protein in carcinogenesis, *BMC Genomics*. **16 Suppl 7**, S5.
428. Qian, J., Hassanein, M., Hoeksema, M. D., Harris, B. K., Zou, Y., Chen, H., Lu, P., Eisenberg, R., Wang, J., Espinosa, A., Ji, X., Harris, F. T., Rahman, S. M. & Massion, P. P. (2015) The RNA binding protein FXR1 is a new driver in the 3q26-29 amplicon and predicts poor prognosis in human cancers, *Proc Natl Acad Sci U S A*. **112**, 3469-74.
429. Iyoda, M., Kasamatsu, A., Ishigami, T., Nakashima, D., Endo-Sakamoto, Y., Ogawara, K., Shiiba, M., Tanzawa, H. & Uzawa, K. (2010) Epithelial cell transforming sequence 2 in human oral cancer, *PLoS One*. **5**, e14082.
430. Justilien, V., Walsh, M. P., Ali, S. A., Thompson, E. A., Murray, N. R. & Fields, A. P. (2014) The PRKCI and SOX2 oncogenes are coamplified and cooperate to activate Hedgehog signaling in lung squamous cell carcinoma, *Cancer Cell*. **25**, 139-51.
431. Fernandez, E. & Mallette, F. A. (2016) The Rise of FXR1: Escaping Cellular Senescence in Head and Neck Squamous Cell Carcinoma, *PLoS Genet*. **12**, e1006344.
432. Wemmert, S., Lindner, Y., Linxweiler, J., Wagenpfeil, S., Bohle, R., Niewald, M. & Schick, B. (2016) Initial evidence for Sec62 as a prognostic marker in advanced head and neck squamous cell carcinoma, *Oncol Lett*. **11**, 1661-1670.
433. Greiner, M., Kreutzer, B., Jung, V., Grobholz, R., Hasenfus, A., Stohr, R. F., Tornillo, L., Dudek, J., Stockle, M., Unteregger, G., Kamradt, J., Wullich, B. & Zimmermann, R. (2011) Silencing of the

- SEC62 gene inhibits migratory and invasive potential of various tumor cells, *Int J Cancer*. **128**, 2284-95.
434. Jung, V., Kindich, R., Kamradt, J., Jung, M., Muller, M., Schulz, W. A., Engers, R., Unteregger, G., Stockle, M., Zimmermann, R. & Wullich, B. (2006) Genomic and expression analysis of the 3q25-q26 amplification unit reveals TLOC1/SEC62 as a probable target gene in prostate cancer, *Mol Cancer Res*. **4**, 169-76.
435. Greiner, M., Kreutzer, B., Lang, S., Jung, V., Cavalie, A., Unteregger, G., Zimmermann, R. & Wullich, B. (2011) Sec62 protein level is crucial for the ER stress tolerance of prostate cancer, *Prostate*. **71**, 1074-83.
436. Yang, G. F., Xie, D., Liu, J. H., Luo, J. H., Li, L. J., Hua, W. F., Wu, H. M., Kung, H. F., Zeng, Y. X. & Guan, X. Y. (2009) Expression and amplification of eIF-5A2 in human epithelial ovarian tumors and overexpression of EIF-5A2 is a new independent predictor of outcome in patients with ovarian carcinoma, *Gynecol Oncol*. **112**, 314-8.
437. He, L. R., Zhao, H. Y., Li, B. K., Liu, Y. H., Liu, M. Z., Guan, X. Y., Bian, X. W., Zeng, Y. X. & Xie, D. (2011) Overexpression of eIF5A-2 is an adverse prognostic marker of survival in stage I non-small cell lung cancer patients, *Int J Cancer*. **129**, 143-50.
438. Zhu, W., Cai, M. Y., Tong, Z. T., Dong, S. S., Mai, S. J., Liao, Y. J., Bian, X. W., Lin, M. C., Kung, H. F., Zeng, Y. X., Guan, X. Y. & Xie, D. (2012) Overexpression of EIF5A2 promotes colorectal carcinoma cell aggressiveness by upregulating MTA1 through C-myc to induce epithelial-mesenchymal transition, *Gut*. **61**, 562-75.
439. Tang, D. J., Dong, S. S., Ma, N. F., Xie, D., Chen, L., Fu, L., Lau, S. H., Li, Y., Li, Y. & Guan, X. Y. (2010) Overexpression of eukaryotic initiation factor 5A2 enhances cell motility and promotes tumor metastasis in hepatocellular carcinoma, *Hepatology*. **51**, 1255-63.
440. Meng, Q. B., Kang, W. M., Yu, J. C., Liu, Y. Q., Ma, Z. Q., Zhou, L., Cui, Q. C. & Zhou, W. X. (2015) Overexpression of eukaryotic translation initiation factor 5A2 (EIF5A2) correlates with cell aggressiveness and poor survival in gastric cancer, *PLoS One*. **10**, e0119229.
441. Tariq, M., Ito, A., Ishfaq, M., Bradshaw, E. & Yoshida, M. (2016) Eukaryotic translation initiation factor 5A (eIF5A) is essential for HIF-1 α activation in hypoxia, *Biochem Biophys Res Commun*. **470**, 417-424.
442. Osawa, M., Umetsu, K., Ohki, T., Nagasawa, T., Suzuki, T. & Takeichi, S. (1997) Molecular evidence for human alpha 2-HS glycoprotein (AHSG) polymorphism, *Hum Genet*. **99**, 18-21.
443. Thompson, P. D., Sakwe, A., Koumangoye, R., Yarbrough, W. G., Ochieng, J. & Marshall, D. R. (2014) Alpha-2 Heremans Schmid Glycoprotein (AHSG) modulates signaling pathways in head and neck squamous cell carcinoma cell line SQ20B, *Exp Cell Res*. **321**, 123-32.
444. Ray, S., Lukyanov, P. & Ochieng, J. (2003) Members of the cystatin superfamily interact with MMP-9 and protect it from autolytic degradation without affecting its gelatinolytic activities, *Biochim Biophys Acta*. **1652**, 91-102.
445. Guillory, B., Sakwe, A. M., Saria, M., Thompson, P., Adhiambo, C., Koumangoye, R., Ballard, B., Binhazim, A., Cone, C., Jahanen-Dechent, W. & Ochieng, J. (2010) Lack of fetuin-A (alpha2-HS-glycoprotein) reduces mammary tumor incidence and prolongs tumor latency via the transforming growth factor-beta signaling pathway in a mouse model of breast cancer, *Am J Pathol*. **177**, 2635-44.
446. Kundranda, M. N., Henderson, M., Carter, K. J., Gorden, L., Binhazim, A., Ray, S., Baptiste, T., Shokrani, M., Leite-Browning, M. L., Jannen-Dechent, W., Matrisian, L. M. & Ochieng, J. (2005) The serum glycoprotein fetuin-A promotes Lewis lung carcinoma tumorigenesis via adhesive-dependent and adhesive-independent mechanisms, *Cancer Res*. **65**, 499-506.
447. Garcia-Echeverria, C. & Sellers, W. R. (2008) Drug discovery approaches targeting the PI3K/Akt pathway in cancer, *Oncogene*. **27**, 5511-26.
448. Butler, A. M., Scotti Buzhardt, M. L., Erdogan, E., Li, S., Inman, K. S., Fields, A. P. & Murray, N. R. (2015) A small molecule inhibitor of atypical protein kinase C signaling inhibits pancreatic cancer cell transformed growth and invasion, *Oncotarget*. **6**, 15297-310.
449. Hu, B., Yang, Y. T., Huang, Y., Zhu, Y. & Lu, Z. J. (2017) POSTAR: a platform for exploring post-transcriptional regulation coordinated by RNA-binding proteins, *Nucleic Acids Res*. **45**, D104-D114.

450. Croft, D., O'Kelly, G., Wu, G., Haw, R., Gillespie, M., Matthews, L., Caudy, M., Garapati, P., Gopinath, G., Jassal, B., Jupe, S., Kalatskaya, I., Mahajan, S., May, B., Ndegwa, N., Schmidt, E., Shamovsky, V., Yung, C., Birney, E., Hermjakob, H., D'Eustachio, P. & Stein, L. (2011) Reactome: a database of reactions, pathways and biological processes, *Nucleic Acids Res.* **39**, D691-7.
451. Hafner, M., Landthaler, M., Burger, L., Khorshid, M., Hausser, J., Berninger, P., Rothballer, A., Ascano, M., Jr., Jungkamp, A. C., Munschauer, M., Ulrich, A., Wardle, G. S., Dewell, S., Zavolan, M. & Tuschl, T. (2010) Transcriptome-wide identification of RNA-binding protein and microRNA target sites by PAR-CLIP, *Cell.* **141**, 129-41.
452. Fabregat, A., Sidiropoulos, K., Garapati, P., Gillespie, M., Hausmann, K., Haw, R., Jassal, B., Jupe, S., Korninger, F., McKay, S., Matthews, L., May, B., Milacic, M., Rothfels, K., Shamovsky, V., Webber, M., Weiser, J., Williams, M., Wu, G., Stein, L., Hermjakob, H. & D'Eustachio, P. (2016) The Reactome pathway Knowledgebase, *Nucleic Acids Res.* **44**, D481-7.
453. Milacic, M., Haw, R., Rothfels, K., Wu, G., Croft, D., Hermjakob, H., D'Eustachio, P. & Stein, L. (2012) Annotating cancer variants and anti-cancer therapeutics in reactome, *Cancers (Basel).* **4**, 1180-211.
454. Gatz, M. L., Silva, G. O., Parker, J. S., Fan, C. & Perou, C. M. (2014) An integrated genomics approach identifies drivers of proliferation in luminal-subtype human breast cancer, *Nat Genet.* **46**, 1051-9.
455. Hyman, E., Kauraniemi, P., Hautaniemi, S., Wolf, M., Mousset, S., Rozenblum, E., Ringner, M., Sauter, G., Monni, O., Elkahoul, A., Kallioniemi, O. P. & Kallioniemi, A. (2002) Impact of DNA amplification on gene expression patterns in breast cancer, *Cancer Res.* **62**, 6240-5.
456. Pollack, J. R., Sorlie, T., Perou, C. M., Rees, C. A., Jeffrey, S. S., Lonning, P. E., Tibshirani, R., Botstein, D., Borresen-Dale, A. L. & Brown, P. O. (2002) Microarray analysis reveals a major direct role of DNA copy number alteration in the transcriptional program of human breast tumors, *Proc Natl Acad Sci U S A.* **99**, 12963-8.
457. Nielsen, J., Christiansen, J., Lykke-Andersen, J., Johnsen, A. H., Wewer, U. M. & Nielsen, F. C. (1999) A family of insulin-like growth factor II mRNA-binding proteins represses translation in late development, *Mol Cell Biol.* **19**, 1262-70.
458. Dai, N., Ji, F., Wright, J., Minichiello, L., Sadreyev, R. & Avruch, J. (2017) IGF2 mRNA binding protein-2 is a tumor promoter that drives cancer proliferation through its client mRNAs IGF2 and HMGA1, *Elife.* **6**.
459. Peng, C. H., Liao, C. T., Peng, S. C., Chen, Y. J., Cheng, A. J., Juang, J. L., Tsai, C. Y., Chen, T. C., Chuang, Y. J., Tang, C. Y., Hsieh, W. P. & Yen, T. C. (2011) A novel molecular signature identified by systems genetics approach predicts prognosis in oral squamous cell carcinoma, *PLoS One.* **6**, e23452.
460. Ye, H., Yu, T., Temam, S., Zober, B. L., Wang, J., Schwartz, J. L., Mao, L., Wong, D. T. & Zhou, X. (2008) Transcriptomic dissection of tongue squamous cell carcinoma, *BMC Genomics.* **9**, 69.
461. Ginos, M. A., Page, G. P., Michalowicz, B. S., Patel, K. J., Volker, S. E., Pambuccian, S. E., Ondrey, F. G., Adams, G. L. & Gaffney, P. M. (2004) Identification of a gene expression signature associated with recurrent disease in squamous cell carcinoma of the head and neck, *Cancer Res.* **64**, 55-63.
462. Pyeon, D., Newton, M. A., Lambert, P. F., den Boon, J. A., Sengupta, S., Marsit, C. J., Woodworth, C. D., Connor, J. P., Haugen, T. H., Smith, E. M., Kelsey, K. T., Turek, L. P. & Ahlquist, P. (2007) Fundamental differences in cell cycle deregulation in human papillomavirus-positive and human papillomavirus-negative head/neck and cervical cancers, *Cancer Res.* **67**, 4605-19.
463. Toruner, G. A., Ulger, C., Alkan, M., Galante, A. T., Rinaggio, J., Wilk, R., Tian, B., Soteropoulos, P., Hameed, M. R., Schwalb, M. N. & Dermody, J. J. (2004) Association between gene expression profile and tumor invasion in oral squamous cell carcinoma, *Cancer Genet Cytogenet.* **154**, 27-35.
464. Kimlin, L. C., Casagrande, G. & Virador, V. M. (2013) In vitro three-dimensional (3D) models in cancer research: an update, *Mol Carcinog.* **52**, 167-82.
465. Keene, J. D. (2007) RNA regulons: coordination of post-transcriptional events, *Nat Rev Genet.* **8**, 533-43.

466. Limesand, K. H., Chibly, A. M. & Fribley, A. (2013) Impact of targeting insulin-like growth factor signaling in head and neck cancers, *Growth Horm IGF Res.* **23**, 135-40.
467. van der Veeken, J., Oliveira, S., Schiffelers, R. M., Storm, G., van Bergen En Henegouwen, P. M. & Roovers, R. C. (2009) Crosstalk between epidermal growth factor receptor- and insulin-like growth factor-1 receptor signaling: implications for cancer therapy, *Curr Cancer Drug Targets.* **9**, 748-60.
468. Ribeiro, F. A., Noguti, J., Oshima, C. T. & Ribeiro, D. A. (2014) Effective targeting of the epidermal growth factor receptor (EGFR) for treating oral cancer: a promising approach, *Anticancer Res.* **34**, 1547-52.
469. Rosenzweig, R., Bronner, V., Zhang, D., Fushman, D. & Glickman, M. H. (2012) Rpn1 and Rpn2 coordinate ubiquitin processing factors at proteasome, *J Biol Chem.* **287**, 14659-71.
470. Rosenzweig, R., Osmulski, P. A., Gaczynska, M. & Glickman, M. H. (2008) The central unit within the 19S regulatory particle of the proteasome, *Nat Struct Mol Biol.* **15**, 573-80.
471. Isono, E., Saeki, Y., Yokosawa, H. & Toh-e, A. (2004) Rpn7 is required for the structural integrity of the 26 S proteasome of *Saccharomyces cerevisiae*, *J Biol Chem.* **279**, 27168-76.
472. Tsolou, A., Nelson, G., Trachana, V., Chondrogianni, N., Saretzki, G., von Zglinicki, T. & Gonos, E. S. (2012) The 19S proteasome subunit Rpn7 stabilizes DNA damage foci upon genotoxic insult, *IUBMB Life.* **64**, 432-42.
473. Gudmundsdottir, K., Lord, C. J. & Ashworth, A. (2007) The proteasome is involved in determining differential utilization of double-strand break repair pathways, *Oncogene.* **26**, 7601-6.
474. Huang, L., Haratake, K., Miyahara, H. & Chiba, T. (2016) Proteasome activators, PA28gamma and PA200, play indispensable roles in male fertility, *Sci Rep.* **6**, 23171.
475. Ortega, J., Heymann, J. B., Kajava, A. V., Ustrell, V., Rechsteiner, M. & Steven, A. C. (2005) The axial channel of the 20S proteasome opens upon binding of the PA200 activator, *J Mol Biol.* **346**, 1221-7.
476. Ustrell, V., Hoffman, L., Pratt, G. & Rechsteiner, M. (2002) PA200, a nuclear proteasome activator involved in DNA repair, *EMBO J.* **21**, 3516-25.
477. Khor, B., Bredemeyer, A. L., Huang, C. Y., Turnbull, I. R., Evans, R., Maggi, L. B., Jr., White, J. M., Walker, L. M., Carnes, K., Hess, R. A. & Sleckman, B. P. (2006) Proteasome activator PA200 is required for normal spermatogenesis, *Mol Cell Biol.* **26**, 2999-3007.
478. Blickwedehl, J., Olejniczak, S., Cummings, R., Sarvaiya, N., Mantilla, A., Chanan-Khan, A., Pandita, T. K., Schmidt, M., Thompson, C. B. & Bangia, N. (2012) The proteasome activator PA200 regulates tumor cell responsiveness to glutamine and resistance to ionizing radiation, *Mol Cancer Res.* **10**, 937-44.
479. Blickwedehl, J., Agarwal, M., Seong, C., Pandita, R. K., Melendy, T., Sung, P., Pandita, T. K. & Bangia, N. (2008) Role for proteasome activator PA200 and postglutamyl proteasome activity in genomic stability, *Proc Natl Acad Sci U S A.* **105**, 16165-70.
480. Chen, D., Frezza, M., Schmitt, S., Kanwar, J. & Dou, Q. P. (2011) Bortezomib as the first proteasome inhibitor anticancer drug: current status and future perspectives, *Curr Cancer Drug Targets.* **11**, 239-53.
481. Langlands, F. E., Dodwell, D., Hanby, A. M., Horgan, K., Millican-Slater, R. A., Speirs, V., Verghese, E. T., Smith, L. & Hughes, T. A. (2014) PSMD9 expression predicts radiotherapy response in breast cancer, *Mol Cancer.* **13**, 73.
482. Luo, T., Fu, J., Xu, A., Su, B., Ren, Y., Li, N., Zhu, J., Zhao, X., Dai, R., Cao, J., Wang, B., Qin, W., Jiang, J., Li, J., Wu, M., Feng, G., Chen, Y. & Wang, H. (2016) PSMD10/gankyrin induces autophagy to promote tumor progression through cytoplasmic interaction with ATG7 and nuclear transactivation of ATG7 expression, *Autophagy.* **12**, 1355-71.
483. Tsvetkov, P., Mendillo, M. L., Zhao, J., Carette, J. E., Merrill, P. H., Cikes, D., Varadarajan, M., van Diemen, F. R., Penninger, J. M., Goldberg, A. L., Brummelkamp, T. R., Santagata, S. & Lindquist, S. (2015) Compromising the 19S proteasome complex protects cells from reduced flux through the proteasome, *Elife.* **4**.
484. Nijhawan, D., Zack, T. I., Ren, Y., Strickland, M. R., Lamothe, R., Schumacher, S. E., Tsherniak, A., Besche, H. C., Rosenbluh, J., Shehata, S., Cowley, G. S., Weir, B. A., Goldberg, A. L., Mesirov, J.

- P., Root, D. E., Bhatia, S. N., Beroukhi, R. & Hahn, W. C. (2012) Cancer vulnerabilities unveiled by genomic loss, *Cell*. **150**, 842-54.
485. Thompson, J. L. (2013) Carfilzomib: a second-generation proteasome inhibitor for the treatment of relapsed and refractory multiple myeloma, *Ann Pharmacother*. **47**, 56-62.
486. Yang, W., Soares, J., Greninger, P., Edelman, E. J., Lightfoot, H., Forbes, S., Bindal, N., Beare, D., Smith, J. A., Thompson, I. R., Ramaswamy, S., Futreal, P. A., Haber, D. A., Stratton, M. R., Benes, C., McDermott, U. & Garnett, M. J. (2013) Genomics of Drug Sensitivity in Cancer (GDSC): a resource for therapeutic biomarker discovery in cancer cells, *Nucleic Acids Res*. **41**, D955-61.
487. de Sousa Abreu, R., Penalva, L. O., Marcotte, E. M. & Vogel, C. (2009) Global signatures of protein and mRNA expression levels, *Mol Biosyst*. **5**, 1512-26.
488. Maier, T., Guell, M. & Serrano, L. (2009) Correlation of mRNA and protein in complex biological samples, *FEBS Lett*. **583**, 3966-73.
489. Glisovic, T., Bachorik, J. L., Yong, J. & Dreyfuss, G. (2008) RNA-binding proteins and post-transcriptional gene regulation, *FEBS Lett*. **582**, 1977-86.
490. Huang, S. H. & O'Sullivan, B. (2013) Oral cancer: Current role of radiotherapy and chemotherapy, *Med Oral Patol Oral Cir Bucal*. **18**, e233-40.
491. Yoshida, S., Ito, D., Nagumo, T., Shiota, T., Hatori, M. & Shintani, S. (2009) Hypoxia induces resistance to 5-fluorouracil in oral cancer cells via G(1) phase cell cycle arrest, *Oral Oncol*. **45**, 109-15.
492. Rockwell, S., Dobrucki, I. T., Kim, E. Y., Marrison, S. T. & Vu, V. T. (2009) Hypoxia and radiation therapy: past history, ongoing research, and future promise, *Curr Mol Med*. **9**, 442-58.
493. Liu, S. Y., Chang, L. C., Pan, L. F., Hung, Y. J., Lee, C. H. & Shieh, Y. S. (2008) Clinicopathologic significance of tumor cell-lined vessel and microenvironment in oral squamous cell carcinoma, *Oral Oncol*. **44**, 277-85.
494. Ishikawa, T., Nakashiro, K., Klosek, S. K., Goda, H., Hara, S., Uchida, D. & Hamakawa, H. (2009) Hypoxia enhances CXCR4 expression by activating HIF-1 in oral squamous cell carcinoma, *Oncol Rep*. **21**, 707-12.
495. Miyazaki, Y., Hara, A., Kato, K., Oyama, T., Yamada, Y., Mori, H. & Shibata, T. (2008) The effect of hypoxic microenvironment on matrix metalloproteinase expression in xenografts of human oral squamous cell carcinoma, *Int J Oncol*. **32**, 145-51.
496. Bengoechea-Alonso, M. T. & Ericsson, J. (2007) SREBP in signal transduction: cholesterol metabolism and beyond, *Curr Opin Cell Biol*. **19**, 215-22.
497. Zagani, R., El-Assaad, W., Gamache, I. & Teodoro, J. G. (2015) Inhibition of adipose triglyceride lipase (ATGL) by the putative tumor suppressor GOS2 or a small molecule inhibitor attenuates the growth of cancer cells, *Oncotarget*. **6**, 28282-95.
498. Grace, S. A., Meeks, M. W., Chen, Y., Cornwell, M., Ding, X., Hou, P., Rutgers, J. K., Crawford, S. E. & Lai, J. P. (2017) Adipose Triglyceride Lipase (ATGL) Expression Is Associated with Adiposity and Tumor Stromal Proliferation in Patients with Pancreatic Ductal Adenocarcinoma, *Anticancer Res*. **37**, 699-703.
499. Zechner, R., Zimmermann, R., Eichmann, T. O., Kohlwein, S. D., Haemmerle, G., Lass, A. & Madeo, F. (2012) FAT SIGNALS--lipases and lipolysis in lipid metabolism and signaling, *Cell Metab*. **15**, 279-91.
500. Das, S. K., Eder, S., Schauer, S., Diwoky, C., Temmel, H., Guertl, B., Gorkiewicz, G., Tamilarasan, K. P., Kumari, P., Trauner, M., Zimmermann, R., Vesely, P., Haemmerle, G., Zechner, R. & Hoefler, G. (2011) Adipose triglyceride lipase contributes to cancer-associated cachexia, *Science*. **333**, 233-8.
501. Das, S. K. & Hoefler, G. (2013) The role of triglyceride lipases in cancer associated cachexia, *Trends Mol Med*. **19**, 292-301.
502. Hirsch, H. A., Iliopoulos, D., Joshi, A., Zhang, Y., Jaeger, S. A., Bulyk, M., Tschlis, P. N., Shirley Liu, X. & Struhl, K. (2010) A transcriptional signature and common gene networks link cancer with lipid metabolism and diverse human diseases, *Cancer Cell*. **17**, 348-61.
503. Santos, C. R. & Schulze, A. (2012) Lipid metabolism in cancer, *FEBS J*. **279**, 2610-23.
504. Braverman, N. E. & Moser, A. B. (2012) Functions of plasmalogen lipids in health and disease, *Biochim Biophys Acta*. **1822**, 1442-52.

505. Roos, D. S. & Choppin, P. W. (1984) Tumorigenicity of cell lines with altered lipid composition, *Proc Natl Acad Sci U S A*. **81**, 7622-6.
506. Howard, B. V., Morris, H. P. & Bailey, J. M. (1972) Ether-lipids, -glycerol phosphate dehydrogenase, and growth rate in tumors and cultured cells, *Cancer Res*. **32**, 1533-8.
507. Snyder, F. & Wood, R. (1969) Alkyl and alk-1-enyl ethers of glycerol in lipids from normal and neoplastic human tissues, *Cancer Res*. **29**, 251-7.
508. Mills, G. B. & Moolenaar, W. H. (2003) The emerging role of lysophosphatidic acid in cancer, *Nat Rev Cancer*. **3**, 582-91.
509. Cheng, J. B. & Russell, D. W. (2004) Mammalian wax biosynthesis. I. Identification of two fatty acyl-Coenzyme A reductases with different substrate specificities and tissue distributions, *J Biol Chem*. **279**, 37789-97.
510. Brown, A. J. & Snyder, F. (1982) Alkyldihydroxyacetone-P synthase. Solubilization, partial purification, new assay method, and evidence for a ping-pong mechanism, *J Biol Chem*. **257**, 8835-9.
511. Wanders, R. J., Komen, J. & Kemp, S. (2011) Fatty acid omega-oxidation as a rescue pathway for fatty acid oxidation disorders in humans, *FEBS J*. **278**, 182-94.
512. Wanders, R. J., Komen, J. & Ferdinandusse, S. (2011) Phytanic acid metabolism in health and disease, *Biochim Biophys Acta*. **1811**, 498-507.
513. Buchert, R., Tawamie, H., Smith, C., Uebe, S., Innes, A. M., Al Hallak, B., Ekici, A. B., Sticht, H., Schwarze, B., Lamont, R. E., Parboosingh, J. S., Bernier, F. P. & Abou Jamra, R. (2014) A peroxisomal disorder of severe intellectual disability, epilepsy, and cataracts due to fatty acyl-CoA reductase 1 deficiency, *Am J Hum Genet*. **95**, 602-10.
514. Liegel, R. P., Ronchetti, A. & Sidjanin, D. J. (2014) Alkylglycerone phosphate synthase (AGPS) deficient mice: models for rhizomelic chondrodysplasia punctate type 3 (RCDP3) malformation syndrome, *Mol Genet Metab Rep*. **1**, 299-311.
515. Xia, J., Sineelnikov, I. V., Han, B. & Wishart, D. S. (2015) MetaboAnalyst 3.0--making metabolomics more meaningful, *Nucleic Acids Res*. **43**, W251-7.
516. Jiang, L., Greenwood, T. R., Artemov, D., Raman, V., Winnard, P. T., Jr., Heeren, R. M., Bhujwala, Z. M. & Glunde, K. (2012) Localized hypoxia results in spatially heterogeneous metabolic signatures in breast tumor models, *Neoplasia*. **14**, 732-41.
517. Chen, C., Pore, N., Behrooz, A., Ismail-Beigi, F. & Maity, A. (2001) Regulation of glut1 mRNA by hypoxia-inducible factor-1. Interaction between H-ras and hypoxia, *J Biol Chem*. **276**, 9519-25.
518. Hatanpaa, K. J., Burma, S., Zhao, D. & Habib, A. A. (2010) Epidermal growth factor receptor in glioma: signal transduction, neuropathology, imaging, and radioresistance, *Neoplasia*. **12**, 675-84.
519. Guo, D., Prins, R. M., Dang, J., Kuga, D., Iwanami, A., Soto, H., Lin, K. Y., Huang, T. T., Akhavan, D., Hock, M. B., Zhu, S., Kofman, A. A., Bensinger, S. J., Yong, W. H., Vinters, H. V., Horvath, S., Watson, A. D., Kuhn, J. G., Robins, H. I., Mehta, M. P., Wen, P. Y., DeAngelis, L. M., Prados, M. D., Mellinghoff, I. K., Cloughesy, T. F. & Mischel, P. S. (2009) EGFR signaling through an Akt-SREBP-1-dependent, rapamycin-resistant pathway sensitizes glioblastomas to antilipogenic therapy, *Sci Signal*. **2**, ra82.
520. Williams, K. J., Argus, J. P., Zhu, Y., Wilks, M. Q., Marbois, B. N., York, A. G., Kidani, Y., Pourzia, A. L., Akhavan, D., Lisiero, D. N., Komisopoulou, E., Henkin, A. H., Soto, H., Chamberlain, B. T., Vergnes, L., Jung, M. E., Torres, J. Z., Liao, L. M., Christofk, H. R., Prins, R. M., Mischel, P. S., Reue, K., Graeber, T. G. & Bensinger, S. J. (2013) An essential requirement for the SCAP/SREBP signaling axis to protect cancer cells from lipotoxicity, *Cancer Res*. **73**, 2850-62.
521. Koizume, S. & Miyagi, Y. (2016) Lipid Droplets: A Key Cellular Organelle Associated with Cancer Cell Survival under Normoxia and Hypoxia, *Int J Mol Sci*. **17**.
522. Lewis, C. A., Brault, C., Peck, B., Bensaad, K., Griffiths, B., Mitter, R., Chakravarty, P., East, P., Dankworth, B., Alibhai, D., Harris, A. L. & Schulze, A. (2015) SREBP maintains lipid biosynthesis and viability of cancer cells under lipid- and oxygen-deprived conditions and defines a gene signature associated with poor survival in glioblastoma multiforme, *Oncogene*. **34**, 5128-40.
523. Fowler, C. J. (2012) Monoacylglycerol lipase - a target for drug development?, *Br J Pharmacol*. **166**, 1568-85.

524. Pacher, P., Batkai, S. & Kunos, G. (2006) The endocannabinoid system as an emerging target of pharmacotherapy, *Pharmacol Rev.* **58**, 389-462.
525. Chouinard, F., Lefebvre, J. S., Navarro, P., Bouchard, L., Ferland, C., Lalancette-Hebert, M., Marsolais, D., Laviolette, M. & Flamand, N. (2011) The endocannabinoid 2-arachidonoyl-glycerol activates human neutrophils: critical role of its hydrolysis and de novo leukotriene B4 biosynthesis, *J Immunol.* **186**, 3188-96.
526. Cao, Z., Mulvihill, M. M., Mukhopadhyay, P., Xu, H., Erdelyi, K., Hao, E., Holovac, E., Hasko, G., Cravatt, B. F., Nomura, D. K. & Pacher, P. (2013) Monoacylglycerol lipase controls endocannabinoid and eicosanoid signaling and hepatic injury in mice, *Gastroenterology.* **144**, 808-817 e15.
527. Schweiger, M., Schreiber, R., Haemmerle, G., Lass, A., Fledelius, C., Jacobsen, P., Tornqvist, H., Zechner, R. & Zimmermann, R. (2006) Adipose triglyceride lipase and hormone-sensitive lipase are the major enzymes in adipose tissue triacylglycerol catabolism, *J Biol Chem.* **281**, 40236-41.
528. Gnerlich, J. L., Yao, K. A., Fitchev, P. S., Goldschmidt, R. A., Bond, M. C., Cornwell, M. & Crawford, S. E. (2013) Peritumoral expression of adipokines and fatty acids in breast cancer, *Ann Surg Oncol.* **20 Suppl 3**, S731-8.
529. Gan, E. S., Cheong, W. F., Chan, K. R., Ong, E. Z., Chai, X., Tan, H. C., Ghosh, S., Wenk, M. R. & Ooi, E. E. (2017) Hypoxia enhances antibody-dependent dengue virus infection, *EMBO J.* **36**, 1348-1363.
530. Nagan, N. & Zoeller, R. A. (2001) Plasmalogens: biosynthesis and functions, *Prog Lipid Res.* **40**, 199-229.
531. Brites, P., Waterham, H. R. & Wanders, R. J. (2004) Functions and biosynthesis of plasmalogens in health and disease, *Biochim Biophys Acta.* **1636**, 219-31.
532. Zoeller, R. A., Morand, O. H. & Raetz, C. R. (1988) A possible role for plasmalogens in protecting animal cells against photosensitized killing, *J Biol Chem.* **263**, 11590-6.
533. Zoeller, R. A., Lake, A. C., Nagan, N., Gaposchkin, D. P., Legner, M. A. & Lieberthal, W. (1999) Plasmalogens as endogenous antioxidants: somatic cell mutants reveal the importance of the vinyl ether, *Biochem J.* **338 (Pt 3)**, 769-76.
534. Zoeller, R. A., Grazia, T. J., LaCamera, P., Park, J., Gaposchkin, D. P. & Farber, H. W. (2002) Increasing plasmalogen levels protects human endothelial cells during hypoxia, *Am J Physiol Heart Circ Physiol.* **283**, H671-9.
535. Piano, V., Benjamin, D. I., Valente, S., Nenci, S., Marrocco, B., Mai, A., Aliverti, A., Nomura, D. K. & Mattevi, A. (2015) Discovery of Inhibitors for the Ether Lipid-Generating Enzyme AGPS as Anti-Cancer Agents, *ACS Chem Biol.* **10**, 2589-97.
536. Buffa, F. M., Harris, A. L., West, C. M. & Miller, C. J. (2010) Large meta-analysis of multiple cancers reveals a common, compact and highly prognostic hypoxia metagene, *Br J Cancer.* **102**, 428-35.
537. Chang, Q., Jurisica, I., Do, T. & Hedley, D. W. (2011) Hypoxia predicts aggressive growth and spontaneous metastasis formation from orthotopically grown primary xenografts of human pancreatic cancer, *Cancer Res.* **71**, 3110-20.
538. Vinci, M., Gowan, S., Boxall, F., Patterson, L., Zimmermann, M., Court, W., Lomas, C., Mendiola, M., Hardisson, D. & Eccles, S. A. (2012) Advances in establishment and analysis of three-dimensional tumor spheroid-based functional assays for target validation and drug evaluation, *BMC Biol.* **10**, 29.
539. Balkwill, F. R., Capasso, M. & Hagemann, T. (2012) The tumor microenvironment at a glance, *J Cell Sci.* **125**, 5591-6.
540. Peters-Golden, M., Gleason, M. M. & Togias, A. (2006) Cysteinyl leukotrienes: multi-functional mediators in allergic rhinitis, *Clin Exp Allergy.* **36**, 689-703.
541. Shirasaki, H., Kanaizumi, E., Watanabe, K., Matsui, T., Sato, J., Narita, S., Rautiainen, M. & Himi, T. (2002) Expression and localization of the cysteinyl leukotriene 1 receptor in human nasal mucosa, *Clin Exp Allergy.* **32**, 1007-12.
542. Figueroa, D. J., Breyer, R. M., Defoe, S. K., Kargman, S., Daugherty, B. L., Waldburger, K., Liu, Q., Clements, M., Zeng, Z., O'Neill, G. P., Jones, T. R., Lynch, K. R., Austin, C. P. & Evans, J. F. (2001)

- Expression of the cysteinyl leukotriene 1 receptor in normal human lung and peripheral blood leukocytes, *Am J Respir Crit Care Med.* **163**, 226-33.
543. Figueroa, D. J., Borish, L., Baramki, D., Philip, G., Austin, C. P. & Evans, J. F. (2003) Expression of cysteinyl leukotriene synthetic and signalling proteins in inflammatory cells in active seasonal allergic rhinitis, *Clin Exp Allergy.* **33**, 1380-8.
544. McKinnon, K. P., Madden, M. C., Noah, T. L. & Devlin, R. B. (1993) In vitro ozone exposure increases release of arachidonic acid products from a human bronchial epithelial cell line, *Toxicol Appl Pharmacol.* **118**, 215-23.
545. Larre, S., Tran, N., Fan, C., Hamadeh, H., Champigneulle, J., Azzouzi, R., Cussenot, O., Mangin, P. & Olivier, J. L. (2008) PGE2 and LTB4 tissue levels in benign and cancerous prostates, *Prostaglandins Other Lipid Mediat.* **87**, 14-9.
546. Dreyling, K. W., Hoppe, U., Peskar, B. A., Morgenroth, K., Kozuschek, W. & Peskar, B. M. (1986) Leukotriene synthesis by human gastrointestinal tissues, *Biochim Biophys Acta.* **878**, 184-93.
547. Zhao, X., Xu, Z. & Li, H. (2017) NSAIDs Use and Reduced Metastasis in Cancer Patients: results from a meta-analysis, *Sci Rep.* **7**, 1875.
548. Diamant, Z., Mantzouranis, E. & Bjermer, L. (2009) Montelukast in the treatment of asthma and beyond, *Expert Rev Clin Immunol.* **5**, 639-58.
549. Gunning, W. T., Kramer, P. M., Steele, V. E. & Pereira, M. A. (2002) Chemoprevention by lipoxygenase and leukotriene pathway inhibitors of vinyl carbamate-induced lung tumors in mice, *Cancer Res.* **62**, 4199-201.
550. Szklarczyk, D., Franceschini, A., Wyder, S., Forslund, K., Heller, D., Huerta-Cepas, J., Simonovic, M., Roth, A., Santos, A., Tsafou, K. P., Kuhn, M., Bork, P., Jensen, L. J. & von Mering, C. (2015) STRING v10: protein-protein interaction networks, integrated over the tree of life, *Nucleic Acids Research.* **43**, D447-D452.
551. Sarau, H. M., Ames, R. S., Chambers, J., Ellis, C., Elshourbagy, N., Foley, J. J., Schmidt, D. B., Muccitelli, R. M., Jenkins, O., Murdock, P. R., Herrity, N. C., Halsey, W., Sathe, G., Muir, A. I., Nuthulaganti, P., Dytko, G. M., Buckley, P. T., Wilson, S., Bergsma, D. J. & Hay, D. W. (1999) Identification, molecular cloning, expression, and characterization of a cysteinyl leukotriene receptor, *Mol Pharmacol.* **56**, 657-63.
552. Sala, A., Voelkel, N., Maclouf, J. & Murphy, R. C. (1990) Leukotriene E4 elimination and metabolism in normal human subjects, *J Biol Chem.* **265**, 21771-8.
553. Wright, H. L., Moots, R. J., Bucknall, R. C. & Edwards, S. W. (2010) Neutrophil function in inflammation and inflammatory diseases, *Rheumatology (Oxford).* **49**, 1618-31.
554. Paggiaro, P. & Bacci, E. (2011) Montelukast in asthma: a review of its efficacy and place in therapy, *Ther Adv Chronic Dis.* **2**, 47-58.
555. Tsai, M. J., Wu, P. H., Sheu, C. C., Hsu, Y. L., Chang, W. A., Hung, J. Y., Yang, C. J., Yang, Y. H., Kuo, P. L. & Huang, M. S. (2016) Cysteinyl Leukotriene Receptor Antagonists Decrease Cancer Risk in Asthma Patients, *Sci Rep.* **6**, 23979.
556. Fang, C. Y., Wu, C. C., Fang, C. L., Chen, W. Y. & Chen, C. L. (2017) Long-term growth comparison studies of FBS and FBS alternatives in six head and neck cell lines, *PLoS One.* **12**, e0178960.
557. Cheng, H., Leff, J. A., Amin, R., Gertz, B. J., De Smet, M., Noonan, N., Rogers, J. D., Malbecq, W., Meisner, D. & Somers, G. (1996) Pharmacokinetics, bioavailability, and safety of montelukast sodium (MK-0476) in healthy males and females, *Pharm Res.* **13**, 445-8.
558. Zhao, J. J., Rogers, J. D., Holland, S. D., Larson, P., Amin, R. D., Haesen, R., Freeman, A., Seiberling, M., Merz, M. & Cheng, H. (1997) Pharmacokinetics and bioavailability of montelukast sodium (MK-0476) in healthy young and elderly volunteers, *Biopharm Drug Dispos.* **18**, 769-77.
559. Schneider, E. K., Huang, J. X., Carbone, V., Baker, M., Azad, M. A., Cooper, M. A., Li, J. & Velkov, T. (2015) Drug-drug plasma protein binding interactions of ivacaftor, *J Mol Recognit.* **28**, 339-48.
560. Wang, M., Maier, P., Wenz, F., Giordano, F. A. & Herskind, C. (2013) Mitogenic signalling in the absence of epidermal growth factor receptor activation in a human glioblastoma cell line, *J Neurooncol.* **115**, 323-31.

561. Wikstrom, K., Juhas, M. & Sjolander, A. (2003) The anti-apoptotic effect of leukotriene D4 involves the prevention of caspase 8 activation and Bid cleavage, *Biochem J.* **371**, 115-24.
562. Kalyankrishna, S. & Grandis, J. R. (2006) Epidermal growth factor receptor biology in head and neck cancer, *J Clin Oncol.* **24**, 2666-72.
563. Wheeler, D. L., Huang, S., Kruser, T. J., Nechrebecki, M. M., Armstrong, E. A., Benavente, S., Gondi, V., Hsu, K. T. & Harari, P. M. (2008) Mechanisms of acquired resistance to cetuximab: role of HER (ErbB) family members, *Oncogene.* **27**, 3944-56.
564. Benavente, S., Huang, S., Armstrong, E. A., Chi, A., Hsu, K. T., Wheeler, D. L. & Harari, P. M. (2009) Establishment and characterization of a model of acquired resistance to epidermal growth factor receptor targeting agents in human cancer cells, *Clin Cancer Res.* **15**, 1585-92.
565. Wang, Z. Y., Martin, D., Molinolo, A. A., Patel, V., Iglesias-Bartolome, R., Degese, M. S., Vitale-Cross, L., Chen, Q. M. & Gutkind, J. S. (2014) mTOR Co-Targeting in Cetuximab Resistance in Head and Neck Cancers Harboring PIK3CA and RAS Mutations, *Jnci-J Natl Cancer I.* **106**.
566. Sunwoo, J. B., Chen, Z., Dong, G., Yeh, N., Crowl Bancroft, C., Sausville, E., Adams, J., Elliott, P. & Van Waes, C. (2001) Novel proteasome inhibitor PS-341 inhibits activation of nuclear factor-kappa B, cell survival, tumor growth, and angiogenesis in squamous cell carcinoma, *Clin Cancer Res.* **7**, 1419-28.
567. Fribley, A., Zeng, Q. & Wang, C. Y. (2004) Proteasome inhibitor PS-341 induces apoptosis through induction of endoplasmic reticulum stress-reactive oxygen species in head and neck squamous cell carcinoma cells, *Mol Cell Biol.* **24**, 9695-704.
568. Zang, Y., Thomas, S. M., Chan, E. T., Kirk, C. J., Freilino, M. L., DeLancey, H. M., Grandis, J. R., Li, C. & Johnson, D. E. (2012) Carfilzomib and ONX 0912 inhibit cell survival and tumor growth of head and neck cancer and their activities are enhanced by suppression of Mcl-1 or autophagy, *Clin Cancer Res.* **18**, 5639-49.
569. Zang, Y., Kirk, C. J. & Johnson, D. E. (2014) Carfilzomib and oprozomib synergize with histone deacetylase inhibitors in head and neck squamous cell carcinoma models of acquired resistance to proteasome inhibitors, *Cancer Biol Ther.* **15**, 1142-52.
570. Li, C., Zang, Y., Sen, M., Leeman-Neill, R. J., Man, D. S., Grandis, J. R. & Johnson, D. E. (2009) Bortezomib up-regulates activated signal transducer and activator of transcription-3 and synergizes with inhibitors of signal transducer and activator of transcription-3 to promote head and neck squamous cell carcinoma cell death, *Mol Cancer Ther.* **8**, 2211-20.
571. Li, C. & Johnson, D. E. (2012) Bortezomib induces autophagy in head and neck squamous cell carcinoma cells via JNK activation, *Cancer Lett.* **314**, 102-7.
572. Argiris, A., Duffy, A. G., Kummar, S., Simone, N. L., Arai, Y., Kim, S. W., Rudy, S. F., Kannabiran, V. R., Yang, X., Jang, M., Chen, Z., Suksta, N., Cooley-Zgela, T., Ramanand, S. G., Ahsan, A., Nyati, M. K., Wright, J. J. & Van Waes, C. (2011) Early tumor progression associated with enhanced EGFR signaling with bortezomib, cetuximab, and radiotherapy for head and neck cancer, *Clin Cancer Res.* **17**, 5755-64.
573. Fukumura, D. & Jain, R. K. (2007) Tumor microenvironment abnormalities: causes, consequences, and strategies to normalize, *J Cell Biochem.* **101**, 937-49.
574. Burke, L., Butler, C. T., Murphy, A., Moran, B., Gallagher, W. M., O'Sullivan, J. & Kennedy, B. N. (2016) Evaluation of Cysteinyl Leukotriene Signaling as a Therapeutic Target for Colorectal Cancer, *Front Cell Dev Biol.* **4**, 103.
575. Bernier, J., Vermorken, J. B. & Koch, W. M. (2006) Adjuvant therapy in patients with resected poor-risk head and neck cancer, *J Clin Oncol.* **24**, 2629-35.
576. Mehra, R., Cohen, R. B. & Burtneess, B. A. (2008) The role of cetuximab for the treatment of squamous cell carcinoma of the head and neck, *Clin Adv Hematol Oncol.* **6**, 742-50.